46807

The Jovian Atmospheres

NASA

The Jovian Atmospheres

Edited by
Michael Allison
and Larry D. Travis
Goddard Space Flight Center
Institute for Space Studies
New York, New York

NASA

PREFACE

We may never stage a better meeting. The Conference on the Jovian Atmospheres was convened at the Goddard Institute for Space Studies on May 6-8, 1985 with the support of Henry Brinton's office at NASA Headquarters. For the space of three days a hundred scientists from over thirty different laboratories, centers, and universities gathered overhead of Tom's Restaurant in upper Manhattan to consider and argue the subtle intricacies of the fluid envelopes of the giant planets.

There is no doubt that the planet Mars and the imminent opportunities for its reconnaissance by spacecraft exert a powerful hold on the imagination of every planetary scientist. But the Pioneer and Voyager observations of the Jovian realm have given the giant planets their own special claim to attention. (And, as Andrew Ingersoll remarks in his conference review, we're not talking about Mars right now.) Other planets have atmospheres. But the Jovian planets *are* atmospheres! Measurements of their elemental and isotopic abundances, as much as for comets, offer important clues to the alchemy of the primordial solar nebula. Their atmospheric motions are inspiring (and confounding) examples of macroscopic organization of chaos far from equilibrium. Nowhere else in the Solar System is the interactive complexity of chemistry, radiation, high pressure physics, electromagnetism, and turbulent fluid dynamics in such full force.

For these reasons we were delighted to be able to pull together researchers from several different areas of planetary atmospheric science and to include representatives from such other pertinent fields as stellar interiors, experimental chemistry, radio astronomy, and geophysical fluid dynamics. We like to think that our organizing committee made some bold and imaginative choices in our selection of invited speakers and reviewers and that the pay-off will be evident to the readers of these pages. The meeting also attracted a number of excellent contributed program and poster papers.

All authors were encouraged to submit their work for publication in a special issue of *Icarus* (1986; <u>65</u>, 159-467). We are grateful to Joe Burns for providing this special publication opportunity and assembling the thirteen papers which appear in that volume.

In these proceedings we include the reviews and contributed papers which did not appear in the special *Icarus* issue (or other publication) as well as the abstracts and a transcript of participant discussion for all the presentations. We thank all the session chairmen for helping to make these discussions as lively and pertinent as they were. We have gone to particular pains to preserve a printed record of these open sessions, having witnessed that some of the best questions and insightful remarks occur outside the pages of the journals. We want to thank all those authors and participants who helped us with the editing of their contributions and apologize to those who did not check their transcripts if the editing affected their meaning. We thank Academic Press for permission to reproduce the abstracts.

The transcription was made possible in the context of our limited resources by the long part-time relay of several word processing operators: Rayna Alexander, Philip Birnbaum, Mary Lynn Garcia, Carolyn Paurowski, Sharon Shively, and Doris Smith. Mary Yastishak was especially helpful in coordinating the

manuscripts and in assisting with the final proofreading. The photographs of conference participants which appear in this publication were made by Patrice Palmer. Lilly Del Valle designed the conference logo. Many of the figures in the text were drafted by Jose Mendoza.

We thank Carl Codan of Sigma Data Services, Inc. for providing logistical support for the meeting. Joseph Ferrier, Lex Lane, Rosa DeLos Santos, and Vicki Shelton helped with the setup of chairs, projection, message relays, and other support services. Carolyn Paurowski served throughout the proceedings as conference secretary.

As we compiled the final assembly of papers for this volume during the months following the Challenger tragedy, it has been distressing to hear of the probable postponement of the Galileo launch according to the torturous designs of one after another delta V-EGA trajectory scenario. Perhaps in the next few years we must be devoted more to scientific scholarship than to interplanetary navigation. But someday we will return to Jupiter and Saturn and have the opportunity to test the steel of our theories and calculations.

Michael Allison
Larry D. Travis

Goddard Institute for Space Studies
New York, New York

CONTENTS

MONDAY POSTER PRESENTATIONS
ATMOSPHERIC STRUCTURE, CLOUDS, AND CHEMISTRY

TUESDAY, MAY 7

SESSION ON GLOBAL DYNAMICS
Chair: P. H. Stone

SESSION ON SYNOPTIC FEATURES AND PROCESSES
Chair: R. F. Beebe

TUESDAY POSTER PRESENTATIONS
ATMOSPHERIC DYNAMICS

WEDNESDAY, MAY 8

SESSION ON FUTURE SPACEFLIGHT OPPORTUNITIES
Chair: W. B. Rossow

SESSION ON URANUS AND NEPTUNE
Chair: G. S. Orton

WEDNESDAY POSTER PRESENTATIONS
OUTER PLANETS

CLOSING SESSION

APPENDICES

WELCOMING REMARKS

James E. Hansen
NASA/Goddard Institute for Space Studies

I'd like to welcome you to GISS and to the Conference on the Jovian Atmospheres, and thank all of you for coming. This is the first planetary conference that we have had at GISS since the Venus atmosphere conference about ten years ago. I'm glad to see many of you who were at that conference and also a lot of new faces. I hope and expect that it won't be that long until we have our next planetary conference.

In looking at the conference notebook that Mike Allison has put together, I was very interested to see right up front a table of physical parameters for the Earth and other planetary atmospheres. One lesson that we have learned in past years from Richard Goody, Don Hunten and others of you is the value in studying the Earth's atmosphere and other planetary atmospheres in the broader context of all the planets. We believe very much in that concept.

For those of you not familiar with the research at the Institute, I should mention that our principal scientific programs are studies of global climate, cloud climatology, and global change on decade and longer timescales, as well as planetary atmospheres and astronomy. Many of us work in both planetary atmospheres and in applications to the Earth's atmosphere. This year we have succeeded in adding to our staff at GISS Tony Del Genio, who has worked with clouds and moist convection in the Earth's atmosphere and also studies of other planetary atmospheres. This summer Michael Prather, an atmospheric chemist at Harvard, is going to be joining us, and he too has done quite a bit of work on other planets as well as on the Earth. So, partly for these reasons, I'm optimistic that we can contribute to progress in this general area of studying planetary atmospheres in a broader context.

As for specific objectives of this conference, Mike Allison suggested last year that this would be a good time to put together some of the information that has been gained from our fly-bys of Jupiter and Saturn. This may help in planning the upcoming Galileo mission to Jupiter, as well as in considerations of other potential future planetary missions. I think that is a good idea, and I'm looking forward to a very stimulating conference.

I'd like to thank all of you again for coming, and I hope you have an enjoyable time in New York. Mike has included in your notebook information on local activities. If you do nothing else, I suggest you walk one block down 112th Street to St. John's Cathedral. St. John's is really remarkable, and I think you'll enjoy it.

MONDAY MORNING

THERMAL AND ORTHO-PARA HYDROGEN STRUCTURE

CHAIR: DONALD M. HUNTEN

PARA HYDROGEN EQUILIBRATION IN THE ATMOSPHERES OF THE OUTER PLANETS

Barney J. Conrath
NASA/Goddard Space Flight Center

The thermodynamic behavior of the atmospheres of the Jovian planets is strongly dependent on the extent to which local thermal equilibration of the ortho and para states of molecular hydrogen is achieved. Voyager IRIS data from Jupiter imply substantial departures of the para hydrogen fraction from equilibrium in the upper troposphere at low latitudes, but with values approaching equilibrium at higher latitudes. Data from Saturn are less sensitive to the ortho-para ratio, but suggest para hydrogen fractions near the equilibrium value. This behavior can be understood, providing the para hydrogen equilibration time exceeds the upper tropospheric radiative time constant. Such would be the case if the equilibration time were that for pure hydrogen ($\sim 10^9$ s) on both planets. Above approximately the 200 K temperature level, para hydrogen conversion can enhance the efficiency of convection, resulting in a substantial increase in overturning times on all of the outer planets. Currently available data cannot definitively establish the ortho-para ratios in the atmospheres of Uranus and Neptune, but suggest values closer to local equilibrium than to the 3:1 "normal" ratio. Modeling of sub-millimeter wavelength measurements of these planets suggest thermal structures with "frozen equilibrium" lapse rates in their convective regions. Measurements from the future Voyager encounters, along with improved ground based observations, should lead to a better understanding of the importance of para hydrogen equilibration in the atmospheres of Uranus and Neptune. Laboratory determinations of para hydrogen equilibrium times in the presence of ammonia ice particles are needed to improve our understanding of the hydrogen thermodynamics on Jupiter and Saturn.

Let me begin by outlining what I will attempt to cover this morning. Basically, I'll start off with a brief introduction to refresh your memory on the thermodynamics of molecular hydrogen and the story on ortho and para hydrogen and how it pertains to the atmospheres of the outer planets. I will cover a little bit of the background of some of the early work of various people, and let me apologize in advance if I forget to give people appropriate credit along the way. I will describe the observational results for Jupiter and Saturn, particularly some work that Peter Gierasch and I and others have attempted to do with the Voyager IRIS data. I'll look at the implications as we see them for some of the dynamics problems on hydrogen atmosphere planets. I'll say a few words about what we know about Uranus and Neptune. Finally, I will attempt to summarize the current outstanding questions in this area.

PRECEDING PAGE BLANK NOT FILMED

3-4
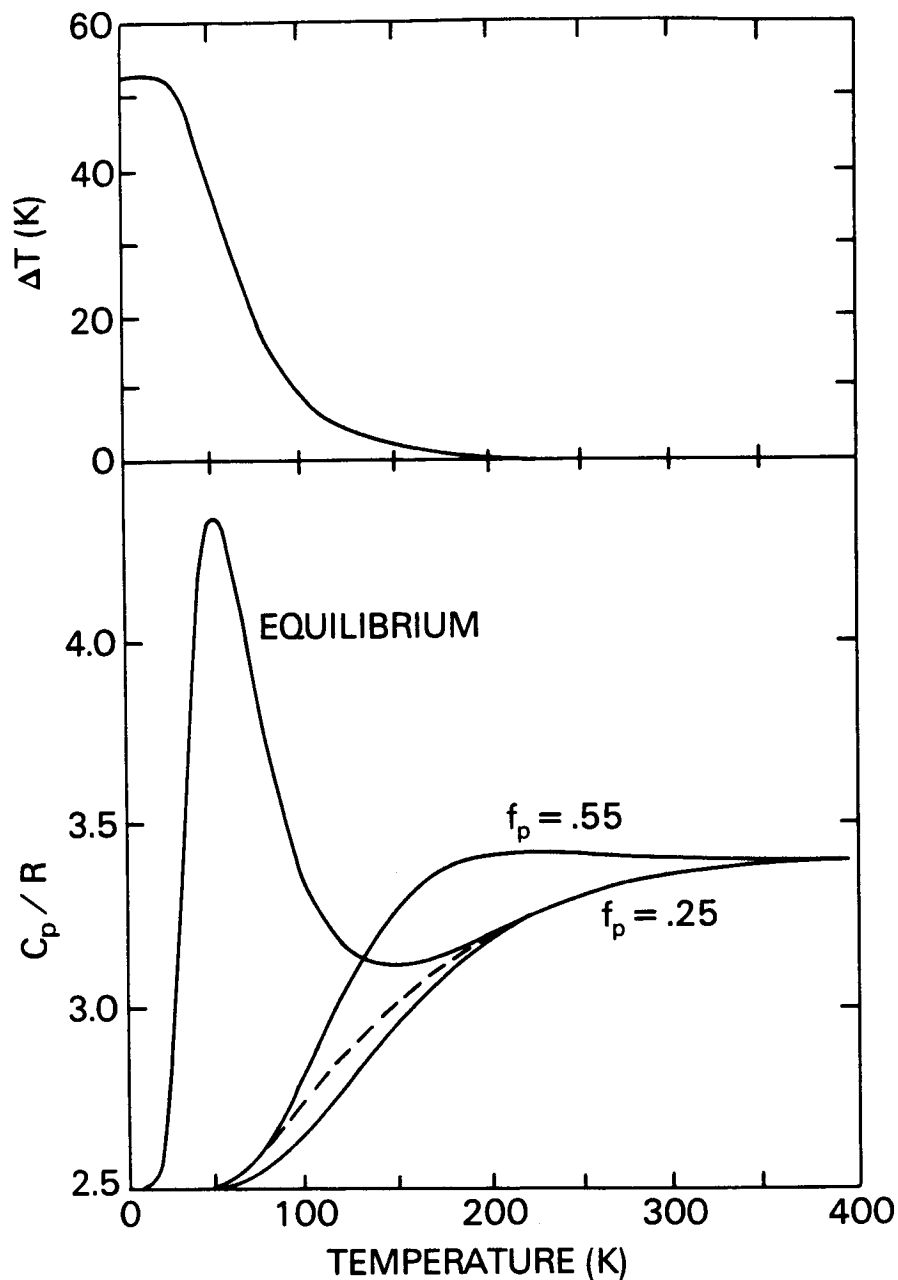
Figure 1. Temperature dependence of relevant thermo-
dynamic properties for a mixture of 90% H_2 and 10% He.
The upper panel indicates the temperature increment ΔT
which results from the equilibration of a parcel of
normal H_2 at a particular temperature. The lower panel
shows the nondimensional specific heats for fixed para
hydrogen fraction f_p compared with that for equilibrium
hydrogen. The dashed line represents the specific heat
which corresponds to the situation where f_p is set at
equilibrium value for the local temperature.

First, let me remind you of the story on molecular hydrogen; there are the ortho and para states. The ortho state corresponds to parallel proton spins, and the para state has anti-parallel spins. The ortho state is essentially a triplet spin state with a spin statistical weight of three; the para state has a spin statistical weight of one. The spin states are quantum mechanically coupled to the rotational states of the hydrogen molecule in such a way that the para state is associated with even rotational quantum numbers, J, and the ortho state has odd rotational quantum numbers. Now the $\Delta J=1$ transitions are highly forbidden in pure hydrogen. Therefore, there tends to be very little communication between the ortho and para states. Thus, if one prepares a sample of hydrogen at a temperature of approximately 300 K or higher and brings it into thermal equilibrium, the ortho-para ratio is essentially the ratio of the spin statistical weights, or three to one. But as the sample is then cooled down to lower temperatures in the case of pure hydrogen, instead of achieving the ortho-para ratio of the local thermodynamic equilibrium, it tends to retain the 3:1 (so-called normal) ortho-para ratio for long periods of time. In the case of pure hydrogen, ultimately there will be an equilibration between the ortho and para states just due to the very weak paramagnetism of the hydrogen molecule itself, but on a time scale (under conditions, say, of the 500 mb level on Jupiter) estimated to be about 10^9 seconds. This time scale decreases as the pressure increases as we get to deeper levels, and the equilibration time should become shorter even for pure hydrogen.

Now, there are catalytic processes which can greatly reduce this equilibration time. For example, the presence of paramagnetic sites on the surfaces of solids will greatly reduce the equilibration time, and this has possibly important consequences in the atmospheres of the outer planets since the cloud particle surfaces may in fact provide some catalysis, which will make the equilibration go much faster. At any rate, this characteristic of hydrogen has some profound spectroscopic and thermodynamic implications.

Hydrogen can have a number of different specific heats depending on the conditions occurring and the resulting degree of equilibration of the ortho and para states. Figure 1 illustrates the specific heat as a function of temperature for a mixture of 90% H_2 and 10% He. The curve labeled "equilibrium" corresponds to the limiting case of rapid conversion and hence strict equilibrium between the ortho and para states. In addition, you can have a specific heat associated with constant para hydrogen fraction, f_p. The para hydrogen fraction of 0.25 corresponds to the 3:1 ortho-para ratio of the normal or high-temperature limit. The dashed line represents a case in which one has a specific heat at constant para hydrogen fraction, but where f_p is taken to be the thermal equilibrium value for the local temperature. I call this case frozen equilibrium, although in the literature this is sometimes referred to as the intermediate specific heat.

To demonstrate the potentially profound effects that para hydrogen equilibration can have on thermodynamics, consider a parcel of hydrogen initially at deep levels where the temperature exceeds 300 K so that one has a 3:1 normal ratio, and move that parcel rapidly without equilibration up into the upper troposphere of a planet (for example, Jupiter where the temperature may be 120 K or so). Then let the parcel equilibrate through some process. Since this

is an exothermic process, the released heat produces a temperature increment. For example, on Jupiter it would be 4-5 K, on Saturn 8-9 K, and it becomes more and more pronounced the colder the upper troposphere is, so when we get to Uranus and Neptune it is quite a dramatic effect.

Let me just briefly mention some of the earlier historical work. In the mid-1960's, Larry Trafton (1967) first started worrying about the problem of the ortho-para ratio. He pointed out the importance of understanding this problem particularly in terms of the adiabatic lapse rate in the convective part of the atmosphere. Later, William Hayden Smith (1978) published a paper in which he emphasized the possible importance of the ortho-para ratio in the atmospheres of the outer planets and attempted to make some estimates of ortho-para ratios based on measurements of equivalent widths of the near infrared hydrogen quadrupole lines. To my knowledge, the first really quantitative attempt at modeling the behavior of para hydrogen fractions in the atmospheres of the outer planets is that due to Massie and Hunten (1982) in which they essentially made use of a one-dimensional aeronomical-type model with eddy mixing. They made various assumptions about para hydrogen equilibration times based on conversion mechanisms involving catalysis on the surfaces of cloud particles, and with this model they were able to calculate para hydrogen fractions as a function of altitude. I think it was really this work which inspired the more recent flurry of activity on hydrogen ortho-para ratio in the atmospheres of the outer planets. In particular, Gierasch (1983) published a brief paper in which he examined the potential dynamic implications of this. Basically in his model, he considered two adjacent atmospheric columns and allowed parcels to come up from depth at high temperatures (above 300 K) with a 3:1 normal ortho-para ratio. The parcels are then allowed to rise and then equilibrated up in the troposphere, releasing heat and producing a temperature increment, and then brought back down with a frozen para hydrogen fraction equal to that appropriate to the temperature near the tropopause. The parcel is then equilibrated again at depth. This produced a buoyancy contrast which in turn could support a thermal wind with velocities comparable to those observed on Jupiter. In fact, he did a similar model for Saturn where with its lower temperature, one can get an even stronger effect, and hence stronger zonal winds.

Largely through the urging of Gierasch and also Don Hunten, we attempted to examine the IRIS data from the point of view of what information we could get on the ortho-para ratio. Figure 2 shows the portion of the spectrum of interest here, between 200-600 wavenumbers, which covers the region of the two broad, collision-induced H_2 lines, S(0) and S(1). The S(0) line corresponds to transitions between para states, and the S(1) line between ortho states. So to first approximation, the ratio of the strengths of the two lines is dependent on the ortho-para ratio. Since this is the thermal emission spectrum, one also must take into account the effect of the vertical thermal structure on the shape of the spectrum. Figure 3 represents calculations for three different para hydrogen fractions, with $f_p = 0.25$ being that corresponding to normal hydrogen (the 3:1 case). The other extreme, 0.35, is approximately the local thermal equilibrium value for the upper troposphere of Jupiter. Clearly, there is substantial sensitivity, one line moving one way and the other line moving the other way. The effect on the S(1) line is less pronounced than that on the S(0) line simply because the S(1) line is formed in a region of
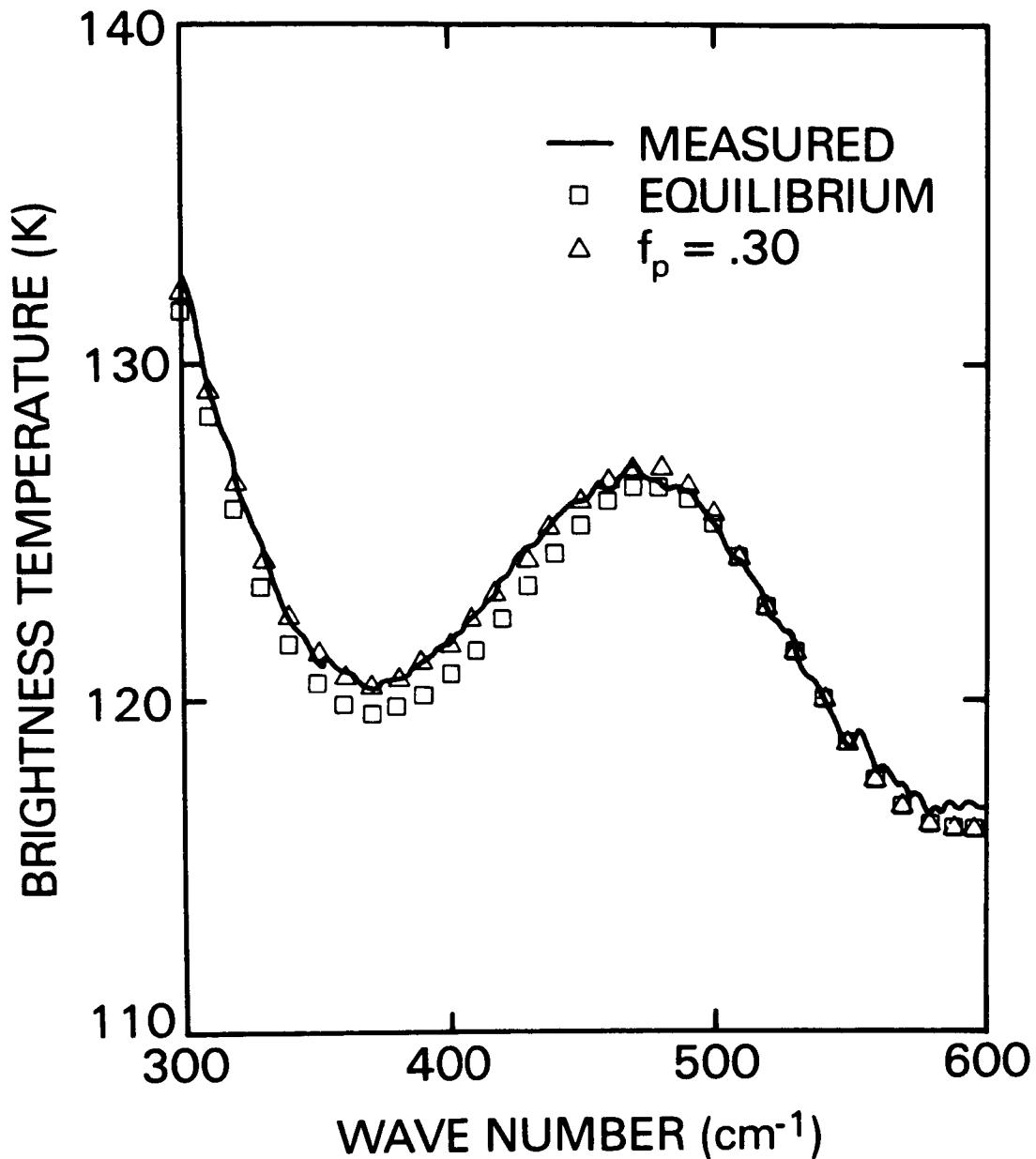
Figure 2. Comparison of the measured Jovian thermal emission spectrum with synthetic spectra calculated for equilibrium f_p and for a height independent value of 0.30. The theoretical spectra were calculated using the vertical temperature profile determined from the Voyager 1 ingress radio occultation. For this example, a height independent $f_p = 0.30$ yields a better fit throughout the region of the S(0) line centered near 370 cm^{-1}.
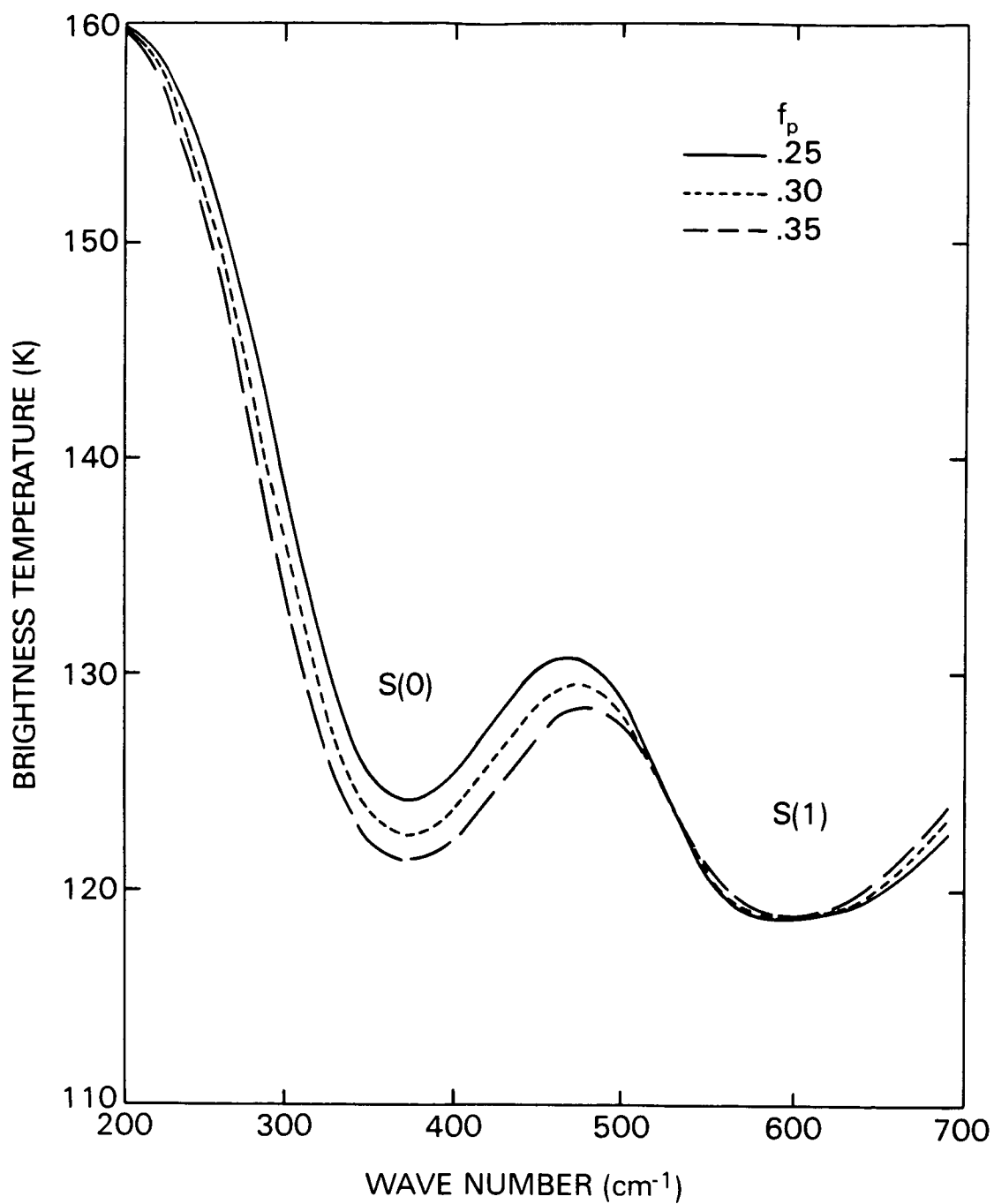
Figure 3. Theoretical Jovian spectra for three different values of the para hydrogen fraction f_p. By virtue of the opposing sensitivities of the $S(0)$ and $S(1)$ lines, the region near 520 cm^{-1} is essentially independent of f_p.

relatively low lapse rates, so the measured gradient of brightness temperature is less sensitive to the opacity of the atmosphere in that region.

In particular, there is a crossover point between the two lines near 520 cm^{-1} which is essentially insensitive to the ortho-para ratio, but rather is sensitive only to the thermal profile in the atmosphere, specifically the temperature in a layer centered near 250 mb. The temperature can be gotten for that region from this point and then by choosing another point on the spectrum, such as that near 320 cm^{-1}, which has a similar nominal optical depth and which is sensitive to the para hydrogen fraction, one can then make a quantitative estimate of the para hydrogen fraction.

We essentially did this with a large volume of Voyager data, and Fig. 4 illustrates the basic result. This set of data was taken from a mapping sequence covering the entire planet from about ± 60 deg latitude. Figure 4 shows the retrieved values of f_p from 536 individual spectra subjected to a running mean with latitude bins five degrees wide and indicates the systematic variation of the para hydrogen fraction as a function of latitude. The normal case would be down at the bottom of the graph corresponding to a para hydrogen fraction of 0.25. If in fact, the atmosphere had been in local thermal equilibrium at the local temperature, we would have anticipated retrieving values corresponding to the solid curve labeled "equilibrium." The reason that this is a function of latitude is that you are looking at different emission angles at different latitudes, so therefore we sample slightly different levels in the atmosphere, and the equilibrium para hydrogen fraction being a function of temperature, will be different for the different levels.

The principal feature of the para hydrogen fraction is its large scale latitudinal variation. Although there are hints of other structure, there does not seem to be any distinct correlation with any other planetary-scale parameters. For example, it does not seem to correlate in any consistent way with the jet structure on the planet. It does not correlate with any of the indicators of the presence of clouds such as temperature in the 5 μm region or measurements of brightness temperature for the continuum between the ammonia lines in the 50 μm region. There are of course always concerns with this type of inference. Are there other opacity effects which are affecting it? If there are cloud opacity effects acting, it must be in a very complicated way because we see no direct correlation for clouds. While the result is sensitive to differential errors in the absorption coefficients, which could in fact lead to systematic errors, it seems doubtful that they would produce a latitudinal-type gradient such as we see here. We seem to be stuck with this large-scale gradient requiring some explanation.

If we attempt the same thing for Saturn, we find that it is more difficult to do the analysis because of lower signal-to-noise at colder temperatures. Also, the upper tropospheric lapse rate on Saturn is lower, so there is less contrast in the lines. Still, to the extent that we've been able to analyze Saturn data, we find, unlike the case for Jupiter, something that appears to be close to equilibrium.
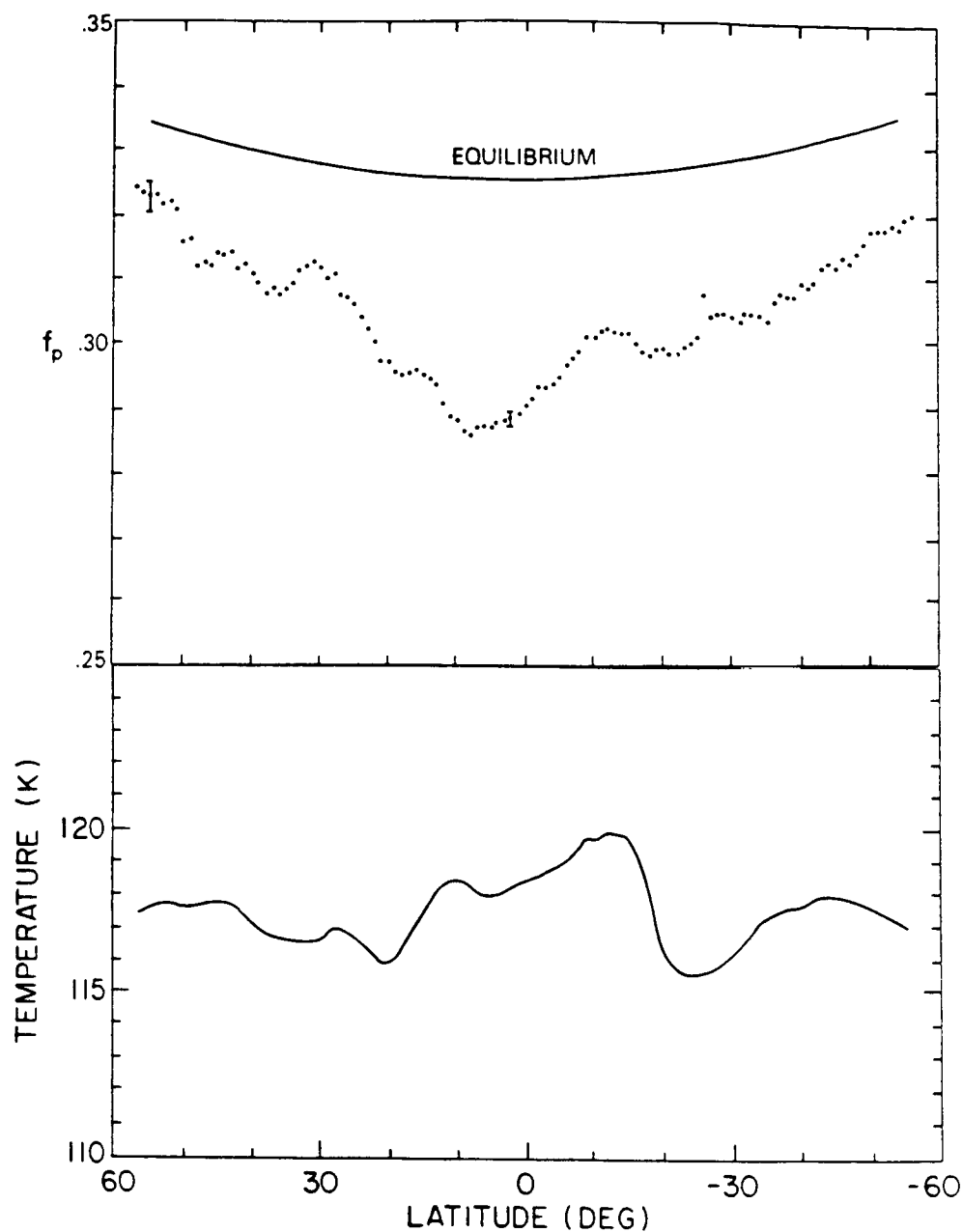
Figure 4. Comparison of inferred para hydrogen fraction and temperature as a function of latitude. The upper panel displays points which correspond to zonal averages of individual f_p determinations over latitude intervals of five degrees calculated at increments of one degree. If the equilibrium value of f_p prevailed at each atmospheric level, the results would lie along the indicated solid line curve. The lower panel shows the meridional temperature profile corresponding to the 270 mb level in the atmosphere.

12

What can we say about the nature of this sort of distribution for the ortho-para ratio? Basically, one looks for a dynamical explanation. We have to explain how the dynamics can have a profound effect on the para hydrogen fraction. At the same time those dynamic processes do not significantly affect the temperature field at this same level. Figure 4 also shows the mean zonal temperatures derived from Voyager data for the same global mapping sequence. Temperature for a layer at 270 mb is displayed as a function of latitude. Here of course, temperature variations are relatively modest, in the vicinity of 3 to 4 degrees at most. How do we perturb the para hydrogen fraction but leave the temperature field relatively unperturbed? One possibility is the following: suppose we have a large-scale meridional circulation with up-welling at the equator and downwelling at the higher latitudes. The rapidly upwelling gas would bring hydrogen up with a lower para hydrogen fraction associated with the warmer temperatures at depth. If the dynamic time scale corresponding to the upwelling is comparable to or less than the para hydrogen relaxation time scale, then the observed perturbation from the local equilibrium value could be produced for the equatorial region. Subsequent transport towards the polar regions with continuing equilibration of the para hydrogen fraction would then be consistent with the f_p values closer to local equilibrium at high latitudes.

Such a scenario would work qualitatively for the para hydrogen fraction, but in order for such a circulation system to leave the temperature field relatively unperturbed, the dynamic time scale would have to be longer than the radiative relaxation time. So this puts constraints on the ratio of the equilibration time of para hydrogen to the radiative relaxation time. Specifically, the para hydrogen relaxation time would have to be longer than the radiative relaxation time. If we take as an upper limit on the hydrogen relaxation time, that for pure hydrogen, an appropriate estimate for the 500 mb level on Jupiter is about 10^9 seconds. The radiative time constant there is about 10^8 seconds, so in that case the para hydrogen relaxation time would exceed the radiative relaxation time. On Saturn, however, they would be about the same order, so we would expect much less perturbation from equilibrium in the para hydrogen fraction on Saturn. As we go out to Uranus and Neptune, it should be even closer to equilibrium because of the relation of the two time scales.

Obviously, we don't know with certainty what the hydrogen relaxation time is. It's not well-constrained; this is one of the big unknowns of the problem. We don't know what the relaxation time of molecular hydrogen is in the presence of ammonia ice crystals, for example (which is something I hope someone will eventually estimate). The other feature of this type of model is the embarrassing fact that the jet scale does not seem to enter into it, and it is hard to conceive of a jet system as not having some meridional circulation associated with it. So why do we not see the influence of the jets in the para hydrogen fraction? An interesting question is whether the para hydrogen fraction is really acting as a quasi-conserved Lagrangian mean tracer for the motion or not.

That is the situation for the observable part of the atmosphere. We can also make some speculative comments on the deeper layers, the convective part of the atmosphere. The ortho-para observations pertain to the upper, stably

stratified portion of the atmosphere. In the deeper levels, we presumably have buoyancy-driven convection. What is the effect of the para hydrogen equilibration in this region? We have attempted to look at that question within the framework of fairly simple mixing length theory. Basically, what one has to do is devise a mixing length theory in which one treats the coupled problem of the transport of the para hydrogen fraction and the heat transport with the constraint being that the heat flux should agree with what is observed. If you do this sort of thing, and assume that the para hydrogen relaxation time is long in the sense that it is close to that of pure hydrogen (which in the deeper layers would probably be 10^7 to 10^8 seconds) then one finds that the efficiency of the convection is enhanced considerably due to the lag in the conversion that occurs in the process. If you do just a standard mixing length calculation, then you come out with an overturning time on the order of 10^4 seconds, while if you include a lag in the para hydrogen conversion, the overturning time lengthens by three orders of magnitude, with a substantial increase in the efficiency of the convection. The para hydrogen conversion acts in an analogous way to latent heat release by water in the Earth's atmosphere. In this case, a substantial fraction of the heat flux would be carried in the form of this latent heat, the energy difference between the ortho and para states. Due to the slowness of the convection, one would come out with a para hydrogen fraction very close to the local thermal equilibrium value and with a lapse rate close to an equilibrium lapse rate. If we consider high-frequency perturbations on such a state, that is displacements of fluid parcels on a time scale short compared to the basic convective scale, the atmosphere would be statically stable to such perturbations because the parcels would essentially follow adiabats which correspond to the frozen equilibrium specific heat, which is a steeper temperature gradient than the equilibrium adiabat. Therefore, such perturbations would in fact be stable in the sense of having a positive value for the square of the Brunt frequency.

This again is mostly speculation, because we don't know what the equilibration times are at these levels. It is based on the assumption of a relatively slow equilibration time, something like that approached by pure hydrogen. This kind of prediction would be made not only for Jupiter but for all of the outer planets including Uranus and Neptune. The lapse rate can't really be checked on Jupiter and Saturn because at those temperatures the equilibrium adiabat, the frozen equilibrium adiabat, and the normal adiabat all lie rather close together. So it is not possible to distinguish these gradients from the available data. As you go to the outer planets, this is no longer the case.

What do we know about Uranus and Neptune? There are several pieces of information available. There have been analyses on, for example, the 4-0 S(0) and S(1) quadrupole lines of hydrogen for these planets. In fact, there is a paper later in the meeting by Baines and Bergstralh on this problem. It will be interesting to hear their latest results. If I understand it correctly, they conclude that the data are generally consistent with an ortho-para ratio closer to the equilibrium than normal. This appears also to be true for a longer wavelength measurement by Orton, Tokunaga, Moseley and others with a spectrum that is at least inconsistent with normal para hydrogen fraction, and probably more nearly consistent with something closer to equilibrium. On the other hand, measurements in the sub-millimeter and millimeter part of the

14

spectrum, which on Uranus and Neptune penetrate down into the convective regions of the planet, seem to be consistent with a temperature lapse rate which corresponds not to the equilibrium, but to the frozen adiabatic lapse rate. This, at least in my opinion, is hard to understand. It is hard to understand how you would have processes which would be establishing a frozen equilibrium lapse rate, which would require motions which are rapid compared to the hydrogen equilibration time, but at the same time able to maintain an equilibrium para hydrogen fraction at that level. It would seem to me that the processes of establishing both a para hydrogen fraction and a temperature lapse rate are most likely one and the same. It is hard to understand how the two different time scales could be operative here. There may be situations in which one could have equilibration occurring in multiple cloud layers (Massie and Hunten alluded to this sort of thing in their paper) where in between one might have a para hydrogen fraction which closely resembles an equilibrium fraction, but nevertheless equilibration would not be occurring on the time scale of the mixing.

In any case, this at least is an open question and one of the big unanswered questions in this area. These observations have all been full disk observations. It will be interesting to try to get spatially resolved observations and Voyager will hopefully do this in January 1986. The Voyager infrared spectrometer should be able to obtain spectra in the region from 200 to 400 cm^{-1} with sufficient signal-to-noise to permit quantitative work. Theoretically calculated spectra indicate that the difference in the shape of the spectrum in this region between the two extremes, normal and equilibrium, is large enough so that it should be possible to make statements at least on the gross para hydrogen fraction, hopefully, as a function if not of detailed spatial resolution on the planet, at least on a regional basis.

Let me then just summarize with a list of what I regard as the current questions in the area. I am sure there are other things to be added to this list. One of the big questions is what really is the para hydrogen equilibration time in the presence of ammonia and methane ice clouds? Until one gets a better answer to this question, it is hard to do much more than speculate on this problem at least in terms of models. What is the mechanism for producing large-scale variation in f_p on Jupiter, and is it really a variation in f_p that we are seeing? I think it's important to get a determination of para hydrogen fraction by other techniques such as ground based measurements in the near infrared hydrogen lines. Work is being done by one or more groups on this area. How important is the latent heat flux in the convective region? We are talking about the region essentially above the 250 K level; this is the only part of the convective region where the para hydrogen fraction is really important. One gets a significant latent heat effect between that level and the top of the convective region. What is the mechanism producing the apparent equilibrium para hydrogen fraction on Uranus and Neptune but a frozen equilibrium lapse rate? That seems to be in conflict with the time scales which one would need. Are there other dynamical processes for which the para hydrogen equilibration is important? This, after all, is perhaps the Jupiter equivalent to moist latent heat processes in the Earth's atmosphere. There has been very little thought given as to exactly how this para hydrogen latent heat process can enter into other dynamical processes on the planet.

REFERENCES

Gierasch, P. J. (1983). Dynamical consequences of orthohydrogen-parahydrogen disequilibrium on Jupiter and Saturn. *Science* 219, 847-849.

Massie, S. T., and D. M. Hunten (1982). Conversion of para and ortho hydrogen in the Jovian planets. *Icarus* 49, 213-226.

Smith, W. H. (1978). On the ortho-para equilibrium of H_2 in the atmospheres of the Jovian planets. *Icarus* 33, 210-216.

Trafton, L. M. (1967). Model atmospheres of the major planets. *Astrophys. J.* 147, 765-781.

DR. POLLACK: If I understand correctly, Peter's original motivation here was to reproduce the pattern of zonal bands. He used the observed variation in the ortho-para ratio to infer temperature variations ΔT, which in turn produced strong thermal winds comparable to observed values. So, if you, in your observations, don't see a significant ΔT, there is a kind of breakdown in the logic for the whole picture.

DR. CONRATH: That theory, I think, is of historical interest at this point. I used it mainly to illustrate the potential. The observations are not consistent with that picture.

DR. HUNTEN: Well, I'd say we've got to be a little wary of believing all the observations in this area because it is very, very difficult. The observations are fine, but the interpretations may be questionable.

DR. INGERSOLL: Do you believe the observations and implications about this large-scale meridional structure? Couldn't you have enhanced vertical mixing at the equator on a smaller scale without the large-scale meridional structure?

DR. CONRATH: This is one of the things we looked at. You also have to keep the heat flux as a function of latitude correct. It seemed to us that since you have a maximum solar heating at low latitudes and less solar heating at high latitudes, that you would get in trouble with heat flux with this type of picture.

DR. HUNTEN: When you say heat flux, you mean thermal IR radiation flux.

DR. CONRATH: Yes, the heat flux, the radiation to space.

DR. W. H. SMITH: First, as far as ortho-para conversions are concerned, it is well understood that ammonia and methane crystals in an undamaged state do not catalyze the relaxation of the hydrogen into an ortho-para equilibrium. Radiation damaged crystals or crystals with paramagnetic impurities may act as a catalyst to induce the equilibrium. As observations have progressed, since 1978 when I wrote my paper on this subject, we have been convinced that some disequilibrium may in fact be present, but primarily in the regions above, say

100 mb. This disequilibration may be photochemically induced, and I wonder why that has not been discussed, particularly with regard to the high regions. It would seem to me that the vertical convection processes will control the equilibration process in the bulk of the atmosphere. Vertical transport of H_2 does not seem to be fast enough to displace the equilibrium very far over most of the observed pressure range.

DR. CONRATH: We were thinking of the dynamic effects from the point of view that perhaps you do have equilibrations occurring efficiently up to some point, perhaps to the top of the main ammonia cloud deck. But the region we're seeing is actually somewhat above this, just below the tropopause, where if you have sufficiently rapid upwelling, you will see the para hydrogen fraction associated with that region where it was last well equilibrated. This was the reason for looking at this type of model.

DR. ATREYA: Barney, if I remember correctly the ΔT is equal for both Uranus and Neptune, around 9 K. Would the absence of an internal heat source on Uranus make any difference?

DR. CONRATH: Not in terms of that simple thermodynamic calculation, but it obviously will in terms of the dynamics if there is not a strong heat flux. Gierasch and I made predictions on Uranus which were an extrapolation from Jupiter and Saturn, and these are probably not relevant in retrospect. I think that all bets are off here because you have such a small internal heat source and such a large obliquity and strong seasonal driving.

DR. ORTON: I'd like to respond to that in part because we are seeing the same frozen equilibrium signature in the sub-millimeter region for both Uranus and Neptune. So this question seems to be rather divorced from the internal heat differences which are substantial between the two planets.

DR. ROSSOW: On your synthetic spectrum, would you comment on how well the synthetic spectrum actually fits your results?

DR. CONRATH: I do not have the figures showing the comparisons with synthetic spectra with me, though they are given in two different publications that describe this. Basically, you get a poor fit at low latitudes if you assume equilibrium and substantially better with a disequilibrium ortho-para ratio.

DR. ROSSOW: What do the remaining differences reflect?

DR. CONRATH: There are still differences in the spectra greater than the statistical noise, particularly in the center of the S(0) line.

DR. ALLEN: When you showed the IRIS results of latitudinal variation, you made the observation that it didn't seem to match the observed pattern of belts and zones. The one thing it does seem to match is the UV image of Jupiter at 2400 Å from Voyager, where there is this correlation between high haze and near equilibrium. I am wondering whether this says anything about the conversion mechanism. Instead of talking about the main ammonia cloud deck, maybe we should talk about the properties of equilibration in the haze layer. Something that produces UV absorption might have characteristics

appropriate for doing the equilibration. Then you see a very nice tie-in between a mechanism for equilibration and possibly something observed there.

DR. CONRATH: Yes, if you look at it from this point of view, this would require less equilibration at low latitudes and more at high latitudes.

DR. ALLEN: Which is what you see.

DR. CONRATH: Your haze levels are pretty high, are they not?

DR. ALLEN: Between 50 and 150 mb.

DR. WEST: I would like to elaborate on that comment just a little bit. One possible way of explaining the distribution of stratospheric aerosols is by looking at the dynamics and diffusion of those aerosols. It's really hard to differentiate anything.

DR. HUNTEN: Barney did comment that it would be nice to have lab measurements of the effects of UV irradiated aerosols, and I would certainly agree. It would cut down at least one degree of freedom in this problem.

SPATIAL AND TEMPORAL VARIABILITY OF INFRARED-OBSERVABLE
PROPERTIES OF THE JOVIAN ATMOSPHERE: A PARTIAL SURVEY

Glenn S. Orton
Jet Propulsion Laboratory, California Institute of Technology

Examination of infrared characteristics of the Jovian atmosphere are made using Voyager IRIS mapping from 1979, ground-based scanning from 1979-1983, and ground-based mapping from 1983 to the present. In general, there is a strong correlation between tropospheric thermal properties and the visual cloud albedo for all observations. The Voyager IRIS maps show no strong evidence for day/night differences. Temperature differences diminish with depth in the troposphere. Temporal changes over several weeks indicate a high correlation between thermal and visual properties, although no changes in the distribution of para H_2 and ortho H_2 are seen. Stratospheric banded organization is different from the troposphere, and there is a temperature enhancement near the north magnetic pole. The spatial distributions of ammonia gas and ammonia ice absorption are different. Stratospheric temperatures exhibit seasonal hemispheric asymmetry. Other temperature changes at and below the 150-mb level correlate with changes in the Jovian visual structure. The stratospheric temperature field is uncorrelated with visual features or temperatures below the 150-mb level. Elevated temperatures are observed near both north and south magnetic pole positions. Both the meridional positions and the relative intensities of stratospheric banded organization change significantly, especially after 1982. Ground-based mapping confirms a correlation between temperatures and various measures of cloud distribution. Complex and unexpected characteristics are observed in the stratospheric temperature field; these include dramatic temporal changes on short time scales.

I want to make a quick survey of thermal infrared features and their variability over the disk and evolution in time. I'll focus on recent work John Martonchik and I have been doing on the Voyager IRIS north/south maps. Also I'll take a quick look at results of scanning of the Jovian central meridian between 1979 and 1984 and mapping of the whole disk which began in a crude form in 1983 and continues through the present. Contributing to the mapping effort are Kevin Baines, Jay Bergstralh, John Caldwell, Terry Martin, Rich Terrile, Alan Tokunaga, and Robert West.

While John and I are also looking at IRIS data for Jupiter with higher spatial resolution, I want to concentrate on the global maps whose characteristic resolution is around 14000 km. These provide a good starting point for a picture of global variations of atmospheric properties. We concentrate on maps combining data from sequences both before and after closest approach. Differences between these inbound and outbound maps appear to be below the noise of the observations. Over the longer several-week period between Voyager 1 and 2

encounters, however, recognizable changes take place. These are clearly evident in meridional maps of zonally-averaged temperatures (Fig. 1). Going deeper in the troposphere, from the 602-cm^{-1} radiances to those at shorter frequencies, strong limb darkening takes place, which also tends to supress the appearance of detailed spatial structure. Without going into the analysis that Conrath and Gierasch (1984) presented in deriving the global variations of the ortho-H_2 and para-H_2 ratios, we can see similar morphological variations by examining the brightness temperature differences between 520 cm^{-1} and 310 cm^{-1}, similar to their primary data base. All longitudinal structure vanishes in such a map, as they described; furthermore, nearly the same distribution is revealed by Voyager 2 maps.
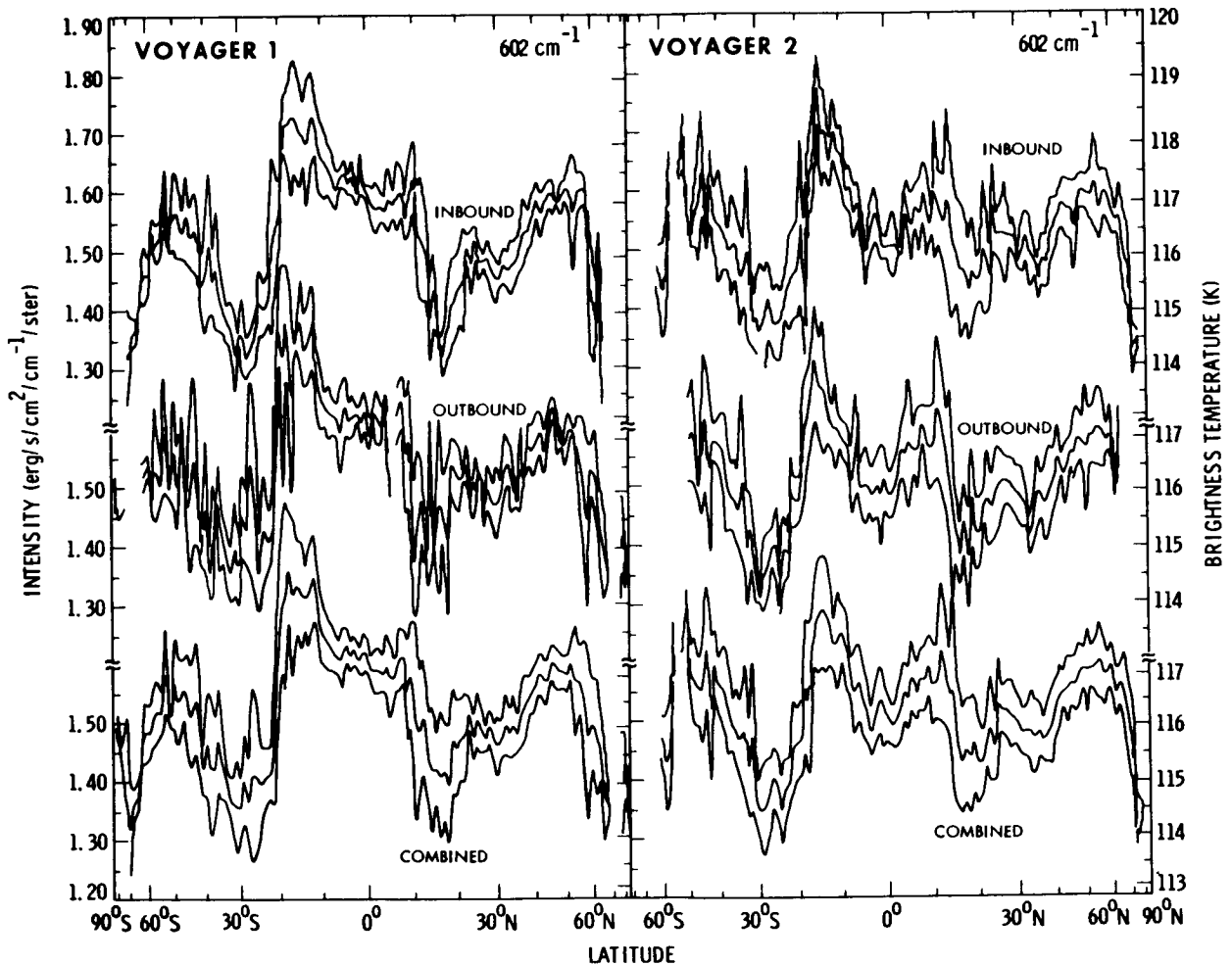
Figure 1. Plot of zonally-averaged radiances observed by Voyagers 1 and 2 at 602 cm^{-1} taken from the IRIS north/south map data. The curves plotted above and below the mean represent the excursions of one standard deviation. Breaks in the curve result from the absence of data in some of the 128 bins corresponding to cosine of latitude.

20

Longitudinal features also tend to disappear for maps of stratospheric thermal radiance. The meridional organization also looks different from that given by the shorter frequencies sensitive to tropospheric temperatures: three bands appear, one near the equator and two at mid-latitudes. One major longitudinal feature is the hot spot which is correlated with the general position of the north magnetic pole. Nothing is seen at the south, either because the south polar feature was not present at the time of each encounter or because it was over the horizon (all Voyager 1 and 2 maps were taken when the spacecraft position was north of the equator). This warm feature is also seen in acetylene (C_2H_2) and ethane (C_2H_6) emission, demonstrating that at 1300 cm^{-1} we are witnessing anomalously warm temperatures rather than nonthermal emission from stimulated methane lines.

Coming back to the troposphere, we can produce a rough measure of the ammonia gas distribution by mapping the difference between the brightness temperatures characteristic of (a) a region strongly influenced by ammonia rotational lines and (b) a nearby continuum. The result is a map which is reminiscent of the deeper tropospheric temperatures shown in Fig. 1, except inverted. The strongest absorption is near the equator with a slow decrease toward higher latitudes. On the other hand, taking the difference between this continuum, which is also sensitive to the presence of ammonia ice, and a spectral radiance nearby which is not so influenced by ammonia ice reveals a very different structure--one that is more reminiscent of the 5-μm structure. This would imply that the horizontal distribution of ammonia ice particles is strongly correlated with the spatial structure of clouds deeper in the atmosphere, to which the 5-μm radiance is sensitive.

Between 1979 and 1984, observations were made from Kitt Peak National Observatory and the NASA Infrared Telescope Facility with angular resolution which corresponded to spatial scales of 7000-14000 km at Jupiter (e.g., Caldwell et al., 1979; Caldwell et al., 1980; Caldwell et al., 1983). Figure 2 shows a summary of some of these scans of the central meridian across the disk. For the filtered radiometry at 17.8 μm, we are sensitive to temperatures near the 200-mb level, and at 7.8 μm to stratospheric temperatures near 10-50 mb. In 1979, the 200-mb temperatures in the northern hemisphere were noticeably warmer than the south, but by 1983-1984 the south was just a little bit warmer than the north. Keeping in mind that Jovian autumnal equinox (for the northern hemisphere) was in late 1979, it appears that seasonal temperature changes lag the insolation cycle by about three years, consistent with radiative equilibration. Note that the cold region appearing at the equator in 1980 is consistent with the broadening of the visually bright region around the equator. At 7.8 μm, the three-banded structure observed by Voyager persists through 1981, but in 1982 things really start to break up. Bands disappear or change latitude position. Also note that seasonal temperature adjustments are quite clear, with the north warmer than the south in 1979 and the opposite in 1984.

Maps of the planet began crudely in 1983 using facilities at the NASA Infrared Telescope Facility, and we are fortunate that the telescope operation was improved by the creation of more efficient mapping software. Banded structure is observable at 17.8 μm (Fig. 3A). At longer wavelengths, consistent with the Voyager IRIS results, the contrast between regions tends to disappear.

17.8 μm

7.8 μm

MARCH 1979
(KPNO)

(VOYAGER 1 IRIS)

(VOYAGER 1 IRIS)

FEB 1980
(KPNO)

MARCH 1981
(IRTF)

FEB 1982
(IRTF)

APRIL 1983
(IRTF)

AUGUST 1984
(IRTF MAP)

JULY 1984
(IRTF MAP)
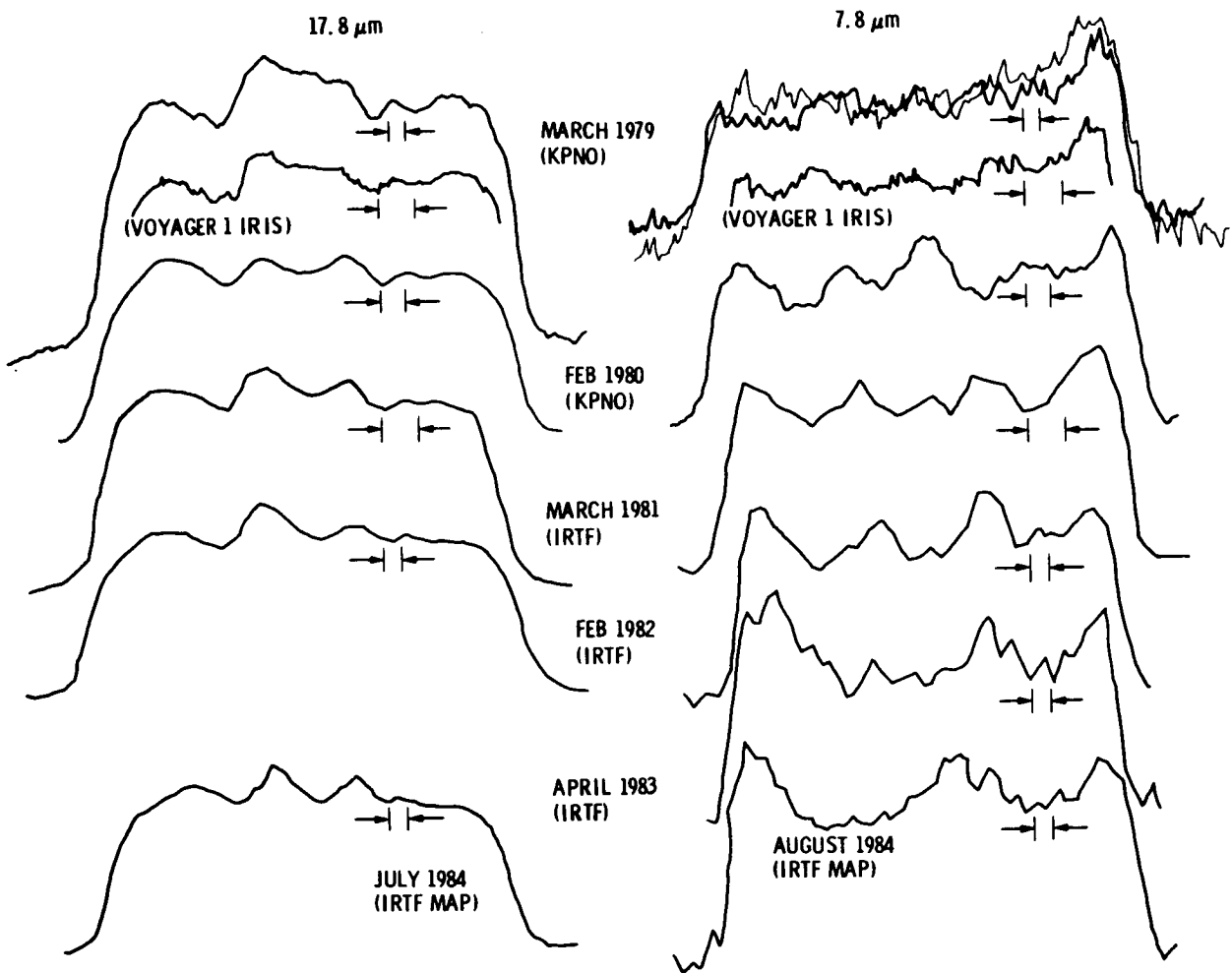
Figure 2. Earth-based scans of the Jovian central meridian near 17.8 μm and 7.8 μm between 1979 and 1984. South is to the left and north to the right. An element of spatial resolution is indicated schematically for each plot. No scan for 17.8 μm was available for 1983. Radiation at 17.8 μm and 7.8 μm are sensitive to temperatures near 200 mb and 10 mb, respectively.

22
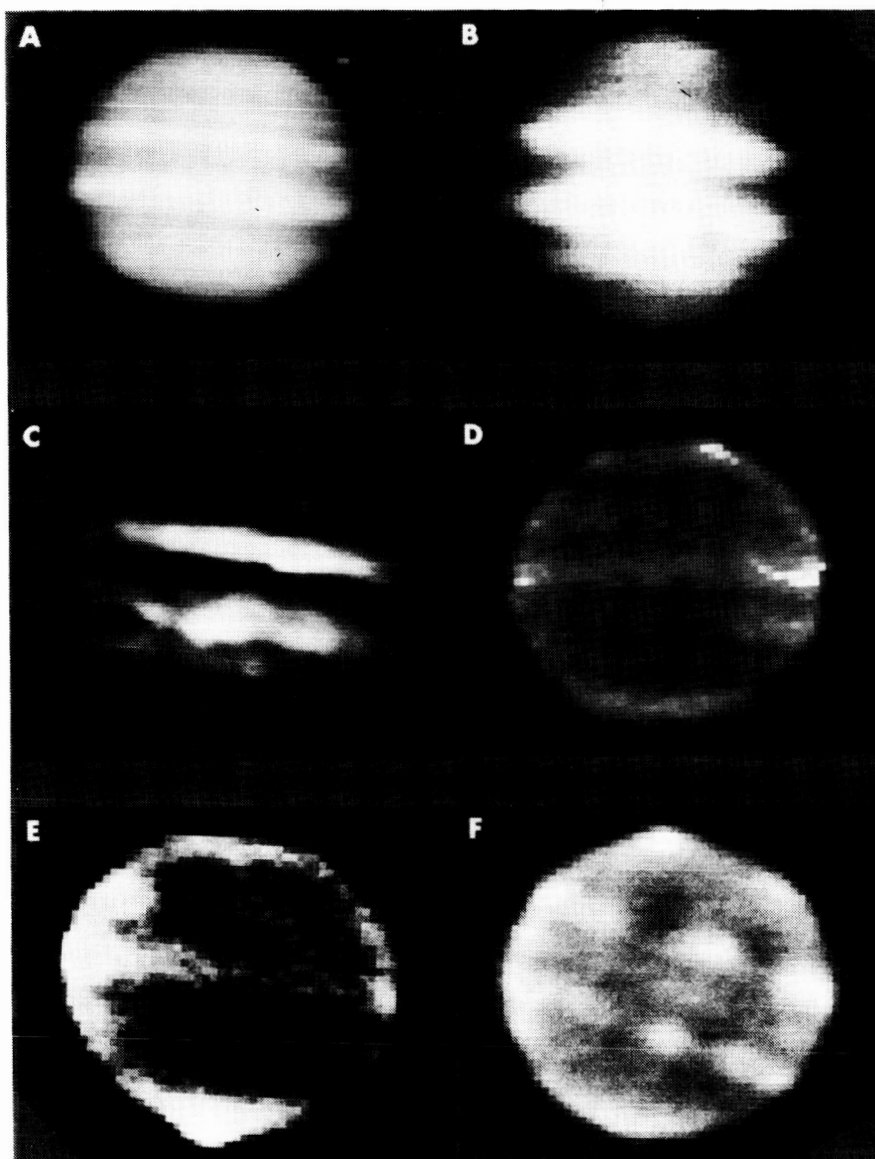
Figure 3. Thermal maps of Jupiter in 1984 and 1985. (A) 17.8-μm
map made on 1984 July 23 with System III longitude of the central
meridian (LCM) = 344 deg at the mid-point of the map observation.
Callisto appears at the upper right. (B) 8.9-μm map of 1984 June 4,
LCM = 210 deg, sensitive to the distribution of NH$_3$ ice clouds. (C)
5-μm map of 1984 April 26, LCM = 148 deg, sensitive to the dis-
tribution of NH$_3$ ice and deeper clouds. (D) 7.8-μm map of 1984
June 7, LCM = 322 deg, showing prominent south polar emission
feature and bright area on rising (left) limb. (E) 7.8-μm map of
1984 August 6, LCM = 222 deg, showing linear feature (distorted by
planetary rotation) north of equator toward setting limb. (F)
7.8-μm map of 1984 June 21, LCM = 98 deg, showing mid-latitude
bright regions of regular spacings and narrow "filamentary" feature
on rising limb. Spatial resolution corresponds to about 5% of the
disk in each image, except for 5-μm which is about 3%.

23

Belt and zone structure, as well as regions such as the Great Red Spot, show up even more clearly in maps of ammonia ice cloud distribution at 8.5 μm (Fig. 3B) or for deeper clouds sensed at 5 μm (Fig. 3C).

One of the most interesting and unexpected results of this mapping work is the appearance of the stratosphere as sensed by 7.8-μm maps (Fig. 3D-3F). In these maps, the limb is brightened as expected, and the familiar three-banded appearance is usually observable. But many changes take place across the disk and in time. Brightenings are associated with both north and south magnetic poles (Fig. 3D), and the bright regions have been tracked while rotating. In the crude partial map in 1983, the equatorial band appeared to be missing, but it had returned by 1984. However, the mid-latitude bands appeared to be missing or extremely faint in 1984 at certain longitudes. Faint features, covering many tens of degrees in latitude and longitude appear occasionally; from time to time they make one limb appear brighter than the other. Usually, however, the limb corresponding to Jovian dawn appears brighter than the sunset limb, for reasons which I don't understand at all. In one map in 1984, a strong linear feature (distorted by the rotation of the planet which takes place during the 40 minutes required to complete a 7.8-μm map) was observed crossing from the equator to about 15-20 deg N (Fig. 3E); the feature was not reobserved a month later. (Subsequent to the conference presentation of this paper, the 1985 appearance showed more of these occasional linear-like features, unlike anything else on the planet.) Furthermore, at certain longitudes, bright areas appeared in the mid-latitude bands with longitudinal separations of some 15-20 degrees (Fig. 3F). These persisted for time scales on the order of months, although rotated with respect to System III.

Only a few types of variable phenomena will be observable by Galileo, and a strong program of regular Earth-based monitoring in certain spectral regions is recommended for the time frame of the mission to supplement the spectral and global coverage available to Galileo remote sensing instruments. For several years preceding and following the nominal mission, such a program will provide an extended baseline to characterize longer-term variability of observable properties at infrared wavelengths. These properties include temperature, gas composition and cloud structure.

ACKNOWLEDGEMENTS

REFERENCES

Caldwell, J., R. D. Cess, B. E. Carlson, A. T. Tokunaga, and F.C. Gillett (1979). Temporal characteristics of the Jovian atmosphere. *Astrophys. J.* 234, L155-L158.

Caldwell, J., A. T. Tokunaga, and F. C. Gillett (1980). Possible infrared aurorae on Jupiter. *Icarus* 41, 667-675.

Caldwell, J., A. T. Tokunaga, and G. S. Orton (1983). Further observations of 8-μm polar brightenings of Jupiter. *Icarus* 53, 133-140.

Conrath, B. J., and P. J. Gierasch (1984). Global variation of the para hydrogen fraction in Jupiter's atmosphere and implications for dynamics on the outer planets. *Icarus* 57, 184-204.

DR. FLASAR: During the Voyager flybys the temperatures of the North Temperate Belt between 24 and 30 deg N latitude were warmer and clouded over. I got the impression that it wasn't clouding over anymore or the cloud cover was breaking up, but what were the temperatures doing? Are they still warm in that region relative to cold temperatures just south of 24 deg S?

DR. ORTON: They seem to be: from 19-24 deg, cold, and from 24-30 deg, warm from the influence of the North Temperate Belt.

DR. FLASAR: Did that temperature structure stay the same?

DR. ORTON: Yes, in spite of the albedo difference. But the albedo in the northern part is actually getting darker now? Is that correct?

DR. FLASAR: Yes, it got darker around 1981. Is that right Reta?

DR. BEEBE: Yes.

DR. ORTON: Although it is hard to see with the resolution we have which is just 10% of the disk.

MS. CUNNINGHAM: You say that the absorptions occur at different levels in the atmosphere. What levels are you actually probing? Is it mostly stratosphere or is it the troposphere?

DR. ORTON: In the far-infrared, we are probing clouds in a spectral region near 245 cm^{-1}. In the absence of a cloud this would be sounding a level near 800-900 millibars.

MODELING THE TEMPORAL AND SPATIAL VARIATIONS OF THE VERTICAL STRUCTURE OF JUPITER'S ATMOSPHERE USING OBSERVATIONS OF THE 3-0 HYDROGEN QUADRUPOLE LINES

C. C. Cunningham, D. M. Hunten, and M. G. Tomasko
University of Arizona

The presentation by Cunningham *et al.* is largely contained in a paper which has been submitted to *Icarus*. The abstract of that paper is reproduced here:

An observational program was established in 1983 to monitor the spatial and temporal variations in the Jovian atmosphere over short and long time scales. The program involves tracking several different longitudes as they rotate around the planet from one limb to another. This tracking experiment was done at many different wavelengths including the 3-0 S(1) and S(0) hydrogen quadrupole lines as well as several broad band methane absorptions. The June 1983 hydrogen quadrupole data has been reduced and equivalent widths have been measured for approximately 25 east-west positions across the planet at 7 different latitudes for both wavelengths. The data for the South Tropical Zone (20 deg S) has been modeled extensively and the effects of the various model parameters on the value of the calculated equivalent widths of both lines was measured as a longitude rotated from the east (or morning) limb to the west (or evening) limb. This increase may be indicative of a diurnal variation in the vertical cloud structure. One plausible explanation appears to be a gradual thinning of the upper NH_3 cloud during the day with the cloud rebuilding during the Jovian night. The value of the equivalent width is also quite sensitive to the height of the NH_3 cloud top and to the value used for the single scattering albedo. A combination of these parameters changing on a diurnal time scale could also explain these observations. This gradual increase from one limb to the other appears in the data for both the North and South Equatorial Belts as well as the equatorial region and the North Tropical Zone. Finally, models that used only normal hydrogen and models that used only equilibrium hydrogen were studied. For all regions the models that used equilibrium hydrogen throughout the vertical structure (between 0 and 2000 mb) fit both quadrupole lines better than the models that used normal hydrogen throughout.

DR. POLLACK: Let me make a mostly philosophical comment on techniques of computing cloud structure based upon work that you'll hear on Wednesday for Uranus. We are working with many free parameters when we try to infer cloud structure in a realistic outer planet. So you need to have as many different types of observational constraints as possible if you are to obtain unambiguous results. For review purposes, it might be nice for you in future work to get data also in methane absorption bands so you can really have enough constraints to pull out what you want.

MS. CUNNINGHAM: We got methane data at the same time as our quadrupole data. It just hasn't been reduced yet.

DR. W. H. SMITH: Bill Cochran and I have a very similar set of data showing the center-to-limb variation of the $S_3(1)$ feature. Recently, I and my co-workers at Washington University have obtained the required laboratory data for interpreting the spectra quantitatively. This includes low temperature measurements of the pressure broadening and shift coefficients for ammonia, methane, and hydrogen at 80 K. Also, the line assignments for the 6450 Å ammonia band are now known. So, with the laboratory data requirements being largely met, we can restrict the number of free parameters much further and can specify the ambient conditions for the lower cloud in terms of pressure, temperature and approach to thermodynamic equilibrium. The only free parameters left are those related to the scattering characteristics of the clouds, their placement, the effective transport processes of the atmospheric gases and cloud particles.

MS. CUNNINGHAM: Are you adding diurnal effects as well?

DR. SMITH: Our original data set was obtained several years ago before CCD's were available, so we have a less extensive data set than you. We also averaged over a range of longitude as well. However, the general shape of the center-to-limb variation is the same, except for the tilt from center to limb which you are tentatively ascribing to a diurnal effect. We do not see any evidence for that effect at the time of our observation. Our analysis has included NH_3 and CH_4 profiles as well. The added constraints on the models has been useful to reduce the range of models which plausibly fit the observations.

DR. LUNINE: You say that your results are not sensitive to the base of the water cloud when you varied the base from something like 1600 to 2400 millibars. Can you rule out a cloud that goes much deeper?

MS. CUNNINGHAM: Our data cannot rule that out, but Gordon Bjoraker has done a very thorough analysis of the deeper regions in the Jovian atmosphere using Voyager data. Our placement of the lower cloud at about 2 bars is based, at least in part, on his work.

DR. LUNINE: Well, I was asking because I was wondering if you have any sensitivity to the cloud level at all and could provide an independent assessment of Gordon's H_2O abundance determinations.

MS. CUNNINGHAM: We can change the pressure at which the lower cloud forms if we also modify the thickness or height of the upper ammonia cloud. There are several families of workable models that will fit the data. At the present time we have constrained the position of the bottom cloud using observations that are more sensitive to that particular region in the atmosphere. It may be possible to make additional constraints on the position of this lower cloud using our broad-band methane data.

DR. INGERSOLL: I hate to use theoretical arguments to shoot down good observations, but diurnal variation at these tropospheric levels are quite hard to

understand. I'm wondering if there is any possible systematic effect between east limb and west limb.

MS. CUNNINGHAM: I've looked pretty carefully because I read about that a lot, too. These bands form a part of the spectrum that is fairly clear of water lines. I obtained some very high air mass solar spectra to look for very small features that might be interfering and affecting the equivalent width of the lines. The region is very clear. This (June) 1983 data is some of our best with respect to the consideration of which part of the spectrum shows a Doppler shift of the quadrupole lines.

DR. BAINES: I discussed similar data, as Bill has mentioned, two years ago. We found then that the observations were very symmetrical from one limb to another. The difference I'm saying here is that we have an equatorial region, but looking at your equatorial region data, you get about 20% greater equivalent width than what we saw. That corresponds to a decrease, as you model it there, to the optical depth of the cloud; I had more like nine, and you are talking about six. I think there is probably a one-to-one correspondence between points. So maybe there is something going on in time there, and maybe that agrees with Reta Beebe and what Glenn Orton showed; that the equatorial region is sort of clearing over a span of three or four years. This data set was taken in 1978, so maybe there is some sort of temporal long-term thing there that we are really quantitatively modeling.

MS. CUNNINGHAM: The equatorial region appears to be a combination of both a belt and a zone. I picked out three particular longitudes to do my tracking experiment. Perhaps these particular longitudes just happened to be more zone-like than belt-like.

DR. WEST: I'd like to follow up Andy's question. It seems to me that one of the most controversial conclusions you come to is the diurnal variation. I'm not aware of any other observations that show that. Are you?

MS. CUNNINGHAM: No. That's why I plan to start looking into our other data in the next few months.

DR. LEOVY: I am concerned about the amplification of the sensitivity for overlying haze. Have you really ruled out the possibility that it is these overlying haze parameters that are causing the diurnal variation?

MS. CUNNINGHAM: I've tried models which distribute the haze over the region from the top of the atmosphere to the top of the ammonia cloud and the calculated equivalent widths were no different than those evaluated with models that had the haze in a concentrated layer. I have also tried models with haze thicknesses that were a factor of four higher than those used in our "best fit" models and the calculated equivalent widths also appear to be insensitive to any reasonable changes in haze thickness.

CHANGES IN SATURN'S SOUTH-TEMPERATE HAZE DISTRIBUTION DURING THE SUMMER OF 1973-1980

L. Trafton
University of Texas at Austin

The presentation by Trafton is largely contained in a paper appearing in *Icarus* (1985; <u>63</u>, 374-405). The abstract of that paper is reproduced here:

We report the results of monitoring Saturn's H_2 quadupole and CH_4 band absorptions outside of the equatorial zone over one-half of Saturn's year. This interval covers most of the perihelion half of Saturn's elliptical orbit, which happens to be approximately bounded by the equinoxes. Marked long-term changes occur in the CH_4 absorption accompanied by weakly opposite changes in the H_2 absorption. Around the 1980 equinox, the H_2 and CH_4 absorptions in the northern hemisphere appear to be discontinuous with those in the southern hemisphere. This discontinuity and the temporal variation of the absorptions are evidence for seasonal changes. The absorption variations can be attributed to a variable haze in Saturn's troposphere, responding to changes in temperature and insolation through the processes of sublimation and freezing. Condensed or frozen CH_4 is very unlikely to contribute any haze. The temporal variation of the absorption in the strong CH_4 bands at south temperate latitudes is consistent with a theoretically expected phase lag of 60° between the tropopause temperature and the seasonally variable insolation. We model the vertical haze distribution of Saturn's south temperate latitudes during 1971-1977 in terms of a distribution having a particle scale height equal to a fraction of the atmospheric scale height. The results are a CH_4/H_2 mixing ratio of $(4.2 \pm 0.4) \times 10^{-3}$, a haze particle albedo of $\omega = 0.995 \pm 0.003$, and a range of variation in the particle to gas scale-height ratio of 0.6 ± 0.2. The haze was lowest near the time of maximum temperature. We also report spatial measurements of the absorption in the 6450 Å NH_3 band made annually since the 1980 equinox. A $20 \pm 4\%$ increase in the NH_3 absorption at south temperate latitudes has occurred since 1973-1976 and the NH_3 absorption at high northern latitudes has increased during spring. Increasing insolation, and the resulting net sublimation of NH_3 crystals, is probably the cause. Significant long-term changes apparently extend to the deepest visible parts of Saturn's atmosphere. An apparently anomalous ortho-para H_2 ratio in 1978 suggests that the southern temperate latitudes experienced an unusual upwelling during that time. This may have signaled a rise in the radiative-convective boundary from deep levels following maximum tropospheric temperature and the associated maximum radiative stability. This would be further evidence that the deep, visible atmosphere is governed by processes such as dynamics and the thermodynamics of phase changes, which have response times much shorter than the radiative time constant.

DR. WEST: I had a lot of trouble understanding your ratios for the S(0) and S(1) lines because you used Bragg's line strengths which differed by a factor of more than four at room temperature and a factor of something like two at colder temperatures for both equilibrium and normal hydrogen. There is no way you can get a ratio anywhere close to one. The S(0) strength should always be weaker than the S(1) strength. What did you use for those...

DR. TRAFTON: I did not use Bragg's experimental line strengths; I used the theoretical ones instead. These imply a ratio which is close to that of hydrogen's at equilibrium for the Voyager temperature distribution (except for 1978). The difference between the laboratory and theoretical values presumably explains the different ratios.

DR. TOMASKO: I wasn't sure I understood how you went about reconciling the 6200 Å weak methane feature. It sounded like you extracted a single scattering albedo to make that data consistent. Is that right? If you used a lower single scattering albedo like 0.98, it wasn't so consistent, but if you used 1 then it was more nearly consistent.

DR. TRAFTON: Exactly. I did it for two extreme cases, and the higher albedo gave the better fit.

DR. TOMASKO: I think the independent absolute photometry of Saturn indicates that the albedo is somewhat closer to the lower value than the higher value. We've done some analysis of methane features on Saturn. When we used the published observed numbers for the single scattering albedo, we have again the same trouble of making the weak features fit when the strong ones do, but we don't see an easy way out of that.

DR. TRAFTON: The validity of what I've done is dependent upon the validity of the haze model. The model assumes a strict scale-height distribution in the scatterers. If that is not true, if there is a top to the haze, then I expect the results to be closer to those that you find for the equatorial region of Saturn and closer to those which you describe. The extent to which this model is valid is the degree to which you get the same derived methane to hydrogen ratio for each independent analysis of each methane band.

DR. BAINES: I hold the opinion that the 6190 Å band is not the band that we should be using to screen atmospheric properties. I think there are problems due to temperatures. I'm having a hard time making that band work for Uranus--I haven't got anywhere on that. There are definitely some weak links. I think Bill Smith will say something about recent measurements in the laboratory system. He definitely sees asymmetries between the shapes, and it's not a single band. That may be a problem in too many of our analyses, that we rely too much on that band, when we should put low weight on it.

DR. TRAFTON: Well, that is just one band out of five in this analysis. The 8600 Å angstrom band also supports this same conclusion.

DR. POLLACK: I wish to pursue the matter of temperature dependence. The absorption spectrum that everybody uses is measured at room temperature in the laboratory. Question: is that valid at the temperatures of the outer planets?

My answer to that is to compare that with absorption coefficients that you get from liquid methane, which gives you a first approximation to that answer. It turns out that at the center of many of the bands, the absorption coefficients are very similar. So that at the center of bands, I think this approximation is safe. On the other hand, as you get towards the wings, you definitely get different results between room temperature coefficients and those of liquid methane, so you are really on thin ice there. I think what that means is that equivalent widths put you on somewhat shaky ground, and if you use the full line shape you are on very shaky grounds. The best thing to do is to be in the center of the band.

DR. TRAFTON: Yes, I agree.

DR. LUNINE: I just want to reply to Jim Pollack: that is that there is a difference in line shapes between liquid methane and methane vapor. Admittedly, liquid methane gives you a first approximation, but it might be dangerous to try to use the liquid methane to specify the absorption coefficients for the vapor, particularly in the far wings of bands. There is a redistribution of line strengths in those bands, for liquid versus gaseous methane. There are some published studies that I can show you.

SEASONAL NORTH-SOUTH ASYMMETRY IN SOLAR RADIATION
AT THE TOP OF JUPITER'S ATMOSPHERE

R. Beebe and R. Suggs
New Mexico State University

The presentation by Beebe and Suggs is largely contained in a paper which has been submitted to *Icarus*. The abstract of that paper is reproduced here:

Although the orbital eccentricity and axial tilt are small, the near temporal coincidence of perihelion and the northernmost excursion of the subsolar point produce asymmetries in the solar radiation incident on Jupiter's atmosphere. Calculations of the incident radiation and the latitudinal gradient of the insolation are presented. North-south asymmetries in the zonal wind and morphology of the large scale cloud systems observed by Voyager 1 and 2 are cited. In the absence of an identified internal mechanism capable of generating the observed asymmetries, seasonal forcing of this magnitude should be considered.

DR. WEST: Well, I think the terminology, "clouds over" and "clears out," is incorrect. I think everywhere on Jupiter is clouded over and what you are seeing is not a difference in clouding over and clearing out, but a difference in the amount of chromophores that are visible at any given latitude at a particular time.

DR. ORTON: A brief comment on the obvious aspects of the particular coincidence of the two effects you've seen taken place. In fact, for the northern hemisphere, we do see large excursions in the rather brief monitoring we've done so far. The north is warmer and gets cooler than southern latitudes, at least in the stratosphere. There is a definite asymmetry in the deeper infrared characteristics as well.

DR. STONE: Just to repeat what is perhaps obvious, you are measuring a difference in the gradient on the seasonal timescale, and therefore a timescale of about ten years, which is also comparable to the radiative time constant.

DR. BEEBE: This is the timescale of the cloud morphology cycle time as well. The observational cycle time was about six years ± three years at latitudes where we have recurring types of phenomena.

DR. BELTON: For how many different epochs do we have the north/south zonal velocity information, and does the asymmetry between north and south stay the same in each one of those epochs?

DR. BEEBE: In the New Mexico State data set, we've got almost 1-1/2 Jovian years, and that is a self-consistent data set. Previous to that, we have to

go back to B. M. Peek's work, which is the most consistent. That takes us back to the turn of the century.

DR. BELTON: Does the asymmetry change, you know...?

DR. BEEBE: No. The jet at 23 deg N has always been recorded as one of the very fastest jets on the planet. In the old traditional nomenclature, the jet at 23 deg N was measured in System I, so it's been traditionally recognized that it is a very fast jet.

DR. ALLISON: Reta, last time I visited your observatory, you had on the wall about 20 photographs of Jupiter taken over the years, and you can see just by visual inspection of that sequence that Jupiter appears to change its overall aspect between what was observed during the Pioneer encounter (sort of a softly banded appearance) to something more resembling its appearance during the Voyager encounter (with more turbulent structure). Have you tried to correlate that kind of change with a seasonal cycle? Is there any straight-forward correlation?

DR. BEEBE: Your observation is influenced to a large extent by what the South Equatorial Belt (SEB) is doing, since it dominates such a large portion of the planet. The SEB activity has been very carefully studied and no correlation between albedo and seasonal change has been found. Recently, Hunt Guitar, a student of mine, determined the rate of zonal translation of the Red Spot at opposition over a 20 year period. Over that period it does appear that the translational speed correlates with the season. The maximum zonal velocity occurs about a quarter of a year before maximum insolation at that latitude.

THERMAL BALANCE OF THE ATMOSPHERES OF JUPITER AND URANUS

A. J. Friedson and A. P. Ingersoll
California Institute of Technology

Two-dimensional, radiative-convective-dynamical models of the visible atmospheres of Jupiter and Uranus are presented. Zonally-averaged temperatures and heat fluxes are calculated numerically as functions of pressure and latitude. In addition to radiative heat fluxes, the dynamical heat flux due to large-scale baroclinic eddies is included and is parametrized using a mixing length theory which gives heat fluxes similar to those of Stone (1972, J. Atmos. Sci., 29, 405-418). The results for Jupiter indicate that the internal heat flow is non-uniform in latitude and nearly balances the net radiative flux leaving the atmosphere. The thermal emission is found to be uniform in latitude in agreement with Pioneer and Voyager observations. Baroclinic eddies are calculated to transport only a small amount of the meridional heat flow necessary to account for the uniformity of thermal emission with latitude. Therefore, we find that the bulk of the meridional heat transfer occurs very deep in the unstable interior of Jupiter as originally proposed by Ingersoll and Porco (1978, Icarus 35, 27-43). The relative importance of baroclinic eddies vs. internal heat flow in the thermal balance of Uranus depends on the ratio of emitted thermal power to absorbed solar power. The thermal balance of Uranus is compared to that of Jupiter for different values of this ratio.

I'd like to tell you about a two-dimensional radiative-convective-dynamical model that calculates the thermal balance in the visible atmospheres of the Jovian planets. It does this by calculating the zonally averaged equilibrium temperatures and heat fluxes on a pressure/latitude grid. Also, it calculates the internal heat flux entering the bottom of the model as a function of latitude. The goal of these calculations is to determine the role of meridional heat transport by baroclinic eddies versus non-uniform internal heat flow in the thermal balance of the planet, and how their roles change when we vary various external parameters that characterize the planet such as the radiative time constant, internal heat source, planetary radius or whatever is an important parameter. First I'll describe the model and how the model calculations are done and then I'll tell you about some preliminary results for Jupiter and Uranus.

In applying the model we have to adopt certain simplifying assumptions. The most important of these is that we assume that the deep atmosphere is convective so that all fluid elements in the convective interior are on the same adiabat. This assumption is supported by the work of Ingersoll and Porco (1978) for Jupiter, and we assume it to work for Uranus as well. We also assume that the dynamical heat flow in stable areas is due to large-scale baroclinic eddies. Other assumptions that we make in the model are that the

opacity is due to H_2 alone, the specific heat is independent of temperature, the albedo is constant with latitude and we ignore seasonal variations and latent heat effects.

I'll show you a list of the heat fluxes that we include in the model. The infrared radiances are calculated using the two-stream approximation. Solar fluxes are fit to other people's work such as Hunten, Tomasko and Wallace (1980) for Jupiter, and Wallace (1980) for Uranus. The dyanamical heat fluxes are calculated wherever the stratification is stable. We used a mixing length formulation that was developed by Ingersoll and Porco (1978) in their *Icarus* paper. In the limit of strong stable stratification, their formulation gives the same expression for heat fluxes in terms of local potential temperature gradients as the work of Stone (1972) in his radiative-dynamic model.

We do a convective adjustment wherever the stratification is unstable. What we do is we adjust the temperature profile back to an adiabat while conserving the enthalpy of the layer. An exception occurs when the unstable layer is in contact with the deep convective interior. In that case, we assume that that layer can extract the heat necessary from the deep convective interior to maintain it on the deep adiabat.

Figure 1 is a plot of fluxes versus latitude for Jupiter, for a ratio of the power emitted from the planet to the absorbed solar power of E = 1.6. The fluxes are expressed in units of the effective temperature of the planet which we used as 125.4 K. You can see that the internal heat flux is non-uniform in latitude, which is an interesting feature that I will try to explain.
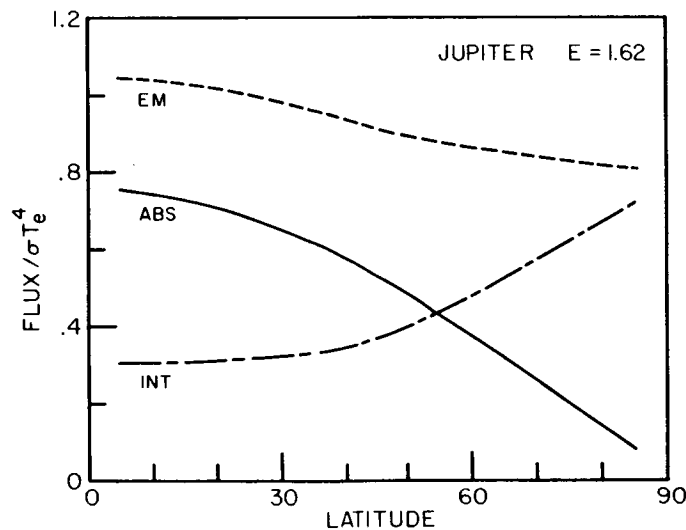
Figure 1. Flux vs. latitude for Jupiter. Ratio of total emitted power to absorbed sunlight is E=1.62. EM is emitted thermal flux, ABS is the absorbed solar flux, and INT is the internal flux. The fluxes are expressed in units of 14 W m^{-2}.

The first thing that you notice about the results for Jupiter is that the dynamical heat flux plays a small, or nearly negligible role on the thermal balance. This is not too surprising since Stone's radiative-dynamical model basically predicted this for Jupiter. The consequence of this is that Jupiter is close to radiative-convective equilibrium at every latitude and therefore, just to conserve energy, the internal heat flux must balance the net emission to space (i.e., IR minus solar radiated flux) to conserve energy. To understand why the internal heat flux is non-uniform in latitude, we can ask an equivalent question, which is why the thermal emission is relativiely uniform. The answer to this is that it's related to the fact that we have taken the adiabat at depth to be uniform with latitude. To see why this would make any difference, one can do the following calculation: you fix the adiabat at depth and work out the grey radiative-convective equilibrium of a column of gas, assuming the solar deposition is all very deep in the convective region. The answer you get is that the thermal emission has to be constant in latitude. The emission in Fig. 1 isn't exactly constant in latitude, but that is because the solar heating has not been all deposited deep in the convecting region in this particular model.

Near the equator, the solar heating stabilizes the atmosphere at a greater depth relative to the poles, producing a 4.4 K difference in the effective temperature from the equator down to 50 deg latitude. The analysis by Pirraglia on Voyager 1 IRIS data indicates that this difference is unlikely to be greater than about 3.5 K.

Figure 2 is a flux versus latitude plot for Uranus, where the fluxes are annual averages. We see that the major difference between this and Jupiter is that we have a uniform internal heat flow when the ratio of emitted to absorbed power is 1.16. Stone has argued that Uranus' long radiative time constant and negligible internal heat source should cause dynamics to be highly stabilizing in the atmosphere. Large-scale eddies, in that case, should be very efficient in transporting heat from the hot pole to the cooler equator. This is basically what we are finding in our model. We are finding that the meridional flux due to large-scale eddies is very efficient and therefore the internal heat flow doesn't have to do any of the meridional heat transport. That is basically the behavior that we find for all ratios of emitted to absorbed power of 1.25 or less.

Now I'll show you a case where basically I jacked up the potential temperature of the interior. In other words I made it hotter in the center so that the internal heat flux is higher. You see in Fig. 3 that the emitted-to-absorbed power here is now 1.5. You get 0.5 K effective temperature difference from equator to pole for the emission, but now you see that the internal heat flow wants to come up and balance the difference in emitted minus absorbed flux towards the equator.

This seems to be a state intermediate between a low-E Uranus and a high-E Jupiter case. So we can at this stage imagine a suite of hypothetical Jovian planets ranging from the low-E Uranus, where large-scale eddy motions dominate, to the high-E Jupiter case, where the internal heat dominates. As the internal heat source becomes larger, the atmosphere becomes more unstable, but the opportunity arises for differential flow of the internal heat to reduce
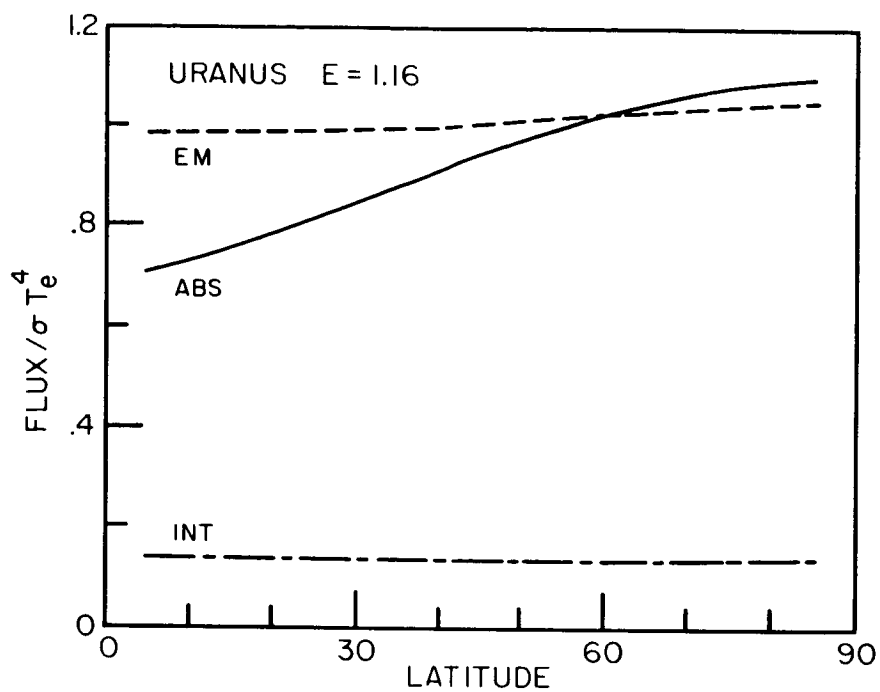
Figure 2. Flux vs. latitude for Uranus. Unit of flux is 0.66 W m^{-2}. The solid curve is the annually-averaged absorbed solar flux.
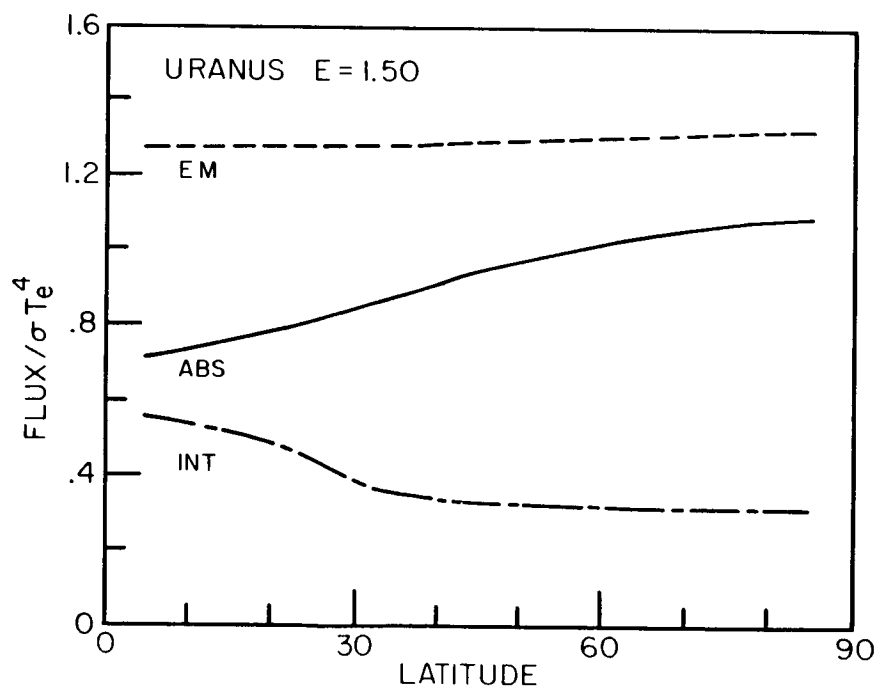
Figure 3. Same as Fig. 2 except here E=1.50.

the effect of temperature difference from the equator to the pole. This is all fine provided that the solar flux is deposited relatively deep in the convective region. If it's shallow then you can get a different result. Should the solar heating occur deep relative to the radiative convective boundary on all the Jovian planets, then we expect that thermal emissions should be fairly uniform in latitude for all these planets. Thank you.

REFERENCES

Hunten, D. M., M. Tomasko, and L. Wallace (1980). Low latitude thermal structure of Jupiter in the region 0.1-5 bars. *Icarus* 43, 143-152.

Ingersoll, A. P., and C. C. Porco (1978). Solar heating and internal heat on Jupiter. *Icarus* 35, 27-43.

Stone, P. H. (1972). A simplified radiative-dynamical model for the static stability of rotating atmospheres. *J. Atmos. Sci.* 29, 405-418.

Wallace, L. (1980). The structure of the Uranus atmosphere. *Icarus* 43, 231-259.

Wallace, L. (1983). The seasonal variation of the thermal structure of the atmosphere of Uranus. *Icarus* 54, 110-132.

DR. STONE: I am not too clear on how the model is constructed. In particular, the heating varies latitudinally. You have a different solar input at different latitudes based on observed albedos, I presume. Then you said that that is being put in fairly deep, so you are calculating the structure at highter levels?

DR. FRIEDSON: Well, I took the solar flux curves for Jupiter from the paper by Hunten, Tomasko and Wallace (1980). I have parametrized the solar input and I have not played too much with that.

DR. HUNTEN: A third of the solar radiation is absorbed above the radiative convective boundary.

DR. STONE: All right, that is put in your model, then, but what did you assume about the heat input at the lower boundary?

DR. FRIEDSON: As you go deep into the atmosphere, our assumption is that you get into a convective region which can maintain all the temperatures as a function of latitude on the same adiabat. Your boundary condition is that your temperature profile, no matter at what latitude, has to approach the same adiabat.

DR. ORTON: For the Jovian models, where is the radiative-convective boundary located, and does that vary with latitude?

DR. FRIEDSON: It varies with latitude generally, but in this particular model the radiative-convective boundary near the pole can be as high as 600 millibars or so. Near the equator, it can be sub-adiabatic, only just slightly so, down to pressures of about one bar.

DR. KAHN: Is there any hope of using the time dependent data and doing a time dependent model here between the limbs and so on? Can we constrain the cloud structure a little bit better that way?

DR. FRIEDSON: I think it is possible that if you really believe our parametrization for horizontal fluxes, which is really just a mixing length theory, you take that as strictly true, and you ignore any horizontal fluxes, then you can possibly use this model to try to probe what the solar flux is doing, what scattering there is and so on, because you have to fit the uniform emission. Right now our model is a bit crude for that, and I think it would need a lot of refinement before I tried anything like that.

DR. BAINES: Because of methane absorption of solar energy, you find that a large part of that solar energy is being deposited around 500-700 millibars for Uranus. The calculations I did around a year or two ago show that you can get a degree difference in the space of ten years. That is not much, but Uranus has a very low effective temperature. It seems that the winds generated may be a function of pole orientation.

DR. HUBBARD: Do your models include a variation of gravity from equator to pole? That can make a difference on the order of the differences in temperature that you are calculating for the equator.

DR. FRIEDSON: No. I hold gravity constant in latitude. Are you saying that it makes a large difference in the effect of column mass abundance?

DR. HUBBARD: Due to the adiabat that you are on to some extent...

DR. FRIEDSON: Well, if it is only changing the adiabat, I have ignored the temperature dependence of the specific heat or whether it is affected by the ortho-para hydrogen ratio. So, you know, the actual model for Uranus right now is rather crude in terms of getting the vertical profiles right. I think qualitatively the behavior will not change much once it is refined.

DR. POLLACK: How do you calculate the meridional dynamical heat fluxes?

DR. FRIEDSON: We use a parametrization that is in terms of local potential temperature gradients. Basically, it is rather complicated to describe, but it is based on a mixing length analysis, and you can find out exactly what the formulae for the fluxes are from Ingersoll and Porco (1978). Usually in our model where we do get significant dynamical heat fluxes, stratification is very stable. In that case we actually have the same parametrization as Stone's (1972) radiative dynamical heat fluxes.

DR. STONE: In those calculations I did in 1972, I neglected beta effects. Things that have been done since then now give us a pretty good idea of

whether the beta effects would be important and how to take them into account. I never myself tried to make any estimate of whether they would be important on Uranus, where you are finding the more stable states. Have you made any estimates of whether beta effects might be important?

DR. FRIEDSON: No. I haven't looked at that, actually.

DR. HUNTEN: What are beta effects?

DR. STONE: Beta is the variation of Coriolis parameter with latitude, which can have strong stabilizing effects on the dynamics.

DR. SROMOVSKY: I'm curious about the time constant for the effect in which the internal heat flux tends to balance the solar deposition. Is that time constant so long that it would inhibit a response to asymmetries in the solar deposition?

DR. FRIEDSON: Well, actually, in the convective envelope, just below say around the 5 bar level and below, you have very short time scales for the convection and the flux can change on the order of hours to maybe a day where it is convectively unstable. If I really believed that we could get a lot of seasonal data on Uranus to watch how the emission changes over the season, then it might be possible to look for the difference in phase response for areas which would be dynamically dominated by the eddies versus areas that are dominated by the internal heat flux.

DR. STONE: In the case of Uranus did you take the average of the whole orbit?

DR. FRIEDSON: Yes, it is annually averaged.

DR. STONE: Because I remember that the mean equator-to-pole temperature difference is relatively small compared to what you could get at the seasonal extreme.

DR. FRIEDSON: Our globally averaged temperature difference for Uranus is very small, and I believe that Wallace's (1983) amplitudes were about 2.5 K, and we just have an annually averaged temperature difference of 1 K. So, yes, I do think you get some variation of emission with season, but I think you have to be able to follow that over a long period of time.

MONDAY AFTERNOON

CLOUDS AND CHEMISTRY

CHAIR: TOBIAS C. OWEN

CLOUDS AND AEROSOLS IN THE JOVIAN ATMOSPHERE: A REVIEW

Robert A. West
Jet Propulsion Laboratory, California Institute of Technology

The presentation by West is largely contained in a paper by West, Strobel and Tomasko. That paper appears in the special issue of *Icarus* (1986; <u>65</u>, 161-217); the abstract is reproduced here:

In this paper we review current ideas about the composition, horizontal and vertical distribution, and microphysical properties of clouds and aerosols in Jupiter's upper troposphere and stratosphere. We also discuss several key photochemical species, their relation to aerosol formation, and their implications for transport processes. We treat photochemistry in the context of comparative planetology and point out important similarities and differences among the outer planet atmospheres. Our approach emphasizes observational data of relevance to cloud properties, and to this end we assemble a wide assortment of ground-based and spacecraft observations. We challenge some widely held views about the distribution of clouds in the troposphere and present a rationale for alternative interpretations.

DR. ROSSOW: I have two questions. First, you showed, very early in your talk, some comparisons of calculated to observed spectra done for 0.1 μm size particles. Then you made the remark that you didn't see the strong absorption features that suggested larger particles. How was that comparison done? In going from small to large particles was the total cloud mass kept the same?

DR. WEST: Yes. Actually there are two parameters in the Marten *et al.* study. There is the particle size and a depletion factor. The distribution of the particles was chosen to be constant, but there was a variable depletion factor. They solved for both the depletion and the particle size and concluded that in the ammonia cloud, the total mass has to be severely depleted compared to what it would be if there were no fallout of particles.

DR. ROSSOW: Yes, O.K. That is really the point—that the particles do get larger, or as you go to more massive clouds the microphysics will, in effect, remove most of the mass as precipitation. What you see up top is small particles and depleted mass. That might well be consistent with the types of depletions they needed.

DR. WEST: I prefer that scenario myself, but they concluded that there aren't any particles smaller than 30 μm.

DR. ROSSOW: But I'm saying that you can also remove the absorption by decreasing the mass. The other question I had was just for information. The

"no water cloud hot spots"...what is the limit on how far down the top of the cloud can be. In other words, you obviously can't see infinitely deep in those hot spots, but if you had to put an upper limit on the temperature of the cloud top such that I could hide one from you, what temperature would that be?

DR. WEST: I'm not sure of the temperature, but I would say it would have to be around 8 bars.

DR. BJORAKER: In terms of temperature, say 270-300 K. If you didn't have any 5 μm opacity due to aerosols, what would limit you is the continuum opacity of pressure-induced hydrogen. That limits you to 5-7 bars.

DR. TRAFTON: You might want to consider some of the data from Jerry Woodman's Ph.D. thesis that he obtained in the mid-1970's from the McDonald Observatory. He obtained methane spectra in the belt, zones, and over the Red Spot. I don't think this is published, but it is available through the University of Texas.

DR. WEST: But isn't that what Sato and Hansen used?

DR. TRAFTON: I'm not sure...

DR. WEST: I believe so, and I showed one of those spectra from Sato and Hansen's paper.

DR. PILCHER: Bob, in any of these cloud models, what is the range of characteristic photon mean free path in the cloud?

DR. WEST: It depends a lot on the absorption coefficient...

DR. PILCHER: Independent of the actual absorption.

DR. WEST: It's hard to estimate. I'd say it's down to the two bar level but between the two bar level and the ammonia cloud there are multiple bounces, and there is also multiple scattering in the ammonia clouds. It has to be greater than up and down to two bars and back. It's probably a factor of two or more greater than that.

DR. PILCHER: The point being that it is a long photon mean free path. You are talking about kilometers, not centimeters. One of the reasons that I ask the question is just a conceptual one. We talk a lot about clouds on Jupiter, and I think a lot of people picture in their minds something like what they see when they look out an airplane window. In fact, in all of these models it has been my impression that we are really dealing with kilometer mean free path. What we are really dealing with is something much more like what we would call a fog on the Earth.

DR. WEST: Yes, I think that that is true.

PHOTOCHEMISTRY OF THE JOVIAN ATMOSPHERE

Darrell F. Strobel
Johns Hopkins University

The review by Strobel is largely contained in a paper by West, Strobel and Tomasko which appears in the special issue of *Icarus* (1986, <u>65</u>, 161-217). The abstract of that paper is reproduced before the open discussion of the previous review by West. Open discussion of the presentation by Strobel follows here.

DR. OWEN: I'd like to use the chairman's prerogative to ask a question. Since you've made this nice discussion on CO, can you say anything similar about the relation of phosphine to red phosphorus given the information that we now have about eddy diffusion coefficients?

DR. STROBEL: I didn't specifically look at that.

DR. POLLACK: Do you have any idea whether diphosphine and hydrazine are observed in the visible and what their spectral characteristics are to see if they make sense in terms of what people think are the spectral absorption coefficients of aerosols in Jupiter's atmosphere? Also, do you have any speculations of comparable things for Uranus and Neptune?

DR. STROBEL: I have no speculations for Uranus and Neptune, but in the case of hydrazine, when I wrote my first paper on ammonia photochemistry, Russ Sowell did some supporting laboratory measurements. We purchased a little bottle of hydrazine and Russ made some absorption measurements. He found the threshold for liquid hydrazine absorption was at 3500 angstroms with a very rapid increase in absorption cross section as you went to shorter wavelengths. The results are given in a footnote in that paper. So, it definitely, in liquid phase, absorbs in the near UV. In the case of diphosphine, I really do not know what its absorption properties are in the solid phase. According to Marty Tomasko, it is not required that there be much real absorption in the visible. So I might direct that part of the question to him.

DR. TOMASKO: You're dealing with nearly conservative scattering; the single scattering albedos are less than 1 but very close to it. It could well be that the sort of upper part of that profile still might fit in quite nicely.

DR. STROBEL: Then of course if you had trace amounts of phosphorus atoms which could provide minute amounts of impurities in some of these substances, you would add to the absorption. Bob West once made the remark that if you take a water droplet and add a little soot to it, the soot will actually absorb more in the water droplet than the soot would by itself.

DR. ALLEN: In your discussion of the HCN profile, you made a passing comment about how the CN could be converted into cyanoacetylene and then go into the

stratosphere. Yet, due to the fact that cyanoacetylene has very large cross sections at much longer wavelengths than does HCN, do you really think that an appreciable fraction of the CN might actually end up in cyanoacetylene?

DR. STROBEL: I'm not sure where that CN will end up when I get to higher altitudes, but I just made the remark to indicate that one should not continue that HCN profile up. What its ultimate form will be will require more analysis, but the first step would be preferential reaction with acetylene rather than CH_4 to recycle HCN.

DR. LEOVY: Is there any question of the kinetics of the gas to particle conversion for the diphosphine or the hydrazine. Could those processes be very slow?

DR. STROBEL: Even if they were slow, you have to remember that the eddy diffusion coefficient is only $10^3 - 10^4$ cm^2s^{-1}. We are talking about years to mix something over a scale height. Certainly, in that length of time, I would assume that one could go from gas to liquid phase and produce a fair sized particle.

DR. HUNTEN: That last graph you showed of the eddy coefficient versus height—it seems to me very unlikely to transport enough heat from the interior.

DR. STROBEL: I wasn't very worried about the heat transport.

DR. HUNTEN: No, but I am. You need values of the order of 10^8 right up to the radiative convective boundary or else you need some other equivalent mechanism, and it would also transport minor constituents, no matter what you call it—eddy diffusion or anything else.

DR. STROBEL: O.K. I wanted an eddy profile I could do analytically, and I'm sure you appreciate that. What I could have done is tried to fit the eddy constraints with some other profile. The point in my calculation is that the mixing ratio has a functional relationship where the second term, the negative one, goes as $1/\kappa$. I'm sure with another eddy profile, I could have found something possibly to fit the heat transport constraints acceptably and still maintain the CO mixing ratio at 10^{-9} without violating the ortho-para H_2 constraint.

DR. HUNTEN: And perhaps have a sudden step down somewhere around the radiative convective boundary. The other question is when you were doing those aerosol calculations you only considered sedimentation and you left out eddy mixing, coagulation and all those things.

DR. STROBEL: Yes. It was just a mass balance calculation. I came up with the simplest model. One should do this in the same vein that one does photochemical calculations, with a real continuity equation.

DR. HUNTEN: Eddy mixing might give you a much bigger loss rate than just the sedimentation.

DR. STROBEL: I checked that, and the velocities were comparable.

DR. ATREYA: We heard from Bob West that Jupiter looks more like sulfur, as the chromophores go. It's very difficult to imagine that sulfur can be produced in photochemistry, and phosphorus comes up again and again as a candidate. The data don't seem to support it. Do you have any speculations on what other candidates might be responsible for the coloration of the clouds?

DR. STROBEL: Other candidates? There are CN compounds, but only trace amounts. You've got phosphorus with the whole hybrid of P_xH_y compounds. The problem is that there are not enough laboratory constraints to really eliminate wild speculation. One would like to have some firmer ground to proceed on. Years ago, at the time we wrote the paper suggesting the Galilean satellites as the source of oxygen atoms, I looked at the sulfur chemistry; and with the few measurements that were available, I found one three-body reaction where the rate coefficients had four or five orders of magnitude differences between two independent measurements. It was very hard to do anything quantitative with sulfur.

DR. ATREYA: But, in any event, the 2.7 μm data, which I think Hal Larson and Gordon Bjoraker have published, indicates that the H_2S mixing ratio is like 3 x 10^{-8}, i.e., it is virtually impossible to get sulfur in the upper atmosphere.

DR. STROBEL: I understand that, but coming in from the top of the atmosphere, there can be a moderate sulfur flux from the Io torus. To the extent that I could do anything with the chemistry, it looked like CS would be the preferential form in which sulfur would accumulate, and it would accumulate at the tropopause just like the CO would from oxygen infall.

WATER VAPOR IN JUPITER'S ATMOSPHERE

G. L. Bjoraker and H. P. Larson
Lunar and Planetary Lab., University of Arizona

V. G. Kunde
NASA/Goddard Space Flight Center

High spectral resolution observations of Jupiter at 2.7 and 5 microns acquired from the Kuiper Airborne Observatory were used to infer the vertical distribution of H_2O between 0.7 and 6 bars. The H_2O mole fraction, qH_2O, is saturated for $P<2$ bars, $qH_2O = 4x10^{-6}$ in the 2 to 4 bar range and it increases to $3x10^{-5}$ at 6 bars where $T = 288$ K. The base of the 5 μm line formation region is determined by pressure-induced H_2 opacity. At this deepest accessible level, the O/H ratio in Jupiter is depleted by a factor of 50 with respect to the solar atmosphere.

High spatial resolution Voyager IRIS spectra of Jupiter's North Tropical Zone, Equatorial Zone, and Hot Spots in the North and South Equatorial Belt were analyzed to determine the spatial variation of H_2O across the planet. The column abundance of H_2O above the 4 bar level is the same in the zones as in the SEB Hot Spots, about 20 cm-amgt. The NEB Hot Spots are desiccated by a factor of 2 or 3 with respect to the global average. The massive H_2O cloud at 5 bars, $T = 273$ K, proposed in solar composition models, is inconsistent with the IRIS data. Instead, a thin H_2O ice cloud would form at 2 bars, $T = 200$ K.

A cloud model for Jupiter's belts and zones was developed in order to fit the IRIS 5 μm spectra. An absorbing cloud located at 2 bars whose 5 μm optical thickness varies between 1 in the Hot Spots and 4 in the coldest zones satisfactorily matches the IRIS data. In contrast, the layered model of Owen and Terrile (1981, J. Geophys. Res. 86, 8797-8814) does not reproduce the continuum level at both the long and short end of the 5 μm window, nor does it fit the observed line to continuum ratios.

No talk about Jupiter at 5 microns is complete without the infrared photograph taken by Rich Terrile using the Palomar 200-inch telescope. There is a wealth of structure in this 5 μm image: one can clearly identify the North Equatorial Belt Hot Spots, the Great Red Spot, and the very cold North Tropical Zone. This high spatial resolution image was acquired using a filter centered at 5 μm with $\lambda/\Delta\lambda = 10$. The next step in exploring Jupiter at 5 μm is to analyze high spectral resolution observations as well. I have used two sets of 5 μm spectra of Jupiter. One set was obtained by Hal Larson using the Kuiper Airborne (KAO) Observatory covering the 40 deg S to 40 deg N latitude range on Jupiter at a resolution of 0.5 cm^{-1}. A complementary set of observations

comes from the Voyager IRIS experiment. The spectral resolution is 4.3 cm^{-1}, and large portions of the planet were observed at spatial resolutions between 1 and 10 degrees of latitude.

The most obvious regions of Jupiter to study initially at 5 μm are the Hot Spots, where the signal to noise ratio is best. Kunde et al. (1982) used the IRIS data between 5 and 50 μm to derive the gas composition for the North Equatorial Belt Hot Spots. In addition, Drossart and Encrenaz (1982) and Drossart et al. (1982) studied the IRIS 5 μm spectra of Hot Spots in both the North and South Equatorial belts as well as a central disk average. They did not analyze the IRIS zone spectra at 5 μm. However, by averaging enough IRIS spectra together we have been able to use the zone data as well as the belt observations in order to measure the spatial variation of the gas composition. Today I am reporting the results of our water vapor analysis.

Water on Jupiter is of interest to many of us in this room. Measurements of H_2O in Jupiter's troposphere allow us to infer the global oxygen to hydrogen ratio (relevant to models of Jupiter's origin), and the location and mass of the H_2O ice cloud. Since this is a clouds and chemistry session, I will focus on this last point. The spatial variation of H_2O on Jupiter is important in studies of dynamics, and the overall oxidation state of the atmosphere determines the stability of disequilibrium species such as PH_3 and CO that have been observed.

Where do we start? We used three observational datasets to study H_2O on Jupiter. We used the airborne and Voyager IRIS spectra at 5 μm that I described previously as well as a recent spectrum of Jupiter at 2.7 μm acquired from the Kuiper Airborne Observatory by Larson et al. (1984). This latter spectrum probes a different portion of the atmosphere because near infrared radiation is dominated by reflected solar flux. Thermal radiation at 5 μm originates near 5 bars, while at 2.7 μm the line formation region is around 0.5 bar. By combining measurements from all of these datasets, we have derived a vertical distribution for H_2O in Jupiter's troposphere.

We used a radiative transfer program to synthesize the infrared spectrum of Jupiter at 5 μm. First, the temperature-pressure profile is specified. The Voyager radio occultation team reported a temperature at 1 bar of 165 K. We used a dry adiabat to extrapolate the temperature down to 7 bars. Next, spectroscopic data for 9 molecules, including H_2O, was fed in. The abundance of each molecule was adjusted to fit the entire 5 μm window. An important source of continuum opacity is due to pressure-induced absorption by H_2. Barney Conrath and Peter Gierasch have discussed the importance of H_2 absorption at 17 and 28 μm. The wings of these lines extend out so far from line center that even at 5 μm, H_2 remains an important opacity source. Unit optical depth occurs at the 5 to 7 bar level, where temperatures are between 270 and 300 K. So, if you have a Jovian model atmosphere with only H_2 and He and no clouds, then pressure induced opacity limits how deep you can see at 5 μm to 7 bars.

Once a cloud is introduced the modeling is more complicated. Bob West, Marty Tomasko, Bob Samuelson and others have calculated the Jovian infrared radiance at a few frequencies using a variety of scattering parameters. Our approach

is to estimate the contribution of gases to the total 5 μm opacity. The remaining opacity is attributed to clouds. In our model we first calculate the spectrum that would be observed from a cloud-free atmosphere. Then a simple purely absorbing cloud is added. This acts as a neutral density filter to the thermal IR radiation. Our model cloud has only two parameters: 5 μm optical thickness and base temperature. These parameters are adjusted in order to fit the continuum radiance at two selected frequencies at each end of Jupiter's 5 μm transmission window.

The calculated synthetic spectrum is convolved with the instrument function for comparison with either the Voyager or KAO observations of Jupiter. A detailed analysis of these observations is given in Bjoraker (1985) and Bjoraker, Larson, and Kunde (1985, 1986). Here I will briefly summarize our results. We have derived a vertical distribution for H_2O in Jupiter's troposphere by fitting strong and weak H_2O lines simultaneously. The H_2O mole fraction on Jupiter changes by about 3 orders of magnitude between 1 and 6 bars. Our upper limit to H_2O from the 2.7 μm airborne data is $3x10^{-8}$ (Larson et al., 1984). This applies to a pressure level near the base of the NH_3 cloud around 0.7 bars. The simplest distribution which reconciles the near IR upper limit with the 5 μm detection of H_2O is a saturated distribution. Between 2 and 4 bars the H_2O mole fraction is $4x10^{-6}$, and it increases to $3x10^{-5}$ at 6 bars.

One consequence of this height dependent H_2O distribution derived from the airborne data is that at 4 to 5 bars the measured abundance is sub-saturated by a factor of 100. This, in turn, implies that Jupiter does not have a massive H_2O cloud near 5 bars. Instead, a thin H_2O ice cloud would form near 2 bars. Is this represenative of the whole planet? One possible explanation is that the airborne data sample primarily the belt regions where most of the 5 μm flux originates. If belts are dynamically dried out with respect to the planet as a whole, then perhaps Jupiter may retain a solar O/H ratio. To test this hypothesis it is necessary to examine the Voyager IRIS 5 μm spectra of Jupiter's zones as well as the belts.

We compared the IRIS spectrum of the North Equatorial Belt Hot Spots to synthetic spectra calculated using various H_2O distributions. A height dependent profile is required to fit strong and weak lines simultaneously. The mole fraction of H_2O in our model of the NEB Hot Spots increases from about 10^{-7} at 2 bars to 10^{-6} at 3.5 bars to $3x10^{-5}$ at 6 bars.

Next, we investigated IRIS 5 μm spectra of cloudy regions in the Equatorial Zone as well as an ensemble of spectra with the coldest 5 μm brightness temperatures, less than 210 K. These latter spectra sample the North and South Tropical Zones as well as the cloudiest portions of the Equatorial Zone. Despite the lower signal to noise ratio compared with belt spectra, the IRIS zone spectra clearly show absorption by H_2O vapor. This represents the first detection of H_2O in spatially resolved spectra of Jupiter's zones. Significantly, the abundance of H_2O in our model which is required to match the zone observations is within a factor of 2 of that derived from the airborne observations of Jupiter's central disk, which included belts and zones. The H_2O mole fraction between 2 and 4 bars in the zones is $2x10^{-6}$, and it increases to $3x10^{-5}$ at 6 bars.

We have assumed that the line formation region for H_2O is the same in Jupiter's belts and zones. Thus, H_2O absorption features in the IRIS spectra of a zone may be compared directly to features in belt spectra to infer relative abundances. Clearly, the degree of cloud cover differs substantially between belts and zones. What if zones have totally opaque clouds at P<4 bars? The absorption features in the IRIS zone spectra might pertain to a completely different altitude than the belt spectra. To test this hypothesis we must investigate several cloud models.

In one class of models the brightness temperature at 5 µm is attributed to a completely opaque cloud at the same physical temperature in Jupiter's atmosphere. To see if the IRIS data are consistent with this idea, we measured the continuum radiance in the IRIS data in various "mini-windows" across Jupiter's 5 µm transmission window. The radiance depends on both the cloud optical thickness at 5 µm and its temperature. In addition, if zones have a totally opaque cloud at some pressure level, then the line formation region for all absorbing gases must be above the cloud. We calculated the line to continuum ratios in the IRIS zone spectra as a function of cloud location. The results of this study are reported in Bjoraker (1985) and Bjoraker, Kunde and Larson (1986). We conclude that an opaque cloud is inconsistent with the IRIS zone spectra. Instead, we find that an absorbing cloud with a 5 µm transmittance ranging from 1 to 4 percent provides a good fit to the IRIS zone observations. The base of the main absorbing cloud deck is near 2 bars, where the temperature is 200 K. Absorption lines in both belt and zone spectra are formed very deep at 5 µm (P=4-5 bars). The main difference is that 5 µm radiation is attenuated to a greater degree in the zones than in the belts.

To summarize, we exclude a massive H_2O cloud in Jupiter's atmosphere at 5 bars for two reasons. First, the H_2O abundance we have derived for the 5 bar level in both belts and zones is about 10^{-5}. This is a factor of 100 below the mole fraction at 5 bars predicted by Weidenschilling and Lewis (1973) assuming a saturated H_2O distribution and a solar O/H ratio. Second, if there were an optically thick cloud in the same temperature region, 250 to 270 K, there would be a prominent signature of black body emission at the long wavelength end of the 5 µm window. This is not observed in any of the IRIS belt or zone spectra. Instead of a massive H_2O cloud, it appears that H_2 pressure induced absorption limits how deep we can see at 5 µm. We do see evidience for a cloud of some kind near 2 bars based on its thermal emission signature at 5 µm. This is, coincidentally, where H_2O ice and condensed NH_4SH are expected to form. Currently, we do not have a spectroscopic signature for either of these condensates. We have only circumstantial evidence for its composition based on measurements of NH_3 and H_2O in the gas phase. Thank you.

REFERENCES

Bjoraker, G. L. (1985). The gas composition and vertical cloud structure of Jupiter's troposphere derived from five micron spectroscopic observations. Ph.D. Dissertation, University of Arizona.

Bjoraker, G. L., H. P. Larson, and V. G. Kunde (1985). The gas composition of

Jupiter derived from 5 micron airborne spectroscopic observations. *Icarus,* submitted.

Bjoraker, G. L., H. P. Larson, and V. G. Kunde (1986). The abundance and distribution of water vapor in Jupiter's atmosphere. *Astrophys. J.,* submitted.

Bjoraker, G. L., V. G. Kunde, and H. P. Larson (1986). The vertical cloud structure of Jupiter's lower troposphere. In preparation.

Drossart, P., and T. Encrenaz (1982). The abundance of water on Jupiter from the Voyager IRIS Data at 5 μm. *Icarus* 52, 483–491.

Drossart, P., T. Encrenaz, V. Kunde, R. Hanel, and M. Combes (1982). An estimate of the PH_3, CH_3D, and GeH_4 abundances on Jupiter from the Voyager IRIS data at 4.5 μm. *Icarus* 49, 416–426.

Kunde, V., R. Hanel, W. Maguire, D. Gautier, J. P. Baluteau, A. Marten, A. Chedin, N. Husson, and N. Scott (1982). The tropospheric gas composition of Jupiter's North Equatorial Belt (NH_3, PH_3, CH_3D, GeH_4, H_2O) and the Jovian D/H isotopic ratio. *Astrophys. J.* 263, 443–467.

Larson, H. P., D. S. Davis, R. Hofmann, and G. L. Bjoraker (1984). The Jovian atmospheric window at 2.7 microns: A search for H_2S. *Icarus* 60, 621–639.

Weidenschilling, S. J., and J. S. Lewis (1973). Atmospheric and cloud structures of the Jovian planets. *Icarus* 20, 465–476.

DR. OWEN: I'm sorry but we really are on a tight time schedule. Time for one question.

DR. LEOVY: Since the water cloud would likely be convective, one might want to look at broken cloud models for a lower cloud. Have you looked at any fractional coverage models (30-50%) for a lower cloud?

DR. BJORAKER: I haven't done that, but clearly the 5 μm images indicate that a heterogeneous cloud model is necessary. A simple gray, absorbing slab is not going to do the trick. An analysis of the center to limb variation of 5 μm continuum radiation should allow you to distinguish between heterogeneous patchy clouds with thick slabs.

VLA OBSERVATIONS OF JUPITER AT 1.3 - 20 cm WAVELENGTHS

Imke de Pater
University of California, Berkeley

In order to study the vertical distribution of ammonia as a function of Jovian latitude, high resolution images have been obtained with the VLA at 1.3, 2, 6 and 20 cm wavelengths. Although the interpretation of the data is quite complicated due to Jupiter's synchrotron radiation, which in fact is the dominant source of radiation at 20 cm, the belt-zone structure is clearly present at 2 and 6 cm wavelengths. At 1.3 cm near the center of the ammonia band, the structure is less pronounced, and at 20 cm it is absent. I am currently trying to fit the data with model atmosphere calculations. Since one probes in and through the visible cloud layers at these wavelengths (temperatures of 135-400 K), and the opacity is likely all provided by ammonia gas, a detailed vertical distribution of this gas can be obtained as a function of Jovian latitude. This ought to give insight in the formation processes of the white cloud layers in the zones and their absence above the belts.

Over the past few years I have obtained much data on Jupiter at radio wavelengths between 1.3 and 20 cm. The various images were constructed from data obtained with the VLA in different array configurations, so that both the small and large scale structures on the disk are visible. The resolution typically is between 1 and 3.5 arc seconds.

At radio wavelengths one typically probes Jupiter's atmosphere between 0.5 and 10 bars, which is precisely the region of cloud formation. Since observations at these wavelengths are only sensitive to ammonia gas, which presumably is the main constituent of the various cloud layers, the radio data provide an excellent means to give additional data on Jupiter's cloud layers.

At 1.3 cm, two bright bands can be seen on the disk, roughly at the position of the NEB and SEB. The brightness contrast is rather weak, however. At 2 cm, the image shows many bands across Jupiter's disk. The brightest coincides with the NEB; this band is about 15 K warmer than its surroundings. At 6 cm, two bands can be seen: the one coinciding with the NEB, and one to the south. The latter, however, is mainly due to Jupiter's synchrotron radiation, which becomes more and more pronounced at the longer wavelengths. At 20 cm, most of the emission is due to Jupiter's synchrotron radiation. No thermal features in excess of about 8 K are visible on the disk. The latitude of the bright bands agrees very well with the latitude of the belts observed at optical and infrared wavelengths. Undoubtedly, they are the same features.

I investigated two different possibilities for explaining the brightness contrast between the zones and belts observed at radio wavelengths: (1) there are either different temperature-pressure (T-P) profiles in belts and zones,

or (2) there is less ammonia gas above the belts than for the zones, which allows one to probe deeper, hotter, levels in Jupiter's belts. Since there are hardly any latitudinal variations at 1.3 and 20 cm, the T-P profiles at $P < 0.5$ bars and $P > 5-6$ bars should be equal. If the belt-zone difference is due to a difference in T-P profiles, the profile should be superadiabatic high up in the atmosphere (0.5-1 bar) in the belts, and subadiabatic deeper down (4-6 bars); or the zones should be subadiabatic high up, and superadiabatic deeper down in the atmosphere. This seems quite unlikely, certainly when taking the dynamics of Jupiter's atmosphere into consideration.

The second possibility, less ammonia gas above belts than zones, is more realistic. Some detailed model atmosphere calculations, when compared to the radio data show that ammonia gas should be depleted by a factor of about 5 high up in the atmosphere above zones as well as belts ($P < 1-2$ bars), and overabundant by a factor of 2 deeper down in the atmosphere ($P > 2$ bars), compared to the solar value. In addition, the depletion above the belts is larger by a factor of about 2 than above the zones, and extends to deeper levels in the atmosphere (zones: down to 1 bar; belts: down to 1.5-2 bars).

A complete comparison between model atmosphere calculations and the data has recently been submitted for publication in *Icarus*.

DR. PILCHER: Does the image at 6 cm exhibit limb darkening, particularly in the upper region?

DR. DE PATER: No, I don't believe that is actually limb darkening.

DR. POLLACK: What altitudes and pressure levels does that factor of 2 less ammonia refer to?

DR. DE PATER: That's between 0.5 and 2 atmospheres.

DR. POLLACK: If you reach the deeper portion of that, the number no longer follows the saturation curve, and a uniform, latitude independent mixing ratio should be achieved.

DR. DE PATER: At $P < 0.6-0.7$ bars ammonia follows the saturation curve.

DR. BELTON: You made a point of the belts not being parallel. Did you have something in mind?

DR. DE PATER: At 6 cm the lower "belt" is actually due to the radiation peaks, and I think it is really a remaining artifact of the synchrotron radiation. I tried to subtract that radiation from the maps.

DR. FLASAR: I don't understand why you ruled out the intrinsic temperature difference of the bright regions.

DR. DE PATER: The temperature profile differences can only occur between 0.5 and 6 bars, otherwise the 1 cm and 20 cm belts don't match the models. It would seem that atmospheric dynamics rule out super- and sub-adiabatic

regions of the sort required to fit the data.

DR. FLASAR: So the actual observations require keeping deep levels at which there are very small temperature contrasts.

DR. DE PATER: Yes.

DR. BAINES: Isn't this one time when radio wavelengths agree with optical wavelengths? Our analysis of visible ammonia lines gives us about the same abundance. Also, from the width of the lines we find the pressure at the bottom of the visible atmosphere to be about 2 bars.

THE VERTICAL STRUCTURE OF JUPITER'S EQUATORIAL AND TROPICAL REGIONS

P. H. Smith
University of Arizona

The presentation by Smith is largely contained in a paper which appears in the special issue of *Icarus* (1986; 65, 264-279). The abstract of the conference presentation is reproduced here:

The complex designs of the Jovian atmosphere can only be understood by examining the planet with every means at our disposal: building unified model atmospheres which are capable of explaining data taken through diverse spectral filters in the continuum, within the absorption bands of selected molecules, and through polarizing filters. At present the synthesis of observational data can only be done for large well-defined features since the various data are taken by different observers usually years apart in time. I have been analyzing two very different data sets which contain information on levels of the atmosphere down to several bars: the Pioneer polarimetry (Smith and Tomasko, 1984, Icarus 58, 35-73) and the methane band images of R. West (1979, Icarus 38, 12-33). When the same model structures are run for both data sets it is encouraging to find that the two-cloud model with a thin overlying haze works well in constraining a large number of available parameters. When the same models are tried on the analysis of hydrogen quadrupole lines (Cunningham and Hunten, 1984, Bull. AAS 16) and also on 5 micron radiation (Bjoracker, 1984, PhD diss., U. Ariz), a unified picture begins to develop. The lower cloud deck is at a pressure level of 2 bars while the upper cloud deck is distributed between about 230 and 700 mb. This upper cloud deck is very likely to be ammonia crystals and has been characterized by an analytic phase function since Mie scattering calculations are not appropriate for nonspherical particles. Above the upper cloud is a thin haze with an optical depth of a few tenths near the 120 mb level. The major difference found between the belt and zone features is the compositional change which causes the lower single scattering albedo in the belts. The belts are also found to have less optical depth in the upper cloud. An optical depth of 7 may be typical for the NTrZ while the SEB model fits the available methane data best with half that value. An earlier model which hypothesized that the ammonia cloud was missing in the belts (Owen and Terrile, 1981, J. Geophys. Res. 86, 8787-8814) gives wildly inaccurate predictions for the observations of the belt polarization. Another morphological difference is the extension of the upper cloud to high altitudes in both the EqZ and the GRS; the haze and cloud material can be clearly differentiated in the polarization models because the cloud is slightly negatively polarizing while the haze needs to be strongly positively polarizing.

UNIDENTIFIED QUESTIONER, DR. X: One question I had was that your predicted base level for the upper cloud seems to be a lot higher than that predicted by other models. Does your analysis still assume that it is predominantly an ammonia ice cloud in the upper layer?

DR. SMITH: You mean at 700 millibars.

DR. X: Right—700 millibars and below.

DR. SMITH: Well, as far as I know, 700 millibars should be the bottom of the ammonia cloud based on the vapor pressure.

DR. X: So it was based on vapor...

DR. SMITH: Yes. It's fixed there. It's assumed to be ammonia and it's evaporating below that level.

VERTICAL CLOUD STRUCTURE MODELS FOR THE NTRZ EQZ, SEB AND STRZ OF JUPITER

B. E. Carlson*
NASA/Goddard Space Flight Center, Institute for Space Studies

R. D. Cess
State University of New York at Stony Brook

Latitude-dependent models of the vertically inhomogeneous Jovian cloud structure are presented. The models assume an atmospheric composition with $[CH_4]/[H_2] = 2.0 \times 10^{-3}$, $[He]/[H_2] = 0.11$ and $[NH_3]/[H_2] = 2.0 \times 10^{-4}$ consistent with the Voyager IRIS measurements and employ refractive indices appropriate for ammonia ice particles and a photochemical stratospheric aerosol layer. The free parameters of the models are determined by fitting the results of multiple scattering calculations to the near-infrared center and limb spectra of Clark and McCord (1979, Icarus 40, 180-188) and the center-to-limb 6190, 6350, 7250, 7500, 8900 and 9500 Å photometric measurements of West (1979, Icarus 38, 12-33). The resulting synthetic center-to-limb profiles are in excellent agreement with the observations. Of the regions studied the tropical zones are the most similar, with the observed differences explained by variations in the vertical extent of the cloudy layers. The Equatorial Zone is a unique region with denser NH_3 clouds than either of the tropical zones. At visible and near-infrared wavelengths the belt-zone contrasts can be explained by opacity differences. The optical depth of the stratospheric aerosol layer is larger in a belt, while the tropospheric clouds are deeper and thinner.

We began this modeling of the vertical cloud structure of the Jovian atmosphere by using the center and limb near-infrared spectra of Clark and McCord (1979). The spectral range of the data is 0.65-2.5 microns. Each spectrum consists of data from 120 individual spectral channels. Thus 240 individual data points were originally considered. The lack of laboratory methane data precludes the modeling of the entire spectral region, therefore roughly only half of the data can be modeled. One of the other problems encountered in working with the Clark and McCord spectra are the uncertainties in the viewing geometry. For this reason our model is also required to reproduce the spatially resolved CCD photometry of West (1979) for which the viewing geometry is known. Of particular interest are the individual belts and zones which were unresolved but contained in the larger field of view of the Clark and McCord measurements.

Our modeling approach is straightforward; we begin by assuming an atmospheric composition consistent with the Voyager analyses of Kunde et al. (1982). Mie theory is used to determine the scattering properties (e.g., single scattering albedo and asymmetry parameter) of the various cloud layers. The cloud layers are modeled as diffuse clouds. As in the real atmosphere, gas absorption occurs within both the clear gas layers and the individual cloud layers in this model. The optical properties for the ammonia ice are taken from Martonchik et al. (1984). Starting with the wavelength where the atmospheric gas opacities are the largest, 2.3 µm, and proceeding to the shorter wavelengths (smaller atmospheric opacities) – we begin by trying to fit the data with simple atmospheric models. First a reflecting layer model is used to infer the cloud top pressure and then a homogeneous cloud model is used to determine the vertical extent of that cloud layer. Where the homogeneous cloud model is no longer able to reproduce the observations, we assume that the atmosphere is no longer homogeneous and add another layer to our model vertical structure. Since both the reflecting layer model and the homogeneous cloud model are unable to reproduce, simultaneously, both the center and limb measurements of Clark and McCord, we were forced to consider, at the outset, a two cloud model. The upper cloud in this model is the stratospheric aerosol layer, while the lower cloud is the tropospheric ammonia cloud layer. The optical properties for the stratospheric aerosol layer are taken from Podolak and Danielson (1977). They found the wavelength dependence of the aerosol extinction to be $\lambda^{-2.5}$. This value is within the range of acceptable values more recently determined by Tomasko.

The vertical cloud structure for the equatorial region of Jupiter that emerges from this investigation is a seven layer model. The seven layers, from top to bottom, are: a clear gas layer; a stratospheric aerosol layer; a second clear gas layer; an ammonia haze; a denser ammonia cloud; a clear gas layer and finally the base cloud layer. This seven layer model was used as the starting point in our investigation into the vertical cloud structure of the tropical zones and equatorial belts using the CCD photometry of Bob West.

Figure 1 shows the model fit to the methane band photometry of the North Tropical Zone, the Equatorial Zone, the South Equatorial Zone and the South Equatorial Belt. The data points plotted are the CCD measurements with their 8% error bars. As can be seen, the model fit is quite good. The wavelength dependence of the optical properties of the stratospheric aerosol layer, taken from Podolak and Danielson, and that of ammonia ice coupled with the wavelength dependent gas absorptions due to hydrogen and methane are able to account for the wavelength dependence of the reflected solar radiation measured at these wavelengths. It is thus not necessary, at these wavelengths, to include any extra absorption due to a chromophore. The relatively poorer, though still acceptable, model fit at 7250 Å is most likely due to the presence of larger cloud particles at the base of the ammonia cloud layer. The presence of larger particles near the cloud base would reconcile the differences in the particle sizes inferred from this study and those determined from the analyses of thermal infrared data. The particle sizes which provide the best fit to the data are 0.6 µm for the ammonia haze layer and 0.8 µm for the ammonia cloud layer. These sizes are representative of the particles found in the upper regions of both layers, as these are the regions most sensitive to reflected solar radiation. The stratospheric aerosol layer is found to contain smaller particles;
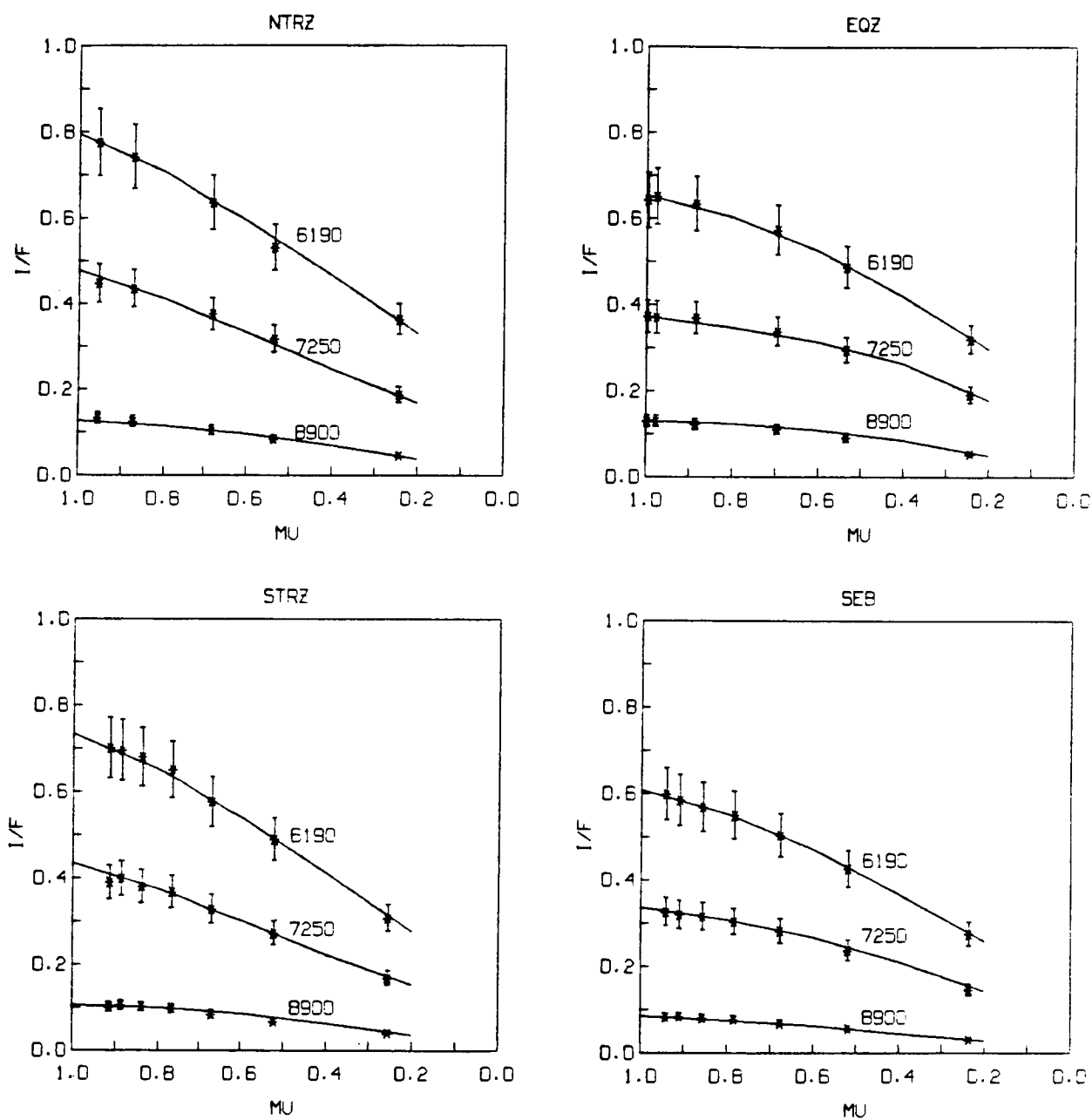
Figure 1. The model fits to the NTrZ, EqZ, STrZ and SEB
methane band photometry.

60

the average particle radius is approximately 0.1 µm. Again this value is within the range of acceptable particle sizes found by Tomasko *et al.* (1986); their preferred particle size is 0.2 with an uncertainty of +0.3/-0.1.

The differences found between the vertical structure of the North Tropical Zone and the South Tropical Zone are found to be due to cloud opacity variations. The optical depth of the ammonia cloud is less in the South Tropical Zone than in the North Tropical Zone. This explains the higher continuum reflectivity found in the NTrZ. The Equatorial Zone is distinct from the other two zones studied here in that the ammonia cloud is optically thicker than that found in either tropical zone. The optical depth due to the ammonia at continuum wavelengths is 2.5 compared with the optical depths of 1.5 and 2.0 found in the North and South Tropical Zones, respectively.

The differences between belts and zones in our analysis are explained by lower cloud top altitudes in belts relative to zones. The top of the ammonia haze layer is at 300 mb in the SEB versus the 200 mb cloud top pressures found for the tropical zones. In addition to the ammonia cloud top altitude variations between belts and zones, there are also differences in the location of the base cloud with latitude. In the SEB the top of the base cloud is encountered at a pressure of 1.8-2.0 bars versus the 1.4-1.6 bar cloud tops found in the zones. We do not, however, find any particle size variations between the base clouds found in belts and those found in zones. This may be due to the fact that the reflected solar radiation modeled here may be more sensitive to certain particle sizes than others. There are some optical depth variations in the base cloud with latitude. These variations may explain some of the variations with latitude found in the 5 µm Voyager IRIS spectra. In particular, the optical depth of the base cloud in the belt is less than that encountered in the zones. This may explain the higher 5 µm emission in belts.

REFERENCES:

Clark, R. N. and T. B. McCord (1979). Jupiter and Saturn: Near-infrared spectral albedos. *Icarus* 40, 180-188.

Kunde, V., R. Hanel, W. Maguire, D. Gautier, J. P. Baluteau, A. Marten, A. Chedin, N. Husson, and N. Scott (1982). The tropospheric gas composition of Jupiter's North Equatorial Belt (NH_3, PH_3, CH_3D, GeH_4, H_2O) and the Jovian D/H ratio. *Astrophys. J.* 263, 443-467.

Martonchik, J. V., G. S. Orton and J. F. Appleby (1984). Optical properties of NH_3 ice from the far infrared through the near ultraviolet. *Applied Opt.* 23, 541-547.

Podolak, M., and R. E. Danielson (1977). Axel dust on Saturn and Titan. *Icarus* 30, 479-492.

Tomasko, M.G., E. Karkoschka, and S. Martinek (1986). Observations of the limb darkening of Jupiter at ultraviolet wavelengths and constraints on the properties and distribution of stratospheric aerosols. *Icarus* 65, 218-243.

West, R. A. (1979). Methane band photometry of Jupiter. I. Absolute relectivities and center-to-limb variations in the 6190-, 7250-, and 8900- Å bands. *Icarus* 38, 12-33.

DR. TOMASKO: What is the opacity of the stratospheric aerosol at continuum wavelengths?

DR. CARLSON: At continuum wavelengths it's tenths.

DR. ALLEN: I wonder whether the spectrum of the chromophores is the single scattering albedo change with wavelength of something on the order of Sato and Hansen. At the wavelength that you're working, the chromophore properties may be the same as the ammonia cloud properties. In fact, you may not be able to distinguish one from the other...

DR. CARLSON: Right--I'm not saying that chromophores are unnecessary at other wavelengths. But I am saying that I do not need extra absorption, in the form of a "chromophore" at these red and near-infrared wavelengths. A chromophore may be required to model the blue portion of the spectrum, but I am not modeling blue data, so I really cannot say. If there is a chromophore, which there most likely is, then to be consistent with the results of this analysis it cannot absorb significantly at wavelengths from 0.6-2.5 μm.

DR. WEST: What is the single scattering albedo of the ammonia particles in those wavelengths?

DR. CARLSON: The single scattering albedo of the ammonia haze layer is adjusted at each wavelength to include the effects of the gas absorption: it is not due to the ammonia haze particles alone. Thus, at 6190 Å the model single scattering albedo is 0.95 while that of ammonia ice alone is 0.997. This is one of the interesting results of this analysis. In comparing the single scattering albedo and the asymmetry parameter of my ammonia haze at 6190 Å with the values determined by Marty Tomasko from the Pioneer data for the stratospheric aerosol layer, I find that these values agree quite nicely. The stratospheric aerosol layer is much darker in my models than that in Marty's models. The single scattering albedo of my stratospheric aerosol layer is 0.64 at 6190 Å.

DR. TOMASKO: I still don't quite understand. You have the haze particles which add some absorbers, and you manage to relate those to some power. But in the ammonia cloud itself, do you have the same kind of material? The ammonia clouds are basically...

DR. CARLSON: The ammonia cloud is modeled as a diffuse cloud. Therefore, in addition to containing ammonia ice particles, the clouds also contain a mixture of methane and hydrogen gas.

DR. TOMASKO: O.K., but in the continuum where the methane doesn't absorb, basically it's 1.0 for the single scattering albedo. I think we had a lot of problems getting the Pioneer data to fit limb darkening if all the absorber is concentrated above, bright clouds beneath. I wonder if you tried to fit your model with the Pioneer data...

62

DR. CARLSON: No, I have not yet tried to model the Pioneer data.

DR. ROSSOW: Marty, keep in mind that the single scattering albedo is not identically one, but 0.98--that's an important difference.

STUDY OF THE AMMONIA ICE CLOUD LAYER IN THE NORTH TROPICAL ZONE OF JUPITER FROM THE INFRARED INTERFEROMETRIC EXPERIMENT ON VOYAGER

William A. Shaffer*, Robert E. Samuelson, and Barney J. Conrath
NASA/Goddard Space Flight Center

An average of 51 Voyager 1 IRIS spectra of Jupiter's North Tropical Zone has been analyzed to infer the abundance, vertical extent, and size distribution of the particles making up the ammonia cloud in this region. It is assumed that the cloud base coincides with the level at which 100% saturation of ammonia vapor occurs. The vertical distribution of particulates above this level is determined by assuming a constant total ammonia mixing ratio (gas plus condensate) and adjusting the two phases so that the vapor is saturated throughout the cloud. A constant scaling factor then adjusts the base number density.

A radiative transfer program is used that includes the effects of absorption and emmission of all relevant gases as well as anisotropic scattering by cloud particles. Mie scattering from a gaussian particle size distribution is assumed. The vertical thermal structure is inferred from a temperature retrieval program that utilizes the collision induced $S(0)$ and $S(1)$ molecular hydrogen lines between 300 and 700 cm^{-1}, and the 1304 cm^{-1} methane band.

A total column abundance of $\simeq 2 \times 10^{-6}$ g cm^{-2} is inferred for the condensate. Acceptable solutions for mean particle radii range from 0.5 to 3.5 μm. These values are considerably smaller than those preferred by Marten et al. (1981, Icarus 46, 233-248) and Orton et al. (1982, Icarus 52, 94-116), though are comparable to the 3 μm mean particle radius derived by Sato and Hansen (1979, J. Atmos. Sci. 36, 1133-1167). Several possible reasons for this apparent discrepancy are suggested.

We have attempted to determine a particulate size of the ammonia cloud on Jupiter's North Tropical Zone from fitting IRIS spectra. In Fig. 1, we plotted two spectra, and the dashed line was obtained by averaging 55 South Pole spectra. The first thing that one notices in the 300-700 wavenumber region is that there is agreement between the two spectra, which indicates a similarity in the tropospheric thermal structure. The second thing that one notices is that there are differences in the 1200-1300 wavenumber regions, indicating differences in the stratospheric structure. Since the tropospheric thermal structures are similar, the differences in the spectra at 200 wavenumbers and 1150 wavenumbers are due primarily to the cloud structure. We have attempted, by fitting these two windows by a cloud model, to obtain the cloud properties in the North Tropical Zone.

---

*NRC Research Associate
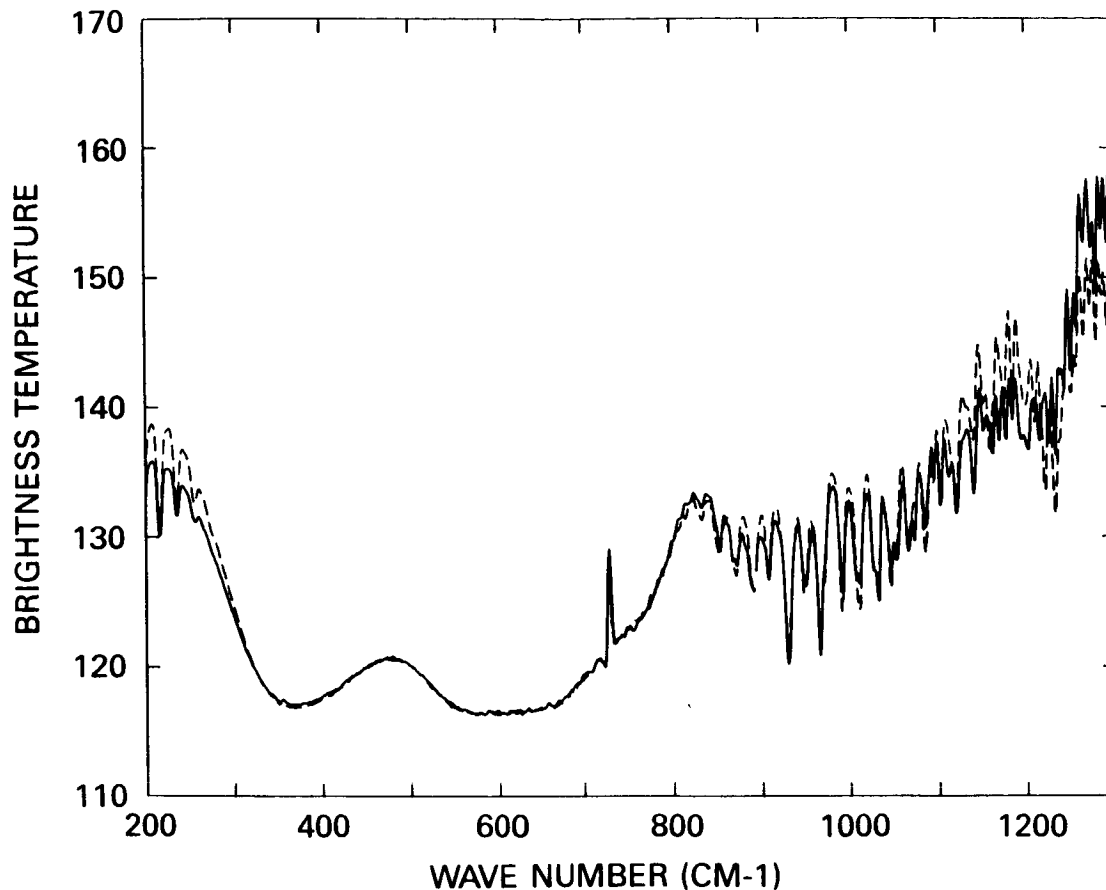
Figure 1. Two Voyager IRIS spectra obtained for large emission angles. The solid line is the average of 46 North Tropical Zone spectra and the dashed line is the average of 55 South Pole Spectra.

In order to save computer time, we chose one wavenumber value in each of the windows to perform the fitting. After we obtained a fit in each of the windows simultaneously using the two wavenumber values, the resulting spectrum was calculated. This was found to be sufficient to obtain a good fit in the entire spectrum. The spectrum we analyzed was not the solid line in Fig. 1. The spectrum analyzed was obtained by averaging 51 North Tropical Zone spectra for small emission angles (Fig. 1 was obtained for large emission angles).

The first step was to obtain a temperature profile from fitting the S(0) and S(1) hydrogen lines and the methane band at 1304 wavenumbers. The cloud model we used assumed one cloud layer with a fixed bottom and a variable, well-defined cloud top. The cloud base was found to be at 700 millibars from the Clausius-Clapeyron equation. The particulate number density profile was determined by assuming that the excess of the assumed ammonia mixing ratio over the saturation mixing ratio went entirely into particulate formation. We used a scale factor of the number density profile to get the number density appropriate

for a given particle size. In our cloud model we solved for three parameters: particle size, the location of the cloud top and the number density scale factor. The radiative transfer program used to calculate the synthetic spectra included absorption, thermal emission, and anisotropic Mie scattering by particulates (assuming a Gaussian distribution of particulates about an assumed mean particle radius). The program used a doubling and adding technique for inhomogeneous atmospheres. We also included phosphine, acetylene, and deuterated methane in the calculations.

Calculating the brightness temperature at the two points in the windows, 210.1 wavenumbers and 1167.9 wavenumbers, for various particle sizes and number density scale factors, we obtained the family of curves shown in Fig. 2. Each point on a curve corresponds to a particular number density scale factor. For this set of curves, the cloud top was arbitrarily fixed at 530 millibars. The tendency in these curves is to move down as the particle size decreases. For example, the curves for 30 to 2 μm particle size move down. At 2 μm they bottom out. For particle sizes smaller than 2 μm the curves move up again. Note, for example, the curves for 1.0 and 0.5 μm.
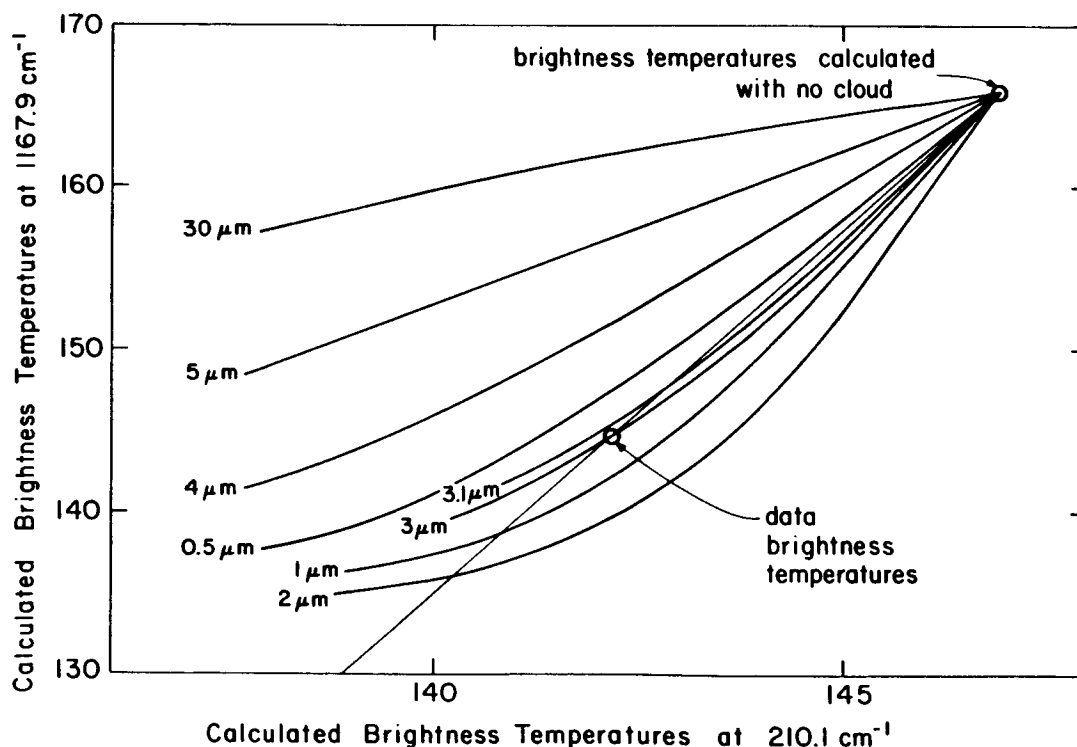
Figure 2. The brightness temperature at 1167.9 wavenumbers as a function of the brightness temperature at 210.1 wavenumbers for a cloud top at 530 mb and various mean particle radii. The straight line contains the points representing a cloud base particulate number density of zero and the Voyager data values.

66

There are two points of interest added to Fig. 2. The first point was obtained by calculating the brightness temperatures assuming no cloud in the radiative transfer program. This point also corresponds to a number density scale factor of zero for all particle sizes. So all the particle size curves share this point. The second point is the point corresponding to the Voyager data values. This point by definition corresponds to a good fit of the data. If one of the particle size curves intersects at this point, for that number density scale factor, we have a good fit in the two windows simultaneously. If we construct a line intersecting these two points, then one notices something about the family of curves. That is, there are two classes of curves. One class of curves is single-rooted; that is, they have one intersection point with the straight line, the intersection point being the no-cloud point or number density scale factor equal to zero. The second class of curves is double-rooted. These curves have two intersection points, the no-cloud point and some point further down the straight line. In the case of single-rooted particle size curves, no simultaneous fit was possible in the two windows. For example, for a 30 micron particle size, an opacity that is sufficient to fit at 210.1 wavenumbers is always too small at 1167.9 wavenumbers. For double-rooted particle sizes a simultaneous fit was possible.

An intersection of the particle curve above the Voyager data values indicates too little opacity in the cloud model. The opacity can be increased by raising the cloud top until the curve intersects at the Voyager data values. The amount that the cloud top must be raised depends upon the distance between the intersection point and the Voyager data values. An intersection that occurs below the Voyager data values indicates too much opacity in the cloud model, and the opacity can be decreased by lowering the cloud top. The cloud top can be lowered until the curve intersects at the Voyager data values. The amount that the cloud top needs to be lowered depends on the distance between the intersection point and the Voyager data values.

We conclude from Fig. 2 that acceptable values of the mean particle radius which will fit both windows simultaneously are larger than 0.5 μm, since 0.5 μm is single-rooted, and smaller than 3.5 μm, since that would also be single-rooted.

In Fig. 3, we've used a 3 μm particle size to calculate the synthetic spectrum shown in the dashed line. For this spectrum, the cloud top was placed at 530 millibars and the cloud mass was 2×10^{-6} g cm^{-2}. The data spectrum is shown with a solid line. An excellent fit is achieved in the two windows, and in the non-window regions in-between, the fit is also good.

Fig. 4 shows an example of the sensitivity of the synthetic spectrum to assumed particle size. The solid line is the Voyager data, and one of the dashed lines is the synthetic spectrum for a 3 μm particle size from Fig. 3. The other dashed line was obtained assuming a 5 μm particle size. This spectrum was obtained by fitting at 210.1 wavenumbers and simultaneously getting the closest possible fit at 1167.9 wavenumbers. Unlike the 3 μm particle size, for the 5 μm particle size it is not possible to fit both windows simultaneously. Fig. 4 shows that in going from a 3 μm to a 5 μm particle size, the synthetic spectrum in the second window blows up and a simultaneous fit is no longer possible.
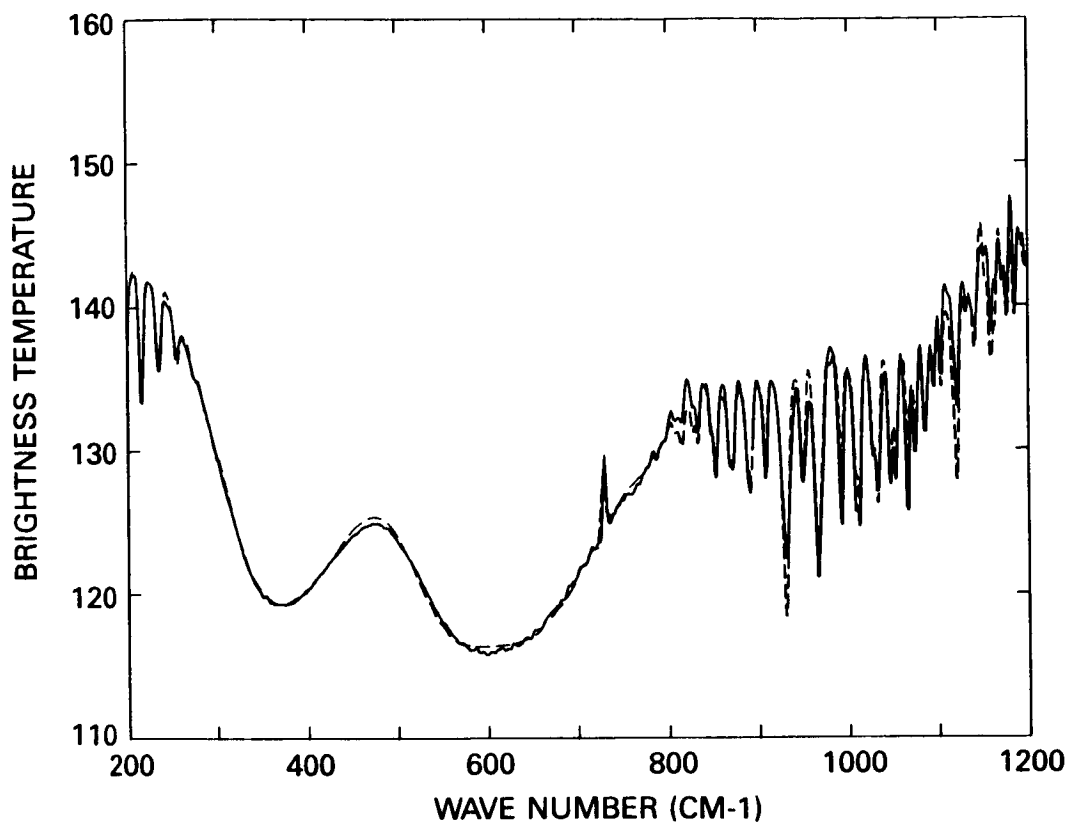
Figure 3. A synthetic spectrum obtained for a cloud with mean particle radius of 3.0 microns, cloud top at 530 mb and cloud mass of 2×10^{-6} g cm^{-2} (shown by dashed line). The solid line is the North Tropical Zone IRIS spectrum.

Now, our results indicating small particle sizes, between 0.5 and 3.5 μm, are contrary to what others have obtained, such as Marten et al. (1981). For example, Marten et al. found that the particle size should be larger than 30 μm and was probably about 100 μm. The reason for the discrepancy between what we have obtained and what they obtained may be due to the region of Jupiter's atmosphere studied. Marten et al. studied the Equatorial Zone, while we have studied the North Tropical Zone. Another reason for the discrepancy between our results and theirs may be due to the cloud model used. We assumed a definite cloud top with a sharp cloud cutoff. Marten et al. assumed a scale height with no cloud top so that the cloud essentially continued on to the top of the atmosphere, although its density was very small. Our results, however, do agree with those obtained by Sato and Hansen (1979), who examined the near-infrared spectrum of Jupiter's North Tropical Zone. We have not considered in this study the possible dependence of the synthetic spectrum on the variation of the cloud base level; nor have we considered different particulate number density profiles or different particle size distributions that are non-Gaussian. These are presently under investigation. Thank you.
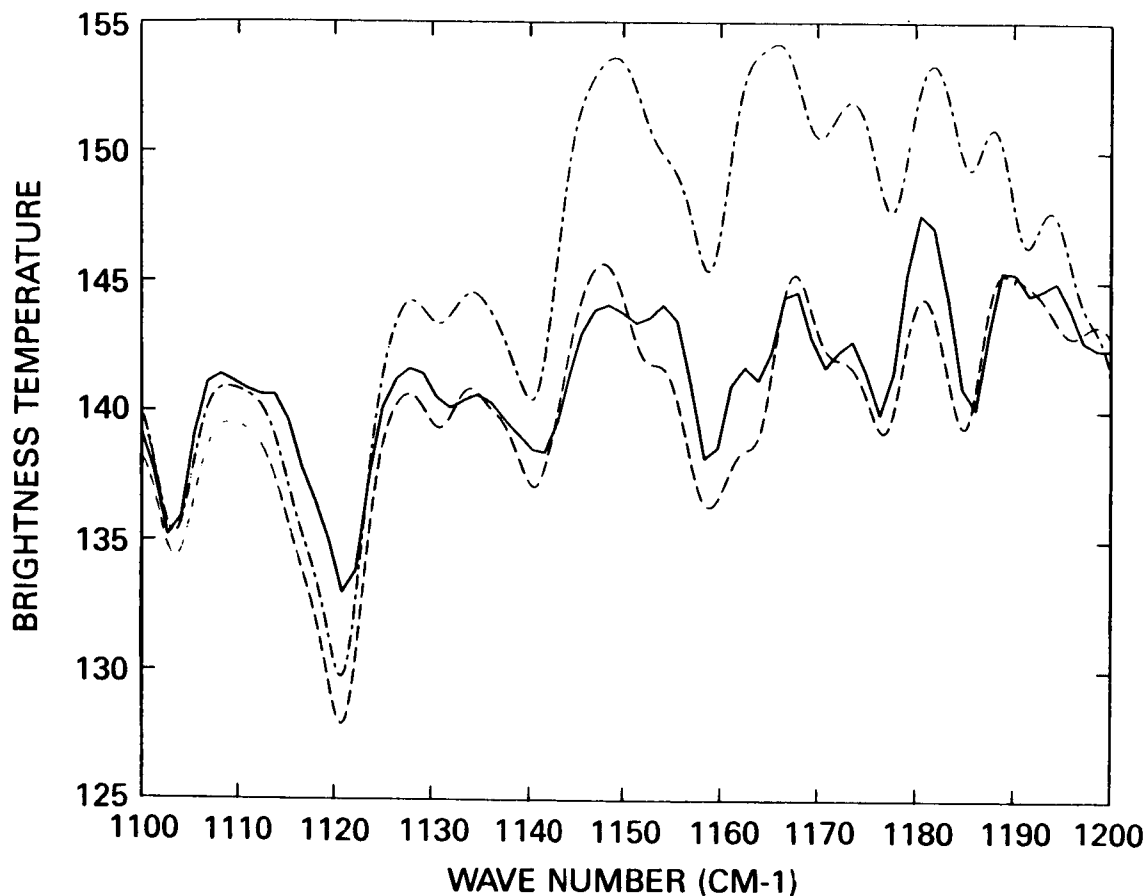
Figure 4. A synthetic spectrum obtained from an attempted fit using a 5.0 micron mean particle radius (dotted-dashed line), showing the best fit possible for an acceptable fit at 210.1 wavenumbers. The dashed line is the 3.0 micron mean particle radius synthetic spectrum. The solid line is the North Tropical Zone IRIS spectrum.

REFERENCES

Kunde, V., R. Hanel, W. Maguire, D. Gautier, J. P. Baluteau, A. Marten, A. Chedin, N. Husson, and N. Scott (1982). The tropospheric gas composition of Jupiter's North Equatorial Belt (NH_3, PH_3, CH_3D, GeH_4, H_2O) and the Jovian D/H isotopic ratio. Astrophys. J. 263, 443-467.

Marten, A., D. Rouan, J.-P. Baluteau, D. Gautier, B. J. Conrath, R. Hanel, V. Kunde, R. Samuelson, A. Chedin, and N. Scott (1981). Study of the ammonia ice cloud layer in the equatorial region of Jupiter from the infrared interferometric experiment on Voyager. Icarus 46, 233-248.

Sato, M., and J. E. Hansen (1979). Jupiter's atmospheric composition and cloud structure deduced from absorption bands in reflected sunlight. J. Atmos. Sci. 36, 1133-1167.

DR. WEST: You mentioned that 1 μm particles were in the range of acceptable fits to your data. I showed a slide showing that for Mie scattering, 1 μm particles show strong resonant features near 1060 wavenumbers. Is that not added in your calculations, or how do you avoid that?

DR. SHAFFER: I believe that the small particle feature that you showed was for 0.1 μm (not 1 μm) which was outside of our acceptable range. No such feature is evident in the spectrum corresponding to the 3 μm particle size.

DR. ROSSOW: Since you derive a number density and a particle size at the base of the cloud, you can calculate the cloud mass density, which should be of order the saturation vapor density at the base of the cloud. Since you assumed a temperature and pressure level, do all those numbers agree? Did you check to see if they do?

DR. SHAFFER: For the synthetic spectrum shown, that is the 3 μm particle size, I believe that only about 60% of the available saturated ammonia actualy goes into cloud formation at the base. However, the apparent excess might be explained by uncertainties in the assumed ammonia mixing ratio profile, or the retrieved temperature profile at this pressure level.

DR. ORTON: To what extent do your results depend on what your assumption was for the distribution of ammonia gas? To what extent did it affect the 210.1 cm^{-1} and 1150 cm^{-1} results?

DR. SHAFFER: We don't expect that it would have much effect on the results, since the particulate number density is not constrained by the ammonia mixing ratio. We didn't try different ammonia profiles. We just used the profile obtained by Kunde *et al.* (1982).

DR. ORTON: The study that Bob West referred to in '83 used 245 cm^{-1} because it was sufficiently far between ammonia line manifolds, and it was pretty far away from ammonia gas absorption.

DR. BEZARD: The spectral region around 1150-1200 cm^{-1} is very sensitive to the cut-off of the Lorentz line shape that you assume. It is sensitive to the far wing shape of the lines of the ν_4 methane band because it's a region of weak gaseous absorption. What did you assume for that line shape, and did you investigate the influence of the cut-off in your calculations?

DR. SHAFFER: The cut-off was 100 wavenumbers.

DR. OWEN: Thank you. I think we should move on.

CONSTRAINTS ON THE COMPOSITION OF JUPITER'S STRATOSPHERIC AEROSOLS FROM ULTRAVIOLET PHOTOMETRY

M. G. Tomasko and E. Karkoschka
University of Arizona

S. Martinek
Pacific-Sierra Research Corp.

The presentation by Tomasko *et al.* is largely contained in a paper which appears in the special issue of *Icarus* (1986; 65, 218-243). The abstract of the conference presentation is reproduced here:

Observations of the limb darkening of Jupiter obtained with the IUE satellite in the spectral range from 0.22 to 0.25 μm near the equator and at a latitude of 40 deg N have been reported by Tomasko and Martinek (1978, Bull. Amer. Astron. Soc. 10, 562), and an analysis of the data has been presented by Karkoschka and Tomasko (1984, Bull. Amer. Astron. Soc. 16, 647). Here we extend the wavelength range over which the imaginary refractive index is derived by including IUE observations at 0.33 μm. This extension of the wavelength coverage appreciably strengthens the available constraints on the composition of the aerosol material. The brightness and limb darkening observations near 40 deg N determine the vertical location (near a pressure level of 25 mb), particle size (~0.2 μm radius), and column number density (5 to 10 x 10^{-8} cm^{-2}), as reported by Karkoschka and Tomasko. At this latitude, the stratospheric aerosols provide so much absorption that their imaginary index of refraction can be derived independent of the absorption produced by the underlying cloud material. The form of the variation of the imaginary index of the stratospheric aerosols determined from the high-latitude data has been compared to published measurements of the imaginary refractive index of several candidate materials produced by irradiating methane-hydrogen or methane-hydrogen-nitrogen mixtures with ultraviolet light (Podolak et al., 1979, Icarus 40, 193-204) or energetic protons (Scattergood and Owen, 1977, Icarus 30, 780-788) as well as recent measurements of Titan tholins (Khare et al., 1984, Icarus 60, 127-137). The material produced by irradiating methane-hydrogen mixtures with energetic particles is not sufficiently absorbing longward of 0.25 μm. Tholins which include a large fraction of nitrogen in the original gas mixture are too absorbing. The best agreement is found for the measurements of acetylene irradiated by ultraviolet light. Near the equator, the stratospheric aerosols provide five to ten times less absorption than at high latitudes, and there is a relation between the absorption produced by the aerosols and the single scattering albedo of the underlying clouds. If the aerosol material is assumed to be the same as that found at higher latitudes, the wavelength dependence of the albedo of the "ammonia" clouds is obtained between 0.22 and 0.33 μm.

DR. ROSSOW: One obvious candidate particle is ammonia. Did you look at the ammonia absorption at these wavelengths?

DR. TOMASKO: As far as I am aware, ammonia absorbs very little at these wavelengths, not nearly enough to be consistent with these kinds of numbers. That's why I was puzzled by the results presented in a paper earlier in this session. I don't think pure ammonia is going to provide these kinds of numbers. Gaseous ammonia only starts to absorb shortward of 2200 Å, and I think the solid phase will be somewhat similar.

DR. ROSSOW: So at longer wavelengths...

DR. TOMASKO: Yes, that's why we like this region between 2500 and 2200 Å. If you remember Bob West's slide, the albedo of Jupiter drops from the visible down to 3000 Å, and rises shortward of 3000 Å due to Rayleigh scattering. At 2500-2200 Å it gets flat, and that is a region where there is no gaseous absorber known as far as I am aware that could do that. We think it's due to the aerosols. Shortward of 2200 Å, ammonia and other gaseous constituents may come in.

DR. ROSSOW: Did you try models with much larger single scattering albedos for the deep cloud?

DR. TOMASKO: At high latitudes, it doesn't make much difference from the curve I showed, which varied between 0.6 and 0.95. At low latitudes, anything goes; there is a whole range of possibilities. If you like to think that the low latitude stratospheric aerosols are different from the high latitude statospheric aerosols, you could make them darker and then require less absorption in the ammonia cloud beneath. That could probably work too.

DR. ROSSOW: So you didn't try retrieving your haze particle properties with an assumed ammonia cloud under it with a high single scattering albedo?

DR. TOMASKO: No, we didn't because we don't understand how that could be consistent in the blue wavelengths where the belts have single scattering albedos of 0.98, and the zones have single scattering albedos of 0.995 or something like that. There's a big difference in the single scattering albedo between belts and zones in the blue, and it can't all be just the ammonia. There has to be some absorber in the ammonia-type cloud particles, I think.

DR. ROSSOW: That wasn't the sense of my question. The sense of my question was what happens to your numbers if you were to put in a higher single scattering albedo for your low latitude...

DR. TOMASKO: Then you would extract even darker aerosol particles; that is, even higher imaginary refractive indices than the ones I've shown, or greater numbers of them, or some combination of the two. That's a big parameter space. There would be many permitted combinations.

THE DISTRIBUTION OF ATOMIC HYDROGEN IN THE JOVIAN ATMOSPHERE

R. M. Killen and J. W. Chamberlain
Rice University

We present an analysis of the Voyager and IUE Lyman alpha spectra of the Jovian equatorial emission in which we derive a zonal asymmetry in the hydrogen column abundance. Using two estimates of the fraction of Lyman alpha which is due to direct excitation by charged particle precipitation from the ionosphere, we have derived upper and lower limits to the H column abundance within and without the perturbed region. We show that the asymmetry in H abundance may be due to localized heating near the homopause with a consequent rise in scale height. The derived exospheric temperature remains fairly constant with longitude. The required additional heat input over the bulge region, 0.02 erg cm^{-2} s^{-1}, is supplied by an additional flux of magnetospheric electrons due to Jupiter's magnetic anomaly.

Voyager ultraviolet spectrometer data indicated a strong longitudinal variation in the Lyman alpha brightness of Jupiter (Sandel *et al.*, 1980). An enhancement was situated at about 110 deg W longitude and exhibited a brightness of 20-21 kR in contrast to the 15-16 kR level for remaining longitudes. The perturbation shows up as well on the night side, although the total magnitude of the intensity is reduced by a factor of about 20. The feature was observed as well by IUE (Skinner *et al.*, 1983) over a period of three years starting in 1978. The Lyman alpha bulge persisted, but was highly variable. We note that the brightness for the perturbed region in the IUE data was 9-15 kR compared to a level 8.5 kR elsewhere. These lower values compared to those from Voyager suggest the possibility of a calibration difference. Nevertheless, the observations show that the feature does persist, and the IUE results show that it is variable.

Our analysis of the Lyman alpha data indicates that the anomalous peak in brightness is due in part to a zonal asymmetry in the hydrogen column abundance. The sources of Lyman alpha that we've considered include reflected interplanetary Lyman alpha, direct excitation by charged particles, and, on the day side, resonance scattering of solar Lyman alpha. It is recognized that a longitudinal variation in the direct excitation by charged particles is one source for the Lyman alpha peak (cf. Gladstone and Shemansky, 1983; Shemansky, 1985). The magnitude of the particle excitation source is taken from the estimates by Shemansky. There is a source which seems to be constant in longitude with a magnitude of 2.5-3 kR, and a source variable in longitude and time with a magnitude of order 4 kR. The longitudinal variation in the charged particle flux is attributed to the magnetic anomaly. Mirror points for charged particles are lowered in the magnetic anomaly region, causing enhanced conductivity. The E-cross-B forces cause a flow of charged particles away from the active sector, and these particles return in the region of the Lyman alpha bulge (cf. Dessler *et al.*, 1981; Hill *et al.*, 1981).

So what we have done is use two different estimates of the amount of Lyman alpha emission due to particle excitation. We next subtract this flux from the total observed to determine the flux due to resonance scattering of solar Lyman alpha, which in turn permits us to infer the enhanced column density of atomic hydrogen required to explain the Lyman alpha bulge. Now, if you assume that the amount of Lyman alpha which is due to particle excitation is constant with longitude, then you will conclude that the column density of atomic hydrogen varies by a factor of three with longitude. However, if you assume instead that there is a particle flux source of 3 kR in the normal component and 7 kR in the bulge, you will conclude that there is a 50 percent enhancement of the column density in the bulge region. Similarly, if you assume that the particle flux source is constant, then the column varies by a factor of 2.5 with time. But if you assume instead that it is the exospheric source that is varying, then you find that no variation in the columm density with time is necessary.

We looked at the night side Lyman alpha and using the hydrogen distribution determined from the analysis of the dayside data, we estimate that about one-third of the nightside Lyman alpha flux is due to resonance scattering of interplanetary Lyman alpha. The remainder should be entirely due to direct excitation by charged particles. Analysis of the variation of Lyman alpha for the nightside suggests that both a zonal variation in column density of hydrogen and particle flux must be present. Furthermore, if one assumes that the particle source is constant with longitude, then an enhancement of about 100 K in the mesospheric temperature of the bulge region is implied. We believe that this is unrealistic, again supporting a variation in the direct excitation by charged particles.

REFERENCES

Dessler, A. J., B. R. Sandel, and S. K. Atreya (1981). The Jovian hydrogen bulge: Evidence for co-rotating magnetospheric convection. *Planet. Space Sci.* 29, 215-224.

Hill, T. W., A. J. Dessler, and L. J. Maher (1981). Corotating magnetospheric convection. *J. Geophys. Res.* 86, 9020-9028.

Sandel, B. R., A. L. Broadfoot, and D. F. Strobel (1980). Discovery of a longitudinal asymmetry in the H Lyman-alpha brightness of Jupiter. *Geophys. Res. Lett.* 7, 5-8.

Shemansky, D. E. (1985). An explanation for the H Ly α longitudinal asymmetry in the equatorial spectrum of Jupiter: An outcrop of paradoxical energy deposition in the exosphere. *J. Geophys. Res.* 90, 2673-2694.

Skinner, T. E., S. T. Durrance, P. D. Feldman, and H. W. Moos (1983). Temporal variation of the Jovian HI Lyman-alpha emission (1979-1982). *Astrophys. J.* 265, L23-L27.

DR. TRAFTON: What can you say about the alternative explanation that the hydrogen was formed over the magnetic pole and drifted down the bulge region by centrifugal force?

MS. KILLEN: Well, I think if that were the case, then the line would show variation along the equator. Isn't that true?

DR. TRAFTON: Yes, that would be the bulge. That was an early alternative explanation.

MS. KILLEN: Well, I think the problem with that is the variation is along the particle drift equator. The variation follows the particle drift equator rather than the true equator.

DR. TRAFTON: Did you find that your mechanism adequately explains this observed tendency?

MS. KILLEN: Yes, if it is coupled with an exospheric source.

DR. STROBEL: I have a number of comments. (1) The Voyager data was given for the center of the disk intensity. The disk averaged intensity is two-thirds of this value and thus in agreement with IUE. (2) If you examine where the major particle precipitation occurs in the auroral regions and assume particle heating drives a thermospheric wind system to transport hydrogen to the bulge region, you encounter a problem. Ion drag will direct transport along flux tube paths, but the field is so contorted when you're in close to Jupiter, you can't get hydrogen to the right spot: the bulge region. I guess that makes a difference. The third comment is that Don Shemansky has written a paper, which just came out, in which he argues that in reanalyzing the Voyager UV data the particle precipitation is actually stronger in the anti-bulge region than in the bulge region.

MS. KILLEN: I think that's only a certain part. It's not all of the particle precipitation.

MONDAY POSTER PRESENTATIONS

ATMOSPHERIC STRUCTURE, CLOUDS, AND CHEMISTRY

SPATIAL VARIATION OF THE THERMAL STRUCTURE OF JUPITER'S ATMOSPHERE

C. Bezanger, B. Bezard, and D. Gautier
Observatoire de Meudon

The radiative seasonal model described by Bezard and Gautier (1985, Icarus 61, 296-310) for the case of Saturn has been adapted to Jupiter. We assume that the atmosphere is radiatively controlled above the 500 mb pressure level and that the temperature at the radiative-convective boundary level is constant for all latitudes. An internal heat source and absorption by methane and aerosols contribute to atmospheric heating. Absorption by aerosols has been adjusted to give a planetary Bond albedo equal to 0.343 (Hanel et al., 1981, J. Geophys Res. 86, 8705-8712). Despite Jupiter's low obliquity, the model predicts seasonal variations of temperature of several degrees for the 1 mb pressure level at mid-latitude regions.

We present here the results from a radiative seasonal model for the strato-sphere and upper troposphere of Jupiter. As in a similar study for Saturn (Bezard and Gautier, 1985), this model includes a multi-layer monochromatic radiative transfer treatment for thermal infrared wavelengths rather than the direct cooling-to-space approximation for each layer that is often employed. Hydrostatic equilibrium is of course assumed, and the thermal structure of the atmosphere is radiatively controlled above the radiative-convective boundary at the 500 mb pressure level. The time-dependent temperature T as a function of pressure p and latitude θ is given by:

$$\frac{dT(p,\theta)}{dt} = \frac{mg(\theta)}{C_p} \frac{dF}{dp} \quad , \tag{1}$$

where m is the mean molecular weight, $g(\theta)$ is the local gravitational acceleration, C_p is the specific heat, and F is the net upward flux comprising the thermal emission and the seasonally dependent solar flux.

Thermal infrared flux is calculated for wavelengths > 7 μm including opacity due to H_2, $H_2 - He$, CH_4, C_2H_6 and C_2H_2 for an atmosphere with 89.7 percent H_2 and 10.3 percent He. Mixing ratios for the hydrocarbons are taken to be: $CH_4/H_2 = 1.95 \times 10^{-3}$, $C_2H_6/H_2 = 2.68 \times 10^{-6}$, and $C_2H_2/H_2 = 3.18 \times 10^{-8}$. The calculation of the solar flux deposition includes absorption by visible and near-infrared bands of CH_4 and the effect of aerosols. The latter are presumed to be homogeneously mixed throughout a semi-infinite layer for $p > 150$ mb and with a single scattering albedo of 0.980 chosen to fit the planetary Bond albedo of 0.343 determined by Hanel et al. (1981).

PRECEDING PAGE BLANK NOT FILMED

The temperature at the radiative-convective boundary at 500 mb is assumed to be constant as a function of time and latitude and equal to 147 K, which thus fits the Jovian effective temperature of 124.4 K observed by Voyager (Hanel et al., 1981). Beginning with an initial thermal profile, we solve Eq. (1) by numerically integrating over several seasonal cycles until the influence of the initial guess is negligible. Continuing the integration to simulate the seasonal variation throughout the period prior to and following the Voyager encounter, we find that temperature variations for mid-latitude regions at the 1 mb pressure level are of the order of several degrees despite the low obliquity for Jupiter.

The results for latitudes 60 deg N and S are shown in Fig. 1 for pressure levels of 1, 10, 100 and 300 mb. Figure 2 illustrates the thermal profiles obtained by our model at five different latitudes for the time of the Voyager encounter. A comparison of our model thermal profile at 10 deg S for the Voyager encounter time with the ingress and egress radio-occultation temperature profiles (at 12 deg S and the equator, respectively) and with an IRIS retrieved profile at a similar latitude indicates that our model is consistent with the observations over the 1-500 mb pressure range.
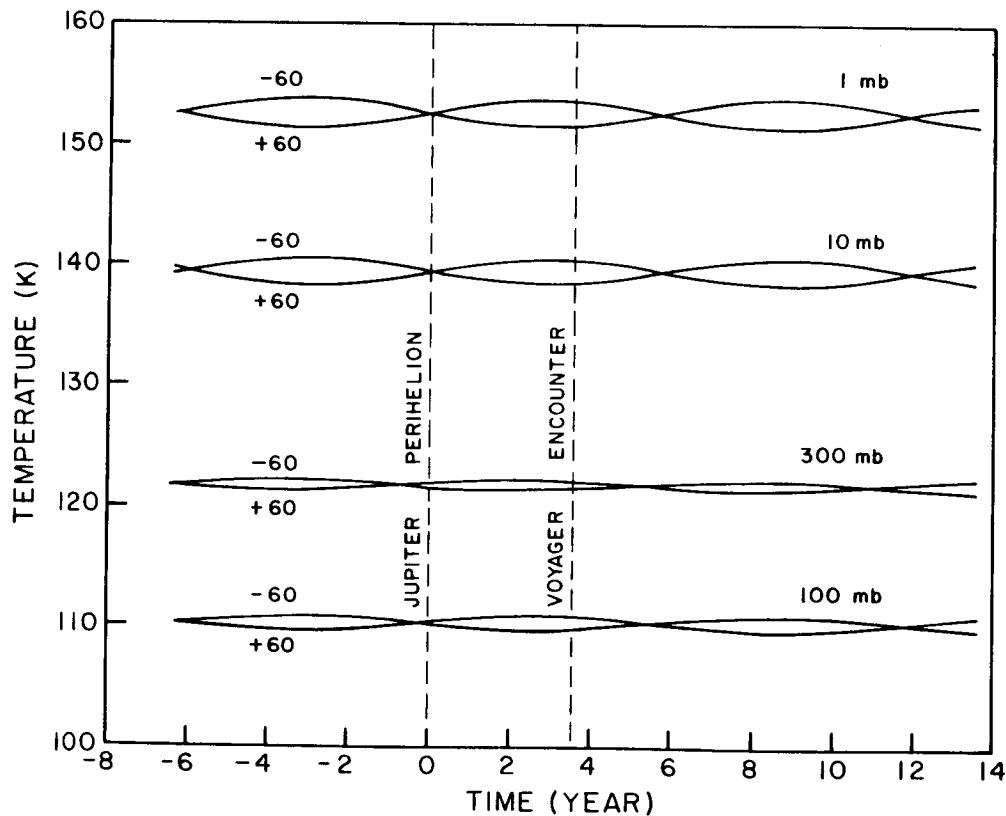
Figure 1. Temporal variations of temperature predicted by the model at four different pressure levels at latitudes of 60 deg. Time origin is Jupiter perihelion.

80

C-2
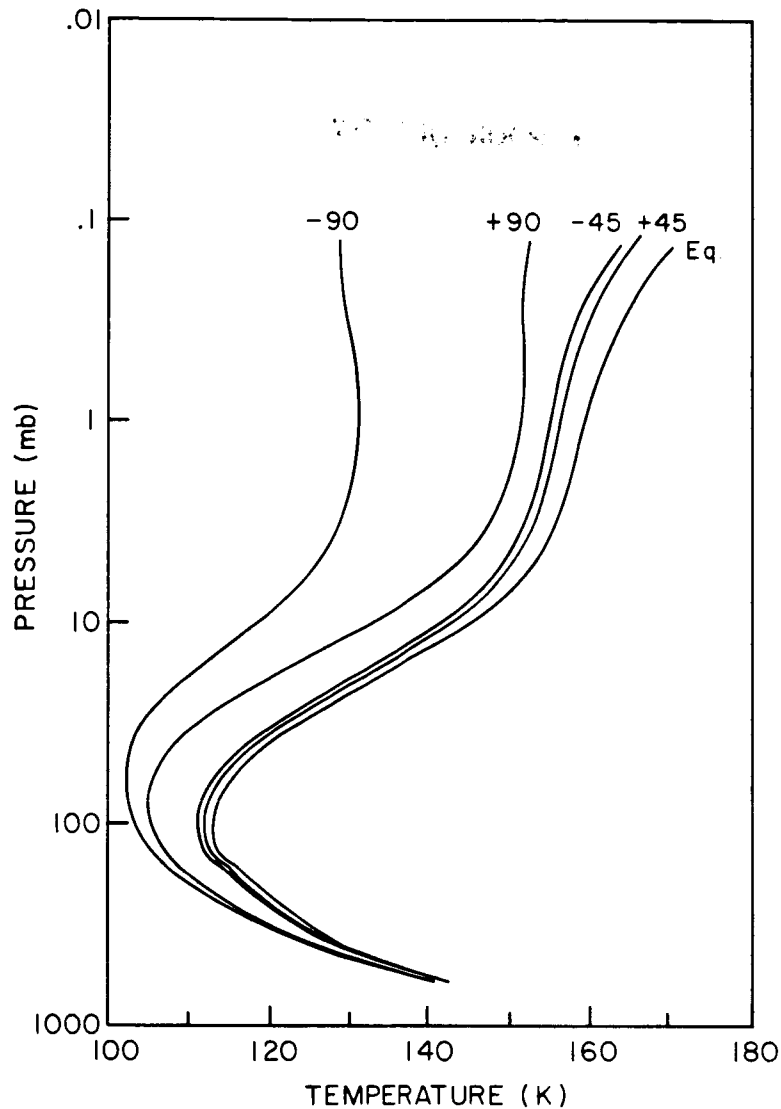
Figure 2. The thermal structure of the atmosphere
of Jupiter as computed by the model for five dif-
ferent latitudes, at the Voyager encounter time.

REFERENCES

Bezard, B., and D. Gautier (1985). A seasonal climate model of the
    atmospheres of the giant planets at the Voyager encounter time: I.
    Saturn's Stratosphere. *Icarus* 61, 296-310.

Hanel, R. A., B. J. Conrath, L. W. Herath, V. G. Kunde, and J. A.
    Pirraglia (1981). Albedo, internal heat, and energy balance of Jupiter:
    Preliminary results of the Voyager infrared investigation. *J. Geophys.*
    Res. 86, 8705-8712.
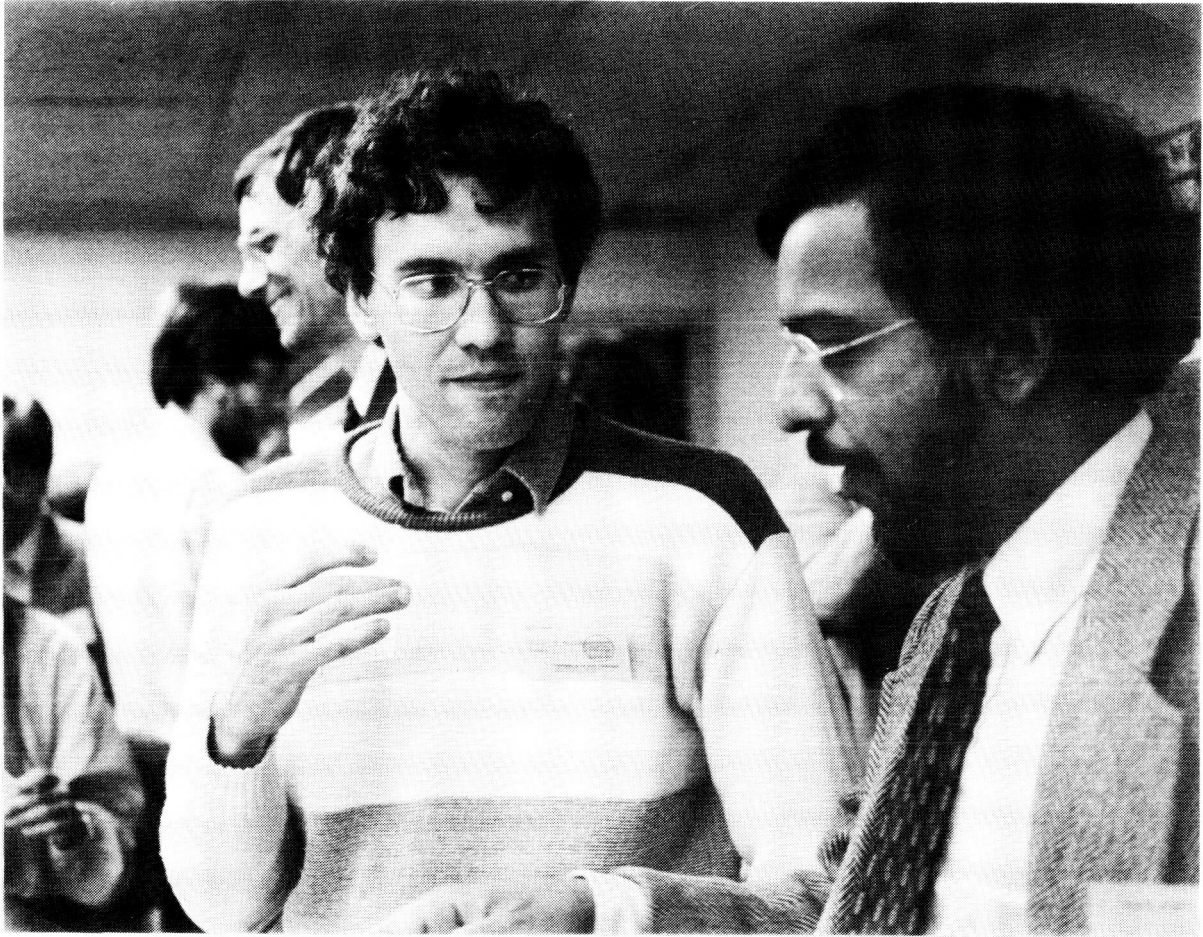
THE SINGLE SCATTERING PHASE FUNCTIONS OF JUPITER'S CLOUDS

L. R. Doose, M. G. Tomasko, and N. D. Castillo
Lunar and Planetary Lab., University of Arizona

The determination of the single scattering phase functions of Jupiter's clouds and a thin upper haze by Tomasko et al. (1978, Icarus 33, 558-592) has been refined and extended to seven latitudes in blue and red light. The phase function is well-constrained by the Pioneer 10 and 11 photometric data sets. Multiple scattering models were computed to match the limb darkening at each latitude at up to 15 phase angles from 12° to 151°. Ground-based observations were used for absolute calibration and to extend the data to lower phase angles. The phase functions were parameterized using the double Henyey-Greenstein function. The three Henyey-Greenstein parameters and the single scattering albedo were determined using a non-linear least squares method for the haze and the clouds below. The phase functions derived for the northern zone and belt are remarkably similar to the phase functions of the corresponding regions in the south, with most of the differences in brightness of the northern and southern features resulting from minor differences in single scattering albedo. Analysis of the Equatorial Region is complicated by the presence of numerous small features, but the phase function required is generally similar to that seen in the more homogeneous regions. Details of the phase functions of the haze and clouds are presented, and the differences between the cloud phase functions at low and high latitudes in red and blue light are discussed.

The phase function for the scattering of light by a cloud particle in Jupiter's atmosphere can serve to constrain the size, shape, and index of refraction of the particle. Atmospheric radiative transfer models which include scattering also require knowledge of the phase function. We have used photometry from Pioneers 10 and 11 covering phase angles from 12° to 151° to determine the phase function of Jupiter's clouds at seven latitudes in blue (0.44 μm) and red (0.64 μm) light. Ground-based observations from Orton (1975) made near the time of the Pioneer encounters have been included to provide data at smaller phase angles.

Figures 1 and 2 illustrate the dependence of the limb darkening of Jupiter over a range of phase angles upon the phase function. This dependence permits the solution for the phase function. Figure 1 shows the angular scattering dependence of four simple Henyey-Greenstein functions and one double Henyey-Greenstein. A Henyey-Greenstein function is described by

$$P(\theta,g) = (1 - g^2)/(1 + g^2 - 2g \cos(\theta)),$$

where θ is the scattering angle and g is the asymmetry parameter. A double Henyey-Greenstein is a linear combination of two such functions:

$$P(\theta) = f\ P_1(\theta,g_1) + (1 - f)\ P_2(\theta,g_2).$$

Double Henyey-Greenstein functions add the possibility of a backscattering peak to the phase function. Figure 2 compares radiative transfer models computed with the phase functions of Fig. 1 to Pioneer limb darkening data. The shape of the limb darkening at any one phase angle cannot be used to determine the phase function. Instead the limb darkening curve at each phase angle tends to constrain the single scattering phase function at the corresponding scattering angle (180°-phase angle). Observations at several phase angles are needed to choose between the phase functions of Fig. 1. Note in Fig. 2a that both the double Henyey-Greenstein and the strongest forward scattering single Henyey-Greenstein give reasonable fits. However at 12° (Fig. 2c) this single Henyey-Greenstein function results in a model which falls far below the data. The data at 34° (Fig. 2b) do not discriminate well between the phase functions. Figure 3 condenses the comparison of data at 15 phase angles on to one graph by plotting only a single data point, near the maximum brightness, for each phase angle against the models. Isotropic scattering (g = 0) fails to fit except at about 70° and 180°. The single Henyey-Greenstein with g = 0.75 fails at angles larger than about 150°. The need for a backward peak in the phase function is again illustrated.
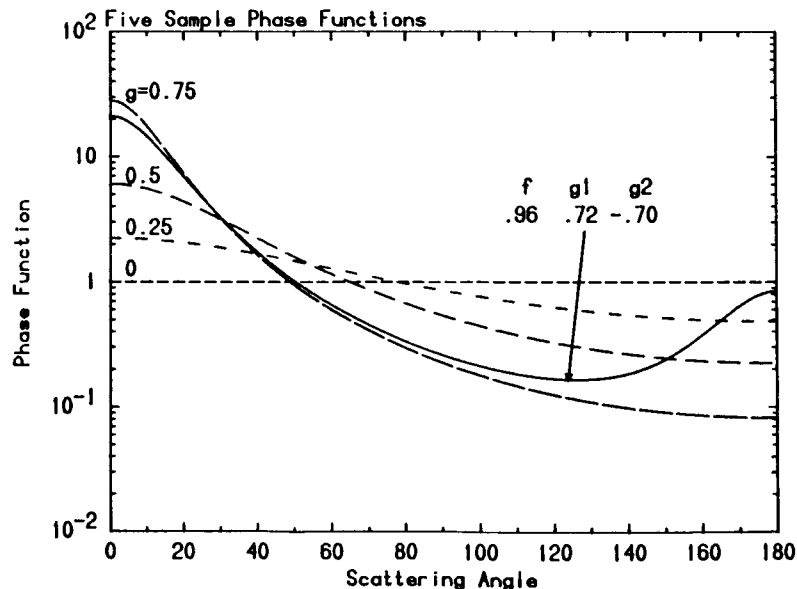
Figure 1. Angular scattering dependence for four single Henyey-Greenstein functions (labeled with asymmetry parameters at left) and one double Henyey-Greenstein function.

IMAGE B1   LATITUDE 18.5 TO 21.5 DEG   150 DEG PHASE

0.75

f   g1   g2
.96   .72   -.70

0.50

0.25

0.00

LONGITUDE (x 10)
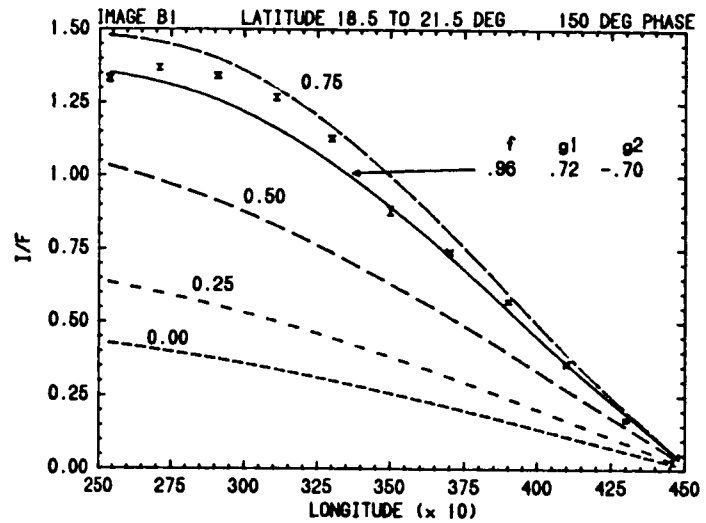
Figure 2. Limb darkening pre-
dicted by radiative transfer
models using the five phase
functions from Fig. 1 are com-
pared to Pioneer photometric
observations at phase angles
of 150° (top), 34° (middle),
and 12° (bottom). The correct
phase function must yield fits
at all phase angles. Only the
double Henyey-Greenstein comes
close. All Pioneer data avail-
able are plotted, but the best
fit was determined by comparing
models to a subset of points
denoted with an X. Cloud fea-
tures cause a fluctuation of
observed limb darkening which
the models cannot follow in
detail.

IMAGE 333   LATITUDE 18.5 TO 21.5 DEG   34 DEG PHASE

LONGITUDE (x 10)

IMAGE A5   LATITUDE 18.5 TO 21.5 DEG   12 DEG PHASE

LONGITUDE (x 10)

85
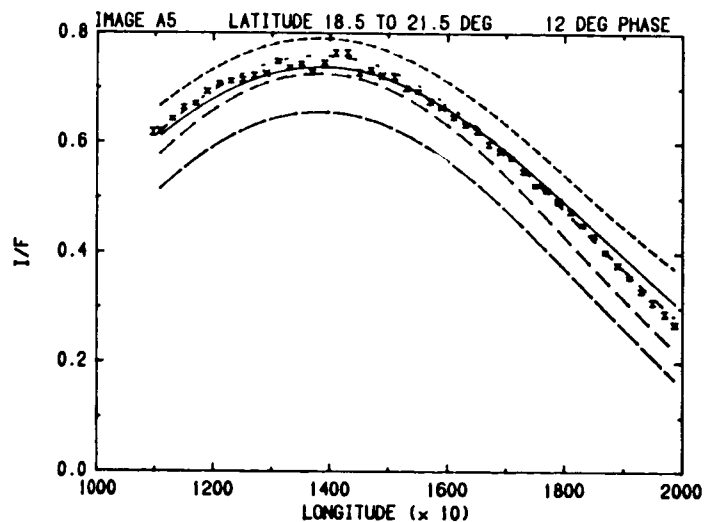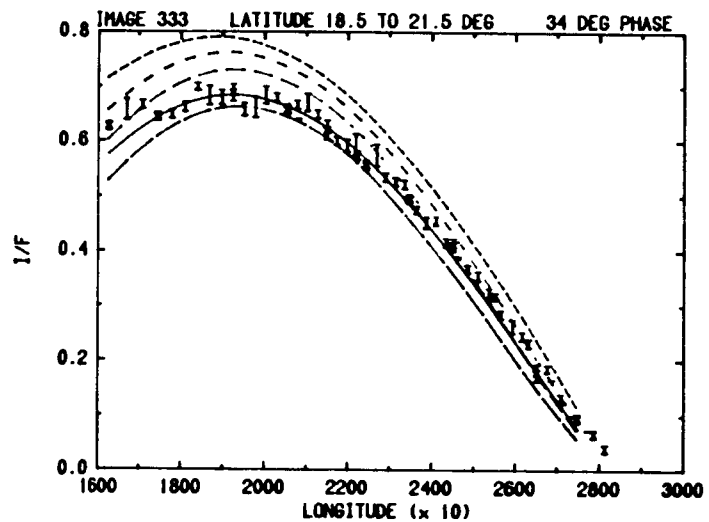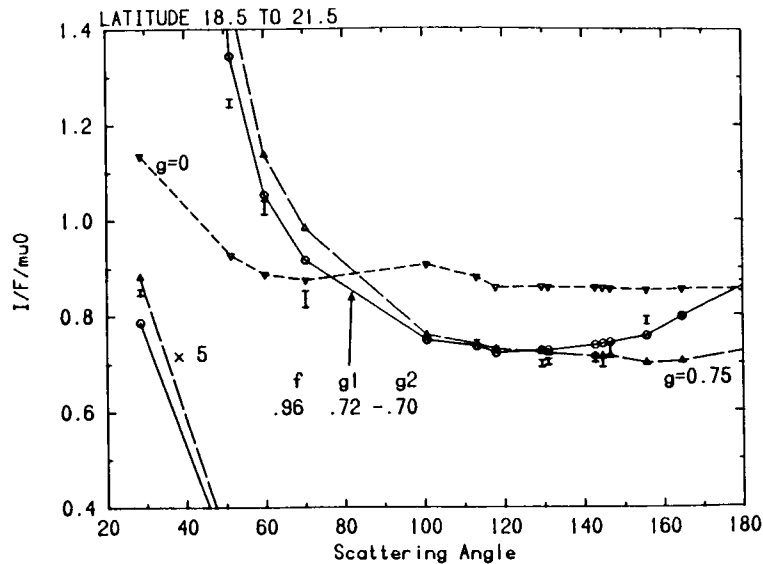
Figure 3. The "normalized reflectivity",
$I/(\mu_0 F)$, for observed points near the maxi-
mum brightness of the limb darkening curve
at 15 phase angles plotted vs. scattering
angle. Isotropic scattering gives a poor
fit. A backscattering peak is needed to
match the small phase angle data.

We used a non-linear least-squares technique to find values for f, g_1, and g_2
and for ω, the single scattering albedo, which optimized the fit to the data
at 15 phase angles. The phase function is constrained best near the scatter-
ing angles where observations exist, as indicated by short vertical lines
near the top of each phase function plot in this paper. No observations
exist at scattering angles less than 29° (phase angles greater than 151°),
hence variations among the functions in this range are not meaningful.

The double Henyey-Greenstein functions which best fit the data are shown in
Figs. 4 through 11. Computation of radiative transfer models requires that
the vertical structure of the atmosphere, in terms of optical depth, phase
function, and single scattering albedo, be specified. We have used two
vertical structures. Structure I contains an optically thin haze above an
optically thick cloud extending downward from the 300 mb level. The phase
function is derived for the cloud. Structure I represents our best estimate
of the true vertical structure for the South Tropical Zone and northern
component of the South Equatorial Belt derived from models which fit the
polarization and photometry in methane bands. Structure II is a single
optically thick cloud including no haze or molecular scattering. Because the
forward peaks of the phase functions are not constrained by our data, we have
not normalized each phase function to the same constant in Figs. 4 through 11.
Instead we have multiplied each by a factor which allows easy comparison of
the shapes over the range of scattering angles for which we have observations.
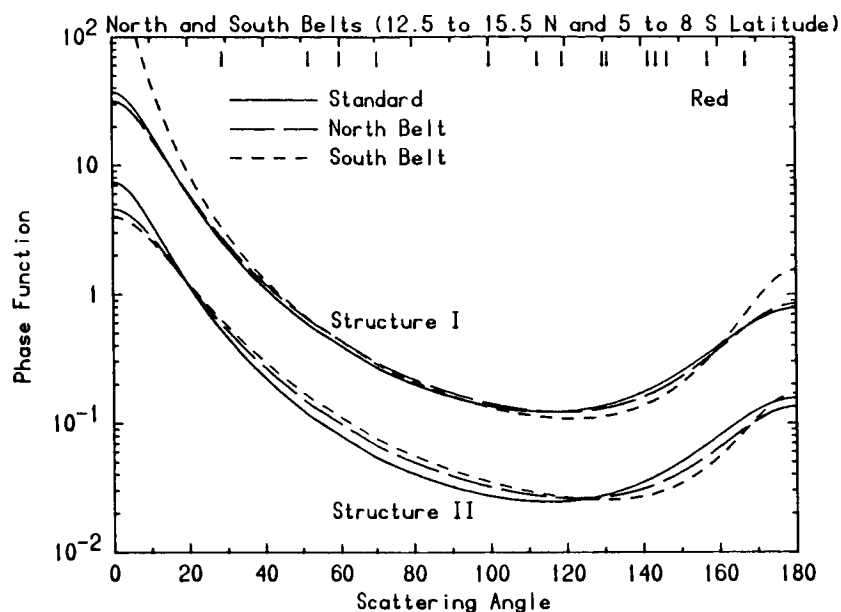
Figure 4. The best-fitting phase functions for a northern belt and a southern belt are similar in shape in red light. The differences are less if Structure I, thought to be closer to the true structure, is used. Vertical bars at the top show the scattering angles of the observations.
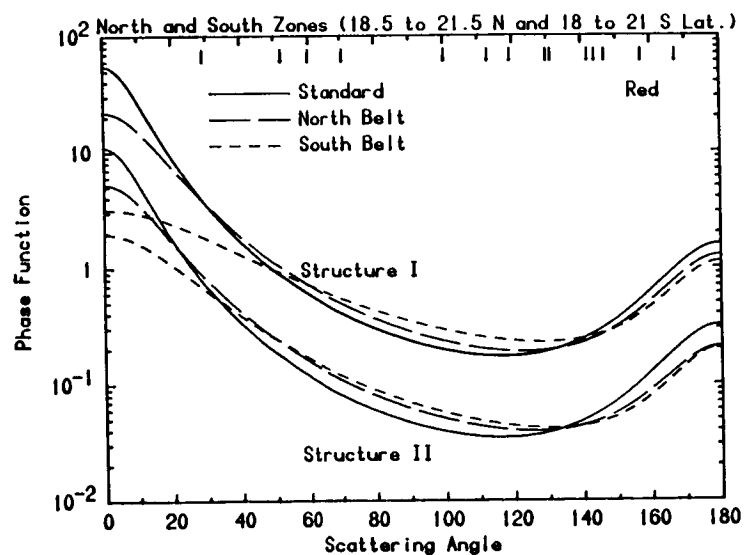
Figure 5. The best-fitting phase functions for a northern zone and a southern zone have similar shapes, and differ only slightly form the standard zone phase function.
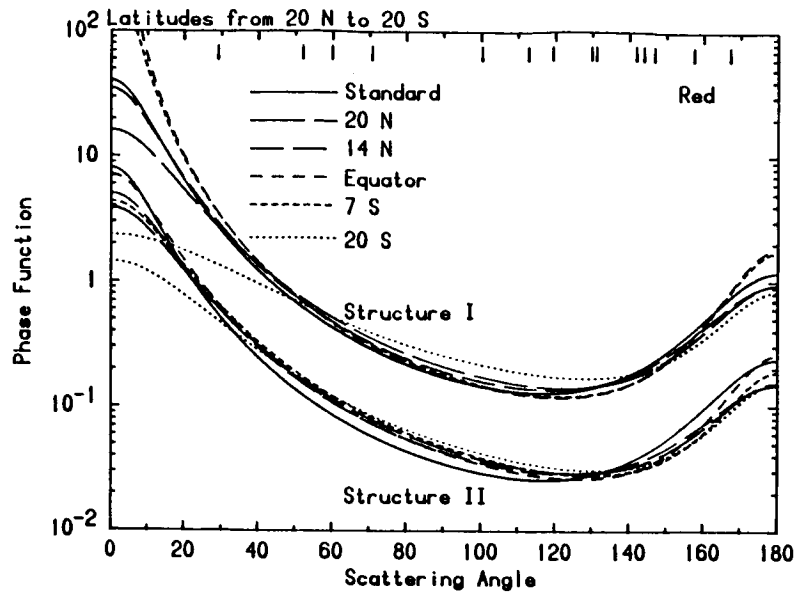
Figure 6. Best-fitting phase functions from six tropical latitudes are all similar in shape in red light. Belts are similar to zones.
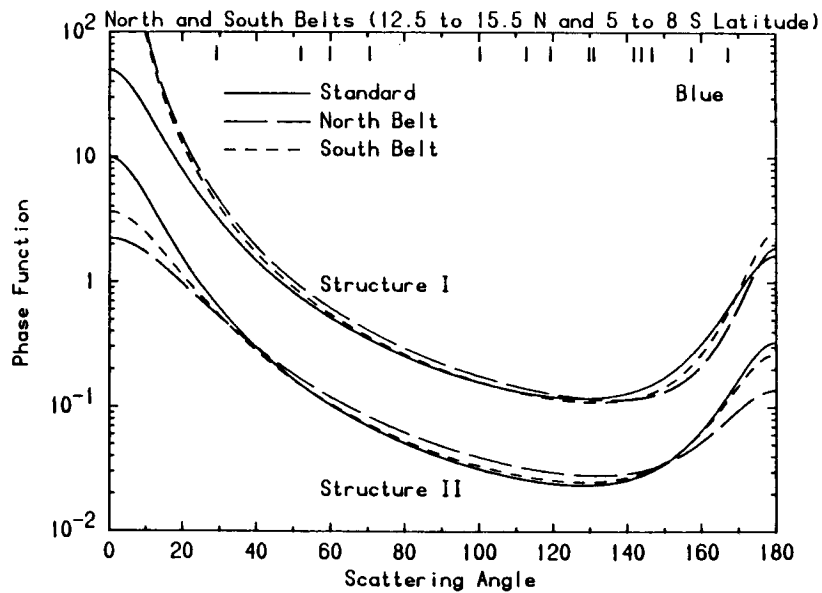
Figure 7. The same belts compared in Fig. 4 in red light are compared here in blue light. The phase functions are again similar in shape to each other and to the standard phase function.
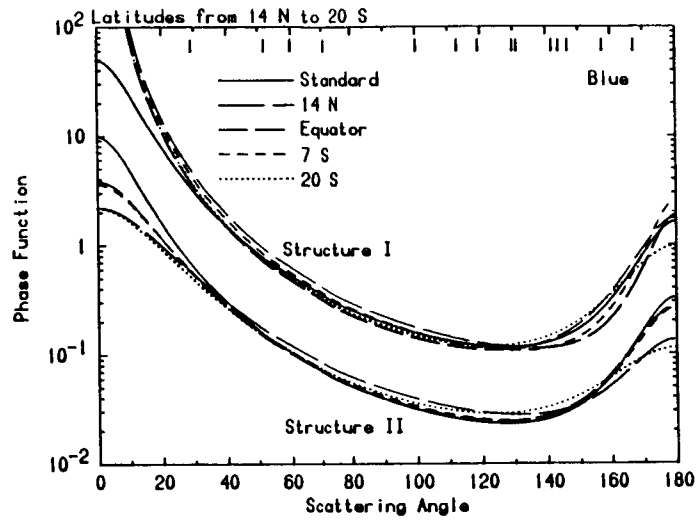
Figure 8. Best-fitting phase functions from
five tropical latitudes are even more similar
in blue light than in red light. Hemispheric
and albedo differences have little effect on
single scattering phase function.
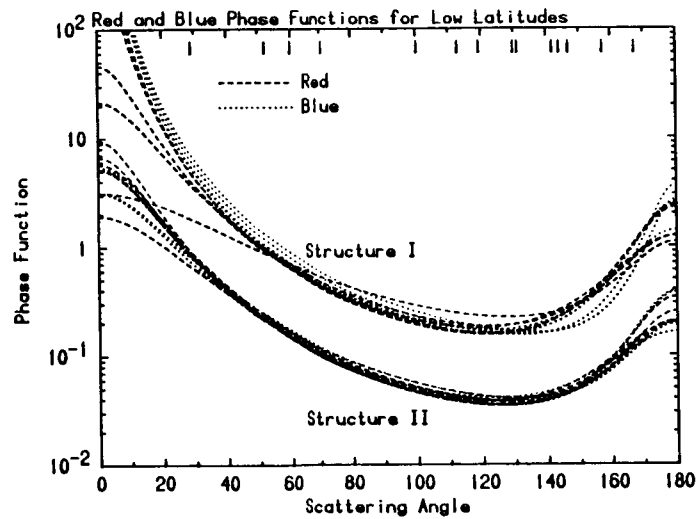
Figure 9. Phase functions derived in the red
and blue are compared for latitudes between 20
deg N and 20 deg S. For Structure I models the
blue phase functions are higher at intermediate
angles and have sharper backward peaks, but even
this marginally significant difference disap-
pears for Structure II models.
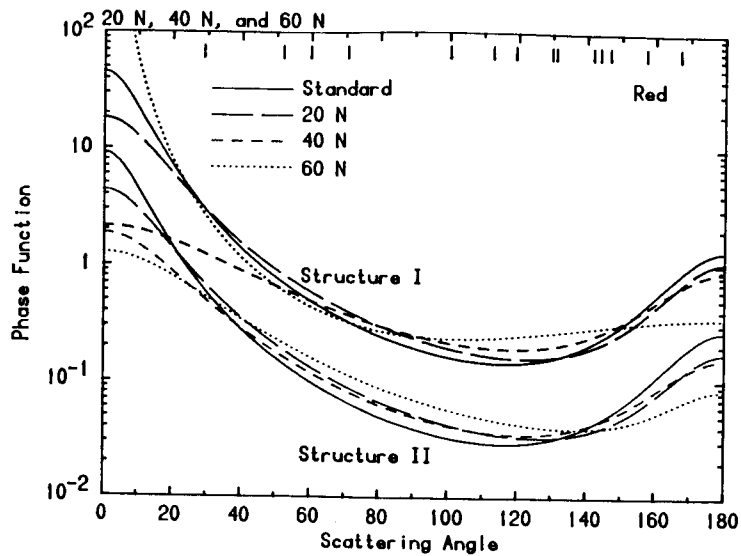
Figure 10. A comparison of three regions shows the latitudinal dependence of the derived phase functions. The particles have significantly different phase functions at 60 deg N.
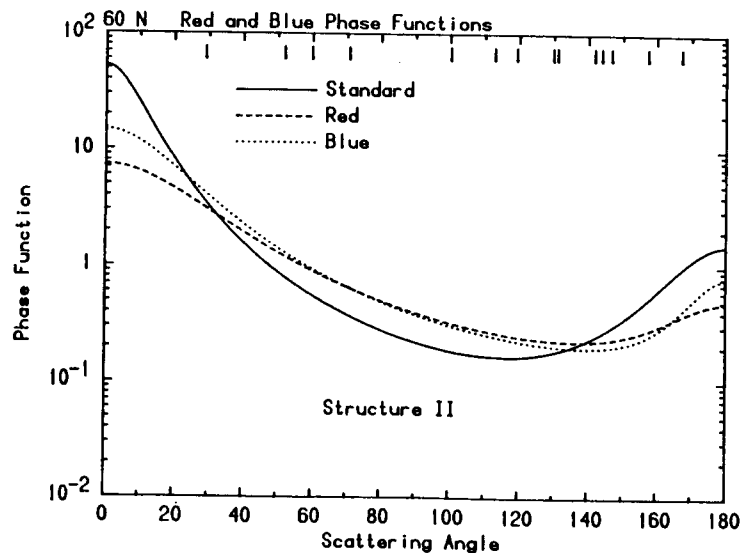
Figure 11. The phase function at 60 deg N has a different shape from the standard in both colors. The backward peak is steeper in blue than in red light, suggesting the presence of smaller particles at high latitudes than at low latitudes.

Figure 4 compares the phase functions for two belts in red light in the north and south hemispheres. Figure 5 is a similar comparison for two zones. In Figs. 4 through 11 the "standard" phase function derived by Tomasko et al. (1978) is included for comparison. Figure 6 compares six tropical latitudes. All of these phase functions are similar to each other and to the standard phase function. The most significant difference occurs at 20 deg S where the phase function is flatter and at the equator and 7 deg S where the backward peak is more pronounced. The difference between the phase functions is marginally significant. The dependence on vertical structure is small. At intermediate scattering angles the phase functions derived using Structure II are 10-20 percent higher than those from Structure I. At large scattering angles this trend is reversed.

Similar comparisons in blue light are shown in Figs. 7 and 8. The phase functions of these low latitude regions appear even more alike in blue light than in red. The dependence on vertical structure is less also, a surprising result considering the larger difference in optical properties in the blue between structures resulting from an increase in optical depth from molecular scattering.

The red and blue phase functions at low latitudes are compared in Fig. 9. For Structure II no significant differences are evident. For Structure I the blue phase functions have a steeper backward peak and a tendency to cross the red phase functions from above to below as the scattering angle increases through intermediate angles. To within our ability to determine the phase functions using double Henyey-Greenstein functions, those at low latitudes are all well represented by the standard phase functions of Tomasko et al. (1978). The lack of dependence on the color of light is indicative of particles large compared to the wavelength.

The phase functions are shown over a wider range of latitudes in Fig. 10. At 60 deg N the phase function is markedly different, being much flatter than those at lower latitudes. This behavior is weakly indicated at 40 deg N also, suggesting a progressive flattening of the function toward higher latitudes beginning somewhere near 40 deg N. Smith and Tomasko (1984) found that the polarization of Jupiter at large phase angles also showed a strong gradient beginning near this latitude. Evidence for an increase in the optical thickness of haze above the clouds at this latitude was also found by Tomasko and Karkoschka. These studies together with Fig. 10 suggest the beginning of a progressive change (with latitude) in the nature of scatterers. Figure 11 shows the phase functions derived at 60 deg N for red and blue light. The flattening of the functions suggests that the scatterers may be smaller than at lower latitudes. In the size range of a few tenths of micrometers the change in the phase function from red to blue becomes predictable. The particles appear smaller (in terms of wavelengths) to the red light, produc- ing a phase function with molecular scattering-like tendencies. This effect is diminished in blue light, in agreement with Fig. 11.

For those who need to use a phase function for radiative transfer modeling, we recommend the double Henyey-Greenstein parameters given in Table 1. For latitudes less than 40 deg the values are those of Tomasko et al. (1978).

We have shown that they apply over a broad range of latitudes. These parameters apply to a model with vertical Structure I, which includes a top haze layer of optical depth 0.25 over a molecular scattering optical depth of 0.04 in the red. In the blue the top layer is molecular scattering with optical depth 0.03 over a haze with optical depth 0.125 over another molecular scattering layer with optical depth 0.05. These layers are above the cloud, which begins at a pressure near 300 mb. The haze has a single Henyey-Greenstein phase function with $g = 0.75$. Its single scattering albedo is 0.95 in the red and 0.995 in the blue. At latitudes larger than 40 deg the haze is thought to be considerably thicker, and a simple optically thick cloud may be a better description of the vertical structure for the purpose of extracting phase functions. The parameters listed are from our solution at 60 deg N using Structure II. For all these latitudes the detailed nature of the forward peak at scattering angles less than 30° may differ from the given phase functions because we have no data to constrain it.

Table 1

Recommended Double Henyey-Greenstein Parameters

	Blue				Red			
	f	g_1	g_2	ω	f	g_1	g_2	ω
Latitudes < 40 deg*								
Belts	0.969	0.8	−0.8	0.97	0.938	0.8	−0.65	0.991
Zones	0.969	0.8	−0.8	0.995	0.938	0.8	−0.7	0.997
Latitudes > 40 deg	0.984	0.65	−0.78	0.988	0.976	0.57	−0.67	0.997

*From Tomasko et al. (1978)

To summarize, for scattering angles at which we are able to constrain the phase functions: (1) In red light at |latitude|<40 deg, belts, zones, and the equatorial region have similar phase functions. (2) This statement is also true for blue light. (3) Red and blue phase functions are similar, indicating the tropospheric cloud particles are large compared to either wavelength. (4) All phase functions derived for low latitudes are in good agreement with those found by Tomasko et al. (1978). (5) At latitudes larger than 40 deg N, the phase functions have less backward peak than at lower latitudes and show a significant difference between red and blue. This suggests the particles are small enough to show a wavelength dependence between 0.44 µm and 0.64 µm. We believe this is due to a thicker (probably photochemical) haze. This interpretation is supported by observations of the polarization and by ultraviolet photometry.

REFERENCES

Orton, G. S. (1975). Spatially resolved absolute spectral reflectivity of Jupiter: 3390-8400 Å. *Icarus* 26, 159-174.

Smith, P. H., and M. G. Tomasko (1984). Photometry and polarimetry of Jupiter at large phase angles. II. Polarimetry of the South Tropical Zone, South Equatorial Belt, and the polar regions from the Pioneer 10 and 11 missions. *Icarus* 58, 35-73.

Tomasko, M. G., E. Karkoschka, and S. Martinek (1986). Observations of the limb darkening of Jupiter at ultraviolet wavelengths and constraints on the properties and distribution of stratospheric aerosols. *Icarus* 65, 218-243.

Tomasko, M. G., R. A. West, and N. D. Castillo (1978). Photometry and polarimetry of Jupiter at large phase angles. I. Analysis of imaging data of a prominent belt and a zone from Pioneer 10. *Icarus* 33, 558-592.

ENHANCED ACETYLENE EMISSION NEAR THE NORTH POLE OF JUPITER

Pierre Drossart, Bruno Bezard, and Therese Encrenaz
Observatoire de Paris, Section de Meudon

Sushil Atreya
University of Michigan

John Lacy
University of Texas

Eugene Serabyn
University of California, Berkeley

Alan Tokunaga
Institute for Astronomy, University of Hawaii

The presentation by Drossart *et al.* is largely contained in a paper which has been submitted to *Icarus*. The abstract of that paper is reproduced here.

We report observations of acetylene emission lines near 13.3 μm on Jupiter recorded at the NASA Infrared Telescope Facility in July, 1984. A strong enhancement in the intensity of the R_7 line of the ν_5 band was recorded within a well-localized region coincident with the southern extension of the footprint of the Io magnetic lines (Dessler, 1983) and with previous observations of localized enhanced emission of CH_4 lines (Caldwell et al., 1980, Icarus 44, 667-675). The line intensity was fairly constant outside this 'bright spot.' Moreover, weak lines of the hot bands $2\nu_5 - \nu_5$, and $(\nu_4 + \nu_5) - \nu_5$ were observed within the bright spot. From the field of view and the precision of the pointing, the zone of activity of the bright spot is found to be: latitude = 59 ± 10 deg and longitude = 178 ± 10 deg (System III, 1965). The location of the spot was found to be constant over a 3 day period. Two interpretations are proposed to explain these observations by (1) a variation of the C_2H_2 abundance and (2) an alteration of the thermal profile in the bright spot. Either may result from precipitation of charged particles near and below the Jovian homopause.

TWO MICRON QUADRUPOLE LINE EMISSION OF H_2 FROM THE JOVIAN AURORAL ZONE

S. Kim and W. Maguire
NASA/Goddard Space Flight Center

Energetic electron bombardment of the H_2 atmosphere in the Jovian auroral zone has been studied using a theoretical model for the vibrational-rotational excitation processes. A non-relativistic electron energy deposition program originally developed by Peterson et al. (1973, Computer Phys. Comm. 5, 239-262) was used. Assuming an incident energy electron spectrum from IUE observations, the calculated intensities of the two micron quadrupole lines from the Jovian auroral zone are shown to be comparable to the intensities of infrared objects in the Orion nebula. Jupiter is fairly dark in the 2-2.5 micron spectral range because of strong absorption of CH_4 and NH_3 vibrational-rotational bands. Consequently, assuming no significant decrease in Jovian auroral activity since the Voyager encounter with Jupiter in 1979, the two micron quadrupole emission of H_2 may be observable by ground-based telescope through the two micron atmospheric window.

Strong 10 micron infrared emission of hydrocarbons in the Jovian auroral zone has been observed from the ground and from the Voyager 1 IRIS instrument. Figure 1 illustrates the infrared emission at 7.8 µm from ground-based observations of the auroral zone. Ultraviolet emission of H_2 has been also detected by Voyager 1 and 2 UV instruments and by the IUE. Yung *et al.* (1982), analyzing the ultraviolet aurora, estimated the electron energy spectrum to be in the range of 1-30 keV.

There are several outstanding scientific questions for these auroral phenomena. Are the particles causing UV aurora also responsible for 10 and 2 micron IR aurora? The derived 1 to 30 keV electrons from UV aurora may not produce the 10 micron IR aurora because these energetic electrons cannot reach hydrocarbon layers in the stratosphere of Jupiter (Fig. 2). A second observation requiring explanation is the discovery of C_2H_4, C_3H_4 and possibly C_6H_6 in the Voyager 1 IRIS spectra of Jupiter's north polar region. To date, we don't have a plausible energetic particle chemistry for creation of these molecules. The third area of investigation is heating and cooling processes in the Jovian auroral zone. This mechanism has been only partially understood.

This presentation is one contribution to solving these outstanding problems. We describe a theoretical model for vibrational excitation and de-excitation processes of H_2, and estimate the 2 micron quadrupole emission flux of H_2. We modified a non-relativistic electron energy deposition program originally developed by Peterson (1973) for calculating the number of vibrational-rotational excitation states of H_2. In the calculation, a continuous slowing-down approximation was used for the energy of incident auroral electrons.
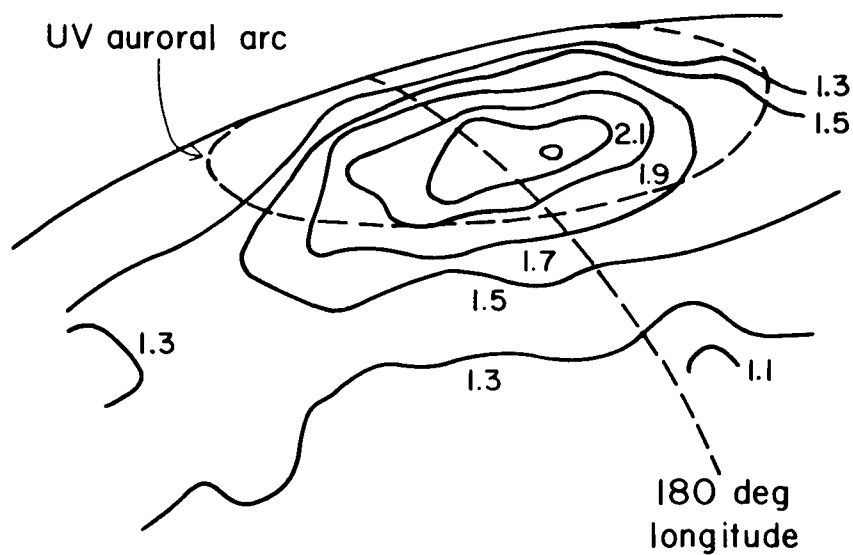
Figure 1. Infrared emission at 7.8 μm for the Jovian auroral zone. Brightness contours are in units of the background intensity.
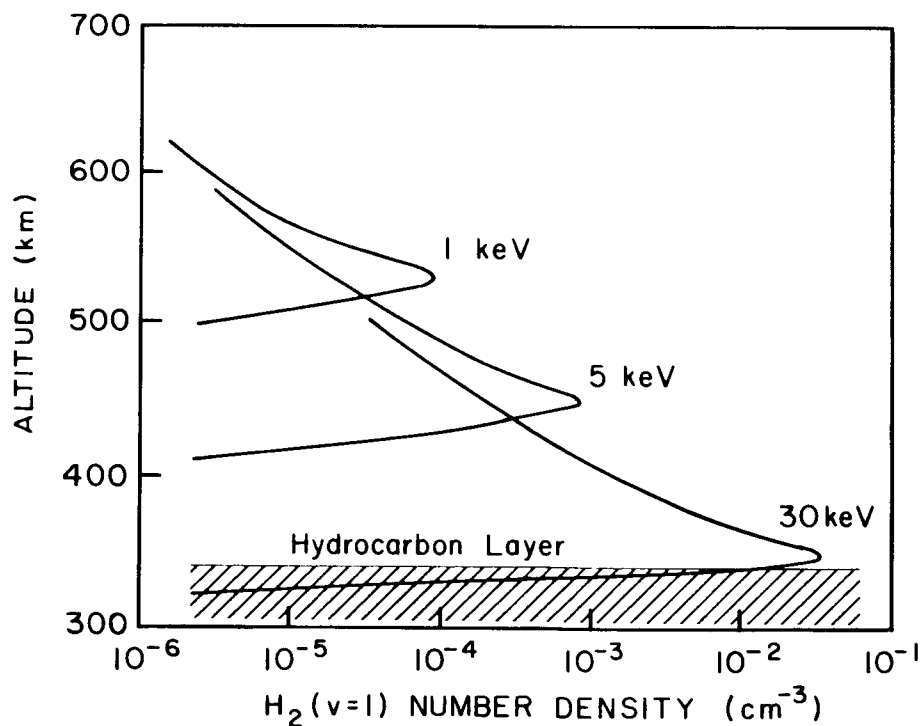
Figure 2. Number densities of $H_2(v=1)$ resulting from the precipitation of an electron of the indicated energy.

An updated cross section compilation for electronic transitions, dissociative excitations, dissociative ionizations, vibrational and rotational excitations was prepared for the input parameters to the electron deposition program. We excluded ohmic dissipation due to currents driven by auroral electric fields. At the present time, we do not have any information about the Jovian auroral electric field. The most uncertain part of the model calculation is the energy flux spectrum of incident electrons on the auroral zone. We used the 1-30 keV electron spectrum derived from UV observations by Yung et al. (1982) for our calculations. For total energy flux, Yung et al. used 10 ergs $cm^{-2}s^{-1}$. This value may be a lower limit for realistic calculations because infrared auroral flux of the 7.8 micron band of CH_4 alone is about 9 erg $cm^{-2}s^{-1}$. Therefore we used 10-100 erg $cm^{-2}s^{-1}$ for the total incident electron flux on the auroral zone. Figure 2 shows results of the number densities of $H_2(v=1)$ as a function of altitude after 1 second irradiation of an auroral electron. The upper, middle, and lower curves correspond to a 1 keV, 5 keV, and 30 keV electron, respectively. Here we arbitrarily set z=0 km at the 1 bar pressure level. A time dependent model of excitation and de-excitation of H_2 has been constructed, with equilibrium number densities of the vibrational de-excitation rate equal to the vibrational excitation rate. The intensity of a quadrupole line is given by

$$I = \frac{h\nu}{4\pi} \int N \frac{A_{ji}}{(A_{ji}+\eta n)} dz.$$

Here h is the Planck constant, ν is the frequency of the quadrupole line, N is the number of excited states per cm^3 per second, A_{ji} is the Einstein coefficient, n is the total number density, η is the total vibrational relaxation coefficient for H_2-He, H_2-CH_4 and H_2-H_2 collisions in units of cm^3 cm^{-1}, and z is the altitude. Table 1 gives a summary for the calculated intensities of the quadrupole lines for 5 keV electrons and a total energy flux of 100 ergs $cm^{-2}s^{-1}$.

Table 1

Calculated Two Micron Quadrupole Line Intensities
(5 keV Electrons, Total Energy Flux = 100 erg $cm^{-2}s^{-1}$)

Line	Position (cm^{-1})	Intensity (erg $cm^{-2}s^{-1}$ $sterad^{-1}$)
$S_1(0)$	4497.84	5.9 x 10^{-3}
$S_1(1)$	4712.91	1.3 x 10^{-2}
$S_1(2)$	4917.01	1.9 x 10^{-3}
$Q_1(1)$	4155.26	2.5 x 10^{-2}
$Q_1(2)$	4143.47	6.4 x 10^{-3}
$Q_1(3)$	4125.87	1.2 x 10^{-2}

Our calculated intensities are comparable to those of infrared objects in the Orion nebula. Since Jupiter is fairly dark in the 2 micron region, the 2 micron quadrupole emission of H_2 may be observable by ground-based telescope through the 2 micron atmospheric window. The observed line intensities can provide the energy spectrum of incoming auroral particles.

REFERENCES

Peterson, L. R., T. Sawada, J. N. Bass, and A. E. S. Green (1973). Electron energy deposition in a gaseous mixture. *Computer Phys. Comm.* 5, 239-262.

Yung, Y. L., G. R. Gladstone, K. M. Chang, J. M. Ajello, and S. K. Srivastava (1982). H_2 fluorescence spectrum from 1200 to 1700 Å by electron impact: Laboratory study and application to Jovian aurora. *Astrophys. J. Lett.* 254, L65-L69.

BROWN DWARFS AND JOVIAN PLANETS: A COMPARISON

J. I. Lunine, W. B. Hubbard, and M. Marley
Lunar and Planetary Laboratory, University of Arizona

The recent detection of a subluminous companion to the M dwarf star VB8 (McCarthy et al., 1985, Astrophys. J. 290, L9) has renewed interest in the characteristics of objects spanning the mass range from Jupiter to hydrogen burning stars. We have constructed atmospheric and interior models for objects in this mass regime, up to 30 Jupiter masses, with emphasis on understanding the relationship of "brown dwarfs" such as the VB8 companion to the better-studied Jovian planets. The atmospheric model solves the equation of radiative transfer assuming frequency dependent molecular opacity sources H_2, He, H_2O, CO, and CH_4 which are important by virtue of the high cosmic abundance of their constituent atoms. Condensation of cosmochemically important materials, iron and silicates, in the atmosphere is possible, and the effect of such grains as opacity sources is assessed. The luminosity of the object is presumed due to degenerate cooling following a collapse phase and possibly deuterium burning (Stevenson, 1978, Proc. Astron. Soc. Austral. 3, 227-229), and an interior model is constructed using as an outer boundary condition the temperature and pressure level at which the atmosphere becomes convective. The interior model is analogous to Jupiter, with a large liquid metallic-hydrogen core and a thinner molecular-hydrogen envelope. At intermediate depths, a zone of neutral atomic hydrogen may be of much greater importance than in the interior of Jupiter. Although the physics of this region is extremely difficult to treat, the assumption that the interior is isentropic allows computation of the temperature-pressure profile through this region by interpolation from lower and higher pressures. The oxidation state of carbon in the outer envelope of a brown dwarf of similar age to Jupiter is a function of the object's mass: a 30 Jupiter-mass object would have CO, rather than CH_4, as the primary carbon species. This makes the wavelength dependence of the atmospheric opacity sensitive to the carbon to oxygen ratio, since the abundance of the primary source of molecular opacity, H_2O, decreases as more oxygen is tied up as CO. We display the infrared spectrum of brown dwarfs of various masses and ages, and assess the possibility of deriving compositional information on these objects from future infrared observations.

The presentation summarized by the above abstract was the preliminary report of work which has now been published in several papers listed below. Details of the work may be found there.

REFERENCES

Hubbard, W. B. (1986). Evolution of super-Jupiters. In *Astrophysics of Brown Dwarfs* (M. Kafatos, Ed.). Cambridge Univ. Press, Cambridge, in press.

Lunine, J. I. (1986). Compositional indicators in infrared spectra of brown drawfs. In *Astrophysics of Brown Dwarfs* (M. Kafatos, Ed.). Cambridge Univ. Press, Cambridge, in press.

Lunine, J. I., W. B. Hubbard, and M. S. Marley (1986). Evolution and infrared spectra of brown dwarfs. *Astrophys. J.*, submitted.

A POSSIBLE DEUTERIUM ANOMALY: IMPLICATIONS OF THE CH_3D/CH_4 MIXING RATIOS IN THE ATMOSPHERES OF JUPITER, SATURN, AND URANUS

Barry L. Lutz
Lowell Observatory

Catherine de Bergh
Observatoire de Meudon

Tobias Owen
State University of New York at Stony Brook

Observations of CH_3D in the atmospheres of the outer planets provide a test of the theory of deuterium fractionation equilibrium in the formation and evolution of these planets. Recent measurements of the CH_3D/CH_4 mixing ratios made for Saturn and Uranus are presented and intercompared with current values for Jupiter, illustrating large differences between the planets. Their implied D/H ratios are compared to D/H ratios derived from measurements of HD/H_2; and, in the cases of Jupiter and Saturn, they may be incompatible. Implications of these comparisons are discussed in terms of the deuterium fractionation chemistry and possible enrichments of deuterium in the core ices of the planets.

INTRODUCTION

Hubbard and MacFarlane (1980) have suggested that equilibrium partitioning of deuterium among various molecular species in the cold protosolar nebula would yield a significant enrichment of it in the icy cores of the giant planets. For Uranus and Neptune, this primordial isotopic fractionation could lead to observable enrichments in the bulk D/H ratios in their present-day atmospheres if a substantial fraction of these atmospheres is derived from the icy cores and thoroughly mixed with subsequently accreted envelopes of hydrogen-rich, nebular composition, and if equilibrium repartitioning of the deuterium is re-established in the atmosphere.

The level of primordial fractionation that may have occurred in the proto-solar nebula is uncertain. Under low-temperature conditions, such as those associated with the canonical solar system formation scenario, the time scale for neutral gas-phase equilibrium partitioning exceeds the age of the universe (Beer and Taylor, 1973). However, catalysis on solid grain surfaces present in the nebular material (Black, 1973) or ion-molecule reactions in the antecedent interstellar cloud (Solomon and Woolf, 1973) can avoid this problem and provide a substantial enhancement of deuterium in the condensible volatiles. Such *ad hoc* processes are sometimes invoked to explain the enhancement of deuterium in certain meteorites as well as in the terrestrial waters.

Whether or not equilibrium repartitioning of the ice-trapped deuterium occurs between the enriched volatiles which outgas from a planet's icy core and any hydrogen envelope which may have accreted subsequent to the core formation is also uncertain. Since there is insufficient time for gas-phase equilibrium to be established at temperatures below about 450 K, an internal heat source is required to drive convective mixing of the hydrogen-rich envelope with the hot interior gases where deuterium exchange can proceed.

If this repartitioning occurs, its effect is to dilute the primordial deuterium enhancement in the outgassed volatiles while increasing the bulk D/H ratio in the overall atmosphere. Based on this scenario and an assumed primordial enrichment by at least a factor of 10, Hubbard and MacFarlane predicted lower limits of about 10^{-4} for the D/H ratios in the atmospheres of Uranus and Neptune.

THE D/H RATIO IN THE OUTER SOLAR SYSTEM

Methane is the most abundant volatile in the atmospheres of the outer planets. Its singly substituted deuteride, CH_3D, is a well-suited tracer of deuterium, and its relative abundance is a test of fractionation equilibrium. Figure 1 shows how D/H ratios are derived from the methane isotopes and from H_2 and HD measurements and gives the relationship between these two ratios if deuterium fractionation has reached equilibrium through chemical exchange reactions of the type shown.

THE MOLECULAR EXCHANGE REACTION
WHICH CONTROLS THE DISTRIBUTION OF
DEUTERIUM IN A MIXTURE
OF H_2 AND CH_4 IS:

$$HD + CH_4 \rightleftharpoons CH_3D + H_2$$

THE $\left[\dfrac{D}{H}\right]$ RATIOS IN EACH
COMPONENT GAS ARE:

$$\left[\frac{D}{H}\right]_{H_2} = \frac{1}{2}\frac{|HD|}{|H_2|}$$

$$\left[\frac{D}{H}\right]_{CH_4} = \frac{1}{4}\frac{|CH_3D|}{|CH_4|}$$

IN EQUILIBRIUM, THE COMPONENT $\left[\dfrac{D}{H}\right]$
RATIOS ARE RELATED BY:

$$\left[\frac{D}{H}\right]_{H_2} = \frac{1}{f}\left[\frac{D}{H}\right]_{CH_4} = \frac{1}{4f}\frac{|CH_3D|}{|CH_4|}$$

Figure 1. Schematic represenation of deuterium fractionation in CH_4 and H_2.
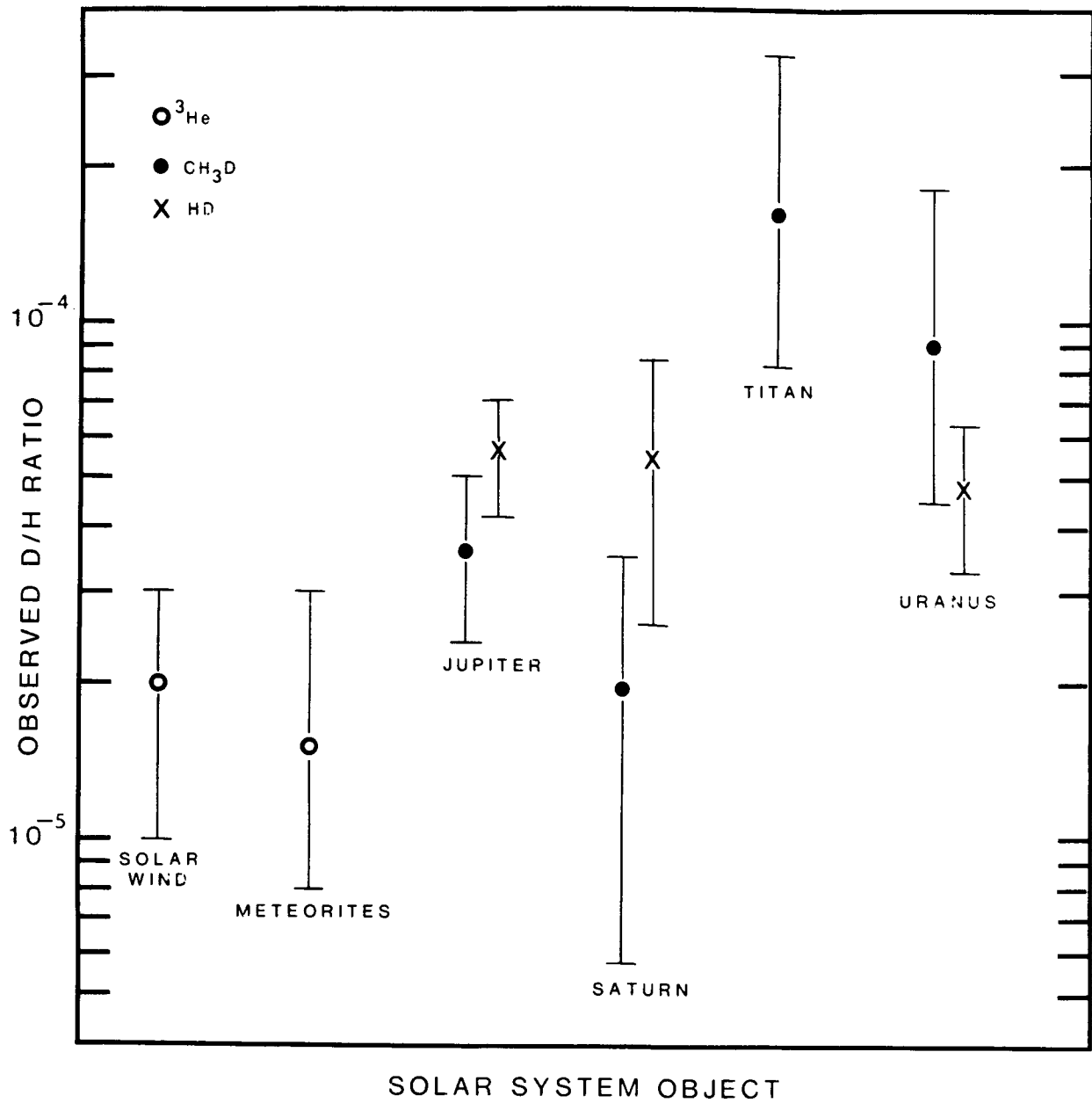
Figure 2. Comparison of the D/H ratios represented in the hydrogen and methane components of outer solar system atmospheres and as deduced from observations of [3]He.

Figure 2 summarizes the current estimates of the D/H ratios in the outer solar system for both the methane and the molecular hydrogen components and compares them with the protosolar values deduced from mass spectroscopic measurements of ^{3}He in the solar wind and in meteorites (Geiss and Reeves, 1981). The ratios derived from methane in the atmospheres of Uranus and Titan are taken from our own simultaneous study of CH_3D and CH_4 absorption in the spectra at 1.6 μm (de Bergh et al., 1985a, 1985b); Saturn's methane ratio is a mean of our ground-based value (de Bergh et al., 1985c) and the recently published Voyager estimate (Courtin et al., 1984); and for Jupiter, the methane ratio is a weighted mean of published ground-based (Beer and Taylor, 1973, 1978; Knacke et al., 1982) and Voyager results (Drossart et al., 1982; Kunde et al., 1982). These values represent the D/H ratios in methane; that is, the D/H ratios are taken as the stoichiometric values $1/4\ [CH_3D/CH_4]$, which, if in equilibrium, would be related to the D/H ratio in hydrogen gas by the fractionation factor f, illustrated in Fig. 1. The ratios for molecular hydrogen are derived from a spectroscopic study of H_2 and HD absorption in the visible spectra of the planets and are taken directly from the literature (Trafton and Ramsay, 1980; Macy and Smith, 1978; Trauger et al., 1977; McKellar et al., 1976).

The comparison of the D/H ratios in methane with the protosolar values derived from the ^{3}He content of the solar wind and of meteorites provides a number of results which, exclusive of the D/H ratios in the atmospheric molecular hydrogen, bear on the Hubbard and MacFarlane deuterium fractionation theory.

1. Deuterium in methane in the atmosphere of Uranus is enhanced relative to the protosolar values derived from the solar wind and meteorites, nominally by a factor of nearly 5. Such an enhancement is consistent with the Hubbard-MacFarlane postulates that, in contrast to Jupiter and Saturn, the present-day atmosphere of Uranus has a significant contribution of volatiles that outgassed from the icy core of Uranus and that those ices are enhanced in deuterium by fractionation.

2. A similar enhancement of deuterium in methane occurs in the atmosphere of Titan, nominally by a factor of 10 over the solar wind and meteoritic values. This enrichment is further supportive of the Hubbard-MacFarlane proposal of core-ice enrichment since Titan's atmosphere is thought to be derived entirely from its interior.

3. The average deuterium content in the methane component of the atmospheres of Jupiter and Saturn is only slightly enhanced over the protosolar values derived from the solar wind and meteorites. Such a marginal enhancement suggests that any deuterium-enriched, interior ices in the cores of these planets have had little or no effect on the isotopic composition of the atmospheric methane. This conclusion is also consistent with the Hubbard-MacFarlane model.

The analogous comparison of the D/H ratios in hydrogen component of the planetary atmospheres with solar wind and meteoritic values is somewhat chancy since the D/H ratios derived from HD and H_2 observations is very uncertain. In addition, recent remeasurements of the molecular parameters needed for analysis of planetary observations (Cochran and Smith, 1983) suggest that the published values of D/H derived from HD and H_2 observations may require an upward

revision by as much as a factor of 2. However, there are trends present in these data which relate to deuterium fractionation, and since they may imply a possible deuterium anomaly in the molecular hydrogen component of the protosolar nebula, they are deserving of speculation.

1. The planetary ratios in molecular hydrogen do not exhibit the differentiation that Hubbard and MacFarlane predicted. This observation appears to contradict the methane results, which show significant differences among the planets, and suggests that, in some cases, the atmospheric deuterium in methane and hydrogen may not be fractionation equilibrium. In fact, for Jupiter and Saturn the D/H ratios may be smaller in methane than in molecular hydrogen, a situation which is chemically impossible if fractionation equilibrium has been reached. If the upward revisions in the hydrogen results are sustained, this discrepancy is assured.

2. For Uranus, fractionation equilibrium may have been established if the published D/H ratio in molecular hydrogen shown in Fig. 1 is accepted, but it is less certain if that ratio is a factor of 2 higher, as the new molecular parameters for hydrogen may suggest. At the level of precision of the current data complicated by the uncertain reliability of the analysis of the HD lines, it is not possible to distinguish between a fractionation equilibrium situation and a coincidental agreement. The apparent agreement among the D/H ratios in molecular hydrogen in the atmospheres in all the planets seems to argue against any significant differential enhancement; but, if the D/H ratio for Titan is indicative of the maximum level of enrichment in the primordial core ices, a measureable enhancement in molecular hydrogen by the outgassing from these ices is unlikely even if equilibrium is reached.

3. The D/H ratios in molecular hydrogen do not appear to be protosolar in any of the atmospheres of the outer planets, regardless of which set of molecular parameters is chosen to derive these ratios. The planetary values are excluded from the range of D/H estimates deduced from the solar wind and meteorite observations, and may indeed be significantly enriched over that range. However, deuterium fractionation is probably not responsible for the enhancement. Apparently high D/H ratios from molecular hydrogen observations could result if the scattering processes that affect the very weak lines of HD have been underestimated or if the possible presence of weak methane absorption in the same spectral region has contaminated the observations.

It seems that these data support the general concept of deuterium enrichment in the ices that make up the cores of the outer planets, but molecular hydrogen in the outer planet atmospheres presents us with a possible deuterium anomaly. Gaseous hydrogen appears uniformly enriched in dueterium over the protosolar value in all the outer planets, but the source of this enrichment does not appear to be the result of fractionation equilibrium with methane and in fact may be in contradiction to the methane results. What processes are needed to be invoked to explain this anomaly is not yet known, but with better observations and improved analyses the constraints needed to define them may be forthcoming.

106

REFERENCES

Beer, R., and F. W. Taylor (1973). The abundance of CH_3D and the D/H ratio in Jupiter. *Astrophys. J.* 179, 309-327.

Beer, R., and F. W. Taylor (1978). The D/H and C/H ratios in Jupiter from the CH_3D phase. *Astrophys. J.* 219, 763-767.

Black, D. C. (1973). Deuterium in the early solar system. *Icarus* 19, 154-159.

Cochran, W. D., and W. H. Smith (1983). Desaturation of H_2 quadrupole lines in the atmospheres of the outer planets. *Astrophys. J. 271, 859-864.*

Courtin, R., D. Gautier, A. Marten, and B. Bezard (1984). *Astrophys. J.* 287, 899-916.

de Bergh, C., B. L. Lutz, T. Owen, J. Brault, and J. Chauville (1985a). Monodeuterated methane in the outer solar system. II. Its detection on Uranus at 1.6 microns. *Astrophys. J.,* in press.

de Bergh, C., B. L. Lutz, T. Owen, and J. Chauville (1985b). Monodeuterated methane in the outer solar system. III. Its abundance on Titan. In preparation.

de Bergh, C., B. L. Lutz, T. Owen, and J. Chauville (1985c). Monodeuterated methane in the outer solar system. IV. Its abundance on Saturn. In preparation.

Drossart, P., T. Encrenaz, V. Kunde, R. Hanel, and M. Combes (1982). An estimate of the PH_3, CH_3D, and GeH_4 abundances on Jupiter from the Voyager IRIS data at 4.5 μm. *Icarus* 49, 416-426.

Geiss, J., and H. Reeves (1981). Deuterium in the solar system. *Astron. Astrophys.* 93, 189-199.

Hubbard, W. B., and J. J. MacFarlane (1980). Theoretical predictions of deuterium abundances in the Jovian planets. *Icarus* 44, 676-682.

Knacke, R. F., S. J. Kim, S. T. Ridgway, and A. T. Tokunaga (1982). The abundances of CH_4, CH_3D, NH_3, and PH_3 in the troposphere of Jupiter derived from high-resolution 1100-1200 cm^{-1} spectra. *Astrophys. J.* 262, 388-395.

Kunde, V. G., R. Hanel, W. Maguire, D. Gautier, J. P. Baluteau, A. Marten, A. Chedin, N. Husson, and N. Scott (1982). The tropospheric gas composition of Jupiter's North Equatorial Belt (NH_3, PH_3, CH_3D, GeH_4, H_2O) and the Jovian D/H isotopic ratio. *Astrophys. J.* 263, 443-467.

Macy, W., Jr., and W. H. Smith (1978). Detection of HD on Saturn and Uranus, and the D/H ratio. *Astrophys. J.* 222, L73–L75.

McKellar, A. R. W., W. Goetz, and D. A. Ramsay (1976). The rotation-vibration spectrum of HD: Wavelength and intensity measurements of the 3–0, 4–0, 5–0, and 6–0 electric dipole bands. *Astrophys. J.* 207, 663–670.

Solomon, P. M., and N. J. Woolf (1973). Interstellar deuterium: Chemical fractionation. *Astrophys. J.* 180, L89–L92.

Trafton, L., and D. A. Ramsay (1980). The D/H in the atmosphere of Uranus: Detection of the $R_5(1)$ line of HD. *Icarus* 41, 423–429.

Trauger, J. T., F. L. Roesler, and M. E. Michelson (1977). The D/H ratios on Jupiter, Saturn, and Uranus based on new HD and H_2 data. *Bull. Amer. Astron. Soc.* 9, 516.

THE ABUNDANCES OF ETHANE TO ACETYLENE IN THE ATMOSPHERES OF JUPITER AND SATURN

K. S. Noll and R. F. Knacke
State University of New York at Stony Brook

A. T. Tokunaga
University of Hawaii

J. H. Lacy
University of Texas, Austin

S. Beck
Northeastern University

E. Serabyn
University of California, Berkeley

The presentation by Noll *et al.* is largely contained in a paper which appears in the special issue of *Icarus* (1986; 65, 257-263). The abstract of that paper is reproduced here.

Infrared spectra near 780 cm^{-1} of Jupiter and Saturn have been obtained to determine the stratospheric abundances of ethane (C_2H_6) and acetylene (C_2H_2). Atmospheric models using Voyager thermal profiles and density profiles with constant mixing ratios result in the mixing ratios, $X(C_2H_2) = 1.0(\pm0.3) \times 10^{-7}$ and $X(C_2H_6) = 5.5(\pm1.5) \times 10^{-6}$ for Jupiter. The results for Saturn are $X(C_2H_2) = 3.0(\pm1.0) \times 10^{-7}$ and $X(C_2H_6) = 7.0(\pm1.5) \times 10^{-6}$. The ratio of ethane to acetylene, $n[C_2H_6]/n[C_2H_2]$, is found to be insensitive to model atmosphere assumptions. The ratio is 55 ± 31 for Jupiter and 23 ± 12 for Saturn from models with uniform mixing ratios. Atmospheric models with density profiles adapted from theoretical photochemical models also result in a higher ratio of ethane to acetylene (by a factor of 2 at the 1 mbar level) on Jupiter. The lower abundance of acetylene on Jupiter suggests that the rate of vertical transport in the stratosphere may be more rapid on Saturn than on Jupiter.

A DETECTED FEATURE AT THE EXPECTED WAVELENTH FOR THE HD $R_5(0)$ LINE IN JUPITER'S AND URANUS' ATMOSPHERES

Wm. Hayden Smith and William Schempp
Washington University

William Macy
Lockheed Research Laboratory

The presentation by Smith *et al.* is largely contained in a paper which has been submitted to *Icarus*. The abstract of that paper is reproduced here.

We have detected a feature at the expected wavelength for the HD $R_5(0)$ line in Jupiter's and Uranus' atmospheres. We also have an upper limit for Neptune. Added to our earlier detection of a similar feature for Saturn, we propose that all evidence from this type of measurement can be interpreted as arising from a D/H ratio of about 10^{-4} for all the major planets. This value is not in agreement with measurements from CH_3D transitions, and is at least fifty times the accepted interstellar medium value of 5×10^{-6}, implying deuterium enhancement in the solar system via fractionation in the proto-solar nebula.

LABORATORY MEASUREMENTS OF MICROWAVE ABSORPTION FROM GASEOUS ATMOSPHERIC CONSTITUENTS UNDER CONDITIONS FOR THE OUTER PLANETS

Paul G. Steffes
Georgia Institute of Technology

Quite often, the interpretive work on the microwave and millimeter-wave absorption profiles, which are inferred from radio occultation measurements or radio astronomical observations of the outer planets, employs theoretically-derived absorption coefficients to account for contributions to the observed opacity from gaseous constituents. Variations of the actual absorption coefficients from those which are theoretically derived, especially under the environmental conditions characteristic of the outer planets, can result in significant errors in the inferred abundances of the absorbing constituents. The recognition of the need to make laboratory measurements of the absorptivity of gases such as NH_3, CH_4, and H_2O in a predominantly H_2 atmosphere, under temperature and pressure conditions simulating the outer planets' atmospheres, and at wavelengths corresponding to both radio occultation and radio astronomical observations, has led to the development of a facility capable of making such measurements at Georgia Tech. We describe the laboratory measurement system, the measurement techniques, and the proposed experimental regimen for Winter 1986; with the goal of obtaining feedback from interested investigators on the relative priorities of the various proposed measurements to be made on specific constituents at specific wavelengths.

INTRODUCTION AND SUMMARY

Radio absorptivity data for planetary atmospheres obtained from spacecraft radio occultation experiments and earth-based radio astronomical observations can be used to infer abundances of microwave absorbing atmospheric constituents in those atmospheres, as long as reliable information regarding the microwave absorbing properties of potential constituents is available. The use of theoretically-derived microwave absorption properties for such atmospheric constituents, or laboratory measurements of such properties under environmental conditions which are significantly different than those of the planetary atmosphere being studied, often lead to significant misinterpretation of available opacity data. Steffes and Eshleman (1981) showed that under environmental conditions corresponding to the middle atmosphere of Venus, the microwave absorption due to atmospheric SO_2 was 50 percent greater than that calculated from Van Vleck-Weiskopff theory. Similarly, the opacity from gaseous H_2SO_4 was found to be a factor of 7 greater than theoretically predicted for conditions of the Venus middle atmosphere (Steffes and Eshleman, 1982). The recognition of the need to make such measurements over a range of temperatures and pressures which correspond to the periapsis altitudes of radio occultation experiments, and over a range of frequencies

which correspond to both radio occultation experiments and radio astronomical observations, has led to the development of a facility at Georgia Tech which is capable of making such measurements.

Recently, we have completed shorter wavelength measurements (1 to 3 cm) of the microwave absorptivity of gaseous sulfuric acid under simulated Venus conditions, as well as completing additional vapor pressure studies of H_2SO_4. In September, 1985, we began reconfiguring the planetary atmospheric simulator so as to begin measurements under simulated conditions for the atmospheres of the outer planets (pressures from 1 to 6 atmospheres, temperatures from 150 K to 300 K, and wavelengths from 1 to 22 cm). Since the outer planet atmospheres are predominantly hydrogen and helium, special procedures are being employed for handling and operating in the simulated atmospheres. The microwave absorbing constituents which will be evaluated included ammonia (NH_3) and methane (CH_4), but other constituents may also be tested. In addition to the laboratory work being conducted, application of the absorptivity measurements to observations will be used to develop more accurate profiles for the abundance and structure of microwave absorbing constituents in the atmospheres of the outer planets.

We believe that this effort fulfills a pressing need in the area of planetary radar and radio astronomy. It will provide a better basis for interpretation of existing radio absorptivity data from Voyager 1 and 2 encounters of Jupiter and Saturn, and from expected encounters with Uranus (January 1986) and Neptune (August 1989). It will continue to provide similar bases for interpretation for a wide range of radio astronomical observations of the atmospheres of Jupiter, Saturn, Uranus, and Neptune. (This is especially relevant to a wide range of observations made with the NRAO Very Large Array (VLA) which is currently capable of operations in the 10-0.8 cm wavelength range.) Finally, this program will continue to provide information which will be extremely useful in data analysis and mission planning for new missions such as Galileo.

JUPITER AND SATURN

Jupiter and Saturn have been the subject of both radio occultation and radio astronomical studies. At Jupiter, microwave absorption in the atmosphere has been measured by Voyager radio occultations from about the 0.6 atm pressure level down to the 1.0 atm pressure level at 13 and 3.6 cm wavelengths (Lindal et al., 1981). At Saturn, the same measurements probed down to the 1.4 atm pressure level. Radio astronomical observations in the 1 to 20 cm wavelength range have probed to even lower altitudes (10 atm pressure or greater--see Berge and Gulkis, 1976). In addition, a large number of radio occultation measurements to be made with the Galileo orbiter, plus data collected with the Galileo entry probe (21.4 cm wavelength) will provide an even larger data base of microwave absorptivity data.

For altitudes with pressures less than about 4 atm, gaseous NH_3 has been recognized as the predominant microwave absorber. Below this altitude, liquid clouds begin to contribute to the observable opacity (see Galileo Probe Project Specification, 1980). Since only a single measurement of the

microwave absorption properties of NH_3 in an H_2/He atmosphere has been made, (at a single pressure and frequency) we propose to make such measurements in a pressure range from 1 to 6 atmospheres, over a temperature range from 150 K to 300 K, and over a wavelength range from 1 to 22 cm. These measurements would provide an invaluable tool for the interpretation of existing and future radio occultation and radio astronomical data, in addition to greatly reducing current uncertainties as to the NH_3 abundances suggested by such data.

URANUS

Uranus presents one of the most exciting and challenging planetary targets of modern astronomy. Radio astronomical measurements made by Gulkis revealed a microwave spectrum vastly different from those of Jupiter and Saturn. This, and other data, led Gulkis et al. (1978) to suggest that the abundance of NH_3 in the Uranus atmosphere may be significantly depleted. In addition, similar studies have suggested a much lower abundance of any microwave absorbing cloud layers than on Jupiter or Saturn (Wallace, 1980).

These results suggest that the upcoming Voyager 2 radio occultation of Uranus may probe to a much deeper level than was probed at Jupiter or Saturn (down to several atmospheres pressure), and that any measured microwave opacity might be that due to methane (CH_4), in addition to, or even to the exclusion of NH_3 (Fox, 1974). With this in mind, we are proposing to measure the absorptivity of CH_4 in an H_2/He atmosphere over a wavelength range from 1 to 22 cm, over a pressure range from 1 to 6 atmospheres, and over a temperature range from 140 K to 200 K. These measurements would provide critically needed data for interpretation of the microwave spectra from radio astronomical observations and for interpretation of absorptivity data from the 1986 Voyager 2 radio occultation experiment.

LABORATORY FACILITY

The experimental approach used to measure the microwave absorptivity and refractivity of gases in a predominantly H_2 atmosphere is similar to that used previously by Steffes and Eshleman (1981 and 1982). As can be seen in Fig. 1, the absorptivity is measured by observing the effects of the introduced gas mixture on Q, or quality factor, of a cavity resonator. The changes in the Q of resonances at numerous frequencies can be monitored by the high resolution spectrum analyzer, since Q is simply the ratio of the frequency of a given resonance to its half-power bandwidth. One resonator provides useful resonances in the 1.3 to 8.5 GHz range, while a smaller unit provides resonances in the 8 to 30 GHz range. The minimum measureable absorptivity, or sensitivity, for this system when operated at 170 K is shown in Fig. 2 as a function of frequency.

One of the major considerations for simulation of the atmospheres of outer planets is refridgeration. Currently, we have available a non-cryogenic refridgerative unit capable of maintaining temperatures down to 140 K. Cryogenic cooling (liquid nitrogen) would be used for lower temperatures.
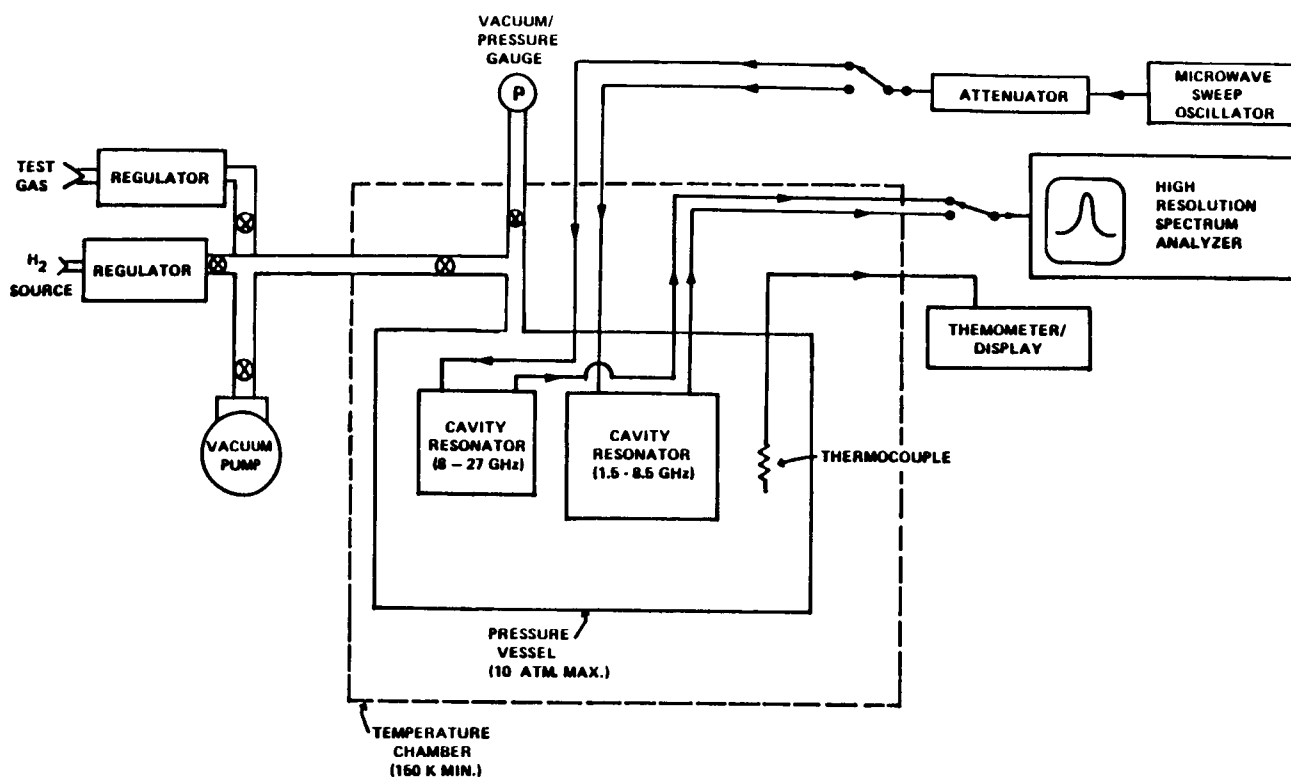
Figure 1. Block diagram of the Georgia Tech Planetary Atmospheres Simulator, as configured for measurements of microwave refraction and absorption of gases under simulated conditions for the outer planets.

Table 1

Minimum Gaseous Abundances Necessary for Measurement by System

Constituent Gas	Abundance of Gas in H_2 atmosphere (total pressure= 6 atm) required for measurement	Partial Pressure of Gas (in atm)	Lowest Possible Temperature for which required abundance can be achieved (K)
NH_3	60 ppm	3.6×10^{-4}	155
H_2-H_2, H_2-He (collisional)	80% H_2 : 20% He	6	20
CH_4	33%	2	120
CO	Not Detectable	---	---

WAVELENGTH (cm)
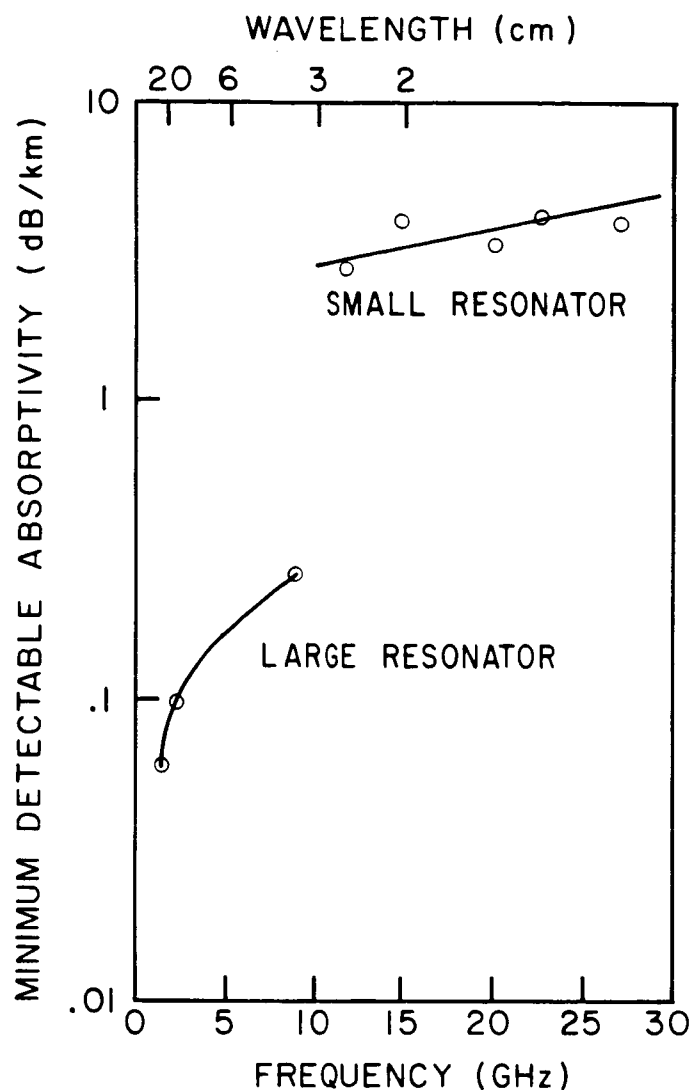
Figure 2. Sensitivity of Planetary
Atmospheres Simulator as a function
of frequency when operated at 170 K.

Another more critical limitation on how low the temperatures can be taken
while still measuring microwave absorption is the saturation vapor pressure
of the gas being tested. As shown in Table 1, the lowest temperature for
which sufficient quantities of gaseous NH_3 would still exist so that the
microwave absorption would be measurable would be $\approx$155 K. While this would
be fine as a Jupiter simulation, it is somewhat above the temperature range
for the other planets. It is hoped that the measurements described can be
tailored to provide much needed absorptivity data for outer planets
constituents which will serve the largest possible number of investigators in
the planetary sciences area.

REFERENCES

Berge, G. L., and S. Gulkis (1976). Millimeter to meter wavelengths. In *Jupiter* (T. Gehrels, Ed.) pp. 621-692.

Fox, K. (1974). On the microwave spectrum of methane in the atmospheres of the outer planets. In *Exploration of the Planetary System* (Woszczyk and Iwaniszewsk, Editors). I.A.U. no 65.

Galileo Probe Project Specification (1980). NASA Document No. JP-590.04.

Gulkis, S., M. A. Janssen and E. T. Olsen (1978). Evidence for the depletion of ammonia in the Uranus atmosphere. *Icarus* 34, 10-19.

Lindal, G. F., G. E. Wood, G. S. Levy, J. D. Anderson, D. N. Sweetnam, H. B. Hotz, W. J. Buckles, D. P. Holmes, P. E. Doms, R. J. Cesarone, S. Mandell, J. K. Campbell, V. R. Eshleman, and G. L. Tyler (1981). The atmosphere of Jupiter: An analysis of the Voyager radio occultation measurements. *J. Geophys. Res.* 86, 8721-8728.

Steffes, P. G., and V. R. Eshleman (1981). Laboratory measurements of the microwave opacity of sulfur dioxide and other cloud-related gases under simulated conditions for the middle atmosphere of Venus. *Icarus* 48, 181-187.

Steffes, P. G., and V. R. Eshleman (1982). Sulfuric acid vapor and other cloud-related gases in the Venus atmosphere: abundances inferred from observed radio opacity. *Icarus* 51, 322-333.

Wallace. L. (1980). The structure of the Uranus atmosphere. *Icarus* 43, 231-259.

TUESDAY MORNING

GLOBAL DYNAMICS

CHAIR: PETER H. STONE

GLOBAL DYNAMICS AND THERMAL STRUCTURE OF JUPITER'S ATMOSPHERE

F. M. Flasar
NASA/Goddard Space Flight Center

Jupiter has an intrinsic luminosity, and most, if not all of its interior is believed to be fluid and of low viscosity. These imply a regime of thermally driven turbulent convection. The convection is likely to be strongly constrained by the planet's rotation, and should maintain an adiabatic interior with small horizontal gradients in temperature. Observations at visible wavelengths depict a cloudy atmosphere with a system of westerly and easterly jets with peak-to-peak amplitudes of up to ~250 m s^{-1} near the equator. Between the visible cloud layer and the adiabatic interior lies a transition zone about which little is known. Latent heat release by condensibles, disequilibrium between ortho- and para-hydrogen, and baroclinic/symmetric instabilities might contribute significantly in maintaining the vertical and horizontal thermal stucture of this region. Theory and observation suggest that, except for a limited range of altitudes, the mean lapse rate in the transition zone is close to dry adiabatic. Horizontal gradients in temperature are not well constrained. How the observed multiple jet system is driven is closely related to how deeply it extends into Jupiter; neither is known. A jet system which extends into the adiabatic interior would imply that the convective eddies themselves are providing the required sources of zonal momentum. Analyses of Voyager images have suggested that the eddies at the observable cloud level tend to transport net zonal momentum counter gradiently into the jets, but this interpretation may suffer from non-uniform and incomplete sampling. Moreover, the momentum transport by any secondary circulation induced by such eddies has not been addressed. In the upper troposphere and lower stratosphere, the observed temperatures suggest a decay of the zonal winds with altitude. This is consistent with a forced mean meridional circulation with frictional and radiative damping, which has upwelling and adiabatic cooling at the latitudes of anticyclonic vorticity. In the upper stratosphere, the meridional temperature anomalies reverse sign. The cause of this is not known and could have either a radiative or dynamical origin. Additionally, there is a global hemispheric gradient, suggestive of a seasonal forcing and implying a global cross-equatorial circulation at high altitudes.

DR. STONE: Would anyone like to make comments or ask questions?

DR. ORTON: Yes, let me ask a question and make a comment in reverse order. First, as I responded yesterday, our monitoring of that strange anomalous area near 24-28 deg N planetographic was not inconsistent with the area remaining warm over several years, although our resolution was only about 10% on the disk in '81 and changed to 5% of the disk only later on. On the other hand in 17.8 microns, it seems stable. We did see that the whitening of the equatorial region was almost simultaneous with the cooling off of the central area right at the equator, you notice between '79, '80 and '81. What we're doing now is waiting for the South Tropical Zone to unwhiten itself and see what happens thermally.

DR. FLASAR: You're saying that the temperature decrease is associated with a whitening of this region?

DR. ORTON: Yes, it appears to. Another thing I want to know is about 7.8 microns. Cess et al. report an anti-correlation between the tropospheric and stratospheric temperature peaks, but we find that by 1982 and later and certainly among the maps of 1984, things got terribly screwy and this correlation is obviously too simplistic. Do you have any answers?

DR. FLASAR: No, I had trouble seeing the ones from the Stony Brook slide that was taken at the Voyager time. Some of those correlations--maybe it was just the way it was plotted--were hard for me to pick out. I think the whole business of the albedo changes on the planet is really weird. It might just be a cosmetic effect as far as dynamics goes, but we don't know yet.

DR. HUNTEN: Certainly this is not original with me, but if you're going to correlate A with B then you should plot A against B, not A and B against C.

DR. FELS: There is an analogous situation at several places on the Earth as Conway Leovy, I think it was, first pointed out. In the stratosphere at 50 km you have the summer poles warm and the winter poles somewhat cooler, whereas in the mesosphere the temperature gradient is reversed and that seems to be the signature of a heating region, a radiative heating region, embedded in a region of strong mechanical friction.

DR. FLASAR: The embarrassing thing is that we already invoked that model at lower altitudes near the tropopause. That's why we need another source of heating in the upper stratosphere.

DR. POLLACK: Mike, you spoke in the beginning part of your talk about counter gradient angular momentum transport by eddies as a way of building up the jets. Would you care to say which eddies are responsible?

DR. FLASAR: One fundamental problem is the relative effect of the eddies we see near the cloud tops, the quasi-geostrophic eddies which are analogous to the kind that have been studied on the Earth, at least at shallow atmospheric levels, and the deeper convective eddies which transport the heat from the interior. That's an open question.

120

DR. POLLACK: Do you see shallow eddies as being basically baroclinic?

DR. FLASAR: I don't know. They could be barotropic. Eddies on the scale of the Rossby deformation radius, $\lesssim 10^3$ km, were not well sampled by the IRIS experiment. If anything, the available data suggest that thermal contrasts are small at these scales.

DR. LIMAYE: You showed some temperature difference from IRIS between Voyager 1 and Voyager 2. What kind of changes in the zonal wind circulation would you see from these temperatures if any?

DR. FLASAR: Well, in a lot of cases the temperature contrast was reduced in Voyager 2 from Voyager 1, so I guess you would tend to see a weakening of that meridional circulation I talked about. We see very little change in the zonal winds, I think, but Andy or Reta would be better able to address this.

DR. SROMOVSKY: The plots of the vertical wind shear that you showed correlating with $\langle U \rangle$ on Saturn and Jupiter, don't show such a good correlation when you get near the equatorial jet: rather than decaying with height, the shear is building.

DR. FLASAR: I think it's good up to the horns, near 8 deg latitude.

DR. SROMOVSKY: What's the current explanation for the failure to follow the correlation at very low latitudes?

DR. FLASAR: Well, as you get too low, the thermal wind equation breaks down, although I would expect that to be good to within 3 degrees on Jupiter. Because the Coriolis parameter is small at low latitudes, however, uncertainties in the meridional gradients in temperature translate into large uncertainties in the computed wind shears.

DR. STONE: I'd like to ask a question. You presented this picture of the zonal winds being the balance between the Coriolis force generated by this overturning circulation and some friction. You present that as a purely kinematic picture; you didn't say why it would do that. But let me ask, what value of the frictional time scale do you need in order to explain the balance in that way?

DR. FLASAR: The vertical damping scale of the jets in the lower stratosphere suggests the frictional damping time is roughly comparable with the radiative time constant, about 10^8 sec.

DR. STONE: This whole thing exposes one of the problems in trying to make deductions about the balances there. You're talking about very long forcing and dissipation time scales and that means you're likely to have a very delicate balance and you pointed that out yourself indirectly when talking about the eddies doing sometimes one kind of transport, sometimes another, then also the mean circulations and the eddies being balanced. Just think of the Earth where it took hundreds of stations and many years of observations before we could sort out those balances and here we've got even longer time scales to deal with.

DR. FLASAR: The situation isn't ideal, but I'm afraid it's all we have.

DR. STONE: Any more questions or comments? Andy Ingersoll?

DR. INGERSOLL: To expand on that, however little you may like the correlation between u' and v', the amplitude of those eddy winds, just the RMS amplitude, is undeniably large enough so that the time constant for the eddies to destroy a zonal wind is three months. So the eddies have a lot of power there if they should ever get their act together.

DR. FLASAR: There are two points to that. One is that we know that there is an excess of angular momentum, so we know the eddies are getting their act together somewhere. The other is this: if the eddies at the cloud tops are doing nothing or are only tending to erode the jets then it's always possible that if there are eddies deep down in the convective cells, they might get their act together faster and maintain these jets. So there are a lot of "ifs".

DR. EMANUEL: I find it paradoxical that, while we admit to the possibility of deep motions in Jupiter that we talk about this angular momentum budget as though it were two-dimensional on spherical surfaces. Is there any good reason to believe that what we're seeing is not simply the consequence of a vertical transport of angular momentum by the mean motions through horizontal planes? Has this really been ruled out as a possibility? Do we really need eddies to explain this?

DR. FLASAR: I think the theorem I talked about is sufficiently general, you don't have to have shallow planes.

DR. EMANUEL: Of course it's true; to get a real excess of angular momentum that has to be true, but are we seeing a real excess of angular momentum, or are we just seeing what appears to be an excess on a spherical surface? In other words, if we had sinking motion in the equatorial plane that would conserve angular momentum but would appear as an angular acceleration.

DR. FLASAR: That's easy to answer. The excess is about 1% of the planetary component of angular momentum: Ωa^2. The Ω comes from System III, which is the radio rotation rate. If that's off, then of course all bets are off; but if you accept that, then it turns out that to get a 1% excess, you have to have sinking motion from about 350 kilometers above the visible cloud tops which is well above the stratosphere, so I tend to discount that. The thing is, we know superrotation and excess angular momentum occur on other bodies such as Venus where there is no question that it's real. So it kind of buoys up your confidence that it may be occurring on Jupiter also, even though we don't fully understand what is going on.

DR. STONE: I would like to make one more comment myself with regard to the question of whether the forcing is primarily the internal heat source or the solar differential heating. The seasonal variation that Reta Beebe showed us yesterday and the solar differential heating might give us a way of getting at the answer to that question. I didn't really worry too much about seasonal change before, simply because the axis is tilted so little. But Reta showed

122

that's too simple minded. Indeed, there does seem to be strong forcing and one should, I think, look for seasonal effects and to the extent that you can find them you know at least that is due to differential solar heaing. You might say that the fact that we haven't seen any strong seasonal changes supports the view that it's the internal heat source that's the more important source. But I think if you go to high enough latitudes at least, you ought to see the effects of the differential heating and it would be very interesting to try to pin down where, if at all, you see those seasonal effects.

DR. FLASAR: That's a good point, and I should also point out that you do have another laboratory that's just a few more A.U. out at Saturn, which is 26 degrees tilted, where the seasonal effects are presumably stronger. So by comparing those two we should get some insight.

DR. STONE: I guess it's time to adjourn for 15 minutes for coffee and more discussion.

JUPITER: NEW ESTIMATES OF MEAN ZONAL FLOW AT THE CLOUD LEVEL

Sanjay S. Limaye
University of Wisconsin-Madison

The presentation by Limaye is largely contained in a paper appearing in the special issue of *Icarus* (1986; <u>65</u>, 335-352). The abstract of that paper is reproduced here:

Previous estimates of the mean zonal flow on Jupiter from Voyager images by Ingersoll et al. (1981, J. Geophys. Res. 86, 8733-8743) and by Limaye et al. (1982, J. Atmos. Sci. 39, 1413-1432) showed good agreement in the locations of the easterly and westerly jets but differed somewhat in magnitude. Recent measurements of the high-speed jet located near 24 deg N (planetographic) latitude by Maxworthy (1984, Planet. Space Sci. 32, 1053-1058) from high spatial and temporal resolution Voyager images indicate that both Ingersoll et al., and Limaye et al. underestimated the magnitude of the jet by more than 30-40 m s^{-1}. In an attempt to examine the differences in the magnitude of the Jovian jets determined from Voyager 1 and 2 images, a new approach to determine the zonal mean east-west component of motion was investigated. The new technique, based on a simple, digital pattern matching approach and applied on pairs of mapped images (cylindrical mosaics) yields a profile of the mean zonal component that reproduces the exact locations of the easterly and westerly jets between ± 60 deg latitude. Not only do the jet magnitudes but also the wings of the jets agree remarkably well from mosaic pair to pair. Further, the latitudinal resolution is five (mid-latitudes) to eight times (equatorial) greater than previous results. Results have been obtained for all of the Voyager 1 and 2 cylindrical mosaics. The correlation coefficient between Voyager 1 and Voyager 2 average mean zonal flow between ± 60 deg latitude determined from violet filter mosaics is 0.9978. A slight latitude offset (averaging + 0.15 deg) possibly due to navigation errors, is detectable in the Voyager 1 data. Independent cloud motion measurements in two high resolution image pairs (orange and violet) acquired from Voyager 1 cameras agree well with the average mean zonal flow for the fastest Jovian jet at 23.8 deg N latitude. Comparison with Maxworthy's results suggests longitudinal variations in cloud motions approaching about 20 m s^{-1} as well as some possible sampling problems. In particular, the jet magnitude is about 163 ± 9 (RMS) m s^{-1}, which compares well with 182 ± 10 m s^{-1} reported by Maxworthy. There is excellent agreement in the location of the peak magnitude as well as its shape.

DR. STONE: I guess we can take one or two comments. Larry Sromovsky.

DR. SROMOVSKY: I know these results are hot off the press. It's a little bit premature to expect a complete study of a lot of these phenomena, but I'd like to inject a note of caution in interpreting these as time variations in the jet until some of the morphological possibilities are also explored. It'd be interesting to determine, given the vertical shear or estimated vertical shear from thermal gradients, what cloud top altitude change would be required to explain that difference. That would be one thing to look at, as well as the scale dependence of this kind of correlation method, which we've already looked at to some degree and I know suggests that this is a good way to measure the winds.

DR. ROSSOW: Sanjay, I guess I missed which of the three techniques you actually used.

DR. LIMAYE: All three techniques essentially give the same answer. Mostly I used the minimum cumulative absolute brightness difference method.

DR. ROSSOW: Since this is mosaic data, how do you remove the effects of the edges in the mosaic?

DR. LIMAYE: They did a very good job of blending in, and I didn't worry too much about it.

DR. ROSSOW: How did they do that?

DR. LIMAYE: It's averaged over overlapping map sections and within a map section the data from the image with the best navigation is kept. For the most part this blending worked quite well. However, there are problems. I'm not saying the mosaics are perfect. I forgot to mention that the brightness normalization also introduces some brightness aliasing over each map region (72 deg longitude). Ideally the longitudinally averaged normalized brightness from mosaics should be the same from mosaic to mosaic. But it seems to vary somewhat, a percent or so from mosaic to mosaic. It appears to be within a couple of percent at least. But these kinds of small problems don't seem to affect the correlation between line scans too much. As I said, I didn't really throw out any data except along that really high speed jet where, because the resolution is not very high, sometimes some correlations are not as good as others and you'll get the wind going 100 m s^{-1} the wrong way. Only a small number of results had to be thrown out because they were too far off from the "expected" or average results. You can also look at the meridional shears as a quality control check. It works—you can't use linear correlation, you shouldn't use linear correlation because the normalization is not perfect. If you look at some of the regions and do a line plot, you'll see the effects of the individual frames being normalized somewhat. And I use that for the difference and it seems to work very well.

DR. BELTON: Regarding the magnitudes of the eddy motions which you should now be able to measure, can you tell me what kind of magnitudes they are and whether you think they will now be statistically significant?

DR. LIMAYE: The variability in the zonal component, or the eddies determined relative to the new mean are not too different from their magnitudes determined in the past, except in some latitude regions where due to sampling problems the eddies may not have been previously estimated properly. Latitudinal shear within a given bin used in the past had not been thought to be much of a problem, at least for the zonal component. The problem comes when you try to correlate the u-component eddies with the meridional component eddies and then you run into navigation and sampling problems.

DR. BELTON: The difference is that you were getting, you showed it in your first slide, navigational errors in the RMS deviations of the meridional velocities--aren't the primed (meridional) velocities much smaller than that?

DR. LIMAYE: No, they're about the same order. The navigational contribution to the RMS variation about the mean meridional velocities does not appear to be large, probably on the order of about 1 m s^{-1}. So most of the eddies you see in the v-component are, within sampling problems, about the same magnitude as the RMS deviations. Another point to note is that meridional component variability is only about half that of the zonal component variablility, i.e., the v-eddies appear to be roughly only half as large as the u-eddies.

DR. STONE: They're about the same order.

DR. LIMAYE: The point to note is that this technique yields the longitudinally averaged zonal component. If you average over a few rotations then you have a zonal and time mean value for the average east-west component of motion. But the technique does work on smaller chunks of data, so there is a possibility of obtaining the "regional" average mean zonal component. Some experimentation is required to determine how small such regions have to be. And it would be a really useful technique to use with the Space Telescope image data for Jupiter and Saturn. I think we have the ability to monitor the mean zonal component over a long time period from a very small number of observations and we can do it efficiently at all (observed) latitudes. From the Voyager mosaics it has been possible to determine the zonal component profile between about 55-60 deg latitude. It appears somewhat unfortunate that the mosaics are in cylindrical projections. One reason the technique appears to fail at higher latitudes may be that the scan lines become too wide at about 55-60 deg latitude, so the actual resolution is quite poor. Of course you have foreshortening in the original images also. So because of unresolved features the results are not very reliable. If you had a different projection you could perhaps extend to higher latitudes, and I'd like to see some of that work get funded.

DR. ALLISON: Sanjay, you know there's a lot of longitudinal structure along the south edge of the equatorial jet. In particular there is this feature that we put on the conference logo which is called J1 in Reta Beebe's catalogue. Do you have any sense of the measurements being loaded on to that feature and being an important part of the temporal change of the equatorial jet at that latitude? Also, do you have any sense of wave dispersive character in any of the structure of the equatorial jet?

DR. LIMAYE: I have not examined the results and systematically compared them to morphology that you see, or don't see, in the equatorial region. I did look

126

to see how sensitive the technique is to the input data. Not all the mosaics are perfect, there are some missing regions. Sometimes you'll get only about 72 degrees worth of data in a mosaic. And since I essentially ran the computer programs blindly without paying too much attention to the gaps or other problems with the mosaics, it is only when I look at the results that I notice some differences which ultimately depend on the image data. If the morphology changes, then the results can change too. And you do see some differences when some regions are missing or when a different filter image may be present in the mosaic. So if I don't take the whole 360 degrees there are some perturbations. So what that tells you is that there are longitudinal differences that appear to be significant. At this point, regarding the 7 deg jet, the morphology did change in that neighborhood over the Voyager observation period, but it is not clear how it affects the zonal component results. I'm not saying the zonal component results are absolutely accurate at that latitude, and I have to go back and study all the mosaics to see what happened. So I can't answer your question completely.[*]

DR. LEOVY: I'd like to ask another question about the eddies, the isotropy or the anisotropy of the eddies is an interesting diagnostic feature. Can you say anything about the relationship between RMS u' and the RMS v'?

DR. LIMAYE: Based on the mosaic results only I do not have any new information. Based on our old results from cloud tracking in similar mosaic images, I would defer my answer to Larry, who is going to talk more about eddies in his paper, which follows mine. One comment I would like to make is that we can take care of some of the sampling problems we have had in determining the zonal circulation at least. The mean meridional component remains a problem, but we could try a mixed approach. We could use the new mean zonal component, and say ignore the mean meridional flow, since it is difficult to obtain from the mosaic data due to its small magnitude. We can then digitally remove the mean zonal component from a mosaic by displacing individual scans in the longitudinal direction proportional to the mean zonal component at that latitude, so that at least longitudinally the clouds are "frozen" in space. This can eliminate one major problem in measuring the meridional component of motion, that of tracking a feature in a pair of images. If you remove the mean flow from one of them so they are essentially co-located, then all you're left with is the eddy component. And I think we might do a better job of measuring the eddies in both the zonal and meridional component that way than by the conventional method of measuring individual cloud motions in original images of Jupiter.

---

[*]It now appears that the change in the 7 deg S jet is in reality a difference in the apparent magnitude of the jet in different color filters from which the mosaics were generated. The mosaics for the first 70 Jovian rotations used almost exclusively blue filter images. All subsequent mosaics (through rotation 112 for Voyager 1 and rotations 266-408) were generated from mostly violet filter images. The morphology in the region just south of the equator is somewhat different, but there is no doubt about the blue-violet difference as it is apparent at the exact time the input images change from blue to violet filter. (See the paper in *Icarus* for additional details.)
-Sanjay Limaye

DR. SROMOVSKY: I'm a little surprised that everybody keeps asking about eddy activity in measurements based on a technique which is inherently unable to see it, and further, that there are many theorists here who are interested in the stability of the jets (and this data is very good at showing curvature in the jet profile), but nobody's asked anything about that.

DR. INGERSOLL: I'd like to ask about that.

DR. LIMAYE: I did compute it, and as I said this is hot off the press. I didn't have enough time to prepare the last slide, but then I thought it would be obvious. I do have a very high latitudinal resolution so that makes the job somewhat easier initially but something that makes the job more difficult is that, it is not immediately clear over what latitude scale I should calculate the derivatives. We're very lucky that 1 degree turned out to be a reasonable choice three years ago when you folks and we computed both du/dy and d^2u/dy^2 in that the errors in u were small enough over the 1 degree bin so that we got a reasonable d^2u/dy^2 profile. In this case the standard error is holding at about 1 m s^{-1} for both Voyager 1 and Voyager 2 results but that is still not small enough for me to take mean meridional derivatives at the highest latitudinal resolution possible from the data. To reduce the error in the derivatives I have to increase the distance over which to calculate the derivatives. And if I increase the distance to a few scans, up to 0.25 degree away, the derivatives are still larger than previous estimates. All the westward jets are unstable by a long shot.

DR. INGERSOLL: By a factor of 2?

DR. LIMAYE: Or even higher. I wish I had a slide but I don't. But it's even higher.

DR. STONE: In defense of the theorists, you really need to know three-dimensional structure to answer anything about stability.

128

CLOUD-TOP MERIDIONAL MOMENTUM TRANSPORTS ON SATURN AND JUPITER

L. A. Sromovsky, H. E. Revercomb, and R. J. Krauss
University of Wisconsin-Madison

Cloud-tracked wind measurements reported by Sromovsky et al. (1983, J. Geophys. Res. 88, 8650-8666), have been analyzed to determine meridional momentum transports in Saturn's northern middle latitudes. Results are expressed in terms of eastward and northward velocity components (u and v), and eddy components u' and v'. At most latitudes between 13 and 44 deg N (planetocentric), the transport by the mean flow ($\langle u \rangle \langle v \rangle$) is measureably southward, tending to support Saturn's large equatorial jet, and completely dominating the eddy transport. Meridional velocities are near zero at the peak of the relatively weak westward jet (centered at 34.5 deg N planetocentric latitude); along the flanks of that jet, measurements indicate divergent flow out of the jet. In this region the dominant eddy transport ($\langle u'v' \rangle$) is northward on the north side of the jet, but not resolvable on the south side. Eddy transports at most other latitudes are not significantly different from measurement error. The conversion of eddy kinetic energy to mean kinetic energy, indicated by the correlation between $\langle u'v' \rangle$ and $d\langle u \rangle/dy$ (where y is meridional distance) is clearly smaller than various values reported for Jupiter, and not significantly different from zero. Both Jovian and Saturnian results may be biased by the tendency for cloud tracking to favor high-contrast (usually more active) features, and thus may not be entirely representative of the cloud level motions as a whole. Attempts to resolve a mean meridional velocity structure in three independent Jupiter data sets have discovered significant correlations between $\langle v \rangle$ and two different trial functions, depending on whether Voyager 1 data is included, or excluded. Neither correlation agrees with the form of Saturn's meridional profile, which has a positive correlation with $d\langle u \rangle/dy$. More measurements are needed to decide the issue.

Here is a preview of what I'm going to talk about. I'll begin with a brief summary of what we know about the Jovian transport results. In essence, there appears to be a large conversion of eddy kinetic energy into mean kinetic energy, but there's a question about sampling. The second topic is the eddy transport measurements for Saturn; these appear to show no significant eddy support of the jet structure. I'll talk about that just a little. The third topic is more of a progress report on my search for meridional transports by the mean flow. Potentially large mean transports have so far been obscured by really huge percentage errors in the meridional velocity measurements. I tried to increase the signal-to-noise ratio in these measurements by doing a lot of judicious averaging and looking for correlations between $\langle v \rangle$ and various functions of $\langle u \rangle$. Tentative results show statistically significant correlations, but Jupiter and Saturn show different kinds of correlations. I'll explain more about this as I go along here.

As a background for discussing transport results I'd first like to present a short, and somewhat sloppy, derivation of what momentum transport is and does. Consider a point at which the eastward velocity is u, the northward velocity is v, and the atmospheric density is ρ. At the same point we note that

$$\rho \cdot u = \text{Eastward momentum per unit volume, and}$$

$$v \cdot \rho \cdot u = \text{rate of northward transport of eastward momentum/unit area.}$$

Consider a volume bounded by two latitudes, labelled here by meridional distance coordinates y_1 and y_2, of thickness H and of longitudinal width W. Assuming zonal symmetry and no vertical transports, the only net momentum transport is meridional. The momentum balance for this volume then becomes

$$\rho \cdot H \cdot W \cdot [(uv)_1 - (uv)_2] = \rho \cdot H \cdot W \cdot (y_2 - y_1)[du/dt],$$

which says that the difference between momentum flow rates into and out of the volume must equal the rate of change of the momentum within the volume. Writing this for a differential volume, and taking a zonal average, we obtain

$$d\langle u\rangle/dt = - d\langle uv\rangle/dy = -d(\langle u\rangle\langle v\rangle)/dy - d\langle u'v'\rangle/dy,$$

where $\langle u\rangle\langle v\rangle$ and $\langle u'v'\rangle$ are transports by mean and eddy flows respectively. The rate of change of kinetic energy, per unit mass, of the zonal mean flow is just the product of $\langle u\rangle$ and $d\langle u\rangle/dt$, i.e.

$$dK/dt = \langle u\rangle \cdot d\langle u\rangle/dt = -\langle u\rangle d\langle uv\rangle/dy$$

$$= - \langle u\rangle d[\langle u\rangle\langle v\rangle]/dy - \langle u\rangle d\langle u'v'\rangle/dy$$

where the second term on the right states that net eddy transport of eastward momentum into an eastward jet tends to increase the kinetic energy of the jet. Thus it's interesting to see correlations between momentum transport derivatives and $\langle u\rangle$. But what we usually look at is the alternate product, which is momentum transport times the derivative of $\langle u\rangle$. These two products are related to the derivative of a product, namely

$$\langle u'v'\rangle d\langle u\rangle/dy = d/dy[\langle u\rangle\langle u'v'\rangle] - \langle u\rangle d\langle u'v'\rangle/dy.$$

We usually talk only about the left hand side of this last equation in deciding whether eddy kinetic energy is being added to by the eddies. This is

justified only when integrated over a suitable atmospheric volume for which the derivative of $\langle u \rangle \langle u'v' \rangle$ converts to a vanishing boundary term. At any rate, $\langle u'v' \rangle \cdot d\langle u \rangle/dy$ has been popularly looked at (cf. Fig. 1.) Maybe we should be looking at $\langle u \rangle \cdot d\langle u'v' \rangle/dy$ also, since it has more local significance.

$$d\langle u \rangle/dy, \ 10^{-5}s^{-1} \ (- - -)$$
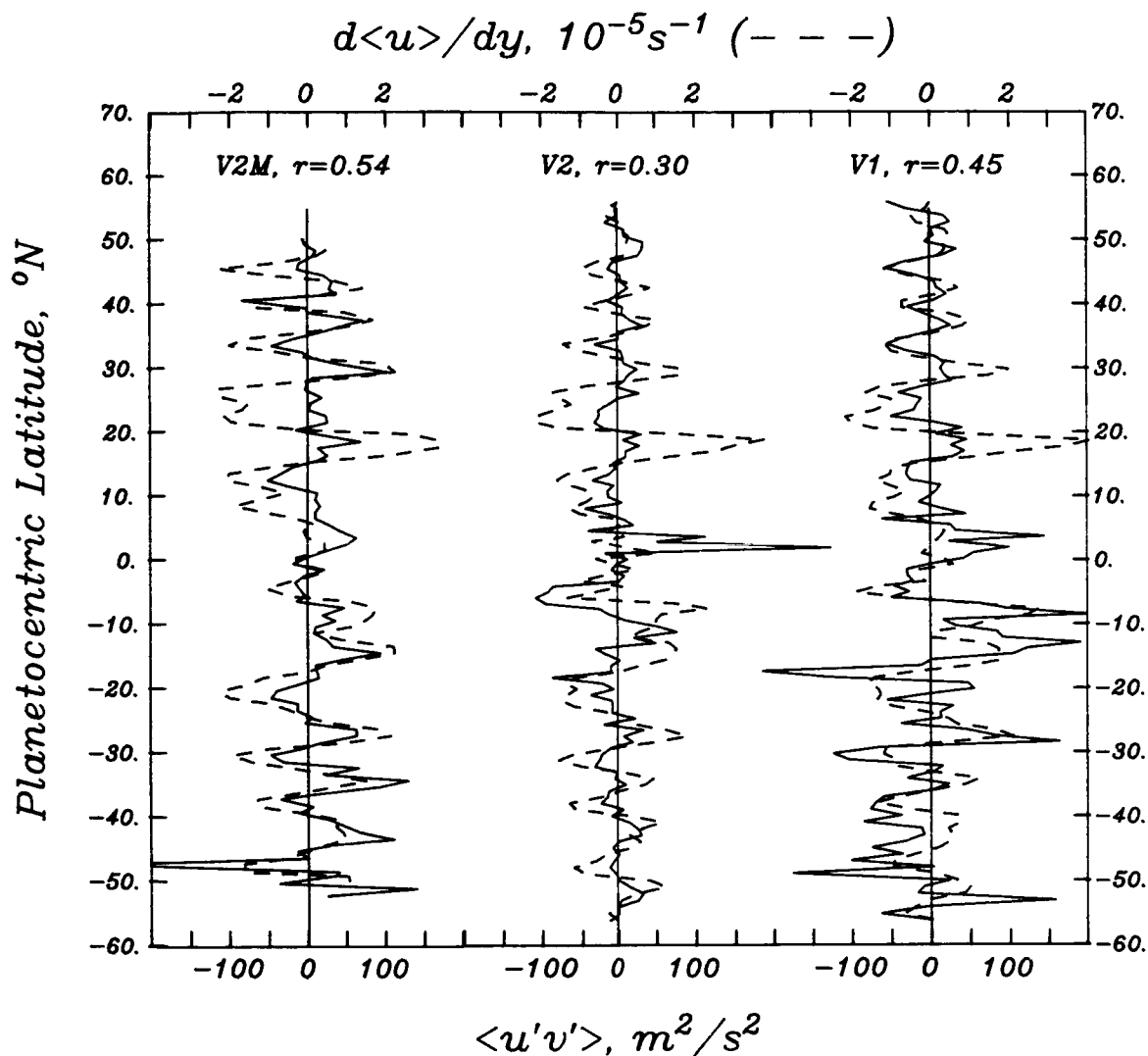
Figure 1. Comparison of Jovian eddy momentum transports [$\langle u'v' \rangle$] with the latitudinal shear of the mean zonal component of motion [$d\langle u \rangle/dy$] for three data sets: Voyager 1 and 2 measurements by Ingersoll et al. (1981), denoted by V1 and V2, and our Voyager 2 measurements (Limaye et al., 1982; Sromovsky et al., 1982), denoted by V2M. A positive correlation between the solid and dashed curves indicates eddy kinetic energy conversion to mean flow kinetic energy.

Figure 1 displays measured eddy transports on Jupiter, where Voyager 1 and 2 results from Ingersoll et al. (1981) are shown in comparison with Voyager 2 results of Limaye et al. (1982). The solid curves represent $\langle u'v' \rangle$, the dashed curves $d\langle u \rangle/dy$. The correlation between them is pretty easy to see in our results; the local correlation is very strong except in the jet at 23 deg N latitude (this looks like 20 deg here because the latitude scale is planetocentric). Over all latitudes measured, the correlation coefficients are, from left to right, 0.54, 0.3, and 0.45. Those are all very significant considering the number of bins which we have here; the chance of random variables correlating this well is less than one percent.

Although the correlations look significant, the differences in these measurements have a disturbing pattern. Ingersoll et al.'s Voyager 1 measurements are noisier than their Voyager 2 measurements (the RMS deviations within a latitude bin are somewhat larger, and the differences between adjacent bins is considerably larger). Our measurements (Limaye et al., 1982) are also fairly noisy because we used low resolution images. Strangely, the noisier measurements are the ones that show the strongest correlation. Now, if you add random noise to correlated variables, you would expect a reduced correlation to appear, not a larger one. So this looks a little bit suspicious in itself; the most noise-free measurements (Ingersoll et al.'s Voyager 2 measurements) are the ones showing the least correlation. Also notable is that the product of these variables has a pretty large average; it's equivalent to an energy conversion rate 10-30 percent of the net flux emitted to space. That is definitely not Earth-like; on Earth the average conversion rate is only about 0.1% of the net flux emitted to space.

When we saw these large correlations we went looking in our data for the eddies that were responsible. What we hoped to see, maybe, were asymmetric eddies something like the upper eddy in Fig. 2, for which the u·v product is large in certain parts of the wave, and very small in others, similar to many baroclinic waves on Earth. We were looking for something like this, although we didn't have a specific target in mind. But we didn't really find anything in the way of obviously asymmetric eddies. Instead, we saw many fairly symmetric eddies and strong motions which we had not sampled uniformly. When we remeasured cloud motions with special efforts to achieve uniform sampling, our correlations became insignificant. We didn't remeasure the motions for the whole globe because it was too costly to do it. But where we did do it we couldn't maintain this fairly strong correlation we had found.

Figure 2 also shows a symmetric eddy imbedded in a mean flow with positive zonal shear; in certain parts of the eddy the u'v' product has a positive correlation with $d\langle u \rangle/dy$, and at other places it has a negative correlation. Thus, in an average over latitude, these positive and negative contributions will result in no net contribution. To upset this balance all that's needed is a non-uniform sampling of the eddy motions. But, for a sampling problem to show up in large scale zonal means, the sampling must be not only non-uniform, it must also be consistently biased. Perhaps the eddies themselves do something to produce more targets in certain regions than others. Of course this is a very speculative suggestion.

132
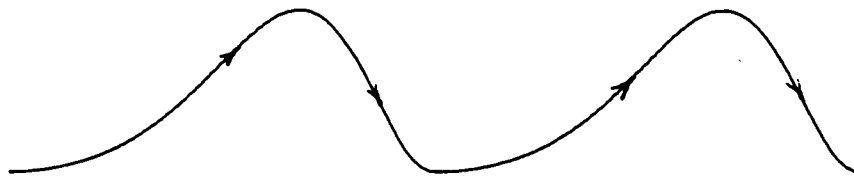
(a) Asymmetric Eddy

$u'v'>0$

$\dfrac{du}{dy}>0$

$u'v'>0$
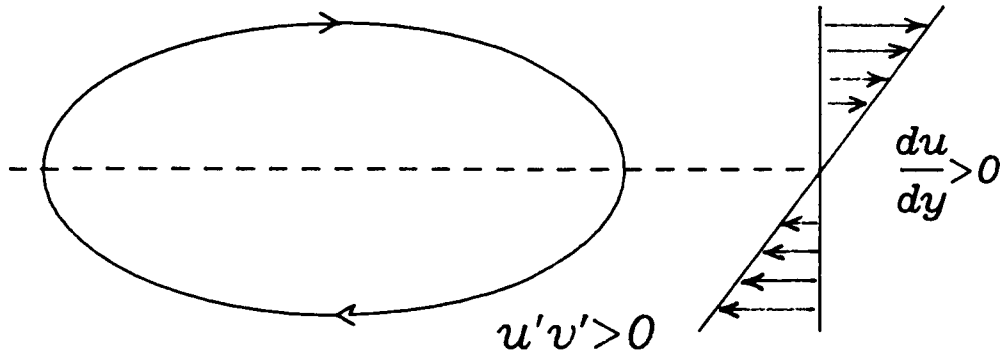
(b) Symmetric Eddy

Figure 2. Latitudinal eddy momentum transports are produced
by asymmetric waves (a) because, at a fixed latitude, the u'v'
products on the gently sloping parts of the wave don't balance
the u'v' products on the steep part of the wave. But symmetric
eddies (b) do balance, unless sampled asymmetrically. A sym-
metric eddy imbedded in a mean positive shear, indicated in the
lower right, could provide eddy transports of the same sign as
the shear itself if over-sampled in upper left and lower right
regions of the circulation.

To summarize this situation, I think there is a problem with sampling in our
data, and the data we used is more susceptible to it. We did obtain the
largest correlation between ⟨u'v'⟩ and d⟨u⟩/dy, and when we tried to do equal
area sampling the correlation became insignificant. Non-uniformity in
sampling probably would be less of an influence on the Ingersoll *et al.*
results because they are based on higher resolution images. So I still have
doubts about what the true situation is. Now let me move to Saturn briefly.
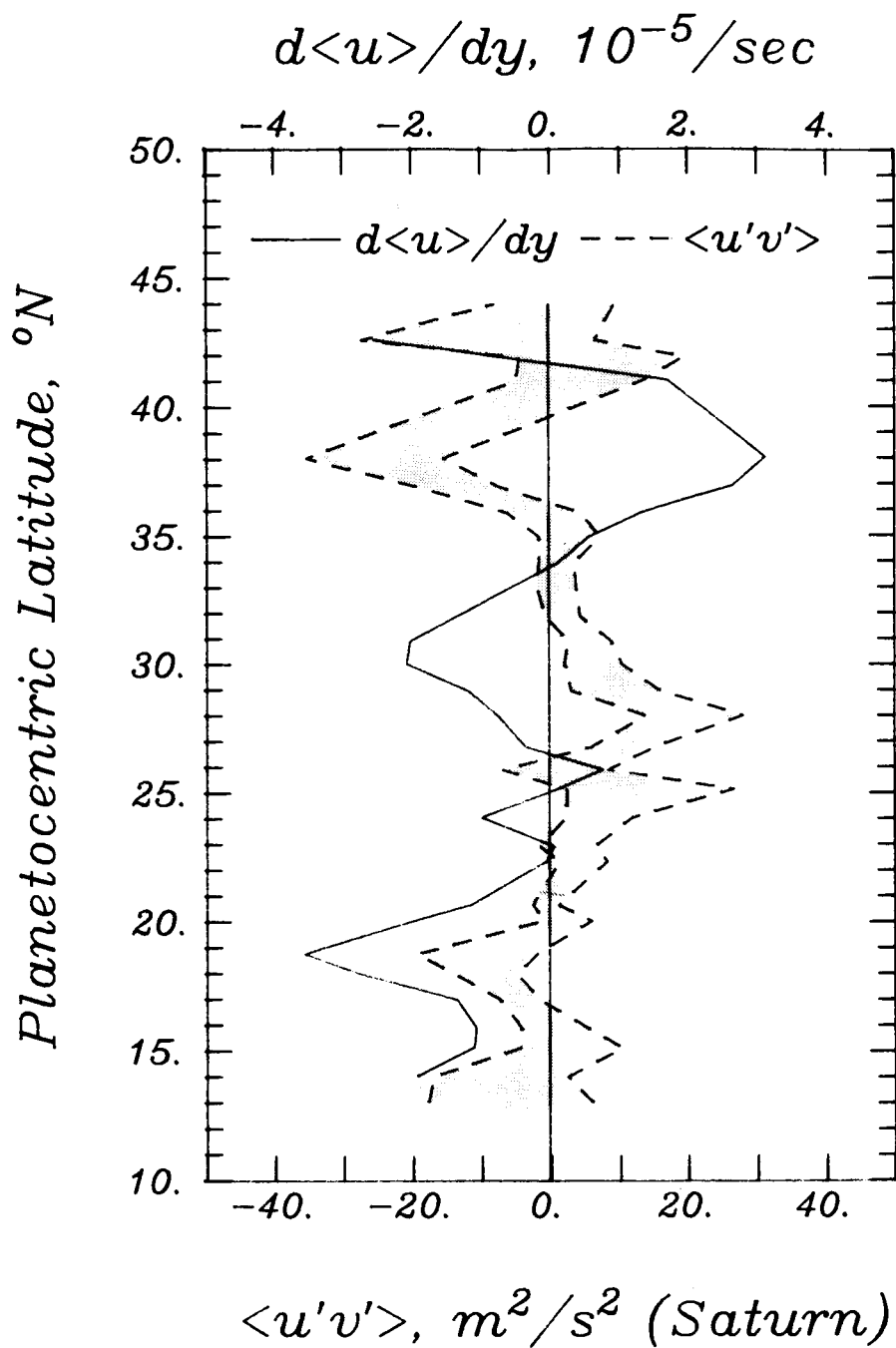
Figure 3. Saturnian eddy momentum transports (shaded region) in comparison with the latitudinal shear in ⟨u⟩ (solid line). These results are from northern mid-latitude measurements by Sromovsky *et al.* (1983). The correlation coefficient over the plotted latitude range is only 0.02, with a 90 percent chance that uncorrelated variables would correlate this well, or better.

Measured eddy transports on Saturn are illustrated in Fig. 3. These results are from a new analysis of measurements described by Sromovsky et al. (1983), consisting of 800 wind vectors measured in northern middle latitudes. The calculated correlation coefficient for our measurements is 0.02 with a probability that random variables could have a correlation this large being about 90%. Independent measurements of about 1000 cloud targets distributed over both hemispheres of Saturn, were obtained by Ingersoll et al. (1984). (These sample numbers should be compared to 8,000 and 10,000 targets measured on Jupiter.) The correlation coefficient for the latter data set is also low, although there is a discrepancy that I haven't straightened out yet. In the Saturn book Ingersoll et al. gave the correlation coefficient as r=0.01, while my calculations for their data yield r=0.12; but, even for the larger value, the chance that this could be random error is 34%. Thus, there doesn't seem to be a significant correlation between $\langle u'v' \rangle$ and $d\langle u \rangle/dy$ on Saturn; the eddy transport of the jets is not as large as we seem to be measuring on Jupiter. Let me move on to the eddy comparison with the mean flow.

Here is the problem with mean transport measurements: because $\langle u \rangle$ is so large a little mean meridional flow can produce a huge transport, and the measured mean transports on Jupiter and Saturn often do overwhelm the eddy transports. This is especially dramatic in the comparison shown in Fig. 4. But the noise in $\langle v \rangle$ is so large that these potentially large transports are highly uncertain, and not to be believed. So I started looking for ways to average results and try to put a better bound on the $\langle v \rangle$ component, and on the associated meridional transport.

The search for mean meridional transports is based on the idea that there is a definite relation between meridional motions and zonal motions, and that the relation is the same for all (or nearly) all of the zonal jets on each planet. You've seen many examples of what kind of meridional flow might appear on Jupiter or Saturn: the typical picture, illustrated in Fig. 5, has rising motions in the zones and descending motions in the belts. A pressure gradient between these two is implied if the motions are geostrophic ("geo" is not quite the right word here); the horizontal pressure gradient provides a balance for the Coriolis force. Add some dissipation to upset the balance, and you might expect meridional motions in the direction of the pressure gradient (an example of "cross isobaric flow"). The steady meridional flow is presumably driven by convection.

If this picture is correct, we should expect the meridional velocities to be related to $f\langle u \rangle$, where f is the Coriolis parameter. If, on the other hand, the meridional transport by mean flows is assumed to balance the measured eddy transports, then $\langle u \rangle\langle v \rangle$ should have a negative correlation with $\langle u'v' \rangle$ or, since this appears to be correlated with $d\langle u \rangle/dy$, we might look for correlations between $\langle u \rangle\langle v \rangle$ and $-d\langle u \rangle/dy$, or just between $\langle v \rangle$ and $-(1/\langle u \rangle)d\langle u \rangle/dy$. Note that if $\langle u \rangle$ is symmetric about the equator (it is, approximately) then both of these functions have a mirror symmetry about the equator: their signs reverse when the sign of the latitude is reversed. It is hard to imagine a combination of symmetric zonal motions and meridional flows which do not have this mirror symmetry. A third simple function with the proper symmetry is $d\langle u \rangle/d\phi$ (ϕ is latitude), although there is no physical basis for picking a sign of the correlation.
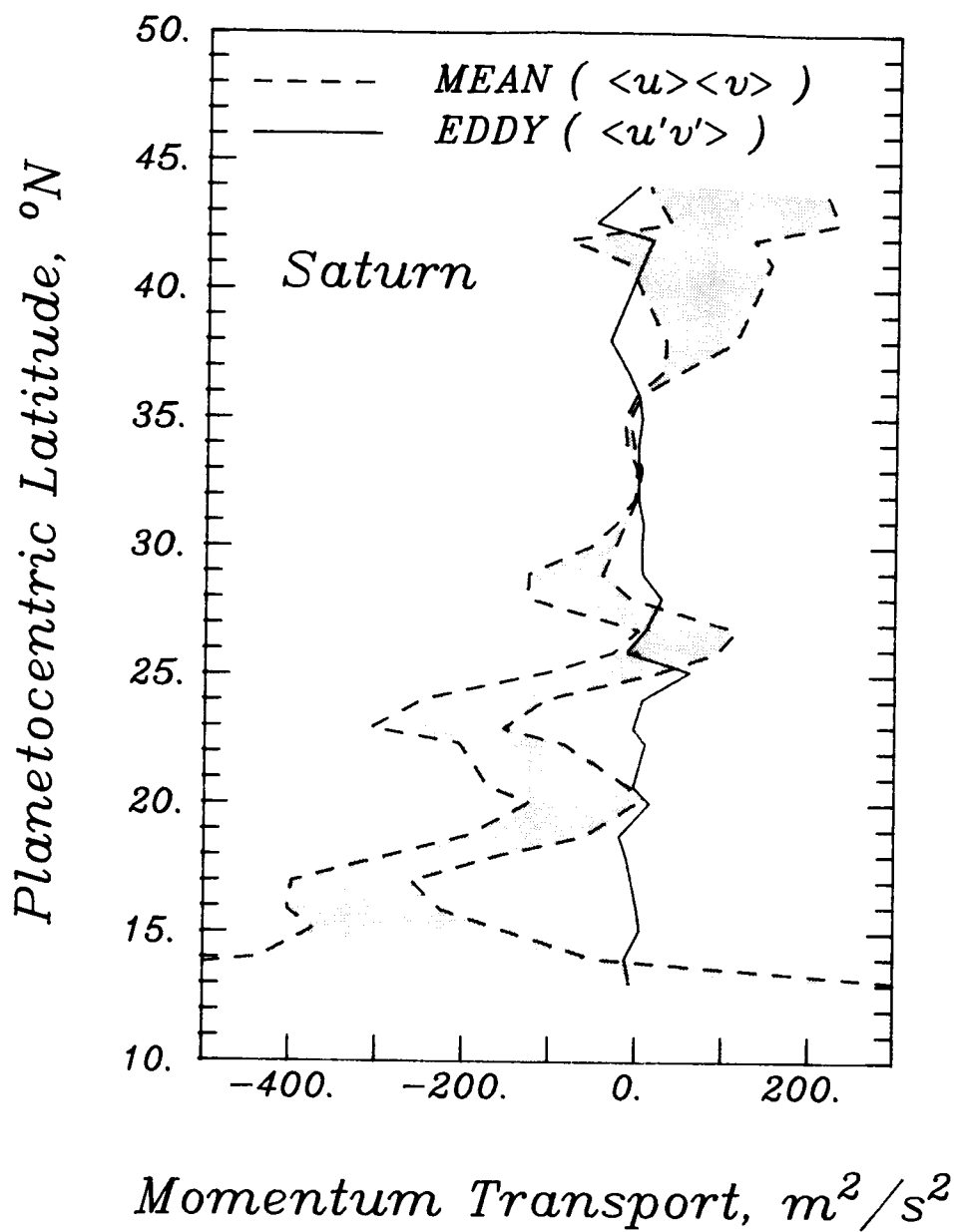
Figure 4. Comparison of mean (shaded band) and eddy (solid curve) momentum transports in Saturn's northern middle latitudes. At low latitudes the mean transport is completely dominant, although the error band for the mean transport is only a formal estimate.
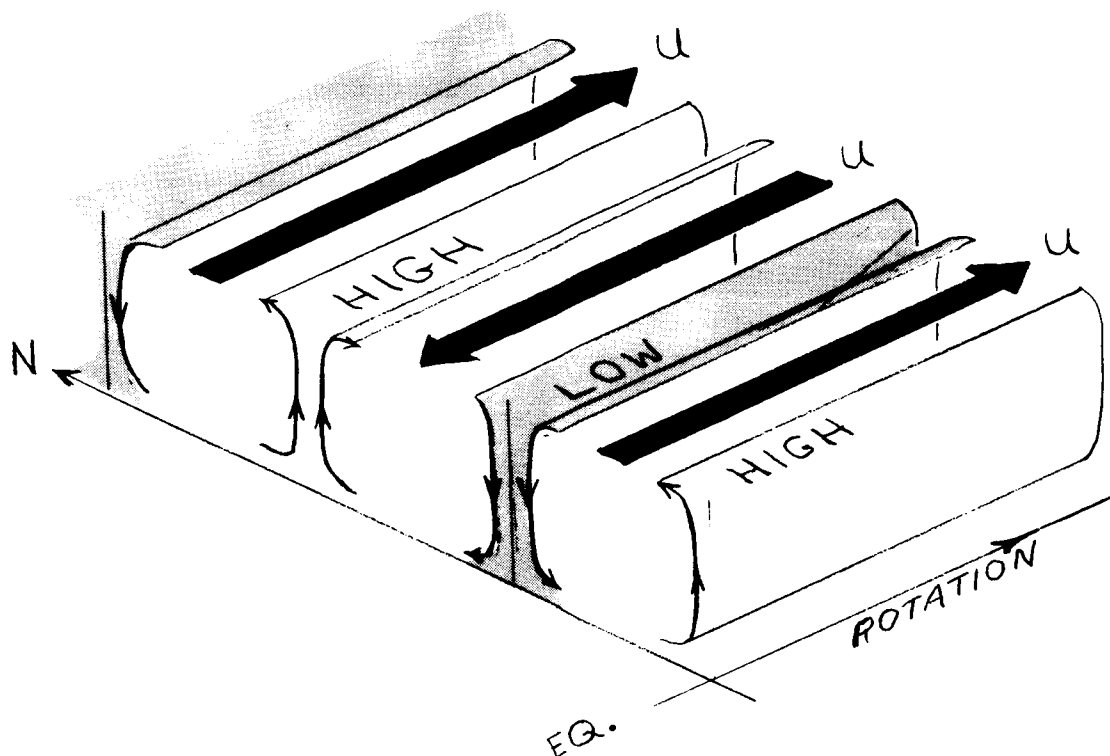
Figure 5. A popular conception of meridional flow on Jupiter and
Saturn (after Ingersoll and Cuzzi, 1969). The Coriolis force on
zonal jets is balanced by the latitudinal pressure gradient between
zones and belts. The zones are pictured as warm high pressure regions
with upwelling motions and meridional divergence at the level of
observation, while the belts are associated with cooler temperatures,
meridional convergence, and downwelling.

Thus we have three distinctly different patterns to look for, none really a
theoretical prediction, but at least two having some physical connotation.
The true patterns might easily be much more complex functions than those
considered here.

The raw measurements of $\langle v \rangle$ are a real jumble of noise, with meridional
velocities reaching nearly 8 m s^{-1}, and little correlation between different
data sets. Just averaging that data and doing a three-point smoothing,
returns a profile which ranges between -2 and +3 m s^{-1}. This, it turns out,
is fairly strongly correlated with $\langle u \rangle$, a function which does not have the
mirror symmetry described previously. That correlation could come about from
a slight error in defining the angle of the Voyager camera relative to the
planet's spin axis. If the images are slightly tilted, the velocity
measurements can be resolved incorrectly along the u and v axes. Half a
degree of tilt would explain the observed correlation. Since there is also no
physical reason for this correlation to exist in true atmospheric motions, I
removed it. The main effect of doing that is in the equatorial region; the
other regions don't change too much. Now the $\langle v \rangle$ profile excursions are down
to ± 2 m s^{-1} at the extremes.

Does this smoothed and corrected v-profile correlate with either of the physically suggested functions: $+ f\langle u\rangle$ from the belt-zone idea, or $-(1/\langle u\rangle)\cdot d\langle u\rangle/dy$, to balance the eddy transport into the jets? Neither of these provide a significant correlation on either Jupiter or Saturn, although on Jupiter we could obtain a significant correlation with the Coriolis force function if we eliminated the Voyager 1 data (the most noisy member of the three Jupiter data sets). If you calculate the correlation coefficient for the entire Jupiter data set, it's hopelessly insignificant.

The third function with the right kind of symmetry to allow correlations with $\langle v\rangle$ is $d\langle u\rangle/d\phi$, although I can't argue that $d\langle u\rangle/d\phi$ ought to correlate with $\langle v\rangle$. Using the complete set of Jupiter data, the correlation between these two is negative between latitudes of 40 deg and 15 deg or so, but positive in the equatorial region. [Between 15 deg and 42 deg latitude the correlation coefficient between $du/d\phi$ and the corrected v is -0.3 which is significant at the 2% level.] To further increase the signal-to-noise ratio in this calculation I tried anti-symmetrizing both the $\langle v\rangle$ profile, and the $d\langle u\rangle/d\phi$ profile, under the assumption that the symmetric component must be erroneous (this is not quite proper because $\langle u\rangle$ is not quite symmetric). The anti-symmetrization does improve the correlation in mid-latitudes, but still does not show a significant correlation in the equatorial region.

Saturn is the next topic. As indicated in Fig. 6, meridional velocities in middle latitudes do not show a significant correlation with $f\langle u\rangle$. The correlation with $d\langle u\rangle/d\phi$, on the other hand, is significant: $r=0.59$, with a chance of random variables correlating this well being less than 1%. The apparent meridional flows on Saturn are divergent in the westward jets and convergent in the eastward jets. This is opposite to the sense that we saw for the complete Jupiter data set. But the picture on Jupiter would change if the noisy Voyager 1 data set were excluded.

To summarize, the conversion of eddy kinetic energy to mean kinetic energy on Jupiter appears to be large, but I think we'd have to be a little suspicious because of the possibility of asymmetric sampling. The conversion on Saturn does appear to be small, and so far not detectable.

There may be some evidence of a $\langle v\rangle$ component which is really measureable. These preliminary results seem to indicate that $\langle v\rangle$ is positively correlated with $d\langle u\rangle/dy$ on Saturn, but negatively correlated on Jupiter: that would imply a meridional convergence in the eastward jets on Saturn and convergence in the westward jets on Jupiter (cf. Fig. 7.) Saturn clearly did not show a significant correlation between $\langle v\rangle$ and $f\langle u\rangle$ which would contradict at least the sense, not the magnitude certainly, of the old belt zone interpretation. The same contradiction would be implied by the entire Jupiter data set, but if the noisier Voyager 1 data is excluded, then there is at least partial consistency with the old belt-zone interpretation. This latter statement points out something that needs to be emphasized: we have only tentative results, especially tentative results concerning mean meridional motions.

Unfortunately this tends to shed some darkness on the eddy question, and not too much light on the mean meridional flow. We hope we can do better with higher resolution imagery and more careful navigation.

138
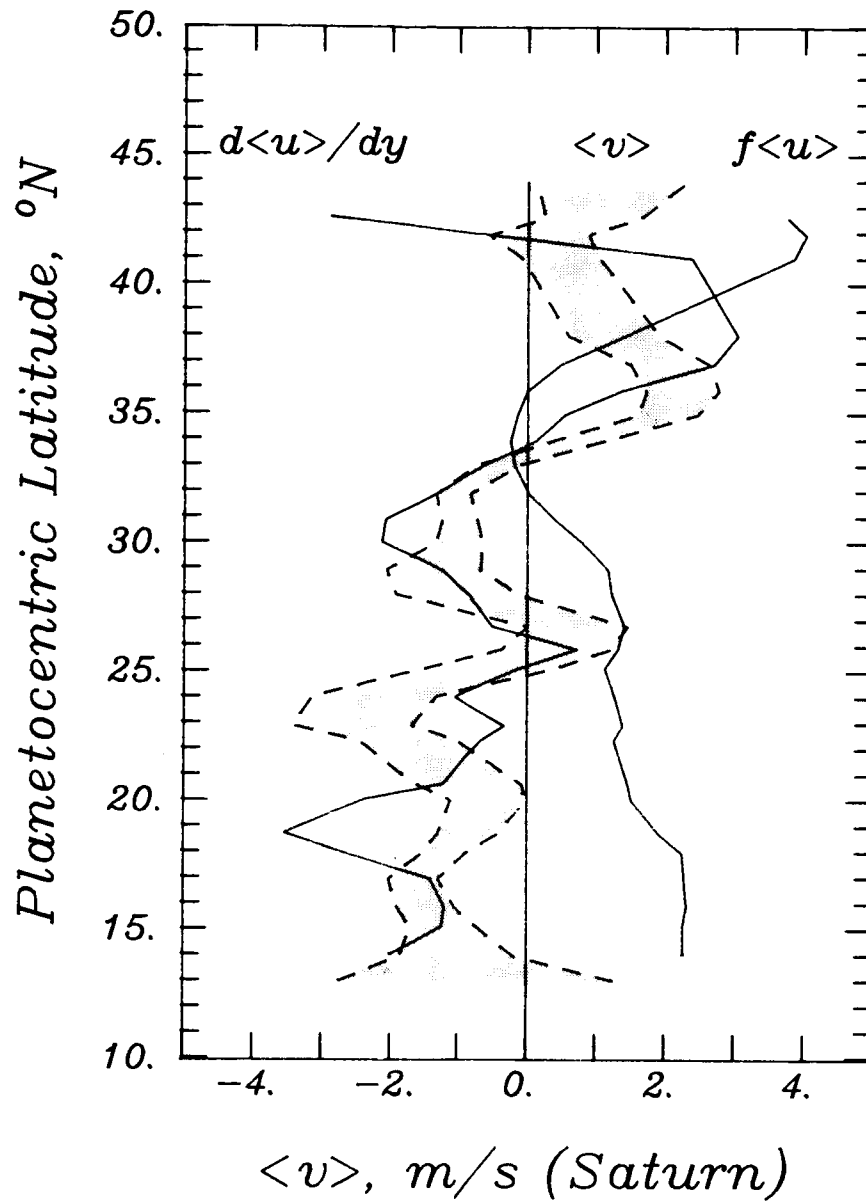
Figure 6. Measured meridional motions on Saturn (shaded band) compared with f·<u> and d<u>/dφ (solid curves). The correlation coefficient between <v> and d<u>/dφ is significant at the 1 percent level.
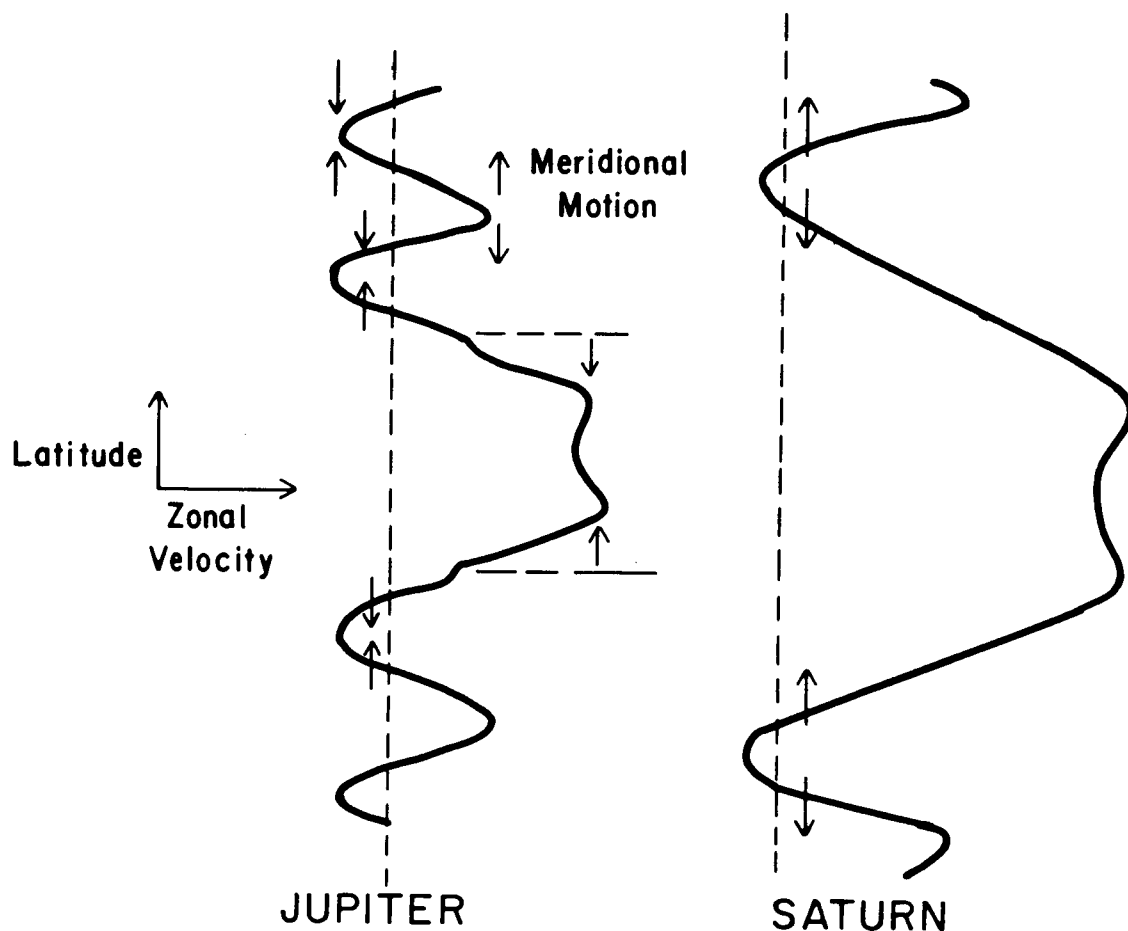
Figure 7. Schematic illustration of tentatively inferred correlation between meridional motion and the latitudinal shear of the zonal wind on Jupiter and Saturn.

REFERENCES

Ingersoll, A.P., and J.N. Cuzzi (1969). Dynamics of Jupiter's cloud bands. *J. Atmos. Sci.* 26, 981-985.

Ingersoll, A. P., R. F. Beebe, J. M. Mitchell, G. W. Garneau, G. M. Yagi, and J. -P. Muller (1981). Interaction of eddies and mean zonal flow on Jupiter as inferred from Voyager 1 and 2 images. *J. Geophys. Res.* 86, 8733-8743.

Ingersoll, A. P., R. F. Beebe, B. J. Conrath, and G. E. Hunt (1984). Structure and dynamics of Saturn's atmosphere. In *Saturn* (T. Gehrels, M. S. Mathews, Ed.), University of Arizona Press, Tucson.

Limaye, S. S., H. E. Revercomb, L. A. Sromovsky, R. J. Krauss, D. A. Santek, V. E. Suomi, S. A. Collins, and C. C. Avis (1982). Jovian winds from Voyager 2. Part I: Zonal mean circulation. *J. Atmos. Sci.* 39, 1413-1432.

Sromovsky, L. A., H. E. Revercomb, V. E. Suomi, S. S. Limaye, and R. J. Krauss (1982). Jovian winds from Voyager 2. Part II: Analysis of eddy transports. *J. Atmos. Sci.* 1433-1445.

Sromovsky, L. A., H. E. Revercomb, R. J. Krauss, and V. E. Suomi (1983). Voyager 2 observations of Saturn's northern mid-latitude cloud features: Morphology, motions, and evolution. *J. Geophys. Res.* 88, 8650-8666.

DR. FLASAR: You made the point that if you're doing local latitude studies of jet structure, you really want to look at the meridional divergence $\langle u'v' \rangle$ correlated with $\langle u \rangle$ rather than $d\langle u \rangle/dy$ correlated with $\langle u'v' \rangle$. Can you get a correlation of the first thing I mentioned, the one that you didn't show, the one between $\langle u \rangle$ and the meridional divergence of $\langle u'v' \rangle$?

DR. SROMOVSKY: No.

DR. FLASAR: Its just hard to calculate that divergence, is that it?

DR. SROMOVSKY: Because $\langle u'v' \rangle$ is so noisy its derivative looks really bad. We did do the integral over all latitudes of $\langle u \rangle d\langle u'v' \rangle/dy$ and compared it with the integral of the normal thing we look at ($\langle u'v' \rangle d\langle u \rangle/dy$) and the results were basically the same. But we didn't look at the detailed local distribution. It should be done but it hasn't been done. It's going to be noisy though, I can say that much.

DR. READ: Just to raise a few notes of healthy theoretical skepticism on interpreting some of these results. First of all, the kind of energy budget that you're talking about inferred from correlations between horizontal momentum fluxes and mean zonal shears, one has to emphasize, is fundamentally incomplete because you simply can't ignore the effect of heat fluxes in deriving the acceleration of the mean flow. You've also stressed the importance of the meridional circulation, which of course Mike Flasar referred to, the fact that that can bring about a cancellation of the effect of these momentum fluxes. So if you're going to do this excercise, you must have the complete information, otherwise you're simply not going to get anywhere in trying to interpret these results. There are some well established theoretical examples where you can write down simple analytical solutions of combinations of eddies and mean flows which have all sorts of exciting looking conversions but by definition do absolutely nothing. These are the so-called "free mode" solutions which satisfy the Charney-Drazin non-acceleration theorem. And these ideas are not just restricted to quasi-geostrophic arguments. Andrews and McIntyre for example, have generalized the whole theory well beyond just the simple quasi-geostrophic arguments. Just one last quick question. Having said that all these correlations may or may not have any real significance, I just want to ask you if you see any evidence of horizontal tilt in the very long lived eddies, the Red Spot and the like, because I gather Tony Maxworthy and Jim Mitchell have claimed to see some evidence of a systematic $\langle u'v' \rangle$ conversion associated with these large eddies.

DR. SROMOVSKY: Has that been published?

DR. READ: I know of at least one place it's been published. In an I.U.T.A.M. conference proceedings which has only just appeared, I think.[*]

DR. STONE: Are you going to answer that question?

DR. SROMOVSKY: The answer is no. (We have not seen evidence of horizontal tilt in the long-lived eddies.)

DR. STONE: OK. Andy Ingersoll.

DR. INGERSOLL: First of all, all of us who have been trying to milk these measurements dry are fully aware of all the other terms. However, I disagree with one statement you (Dr. Read) made and that is that you can get nothing out of an incomplete picture. You get a diagnostic which, if it is statistically true—and I will admit there is controversy about that—but, if it is statistically true that there is a correlation between one thing and another, you may not have the whole picture of the whole momentum or energy conversion, but you have one number that is true. And if you have a theoretical model that disagrees with that number, you've got a problem with that theoretical model.

DR. LEOVY: I raise again my question about the isotropy of $\langle u' \rangle$ versus $\langle v' \rangle$ and let me mention the reason that I think it's important. It's because what one would like to do is to isolate the scale at which the energy is coming in if possible, and one would expect the eddies to be more or less isotropic at the scale at which the energy is coming in, and to get more and more longitudinal at the larger scales. Do you have any information on that?

DR. SROMOVSKY: Are you asking about the longitudinal distribution?

DR. LEOVY: I'm asking about first the relationship between RMS u' and RMS v', and second, is there any possibility of getting scale dependent information on that?

DR. SROMOVSKY: RMS u' tends to be larger than RMS v'. I can't give you any information on scale dependence. I'm not sure how to answer anything more than that.

DR. POLLACK: A very naive question, and that is, does the fact that you get a correlation of one sign from Jupiter for your $\langle v \rangle$ correlation with $d\langle u \rangle/dy$ and an opposite sign for Saturn make you potentially suspicious that all this is noise really and not real correlation?

---

[*]Editor's note: Dr. Read is referring to Mitchell, J., and T. Maxworthy (1984). Large scale turbulence in the Jovian atmosphere. In *Turbulence and Chaotic Phenomena in Fluids* (T. Tatsumi, Ed.), pp. 543-547. Elsevier Science Publishers B.V., North Holland. This was a contribution to an International Union of Theoretical and Applied Mechanics Conference Proceedings. A more complete account of their work appears in (1985) Turbulence and Predictability in Geophysical Fluid Dynamics and Climate Dynamics (M. Ghil, Ed.), pp. 226-240. North-Holland Physics Publishing, Amsterdam.

DR. SROMOVSKY: Yes. Well, I'm less suspicious on Saturn actually; the results of the Saturn mean flow calculation are fairly consistent with the visual impression you get just looking at the images, and the noise on Saturn is pretty low in the one jet where we see a lot of eddy activity. On Jupiter the eddies are stronger, it's easier to make mistakes. The agreement between the three Voyager data sets is not quite as good as their estimated errors say they should be, so I'm more suspicious of the results on Jupiter and I think possibly larger error bars should be attached to those. And I'd like to see better measurements on Jupiter, which is possible. I am suspicious, but more suspicious of Jupiter actually.

DR. LIMAYE: Let me just add one thing to Conway Leovy's question. I guess I'll try to answer your question, at least one small part of it. I think the disagreement between the three previous Voyager estimates for Jupiter's mean $\langle u \rangle$ component is large enough so that it totally becomes a problem as to what is a u eddy. But now I think the results I presented earlier suggest that the mean flow appears to be very stable. So we can redefine what the $\langle u \rangle$ component is. I was about to take the new mean $\langle u \rangle$, use the old measurements and calculate $\langle u'v' \rangle$. I resisted that temptation very greatly, because, frankly I don't know how to interpret what I would get. But we hope we can now use the mean flow and redefine some of the eddies.

DR. BEEBE: Some comments about those atmospheres. When you look at the atmosphere of Saturn, most of the turbulence you can see is in the westward jets. They're in the middle of the lowest albedo regions. You get the impression that you've got convection punching up through the cloud deck and you're actually seeing divergence of convection to the north and the south. The high speed jets on Saturn are much more spatially homogeneous with feathery structures that trail off along their edges. After you've worked in both north and south hemispheres looking at the morphology as you measure the features, you get the impression that the high speed jets are decoupled from the local convection. In the case of Jupiter's atmosphere all of the semi-permanent high albedo regions that we call zones are bounded on the poleward side by an eastward jet. There is chaotic structure along their equatorward side associated with the westward flows, and there seems to be divergence from those westward flows both north and south. But it looks as though the whole cloud deck that we're seeing on Jupiter is really still involved in the convective interface of the atmosphere and that doesn't appear to be the case in Saturn's atmosphere.

CONVECTIVE FORCING OF GLOBAL CIRCULATIONS
ON THE JOVIAN PLANETS

David H. Hathaway
NASA/Marshall Space Flight Center

Examples of convection in rotating layers are presented to illustrate how convection can drive global circulations on the Jovian planets. One example is derived from an analytical solution for the onset of convection in a rotating, ideal fluid layer (Hathaway, 1984, Ap. J. 276, 316-324.) For rapid rotation the convective motions become largely two-dimensional and produce Reynold stresses which drive large scale flows. The initial tendency is to produce a prograde equatorial jet and a meridional circulation which is directed toward the poles in the surface layers. Fully nonlinear numerical simulations for the slowly rotating solar convection zone show that the meridional circu- lation does not reach the poles (Glatzmaier, 1984, J. Comp. Phys 55, 461-484). Instead a multicellular meridional circulation is produced which has a downward flowing branch in the mid-latitudes. For more rapidly rotating objects such as Jupiter and Saturn this meridional circulation may consist of a larger number of cells. Axisymmetric convective models then show that prograde jets form at the downflow latitudes. A nonlinear numerical simulation of convection in a pro- grade jet is presented to illustrate the interactions which occur between convection and these jets. Without rotation the convection removes energy and momentum from the jet. With rotation the convec- tion feeds energy and momentum into the jet. The conversion rates are similar to those found for motions in the vicinity of Jupiter's North Temperate Belt. A movie of this simulation will be shown.

Those of us who would like to construct realistic models for the dynamics of Jupiter's atmosphere and interior are faced with a bit of a dilemma...actually it's a major problem. There is a very wide range of length scales that are dynamically important for forcing flows on the giant planets. The planetary rotation is important for a broad range of lengths from the global scale of tens of thousands of kilometers down to a scale of 100 kilometers or less. What I would like to present today are two examples of these dynamically impor- tant flows. The first is from an analytical model that I have developed with the hope of getting a handle on how to parameterize small scale convection in a global circulation model. The second example is a numerical simulation of convection in a zonal flow which illustrates the interactions between the con- vection, rotation and a zonal shear flow.

The first slide shows an example of the type of flow that is produced from the analytical solution of the equations of motion for convection in a rotating layer. The solution is for an ideal fluid, that is, a fluid without dissipa- tion, in a rotating layer in which the rotation vector is tilted from the

vertical to represent various latitudes (Hathaway, 1984). This example represents a fairly rapidly rotating case in which the ratio of the buoyancy time to the rotation period is about three. What is found is that the fluid tends to flow upward and toward the pole in a direction nearly parallel to the rotation axis but with much spiraling about this trajectory. Much of the kinetic energy in the flow is in the horizontal spiraling motions rather than the vertical flow.

This solution is used to produce a stress tensor that can be employed in a global circulation model for the large scale flows. The stress tensor is formed by taking the product of the different components of the fluid velocity and then averaging over the volume of the convective eddy. The second slide (Fig. 1) shows the latitude dependence of the stress tensor components for cells like those shown in the first slide. The curves are labeled with the tensor components in spherical polar coordinates. Comparing the diagonal components shows that there is about a factor of 10 more kinetic energy in the horizontal motions than in the vertical motions for this case where rotation is three times faster than buoyancy. More important for forcing the global circulations are the off diagonal components, the products of eastward and northward velocities or northward and radial velocities. The stress tensor shown here gives an equatorward flux of zonal momentum, given by the $\theta\phi$ component, which converges at the equator and would tend to produce a rapidly rotating equator. There is also an upward flux of latitudinal momentum that would tend to produce a meridional circulation that is directed toward the poles in the surface layers.
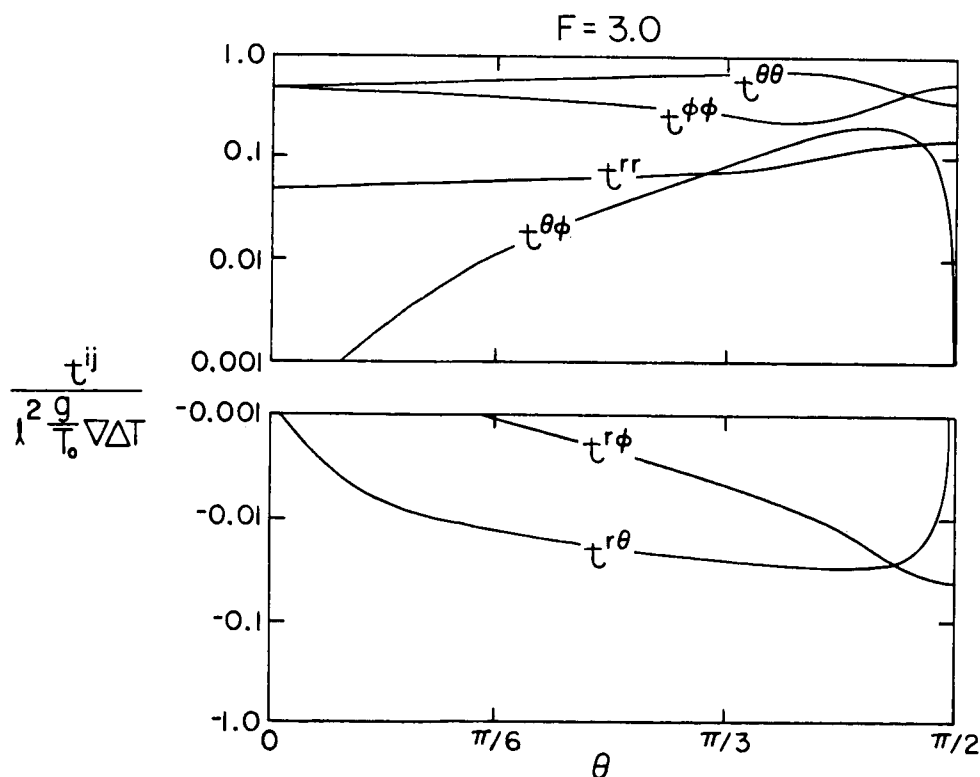
Figure 1. Latitude dependence of the stress tensor components.

RADIAL VELOCITY CONTOURS

$Ra = 10^4$ $Ta = 10^6$

$\Delta T_\theta = 128 \cdot \Delta T_r$
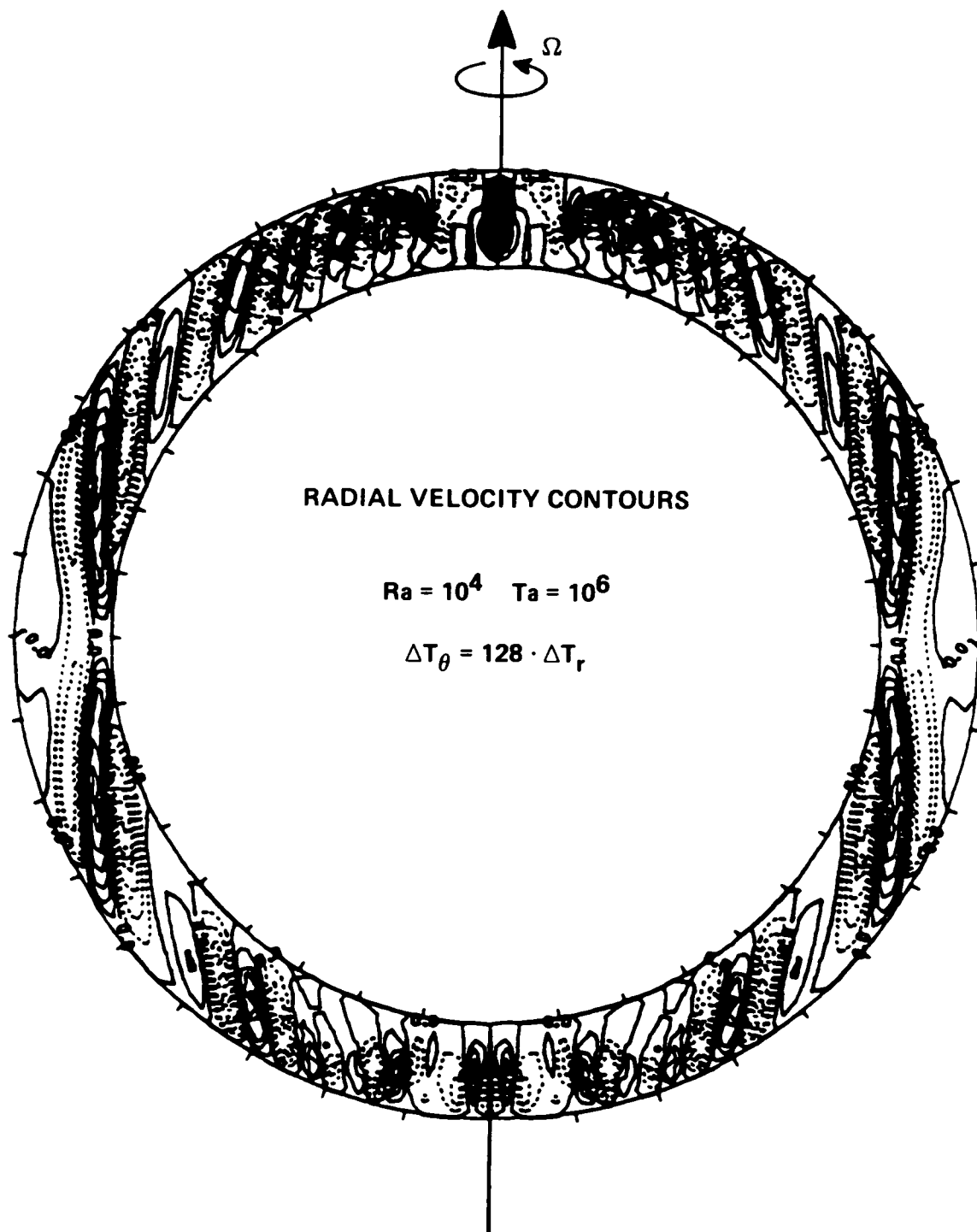
Figure 2.   Contour plot of the radial velocity for an axisymmetric flow forced by a thermal gradient.

This linear convection model only gives the initial tendencies for the global circulation. The actual flows produced by this stress tensor can only be determined from a global circulation model which includes both the stress tensor and the nonlinear interactions between the various flow components. A variety of effects and feedbacks can alter the form of the global circulation from what might be expected given the form of the stress tensor. Fully non-linear models which explicity calculate the convection as well as the global circulation have been produced by Gilman (1977) and Glatzmaier (1984) for the Sun. They find that for the Sun, which is a slow rotator, the stresses produced by the convection do, in fact, produce a rapidly rotating equator and a meridional circulation which is directed toward the poles in the surface layers. However, the meridional circulation does not travel all the way to the poles but instead turns inward at midlatitudes. I propose that on rapidly rotating objects like Jupiter and Saturn this process may go even further and break up the meridional circulation into a series of cells. If I cheat a bit (actually I have to cheat a lot) I can produce a circulation that does just that.

The third slide (Fig. 2) shows the result of a calculation for an axisymmetric flow which is forced by a thermal gradient rather than by a stress tensor. Here the equator is hot and the poles are cold. This tends to drive a meridional circulation in a manner similar to that of the stress tensor. With rapid rotation, here rotation is ten times faster than buoyancy, the meridional circulation breaks up into a series of cells whose sides are nearly parallel to the rotation axis. This slide shows a contour plot of the radial velocity. Associated with this radial flow is a zonal flow in the form of a series of prograde and retrograde jets. Prograde jets are formed in the downdrafts and retrograde jets are formed in the updrafts essentially by conservation of angular momentum in the flow. In this calculation I don't get a rapidly rotating equator because I only include the axisymmetric motions and don't have the stress tensor forcing by the small scale convection.

The second part of this talk is concerned with what happens to small scale convection which is imbedded in zonal shear flows like those produced in the meridional circulation shown in this last slide. The fourth slide (Fig. 3) shows the basic idea behind this study. Consider a zonal flow with a jet-like profile in latitude together with convection in the form of a chevron pattern. (Cloud patterns of this type can be seen on Jupiter, particularly around the 23 deg N latitude jet.) Without rotation the fluid rises along the axes of these convective rolls, spreads outward at the top and then sinks downward in the downdrafts. We find that there is a correlation between the velocity components such that westward flows are associated with flow into the jet maxima and eastward flows are associated with flows into the jet minima. This process extracts momentum and energy from the zonal jet. We get the opposite effect if we look at what happens with rotation. If we take all these horizontal vectors and turn them by the Coriolis force then the velocity correlations are reversed. The fluid moving into the jet maxima is moving to the east and the fluid moving into the jet minima is moving to the west. These velocity correlations feed momentum and energy into the jet.

To see what type of convection pattern is formed, and how it interacts with the jet, Richard Somerville and I have run some numerical calculations for

a) Without Rotation

Convective Flow   Mean Flow

b) With Rotation
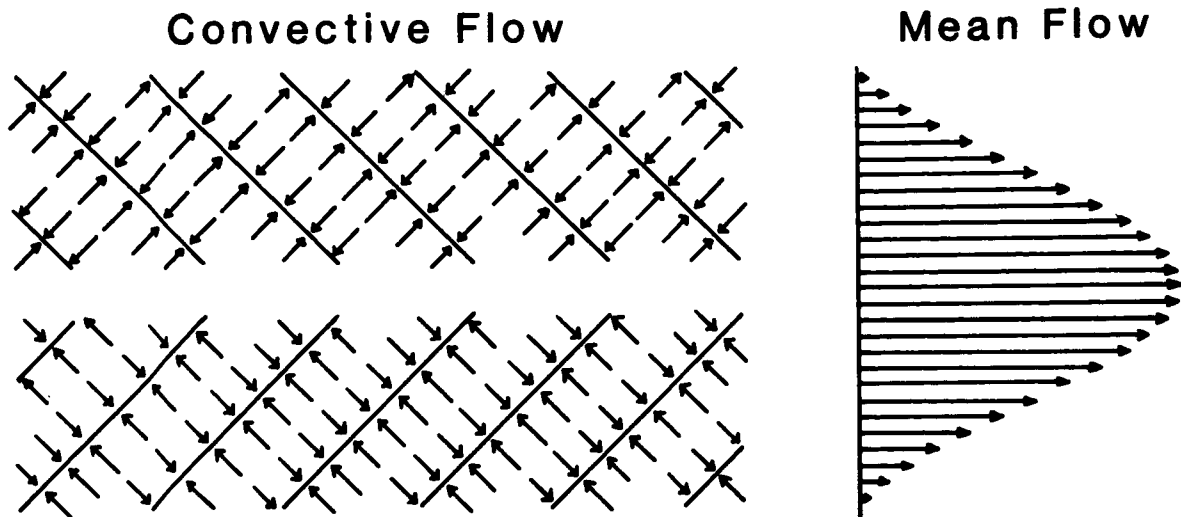
Convective Flow   Mean Flow
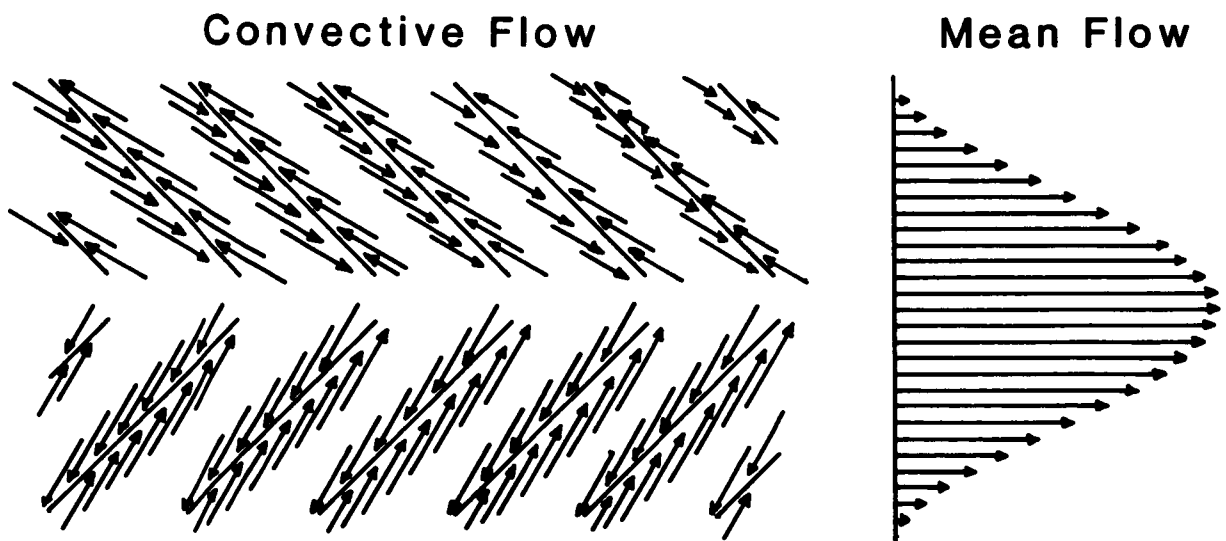
Figure 3. Schematic depiction of correlation between convective velocity components and the zonal mean flow.

three-dimensional and time-dependent convection in a jet-like zonal flow. This prescribed zonal flow has a sine-squared profile in latitude and is constant with depth. The computational domain is periodic in both horizontal directions so the jet profile repeats to the north and south. The jet maximum (eastward) is located halfway between the northern and southern boundaries.

The next slide shows the convective motions for the nonrotating case. On either side of the jet maximum, where the shear is strongest, convection cells are produced which are aligned with the shear flow in an east/west direction. A chevron pattern is not produced in this nonrotating case.

The next slide shows the convective motions for a moderately rotating case in which the rotation period and the buoyancy time are about equal. Here the convection starts to form a chevron pattern and the fluid motion is turned by the Coriolis force so that the velocity components are correlated in the same sense as suggested by the slide shown earlier (Fig. 3). The next slide shows a simulation in which the rotation rate has been increased slightly. Here the chevron pattern is more striking and there is a larger correlation between the velocity components that would feed momentum into the jet. The next slide shows a rapidly rotating case in which the convection is actually quenched where the shear is large. The tilted rotation vector stabilizes convective rolls oriented east/west while the shear flow stabilizes convective rolls oriented north/south. Where these two processes compete the convection is inhibited leaving convection only in the maximum of the jet where the shear vanishes.

I now have 3000 transparencies to show you in the form of a movie. The first part of the movie shows the basic state--hot on the bottom, cool on the top and with the imposed zonal flow. Again, the domain is periodic in both hori-zontal directions so that fluid that flows off the east end reappears at the west end and flow off the north face returns at the south face.

The second part of the movie shows the nonrotating case. This was started from the basic state with small random perturbations in the temperature field. It takes a while for the convection to get started but a pattern starts to form after a while. This pattern has convective rolls aligned with the shear where the shear is strong and then ridges or cells that move along with the flow in the flow maximum. On the two vertical faces of the domain you can see the overturning motions.

DR. STONE: Does the convection interact with the mean flow here or not?

DR. HATHAWAY: It does. I have the imposed mean flow and an additional mean flow is produced by the convection. In the following slides I'll show what the mean flow actually looks like.

The third part of the movie shows a rotating case which was also started from the basic state with small random perturbations in the temperature field. The convection takes a bit longer to get started here because of the stabilizing effects of rotation. We first see the wave-like features in the jet maximum and somewhat later the convection on either side where the shear is stronger.

But it does end up forming a chevron pattern by cells that are tilted into the flow where the shear is strong. It's a bit hard to see exactly how the velocities are correlated in these cells, but the slides I'll show afterwards indicate that there is a flux of momentum into the jet rather than out of it.

DR. LEOVY: Is that flux both in the horizontal and the vertical or just in the horizontal?

DR. HATHAWAY: Primarily in the horizontal, but there is an added twist to the story at the end.

That's the end of the movie. We should now go on to the next slide.

This slide (Fig. 4) shows the mean flow for the nonrotating case. Latitude increases upward and eastward flows are plotted toward the right. The dotted line is the imposed zonal flow. The solid line is the zonal flow after the convection has had a chance to interact with the flow. For this nonrotating case eastward momentum is taken out of the peak of the jet and deposited in the troughs so that there is less momemtum and kinetic energy in the mean flow. In the right hand panel of this slide are plotted the quantities that others have used in analyzing the Voyager images of Jupiter and Saturn. The latitudinal flux of zonal momentum is shown with a dashed line and the gradient of the mean zonal flow is shown with a solid line. These two quantities are anti-correlated indicating that the flux is down the gradient. Momentum is removed from the jet and added to the convection.
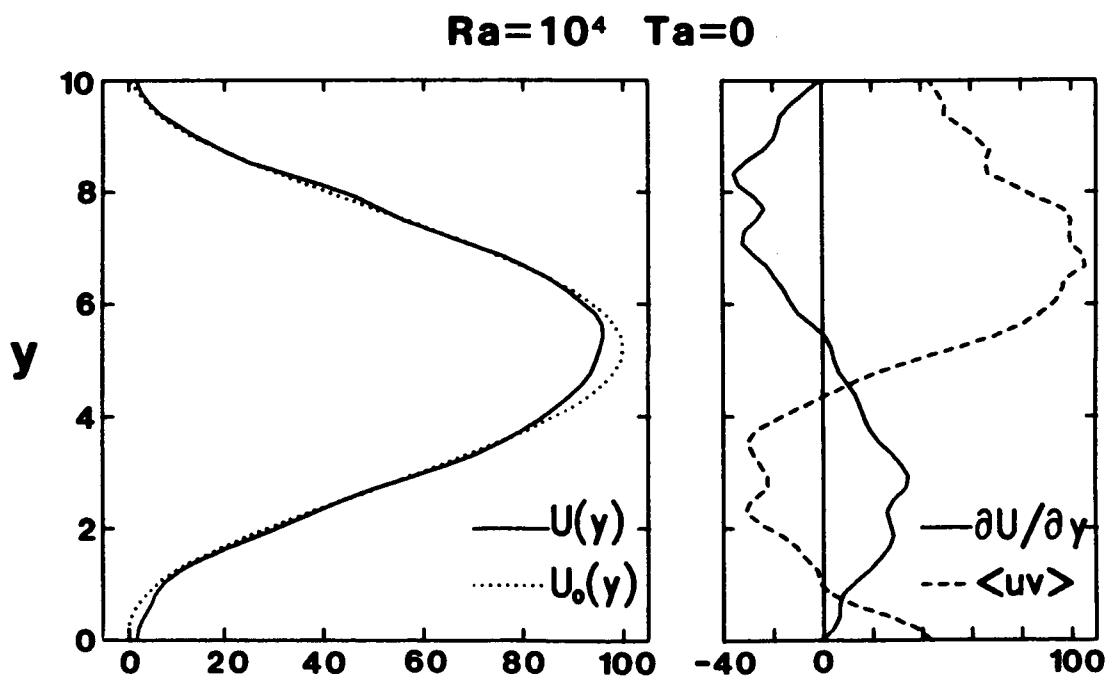
Figure 4. Zonal mean velocity, its latitudinal gradient, and the eddy momentum flux as computed for a nonrotating model.

The next slide (Fig. 5) shows the same quantities for the rotating case shown in the movie. The left hand panel shows that the mean flow is slightly enhanced although the effect is not very large. However, the right hand panel shows a positive correlation between the momentum flux and the momentum gradient which indicates a flux of momentum up the gradient that feeds momentum into the jet. If I apply this model to Jupiter, taking the depth of the layer as 1000 km and the distance between jet maxima as 10,000 km, then the jet has a maximum velocity of about 100 m s^{-1} and the momentum flux is as high as 35 m^{2}s^{-2}. This corresponds well with the magnitude of the momentum flux found by Ingersoll *et al.* (1981). Judging from the last talk there seems to be a question as to what the magnitude of this effect really is but there does seem to be agreement on the sign of this momentum flux for Jupiter.

In spite of the magnitude of the momentum flux we find in these simulations, we don't produce a very strong jet. The next slide (Fig. 6) shows the final twist to this story. It turns out that there are several other terms that act on the mean flow. One that hasn't been mentioned is the Coriolis force on the vertical flow. Downflows produce eastward flows and upflows produce westward flows. We find that there is a meridional circulation induced by the convection in this last simulation with rising motion on the equatorward side of the jet and falling motion on the poleward side. The Coriolis force acting on these vertical flows is nearly anticorrelated with the divergence of the momentum flux as shown in this slide. These two forcing terms for the mean zonal flow counteract each other so that a stronger jet is not produced. When we look at the other forcing terms we find that they are unimportant for the depth-averaged zonal flow. The Coriolis force acting on the induced latitudinal flow gives no net contribution, the force is in one direction on the top and in the opposite direction on the bottom.

Ra=10⁴ Ta=3×10⁴
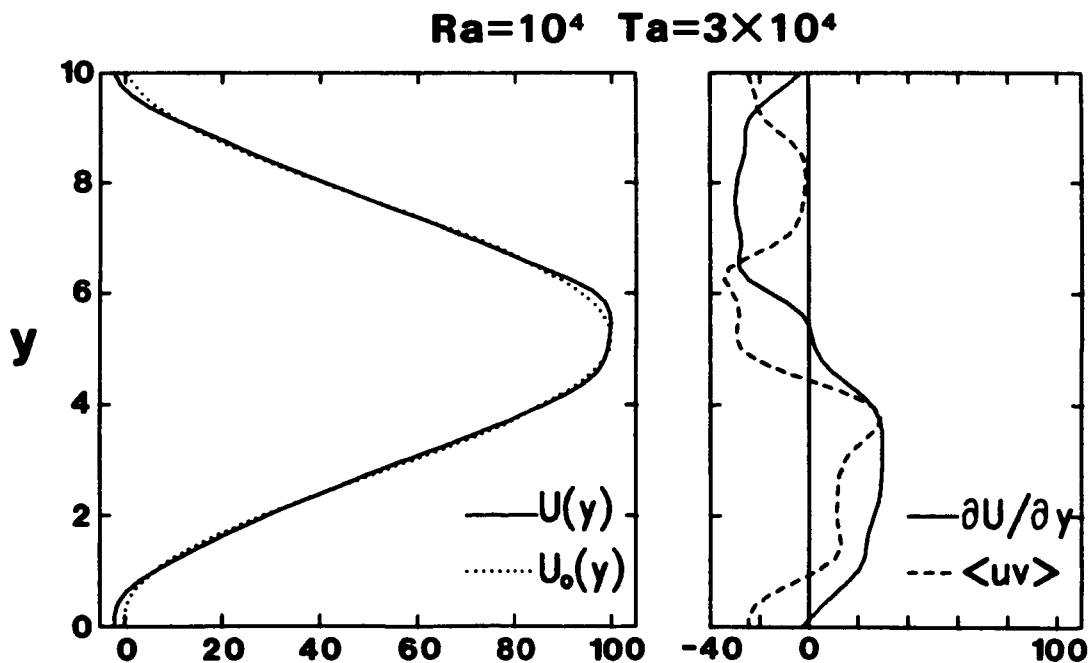
Figure 5. Zonal mean velocity, its latitudinal gradient, and the eddy momentum flux as computed for a model with rotation.

Ra=10⁴ Ta=3×10⁴
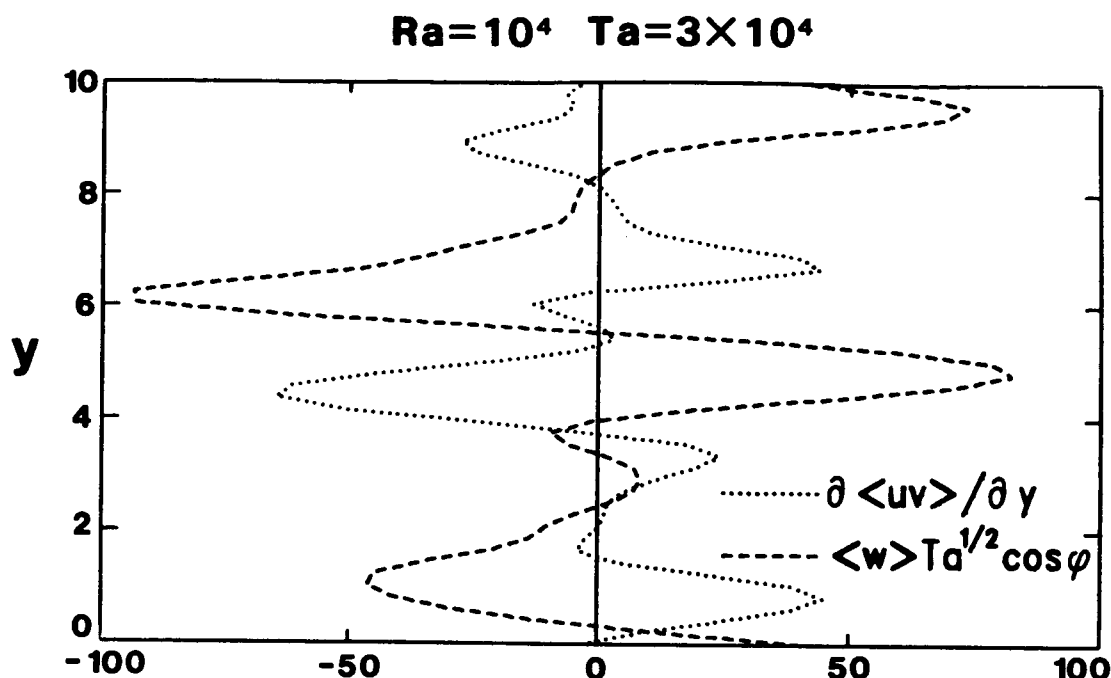
Figure 6. The Coriolis torque on vertical motion and the divergence of eddy momentum flux as computed for the rotating model.

This induced meridional circulation may be of interest to those concerned with the cloud structure and aerosols. I think it's also the same type of circulation that Michael Flasar presented in his model of overturning flow around the jets at stratospheric levels. I hope that this drives home the point that there are additional forcing terms that we need to look at. Although the Coriolis force on the mean vertical flow may be one of the hardest things to measure, in this model, at least, it was probably the dominant term. With that I'll end my talk.

REFERENCES

Gilman, P. A. (1977). Nonlinear dynamics of Boussinesq convection in a deep rotating spherical shell. I. Geophys. Astrophys. Fluid Dynam. 8, 93-135.

Galtzmaier, G. A. (1984). Numerical simulations of stellar convective dynamos. I. The model and the method. J. Comput. Phys. 55, 461-484.

Hathaway, D. H. (1984). A convective model for turbulent mixing in rotating convection zones. Astrophys. J. 276, 316-324.

Ingersoll, A. P., R. F. Beebe, J. L. Mitchell, G. W. Garneau, G. M. Yagi, and J. P. Mueller (1981). Interactions of eddies and mean zonal flow on Jupiter as inferred from Voyager 1 and 2 images. J. Geophys. Res. 86, 8733-8743.

DR. STONE: I'd like to ask a question myself. Were those equilibrium solutions that you were showing? They had fully evolved as much as they could?

DR. HATHAWAY: I think you can see from the movie, I ran it until they were statistically steady. As far as I could tell it looked like there weren't going to be any more changes. They certainly do produce small fluctuations but I think the statistics were fairly steady at the time I stopped calculations.

DR. HUBBARD: Can I ask you to defend your results in terms of what I would consider to be a more realistic interior model. I mean, you're taking a layer as I understand it, which is 1000 km thick or so and you have some sort of rigid lower boundary to it whereas on the real Jupiter the equation of state gradually goes over to a non-ideal form over something like that depth. But there is certainly no abrupt transition to some other domain.

DR. HATHAWAY: Yes. My choice of depth was motivated by one thing and that was to get the size of the cells somewhat similar to what we observe in the north temperate belt and there are a lot of things that can change that. Within this model I have rigid tops and bottoms, the size of the convection tends to be on the order of the depth of the layer. What you get for more realistic situations is a little hard to say. I mean, there are problems even in the Earth's atmosphere in producing very broad meso-scale eddies where the width of the eddies are much bigger than the depth of the layer. It was a bit of an arbitrary decision, but the choice shouldn't change the character of the interaction much. The previous calculation I showed for the spherical shells chose the depth to be where the fluid changes from molecular to metallic hydrogen. This seems to be a more reasonable place to put an interface.

DR. EMANUEL: What do you imagine might change if you were to repeat the experiment on the equatorial beta plane? I guess what I'm driving at is, is it possible that this mechanism might have anything to do with the equatorial jet?

DR. HATHAWAY: It could. Basically all you need to get the equatorial jet with the convection are cells that are elongated in the north/south direction. That's basically the thing you need. You can go through the same exercise drawing vectors and seeing which way the Coriolis force turns them. I think that the key for producing equatorial acceleration is cells that are elongating north/south. That is also the sense you get out of convective models in spherical shells or those I've done on inclined planes where the rotation vector is tilted. The rotation vector tends to elongate cells in that direction. However, I can't do these calculations on a beta plane. A beta plane has a rotation vector which tilts more as you go toward the north. I've got periodic boundary conditions, so I can't do that.

DR. FELS: I'm sorry. I'm not quite clear on just what's in your model. It's a fully non-linear invisid...?

DR. HATHAWAY: Which one, the latter model?

DR. FELS: The one that generated the movie, yeah.

DR. HATHAWAY: The one that generated the movie is wholly viscous. I've solved the Navier-Stokes equations in a plane parallel layer with a rigid top and bottom and rotation about an axis that's tilted from the vertical. I then impose the jet, and then solve the equations for the flow, and see how it evolves. I still have to include something that's essentially forcing the basic jet. The convection here doesn't maintain it afterward. It does feed momentum into it, but it doesn't really maintain it.

DR. INGERSOLL: Sort of a body force?

DR. HATHAWAY: Yes, I need a pressure gradient, or some other forcing. That's why I had two parts to my talk. In the first part of my talk I wanted to suggest that you can produce jets by these meridional circulations and it may be that these maintain the jets. Once you have convection, you then get these momentum fluxes.

DR. STONE: Don't you have an externally imposed meridional pressure gradient?

DR. HATHAWAY: That's right. That's what I have within the model.

DR. STONE: There's no feedback on that pressure gradient?

DR. HATHAWAY: That's right.

DR. FELS: So would the jet grind down?

DR. HATHAWAY: It depends on what you have for forcing, whether it's strictly by the meridional flow or by a thermal wind or what. That something isn't specified. I just have a force within my equations that maintains that basic shear profile and then the convection interacts with the shear and produces its own flow which in one case was opposed to the imposed flow and in the other case was to increase the imposed flow.

DR. CANUTO: Can I ask a question about these Reynolds stresses you have computed? You show a computed graph of $\tau^{r\phi}$ versus θ and presuming the geometry was right, do you really believe that the absolute values are also correct? You use a linear model for those.

DR. HATHAWAY: What I have to do there is go to mixing length theory to get an amplitude for motions.

DR. CANUTO: That's what you do to get the absolute value?

DR. HATHAWAY: That's right. With my linear model all I can do is describe the geometry of the flow, for the amplitude I have to go to mixing length theory.

DR. STOKER: You talked about vertical motion flowing along the parallel to the rotation vector. Does that happen for more shallow flows? I mean, if your flow is 100 km rather than 1000 km, will it still...

DR. HATHAWAY: It depends upon the ratio of the time scales. If you have shallow flows that are very rapid with respect to the rotation period, I wouldn't expect that. If the flows are slow so that a turnover time is very long compared to rotation period I would expect the same thing, that you get a sloping flow nearly in the direction of the rotation axis.

CONVECTION WITHOUT EDDY VISCOSITY: AN ATTEMPT
TO MODEL THE INTERIORS OF GIANT PLANETS

A. P. Ingersoll
California Institute of Technology

Meteorologists are lucky. In the theory of hydrostatic quasi-geostrophic flow in the earth's atmosphere the principal results do not depend on the eddy viscosity. This contrasts with published theories of convection in deep rotating fluid spheres, where the wavelength of the fastest growing disturbance varies as $E^{1/3}$, where E the Ekman number is proportional to the eddy viscosity. A new theory [an extension of work by A. P. Ingersoll and D. Pollard (1982, Icarus 52, 62-80)] of quasi-columnar motions in stably stratified fluid spheres attempts to capture the luck of the meteorologists. The theory allows one to investigate the stability of barotropic and baroclinic zonal flows that extend into the planetary interior. It is hypothesized that the internal heat of Jupiter and Saturn comes out not radially but on sloping surfaces defined by the internal entropy distribution. To test the hypothesis one searches for basic states in which the wavelength of the fastest-growing disturbance remains finite as E tends to zero, and in which the heat flux vector is radially outward and poleward. A status report on this search will be presented.

You've seen what happens to a nice guy like myself who tries to observe something and measure something, so for this talk I'm going to be a theoretician. I'd like to test a hypothesis. I don't necessarily believe the hypothesis, but I want to develop theoretical models that will provide us with some tests, especially if we have some data. The hypothesis is that the zonal flows and other large scale structures that we see are due to large scale motions in the interior driven by convection of internal heat (see Fig. 1). A number of collaborators have helped with this work. (D. Pollard, 1982; R. L. Miller, 1986; S. Schilpf, in progress.)

Eddy viscosity is sort of a distasteful subject, since you never know it in advance or even its sign or magnitude or the exponent of its magnitude and I don't like it. But it's a useful way to classify the two kinds of convection that I want to talk about. One is viscous convection, starting with Rayleigh and Benard plane parallel convection, but including configurations of rotating spheres. The general feature of this kind of convection is that the entropy gradient is decreasing as you go outward, so it's unstable stratification. There's nothing wrong with this kind of convection, except that if you're going to invoke it to explain the zonal flows on Jupiter, you get into trouble. Let me explain that. If you pick the eddy viscosity to be a small number, you find that the scale of the convection, which is the diameter of the little columns shown in Fig. 1, goes to zero as the eddy viscosity that you choose goes to zero. Eventually you get into scales that are just too small to account for the zonal jets. So if you're going to pursue the hypothesis

that the zonal jets are related to the cylinders and those are related to the columns, then you've got trouble if the eddy viscosity is small. On the other hand, if you choose a large enough eddy viscosity to get large scales, you've got another problem if you're going to invoke this kind of convection on Jupiter, and that is that you've increased the dissipation of the mechanical energy. According to the hypothesis we've got shear flows of the same order that we see in the atmosphere extending way into the fluid, and with the large viscosity down there you're going to get more energy being dissipated than the planet has available.

I tend to reject viscous convection, or if not reject it at least look elsewhere for the kind of convection that I'm going to invoke for Jupiter. There is another place to look and that is the Earth's atmosphere which is stably stratified, with entropy increasing as you go up. On the Earth convection takes place on sloping surfaces of potential temperature and this is of course the theory of baroclinic instability which is quite successful. It's robust, the scale size does not depend on some undetermined eddy viscosity. It depends on fairly easy to measure quantities. Its radius of deformation involves the entropy gradient, and it kind of explains our weather at mid-latitudes. Also, you don't need a lot of fancy computation to get nice models. Of course this has been formulated for thin atmospheres with solid boundaries.
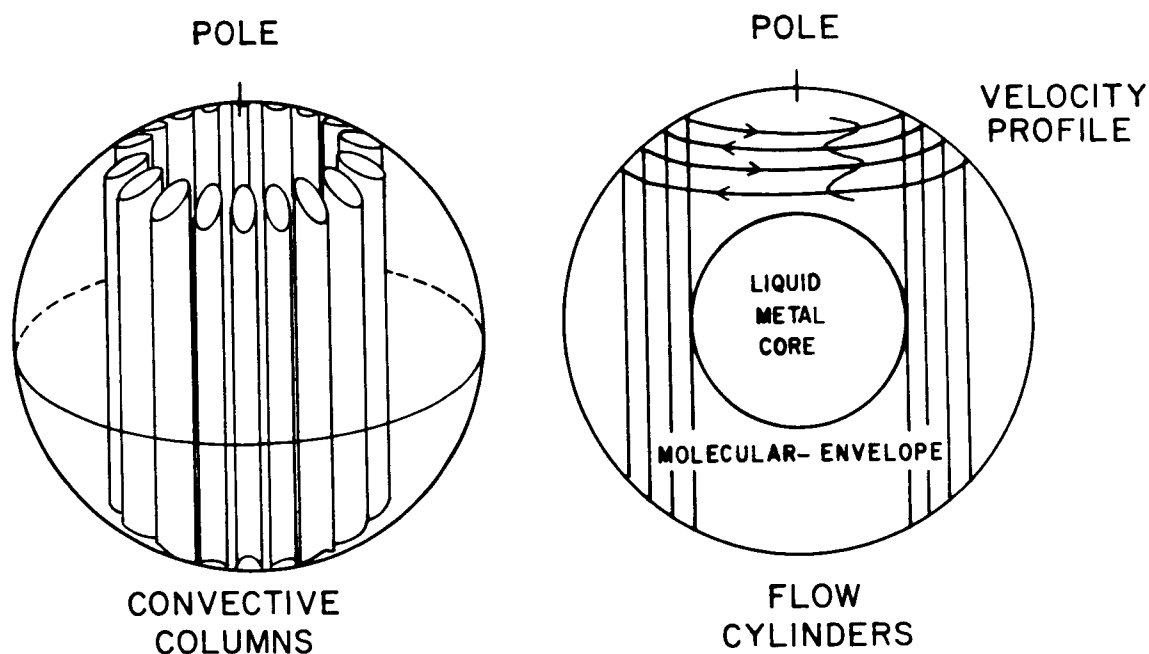
Figure 1. Schematic geometry for models of deep interior convection and zonal flow in the Jovian planets. The scale of the convection is indicated by the diameter of the columns in the illustration on the left. According to the hypothesis under study the columnar convection supports the observed zonal flow as cylinders of motion extending through the fluid interior as shown in the illustration on the right.

Well, the question is, can we somehow apply this idea of convection in stably stratified media to a full sphere of density, varying from some internal value down to zero at the surface, as in the interior of Jupiter and Saturn? So the goals of this research are ambitious. I'd like to redo all of text-book meteorology. I'd like to take Holton—page by page—and solve the normal mode oscillation problem, the problem of barotropic instabilities, the problems of baroclinic instabilities, all of these textbook problems. I want to throw in non-linear calculations, do it all again, having abandoned the thin layer approximation but kept the quasi-geostrophic approximation. It turns out that you can do that if you are dealing with quasi-columnar motions of the sort depicted in Fig. 2 showing the first three modes under study. I want to proceed with the hypothesis that the fluid is stably stratified, which means that entropy increases as you go out along its spherical radius, but on the other hand, is not spherically symmetric either so that there are horizontal entropy gradients; i.e., there are horizontal temperature gradients that can drive some sloping convection.

So that's what I'd like to do, and I'm only half way through it. Of course you don't know where the end is so I'm probably only 10% of the way through it. I have a few achievements. There is a nice quasi-geostrophic system of equations. It's a little different but it somewhat resembles the old system. It's got some new terms cropping up here and there. It's lots of fun, and I've been solving a few simple problems. The first one was the normal mode oscillations of the otherwise uniformly rotating planet. I get solutions that look like Rossby waves but they go to the east, not to the west, and that's because the effective beta parameter for the system has the opposite sign (cf. Ingersoll and Miller, 1986).

EQUATOR

Possible disturbance modes

EQUATOR

Possible basic state
($\bar{S}$ entropy Contours)
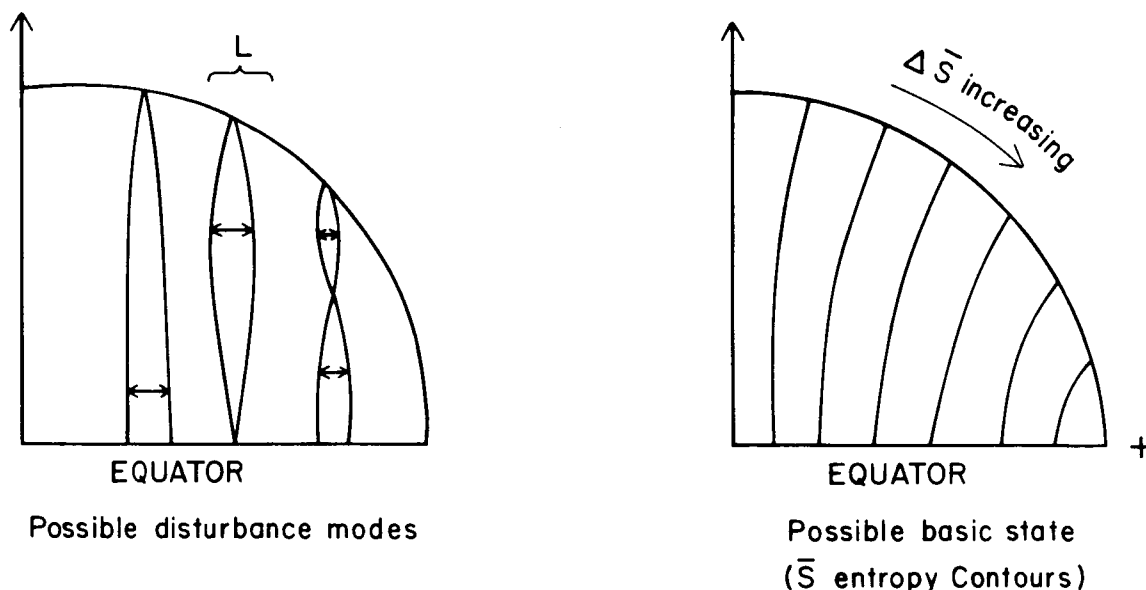
Figure 2. Schematic depiction of possible normal mode oscillations (left) and a possible configuration for the basic state distribution of entropy (right) for convection within the fluid interiors of rotating Jovian planets.

If one of the columns moves toward the axis of rotation, you stretch it and so the beta effect has the opposite sign as in the terrestrial problem. It is possible to match the wavelength of these features... *[Dr. Ingersoll holds up a copy of the conference notebook and refers to the schematic depiction of the equatorial plumes on the logo.]* ...according to these solutions and the 100 m s^{-1} wind speed if you assume the presence of a latitudinal duct at ± 9 deg latitude. Of course this is just forcing it to fit.

I've also solved the barotropic stability problem for a particularly simple case with no buoyancy forces at all and a totally adiabatic interior. You have differentially rotating cylinders and you want to know the criterion for shear instability. How much curvature can the differential rotation profile take before the instabilities will set it? It's very much like the barotropic problem in meteorology. Pollard and I, in our 1982 *Icarus* paper, investigated the deep barotropic instability in the long-wave limit for longitudinal disturbances. Now Miller and I have investigated this as a function of longitudinal wavenumber and have shown that the new criterion really does control the stability of the assumed flow. If you take the measured zonal velocity profile projected on the surface of the sphere and take its second derivative, the Voyager data show that every westward jet is unstable according to the simple barotropic stability criterion. Only the 23 degree jet is unstable according to the deep sphere criterion. And of course the sign of beta for the deep cylindrical case is opposite to that for the terrestrial case and the new criteria apply to the eastward jets, not to the westward jets. But it must be remembered that this has been derived for an adiabatic sphere.

I'm having problems with the baroclinic calculation, and this may be telling me something. I am objective enough that if it really tells me it's the wrong theory I will so state and so conclude. One problem is that there are too many possible basic state configurations for the entropy distribution. The real basic state should emerge from a fully non-linear calculation, but quasi-geostrophic theory can't give this. (There is the same problem in meteorology.) We've run a lot of cases with various entropy distributions and so far all the kinds of instabilities that emerge, all the growing oscillations, are small-scale even though the entropy gradient is increasing spherically outward. In other words the convection looks like what I call viscous convection. It wants to take place on small scales, and that really violates the scaling that I put into this whole theory. Maybe Busse is right. Maybe we just need a big eddy viscosity and there is no preference for large-scale motions. I'd like to be able to come to a conclusion at least and I'm not quite ready to do that nor have I put in buoyancy forces, i.e., baroclinicity, and at the same time shear. That lies ahead. So this is a progress report.

REFERENCES

Holton, J. R. (1979). *An Introduction to Dynamic Meteorology*, Second Edition, Academic Press, New York.

Ingersoll, A. P., and C. C. Porco (1978). Solar heating and internal heat on Jupiter. *Icarus* <u>35</u>, 27-43.

Ingersoll, A. P., and D. Pollard (1982). Motion in the interiors and atmospheres of Jupiter and Saturn: scale analysis, anelastic equations, barotropic stability criterion. *Icarus* 52, 62–80.

Ingersoll, A. P., and R. L. Miller (1986). Motions in the interiors and atmospheres of Jupiter and Saturn 2: barotropic instabilities and normal modes of an adiabatic planet. *Icarus* 65, 370–382.

DR. ROSSOW: Andy, could you just explain again the basic state for those of us who still think in terms of spheres? On a spherical surface do you end up with a gradient both radially and horizontally?

DR. INGERSOLL: Constant entropy lines are shown in my cartoon (Fig. 2). This is just one example of what you might try. The highest entropy is over on the right. This would be a planet heated by the sun, like Jupiter, but also radiating into space. If you go out along any spherical radius, entropy is increasing, so it's stably stratified. On the other hand, you do have horizontal entropy gradients so it's baroclinic. And the idea is the sloping convection would take place along these surfaces and would duct heat outwards and polewards just as it should to satisfy energy conservation. Ingersoll and Porco (1978), if I may cite myself.

DR. FLASAR: You mentioned that as the eddy viscosity goes down for the convective modes that the scales get shorter and that bothers you, but is that really so bad? Why can't the heat transporting convective modes drive larger scales? I mean, drive larger eddies which in turn drive the jets. Why does that bother you necessarily?

DR. INGERSOLL: It's only something that bothers me, it's not a proof of something. Numerical models of viscous convection are always done at moderate Reynolds numbers and moderate Rayleigh numbers, because you can't just shoot those numbers way up and have a convergent numerical scheme; and at those values, the scale of the eddies is about the same scale as the mean flow that they drive. No one really knows what those models are going to do at much higher scales and it may be that little tiny eddies will drive great big cells.

DR. LEOVY: I very much appreciate your desire to redo Holton and I got the same feeling just from reading your paper with Pollard, but there are two aspects of the barotropic situation that I'd like to ask about. Two aspects of the kind of barotropic analogy that you and Pollard describe intrigue me. One is that, for that barotropic vorticity equation one gets 2-D turbulence with upscale energy and downscale enstrophy cascades, and the second is this: there may be the possibility of Rossby wave solitons in this type of system. Have you investigated whether either of those are possible in the barotropic case?

DR. INGERSOLL: There's only one obviously conserved quantity, which is energy, in this system. I don't see any enstrophy sitting around...

DR. LEOVY: Do you have a vorticity?

DR. INGERSOLL: I'm just telling you what I know so far. There's a vorticity, but the vertical equation is totally different from anything you're used to. You can't combine it into a single potential vorticity equation. You just can't do that in this system the way you can in the other systems and so there's only one conserved thing and it's energy. You could say there are low frequency inertial oscillations too, so in a sense it's got more degrees of freedom. It has more than just a Rossby-type wave mode. The quasi-geostrophic system filters out inertia-gravity waves. This system doesn't filter them out.

DR. EMANUEL: In your reworking of Holton, did you get around to generalizing the Charney-Stern theorem? In other words, do we really know for a deep rotating fluid like this what the criterion for internal instability really is? Is there a generalization? Can we state with any confidence that an instability criterion is really satisfied because I think, as you pointed out earlier, just looking at the horizontal variation of U along spherical surfaces is insufficient, it's not really a critical look at the stability criterion.

DR. INGERSOLL: I haven't found any lovely theorems. What I call the Rayleigh criterion is certainly an integral constraint. I could only derive that assuming something about the perturbations, namely they have long wavelength. Otherwise I just had to root it out numerically. So I don't know the answer.

DR. EMANUEL: And that was a strictly two-dimensional analysis?

DR. INGERSOLL: If you assume long wavelengths you can turn it into two dimensions, one of which has perturbations proportional to e^{ikx}. The numerical three dimensional analysis is non-separable in the spatial coordinates. It's kind of a nasty thing.

DR. HATHAWAY: A comment about eddy viscosity. You suggest as you make that viscosity smaller and smaller you get a smaller scale of convection that is preferred, when what really happens is that you just open up the spectrum to those smaller scales. It may still be the large scale convection that dominates. If you in fact look at growth rates for convection in a purely inviscid fluid, the spectrum rises from zero and then flattens out completely off to infinity. The maximum is out at infinity but you get this broad spectrum that is included.

DR. INGERSOLL: Well I was citing the linear stability analyses of Busse and company when I said that. It's true that in a fully nonlinear calculation, the fastest growing disturbance is not necessarily the one that's preferred.

DR. HATHAWAY: Then a question. Can you get Jupiter's internal heat flux out for a model that has an entropy maximum at the surface and the equator?

DR. INGERSOLL: That is the kind of self-consistency test that must be applied. I will believe the model if I can and I won't believe it if I can't. But it's hard to prove you can't do something because you may not have tried it the right way. You can try it a million times and the million plus first time it works. That's kind of the problem I'm having right now.

DR. TAYLOR: At the beginning you explained a desire to have more data. Could you say what kind of data you'd like to have and in detail how you would use it to test different aspects of this?

DR. INGERSOLL: I'm going to spend tonight writing my conference review and I'll tell you tomorrow about what you can expect from Galileo, Voyager, and what I'd like if I had some other spacecraft...You think I'm just going to review what you people said.

[Laughter from conference participants.]

CONVECTIVE ADJUSTMENT IN BAROCLINIC ATMOSPHERES

Kerry A. Emanuel
Massachusetts Institute of Technology

Local convection in planetary atmospheres is generally considered to result from the action of gravity on small regions of anomalous density. We show that in rotating baroclinic fluids the total potential energy for small-scale convection contains a centrifugal as well as a gravitational contribution. Convective adjustment in such an atmosphere results in the establishment of near adiabatic lapse rates of temperature along suitably defined surfaces of constant angular momentum, rather than in the vertical. This leads in general to sub-adiabatic vertical lapse rates. We demonstrate by example that such an adjustment actually occurs in the earth's atmosphere and estimate the magnitude of the effect for several other planetary atmospheres.

Among the more important processes operative in many planetary and stellar atmospheres is small-scale bouyant convection, whose presence is often inferred from the observation of adiabatic lapse rates of temperature, a condition which both theory and experiment show will result from the action of convection at very high Rayleigh number. Conversely, the observation of sub-adiabatic lapse rates appears to rule out the action of bouyant convection. The purpose of this presentation is to demonstrate that small-scale convection in rotating baroclinic flows is driven by centrifugal as well as gravitational bouyancy and results in the establishment of adiabatic lapse rates along locally defined angular momentum surfaces and sub-adiabatic lapse rates in the vertical. We estimate the magnitude of this effect in planetary atmospheres and discuss a technique for inferring the lapse rates along angular momentum surfaces from vertical profiles of wind and temperature. This work represents a generalization to planetary atmospheres of the theory of slantwise convection in the earth's atmosphere developed by Emanuel (1983a,b), and may be considered a nonlinear extension of the theory of symmetric instability developed by Solberg (1933), Stone (1966), and others.

Consider a geostrophically and hydrostatically balanced baroclinic flow on a segment of a sphere sufficiently small that the variation of the local normal component of the planetary rotation may be neglected. Figure 1 shows a hypothetical distribution of isotherms on a constant pressure surface in such a segment. In order that the flow remain close to geostrophic, the length and velocity scales associated with the pattern must be such that the Rossby number, defined $R_o \equiv U_o/fL$ is much less than unity. Here U_o and L are velocity and length scales, and f is the Coriolis parameter. It is helpful to define a local coordinate system which has its x-axis parallel to the isotherms, as illustrated in Fig. 1.
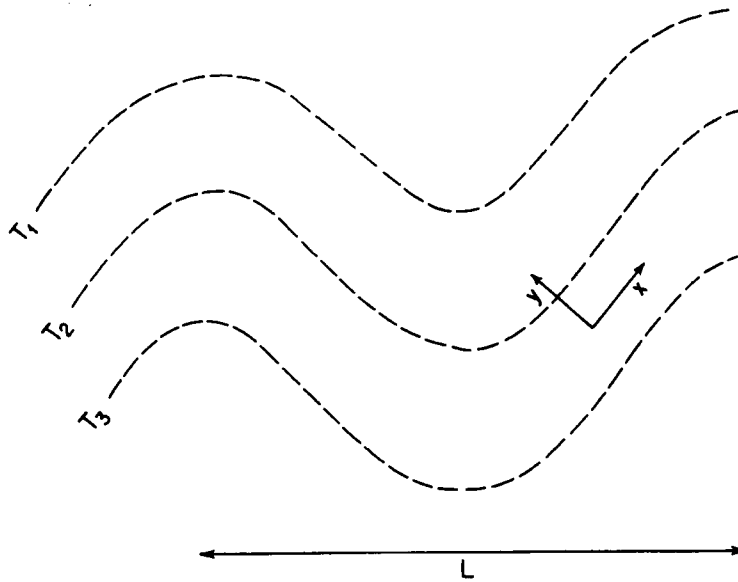
Figure 1. Definition of coordinate system with
respect to large-scale pattern of isotherms on
an isobaric surface.

In this coordinate system, the inviscid equations of motion may be written

$$\frac{du}{dt} = fv \equiv f\frac{dy}{dt} , \tag{1}$$

$$\frac{dv}{dt} = f(u_g - u) \tag{2}$$

where u and v are the components of velocity in the x and y directions and u_g is the geostrophic velocity. Equation (1) applies as long as the parcel remains in a flow for which pressure gradients parallel to x are small. By virtue of (1), a quantity M, defined

$$M \equiv u - fy \tag{3}$$

is conserved following the motion of fluid parcels and (1) and (2) may be rewritten

$$\frac{dM}{dt} = 0 , \tag{4}$$

$$\frac{dv}{dt} = -f(M-M_g), \tag{5}$$

where M_g is the geostrophic value of M. The quantity M represents a linearization of the angular momentum per unit mass of the fluid.

164

C-3

It has been demonstrated by Emanuel (1983a) that provided the ensuing convection is characterized by length scales along the total acceleration vector that are large compared to length scales normal to this vector, the effect of the convection on the pressure field may be neglected so that M_g may be regarded as a fixed function of space in (5). Similarly, if the temperature perturbations are small compared to the mean temperature, the inviscid equation of vertical motion may be approximated by

$$\frac{dw}{dt} = \frac{g}{\theta} (\theta - \theta_a),$$ (6)

where g is the acceleration of gravity, θ is the potential temperature and θ_a is the ambient potential temperature, also a fixed function of space. The thermal wind equation relates M_g to θ_a:

$$f \frac{dM_g}{dz} = - \frac{g}{\theta_a} \frac{\partial \theta_a}{\partial y} ,$$ (7)

The system is closed by the equation for the parcel potential temperature:

$$c_p \frac{d \ln \theta}{dt} = \frac{\dot{H}}{T}$$ (8)

where c_p is the heat capacity at constant pressure, $\dot{H}$ is the diabatic heating rate, and T is the absolute temperature. The diabatic heating includes effects of radiative transfer and latent heat release associated with phase changes. The latter will generally result in a parcel potential temperature which is a function of pressure. We note that (6) does not include effects due to changing proportions of chemical constituents or to the presence of suspended liquids or solids.

Note that equations (5) and (6) for the lateral and vertical accelerations are formally identical in form as they both depend on the differences between conserved parcel quantities and fixed ambient properties. This is simply to say that there is no qualitative difference between centripetal and gravitational acceleration. In a baroclinic flow, M_g varies with height so that, according to (5), vertically displaced parcels will always suffer lateral as well as vertical accelerations; convection in this case will therefore be "slantwise" rather than vertical. An extensive discussion of the nature of slantwise convection in the earth's atmosphere may be found in Emanuel (1983a,b); here we summarize and extend the main results as they pertain to convection in planetary atmospheres.

The relations (5) and (6) imply that unstable convection will occur if a displacement results in accelerations in the same directions as the displacement; they also imply that the parcel will come to rest at or oscillate about stable

equilibrium points where $M = M_g$ and $\theta = \theta_a$. The total potential energy available to drive parcels between their initial unstable equilibrium points and their final stable equilibria is the path integral of the vector force (per unit mass) $\underset{\sim}{F}$:

$$\text{TPE} = \int_1^2 \underset{\sim}{F} \cdot d\underset{\sim}{\ell} = \int_1^2 \left\{ -f(M-M_g)\hat{j} + \frac{g}{\theta}(\theta-\theta_a)\hat{k} \right\} \cdot d\underset{\sim}{\ell} \;, \tag{9}$$

where TPE is the "total potential energy" and (5) and (6) have been substituted as the lateral and vertical components of the force per unit mass. The unit vectors in y and z are $\hat{j}$ and $\hat{k}$.

Now by virtue of (7), the force vector is irrotational:

$$\nabla \times \underset{\sim}{F} = 0 \;,$$

so that the choice of integration path is immaterial. For convenience, we choose a path along a surface of constant M and redefine the potential energy:

$$\text{TPE} = \int_1^2 \Big|_{M_g} \frac{g}{\theta}(\theta-\theta_a)dz \;, \tag{10}$$

which simply means that the total potential energy for small-scale convection is the integral of the parcel bouyancy as it is lifted along surfaces of constant geostrophic pseudo-angular momentum, M_g. (We note that this in no way implies that the ensuing convection will result in motions along M_g surfaces.) This definition of potential energy represents a simple generalization of the classical expression which is identical to (10) except that the path of integration is in the vertical direction. In a barotropic flow, M_g surfaces are vertical and (10) reduces to the classical expression. The important implication of (10) for our present purpose is that the state of neutrality to small-scale convection is characterized by adiabatic lapse rates along M_g surfaces. That this type of adjustment actually occurs in the earth's atmosphere is illustrated in Fig. 2, which shows a temperature sounding measured by an instrumented aircraft flying down an M surface, a vertical sounding, and a pseudo-adiabat for processes involving phase change of water between vapor and ice. While the vertical sounding is definitely sub-adiabatic, the M-surface sounding is almost perfectly adiabatic. An interpretation of the convective dynamics of this atmosphere based only on the vertical sounding would be most misleading. If the vertical sounding measures horizontal wind as well, however, it is possible to roughly estimate the M_g-surface temperature structure from the vertical sounding.

Suppose that a baroclinic flow is characterized by zonal winds which increase with height. Then, as illustrated in Fig. 3, M_g surfaces will slope poleward with increasing height. We estimate the temperature structure along a particular M_g surface using the thermal wind equation and geometry.

166

Figure 2. Earth atmospheric
temperature soundings shortly
after midnight Eastern Standard
Time on 16 November 1983. Solid
line: Aircraft sounding along
M surface from central Maine
to coastal New Hampshire.
Departures of M (m s^{-1}) from
value at 412 mb indicated in
parentheses at left. Dash-
dot line: Vertical sounding
made by spiral ascent of air-
craft at Brunswick, Maine.
Dashed line: Moist adiabat for
vapor-ice transition corres-
ponding to ice equivalent
potential temperature of 315 K.
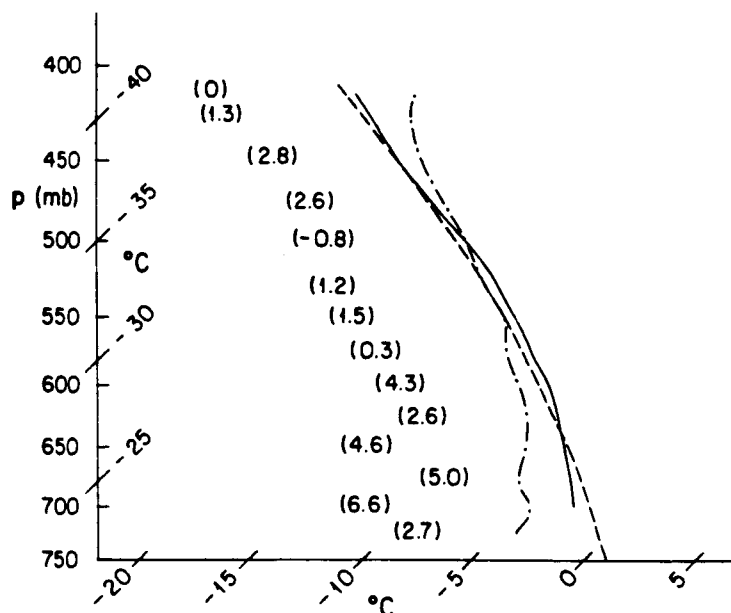
Figure 3. Geometry used to esti-
mate distribution of potential
temperature along the M_g surface.
See text for explanation.
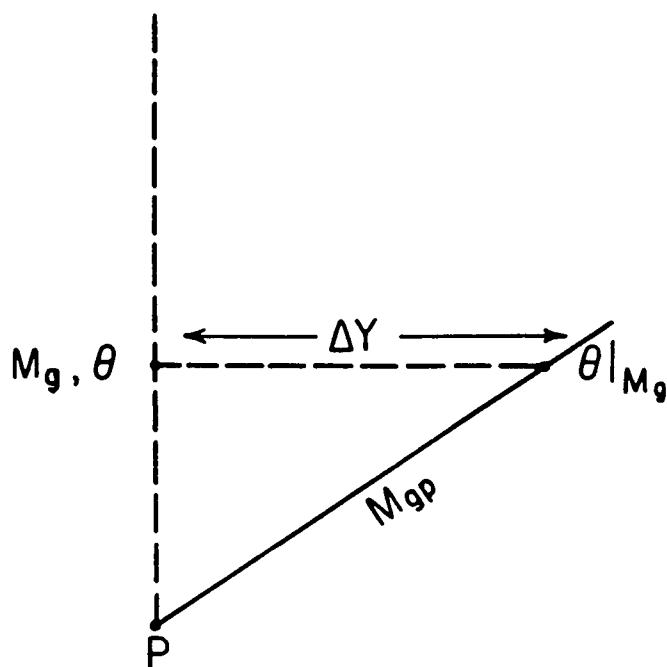
It is first necessary to define a level p at which we wish to examine the stability with respect to overlying fluid. This is important when phase changes occur, since the shape of an adiabat will depend on the temperature, pressure, and chemical composition of the starting parcel. When there are no phase changes, the choice of this level is arbitrary. We now wish to estimate the temperature structure along an M_g surface intersecting p from a vertical sounding which also passes through p. At an arbitrary height the potential temperature along the M_g surface is related to that of the vertical sounding by

$$\ln\theta\Big|_{M_g} = \ln\theta + \Delta Y \frac{\partial\ln\theta}{\partial y} \tag{11}$$

where ΔY is the horizontal distance between the M_g surface and the vertical sounding. Provided the horizontal gradient of M_g is constant this distance is given by

$$\Delta Y = \frac{\Delta M_g}{\partial M_g/\partial y} \tag{12}$$

where ΔM_g is the difference between the M_g at the vertical sounding and the M_g characterizing the parcel level p. From the definition of M, (3),

$$\Delta M_g = U_{gp} - U_g$$

and   (13)

$$\frac{\partial M_g}{\partial y} = -\eta_g$$

where η_g is the vertical component of absolute geostrophic vorticity, and U_{gp} is the geostrophic wind at level p. Substituting the relations (13) into (12) and (12) into (11), and using (7), there results

$$\ln\theta\Big|_M = \ln\theta - \frac{1}{g}\frac{f}{\eta_g}\frac{\partial U_g}{\partial z}(U_g - U_{gp}). \tag{14}$$

Given an estimate of η_g, this may be used to directly infer the temperature structure along a particular M_g surface from a vertical sounding of θ and U, provided one is willing to approximate U_g by U. If phase changes are not important, stability can be assessed by infinitesimal displacements from level p and (14) can be used as a linear stability estimate:

168

$$\frac{\partial \ln\theta}{\partial z}\bigg|_{M_g} = \frac{\partial \ln\theta}{\partial z} - \frac{1}{g}\frac{f}{\eta_g}(\partial U_g/\partial z)^2 \qquad (15)$$

In this case, generalized convective neutrality occurs when

$$Ri \equiv \frac{g\partial \ln\theta/\partial z}{(\partial U_g/\partial z)^2} = f/\eta_g \ ,$$

where Ri is the Richardson number. This is nearly identical to the linear neutral condition derived by Stone (1966).

When phase changes drive the convection, parcels may be stable to small displacements but unstable for finite displacements. Here it is important to use (14) to assess the stability of the flow with respect to particular parcels. We note that if (14) is substituted into (10) for the total potential energy there results

$$TPE = \frac{1}{2}\frac{f}{\eta_g}(U_{g_2} - U_{g_1})^2 + \int_1^2 \bigg|_y \frac{g}{\theta}(\theta - \theta_a)dz \ , \qquad (16)$$

if η_g is constant. The total potential energy is the sum of the bouyant energy of a vertically lifted parcel and the available kinetic energy of the geostrophic wind.

Now we will estimate vertical lapse rates in convectively adjusted planetary atmospheres. We have argued that generalized convective adjustment will result in adiabatic lapse rates along surfaces of constant M_g. If phase changes are unimportant, this state will be characterized by zero lapse rates of potential temperature along M_g surfaces.[*] According to (15), then, the vertical lapse rate will be given by

$$\frac{\partial \ln\theta}{\partial z} = \frac{1}{g}\frac{f}{\eta_g}(\partial U_g/\partial z)^2 \qquad (17)$$

---

[*]If phase changes are not negligible, then the arguments which follow will still be valid if θ is replaced by $\theta_e{}^*$, where the latter is the temperature a parcel would have if a) it were saturated with the constituent whose phase change is being considered and b) it were then lifted first to zero pressure, all condensate removed, and then brought adiabatically to a reference pressure.

Using (7), this may alternatively be expressed

$$\frac{\partial \ln\theta}{\partial z} \simeq \frac{g}{f\eta_g} \left(\frac{\partial \ln\theta}{\partial y}\right)^2 \qquad (18)$$

A nondimensional measure of the significance of this lapse rate is formed by comparing it to the dry adiabatic lapse rate of absolute temperaure (g/c_p):

$$\chi \equiv \frac{\partial \theta/\partial z}{g/c_p} \simeq \frac{c_p \theta}{g^2} \, (\partial U_g/\partial z)^2 \quad \text{or} \quad \frac{c_p}{\theta f^2} \left(\frac{\partial \theta}{\partial y}\right) \qquad (19)$$

where we have used f as an estimate of η_g. Table 1 shows estimates of χ for the five major planets for which reasonable data were available to the author. The estimates are based on mean conditions in the tropospheres of the planets. Of the five planets, only Earth and Mars may be expected to show significant departures of vertical lapse rates from adiabatic values within convectively adjusted layers.

Table 1

Estimates of χ for the Tropospheres of Five Planets

	χ
Venus[*]	2×10^{-2}
Earth	3×10^{-1}
Mars	4×10^{-1}
Jupiter	5×10^{-4}
Saturn	5×10^{-4}

---

[*]Because the large-scale flow on Venus is in cyclo-strophic rather than geostrophic balance, the above relation for χ in terms of the horizontal potential temperature gradient will be modified for this application. A straightforward analysis of the cyclo-strophic balance equation suggests, however, that the expression for χ in terms of the vertical wind shear is the same, to order of magnitude, as the result derived above.

To summarize, convective adjustment in rotating baroclinic fluids is brought about by the action of both gravitational and centrifugal accelerations. The net effect of the adjustment is to drive temperature lapse rates toward adiabatic values along surfaces of constant geostrophic angular momentum; these surfaces are vertical in a barotropic flow but have a finite slope under baroclinic conditions. We have presented observations which demonstrate that moist slantwise adjustment does indeed occur in the earth's atmosphere, and developed a method for inferring M_g surface temperature structure from vertical soundings. Estimates of the departure of vertical lapse rates from adiabatic values within convectively adjusted regions of five planetary atmospheres show that the effect is significant only in the tropospheres of Earth and Mars.

REFERENCES

Emanuel, K. A. (1983a). The Lagrangian parcel dynamics of moist symmetric instability. *J. Atmos. Sci.* 40, 2369-2376.

Emanuel, K. A. (1983b). On assessing local conditional symmetric istability from atmospheric sounding. *Mon. Wea. Rev.* 111, 2016-2033.

Solberg, H. (1933). Le mouvement d'inertie de L'atmosphere stable et son role dans la theorie des cyclones. Memoir of the U.G.G.I., Lisbon, Dupont Press, 66-82.

Stone, P. H. (1966). On non-geostrophic baroclinic stability. *J. Atmos. Sci.* 23, 390-400.

DR. STONE: Are there comments? Bill Rossow?

DR. ROSSOW: I have two comments and I think I'll do them in reverse-sensible order to get the first comment in. The point you made to start with, that the radiative time scale is very long compared to the convective adjustment time also raises another whole class of phenomena, namely that if you were to try to run a numerical model with that condition in it, which I've had the pleasure of doing, what you find is that it almost never convects. It only does so every third Thursday under a blue moon because that's all it needs to do to satisfy the balance. What happens in that case is that the large scale dynamics, which are busy doing other things like taking care of horizontal temperature gradients, control the static stability, and the convection doesn't really matter much. That may be a possible problem for all these kinds of puzzles, that we're not really looking at something which is smoothly balanced, that the processes are going on all the time. The question I had was, does your analysis essentially say that small scale convection of the usual kind should maintain the entropy state that Andy starts out assuming as his basic state?

DR. EMANUEL: I'll have to take your comment before your question. I suppose in a sense it depends on how you define convective time scales. For example, if we really did have a radiative convective equilibrium, we would compare something like the radiative time scale with a time scale characterizing the

fluxes and heat in convection. What I really wish to point out is that some, say, viscously determined time scale of convection has to be very very quick. So in these circumstances you would imagine actually seeing a lapse rate close to adiabatic. So far as the initial condition Andy Ingersoll used, I'm not sure I exactly understand the initial condition, but if it's a spherical rotation, if there are no perturbations on that, if you're starting off with just solid body rotation, then of course angular momentum surfaces are cylinders, and then if you postulate that you have convective equilibrium then it's quite proper to take the entropy to be constant along cylinders. They won't stay that way if the cylinders are deformed by the motion that develops.

DR. ROSSOW: It sounded to me that what you were really saying, your sort of definition of total potential, is that the proper direction for neutral bouyant stability in a rotating fluid is along something like the rotation axis and that sounded like where Andy Ingersoll started.

DR. EMANUEL: Yes, that's right. My only point is that that's true, but it's along the total vorticity vector including the vorticity of the large scale flow if it exists, not just the planetary vorticity.

DR. FELS: I'm sorry, I'm very confused about the relationship between this and the conventional old fashioned vertical stabilization by baroclinic instability. Now is this a reworking or is this on a much smaller scale?

DR. EMANUEL: No, it isn't. In fact, I should make a very strong distinction between what I'm talking about and what is conventionally called baroclinic instability. There's a tremendous amount of confusion on this problem. I'm really talking about a kind of convection which has been called symmetric instability. I guess I have to disagree with Andy Ingersoll on his characterization of baroclinic instability as sloping convection, although he's not the first to have done that; I think that Hide in fact characterized it that way as well, because in fact baroclinic instability is trying to redistribute potential vorticity principally. In my case we're dealing with something that's fundementally trying to redistribute heat but I'm only claiming it's redistributing heat along angular momentum surfaces.

DR. FELS: You're talking about inertial instability here.

DR. EMANUEL: Baroclinic inertial instability, yeah.

DR. STONE: Larry Trafton.

DR. TRAFTON: How would you characterize the latitudinal dependence of the degree of subadiabaticity? Would it disappear at the equator for example?

DR. EMANUEL: Yes, it would have to disappear at the equator and presumably it would have to disappear, well, it's not true that it has to disappear at the pole for large scale asymmetries which, for example, cause flow across the pole. That happens in the Earth's atmosphere. But I would suppose that on the average it would be maximum somewhere in the middle latitudes, so you would expect on the average the most sub-adiabatic lapse rates somewhere in the middle latitudes.

DR. ALLISON: One more thing about your results. Can you tell me how to re-express your statification parameter χ in terms of the Richardson number?

DR. EMANUEL: Uh, let me think about that. Essentially, the adjustment problem can be phrased as making the Richardson number close to unity everywhere. But that doesn't tell you the answer to the question of how sub-adiabatic the fluid is, because that depends on the individual magnitudes of the horizontal temperature gradient and the stratification. So you can't really express the sub-adiabaticity just in terms of the Richardson number. You need something else as well.

DR. STONE: I have a plea for one more question from Mike Belton.

DR. BELTON: It's probably silly, but there is one way of maybe getting to lapse rates deeper down and that is to look for silly results for abundances using thermal spectroscopy. So for example in Uranus we have a problem with ammonia and one of the ideas that was being kicked around was that maybe there was a sub-adiabatic region deep down in the atmosphere which seemed ridiculous. Then yesterday we heard "Well maybe there's no water on Jupiter, or very little water," but that could be interpreted possibly as a sub-adiabatic lapse rate in that region, say at 3 bars, 2 bars. The problem with it, and probably why it's silly, is that it requires an enormous sub-adiabaticity, and that doesn't seem to be in the cards.

DR. EMANUEL: Not unless there are extremely large horizontal temperature gradients...

DR. STONE: Alright. Now I think we can adjourn. Thank you all.

During the lunch break on the second day of the meeting several scientists attended a tour of the nearby Cathedral of St. John the Divine led by conference participant Canon Jonathan King. The tour included a review of a stained glass window depicting the planets, excuted by Ernest W. Lakeman in 1934. The slanted equatorial feature rendered for Jupiter was interpreted by Dr. Conway Leovy as an example of an atmospheric breaking wave or "surf zone" as a part of his review presentation for the afternoon session. (The illustration here has been reproduced from an original color photograph by Gregory Thorp by permission of The Cathedral Shop; 1047 Amsterdam Avenue; New York, NY.)

TUESDAY AFTERNOON

SYNOPTIC FEATURES AND PROCESSES

CHAIR: RETA F. BEEBE

EDDY PROCESSES IN THE GENERAL CIRCULATION
OF THE JOVIAN ATMOSPHERES

Conway Leovy
University of Washington (Seattle)

Two fundamentally different views of the general circulation of Jovian atmospheres have emerged. According to one view, espoused by G. Williams, the observed jet streams at the cloud tops are controlled by the vorticity transfers of small scale eddies generated by planetary wave instabilities within a shallow atmospheric layer. According to the alternate point of view argued by F. H. Busse, A. P. Ingersoll and their colleagues, the zonal jets are surface manifestations of deep interior convection organized into cylindrical motion with axes parallel to the planetary rotation axis. Both approaches may be considered in the context of the very different roles assumed by the potential vorticity. A possible reconciliation of the two kinds of dynamical systems is considered in which the interior motion is overlaid with a statically stable "capping layer" driven by turbulent energy injection from below. A simple model for the eddy driving of quasi-geostrophic dynamics in the capping layer is presented which is consistent with the tentative evidence for up-gradient momentum flux on Jupiter and IRIS observations of thermal contrast correlations with cyclonic and anticyclonic shear zones. Certain synoptic-scale cloud features in Jupiter's atmosphere are interpreted as breaking waves, which may also influence the lateral mixing of tracers such as the ortho-para hydrogen ratio.

Two basic ways of looking at the dynamics of the atmospheres of the giant planets have emerged in the last few years. One of these regards the visible surface features and wind systems as manifestations of "shallow layer" dynamics. According to this view these features can be understood in terms of energy generation, scale interactions, and dissipation within the layer, no more than a few scale heights deep, that is directly observable. The leading proponent of this point of view is Gareth Williams (1979). The alternative point of view is that the observable features are surface manifestations of the dynamics of the deep interior. Among the proponents of this view are Busse, and Ingersoll and Pollard (1982).

In both approaches, potential vorticity plays a central role, but it enters in fundamentally different ways. In the shallow layer view, the relevant component of vorticity is in the direction of the local vertical, and its variations arise largely from variations of the vertical component of planetary vorticity as fluid parcels move meridionally in the thin layer. These variations are responsible for the "β-effect", and the dynamics is analogous in many ways to those of Earth's atmosphere and oceans. In the deep dynamics view, the relevant component of vorticity is parallel to the planetary rotation axis and variations arise largely from stretching of axially aligned fluid columns as

177

they move toward or away from the rotation axis. Such a dynamical regime would be fundamentally different from that of Earth's atmosphere and oceans.

There is some observational justification for each point of view. In support of the shallow layer dynamics point of view, Williams has shown that the multiple jet structure and certain features of the Jovian eddies are produced by an "earth-like" shallow layer dynamics model driven by solar forcing. On the other hand, such features as the longevity of the Great Red Spot (GRS) and large ovals, the high speed of Saturn's zonal jets, and the large negative values of the meridional gradient of absolute vorticity observed near Jupiter's easterly jets seem to require a strong influence of deep dynamics, though they do not necessarily indicate cylindrical structures parallel to the rotation axis.

Can these two points of view be reconciled? In this paper, some features of the deep dynamics scheme are first reviewed, and a scheme for surface layer dynamics is proposed in which the statically stable cloud level region acts as a "capping layer", driven by turbulent energy injection from the interior. In this layer, the amplitude of large scale deep circulation features decreases with altitude. The possible roles of breaking internal gravity waves and Rossby waves, and the influence of lateral mixing of tracers such as the ortho-para hydrogen ratio are also briefly discussed.

POTENTIAL VORTICITY IN THE DEEP INTERIOR

Figure 1 is a sketch of a possible structure for deep dynamics. The cylindrical sheets parallel to the rotation axis represent surfaces on which the zonal flow has a maximum. They are shown in the extreme idealization in which the zonal flow penetrates right through the planet, in which case there would be perfect symmetry beyween the upper and lower hemispheres. Superposed on this planetary scale flow are eddies consisting of tall thin axial cylinders. Such a regime might occur in the interior where potential density variations are sufficiently small that bouyancy forces are of the same order as vertical Coriolis forces and the dissipative time scale is not too short, i.e., probably not everywhere, but possibly in large regions of the interior.

Under these conditions, eddy motions could occur in planes perpendicular to the axis and would satisfy the circulation theorem in the form

$$\frac{dC}{dt} \simeq \frac{d}{dt} (\eta \delta A) \simeq 0 \tag{1}$$

where C is the absolute circulation around a small closed curve of area δA perpendicular to the rotation axis, and η is the sum of the planetary and relative vorticities. For long thin columns oriented parallel to the axial coordinate h, the continuity equation is

$$\frac{d}{dt} (M \delta A) = 0 \tag{2}$$

where M is the mass per unit area of the column, i.e.,

$$M = \int \rho dh,$$

where ρ is density, and integration is over the length of the column. Combining (1) and (2) gives

$$\frac{d\zeta}{dt} - v\ (2\Omega + \zeta) \cdot \left(\frac{d\ell nM}{dr}\right) \simeq 0 \tag{3}$$

where r is the coordinate perpendicular to the axis, v is the associated fluid velocity, Ω is the planetary rotation rate, and ζ is the relative vorticity. This equation is analogous to the barotropic vorticity equation on a β-plane

$$\frac{d\hat{\zeta}}{dt} + \hat{v}\beta = 0 \tag{4}$$

where $\hat{\zeta}$ is the vertical (not axial) component of relative vorticity, $\hat{v}$ is the meridional velocity, and β is the meridional gradient of planetary vorticity, $\beta \equiv 2\ \Omega\ \cos\phi/a$ at latitude ϕ and planetary radius a.
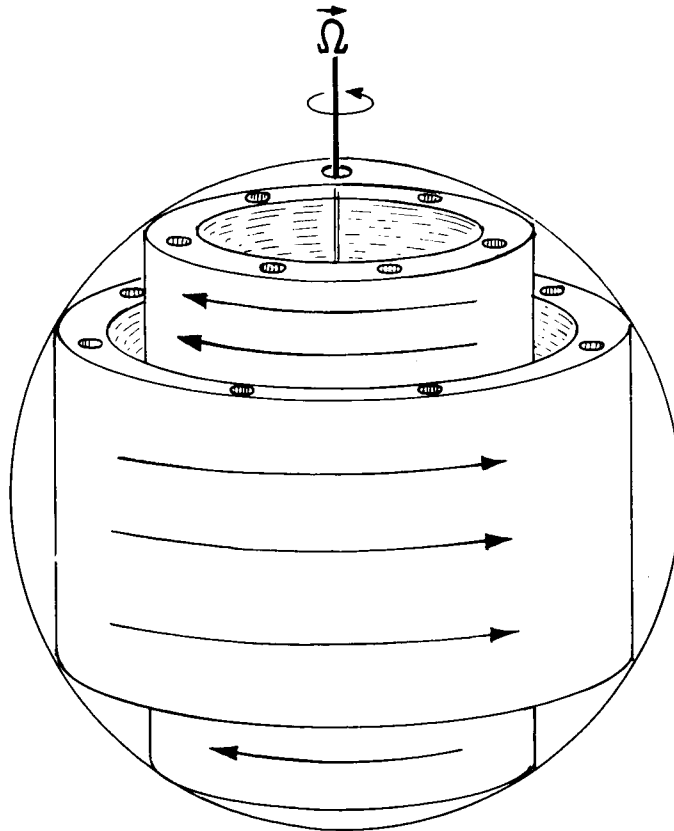
Figure 1. Possible cylindrical convection geometry in Jupiter's atmosphere.

Ingersoll and Pollard pointed out the possible applicability of equation (3) to the deep interiors of the atmospheres of the giant planets. They also called attention to two features of this equation: (a) It has small amplitude solutions analogous to Rossby waves, except that they propagate eastward rather than westward relative to the zonal wind $\bar{u}$ in which they are imbedded. Thus, observations of waves with slow eastward propagation speed might be diagnostic of deep dynamics. (b) For this deep dynamics model, there is a threshold of wave instability in regions where

$$\bar{u}_{rr} \approx 2\Omega \frac{d \ln M}{dr} \quad .$$

For isentropic columns whose length is constrained by the spherical shape of the planet, Ingersoll and Pollard have shown that this condition is approximately equivalent to

$$\bar{u}_{yy} \approx - 3\beta.$$

This condition can be contrasted with the more familiar threshold condition

$$\bar{u}_{yy} \approx \beta,$$

where y is the meridional coordinate, for a barotropic thin atmosphere. The large observed curvatures of the Jovian eastward jets might be indications of deep velocity structure.

The analogy between equations (3) and (4) encourages speculation about other possible aspects of deep dynamics. For example, should one expect an upscale cascade, analogous to that in barotropic flows, in which energy introduced at small scales is transferred upscale eventually appearing in zonally aligned jets like the cylindrical sheets sketched in Fig. 1? Does this system admit solutions corresponding to long-lived large scale features analogous to Rossby wave solitons or modons?

EDDY DRIVING OF THE SURFACE LAYER

We suppose that deep rooted zonal flow systems, perhaps like those represented by the cylindrical sheets in Fig. 1, exist in the interior, and ask how they might be modified by large scale zonal shear in the surface layer. In particular, we examine how such large scale zonal wind shear might be driven by convective eddies impinging on the surface layer from the interior.

In the surface layer, energy input is presumed to take place at a scale comparable to the Rossby radius of deformation,

$$L_R \sim NH/2\Omega \sin\phi \quad ,$$

where N is the bouyancy frequency and H the scale height. Smaller scale convective eddies impinging on the surface layer would spread laterally until they reach the scale L_R. Based on the bouyancy frequency and scale height just below Jupiter's tropopause, $L_R \lesssim 2000$ km. This scale corresponds to a

zonal wavenumber of 30 or more at middle latitudes. At scale L_R, the eddies should be horizontally isotropic, but energy would be transferred upscale in eddies of increasingly zonal orientation until the scale of the jets is reached. This energy decascade is expected to occur in the surface layer, and might occur in the deep interior. The jet scale L_j in the interior, if dominated by a potential vorticity conserving dynamics like that sketched in the last section would be

$$\hat{L}_j \sim \pi \left[|2\Omega(\frac{1}{M}\frac{dM}{dr})|/|\bar{u}| \right]^{-\frac{1}{2}} .$$

In a barotropic surface layer, that scale would be

$$\hat{L}_j \sim \pi \left[\beta/|\bar{u}| \right]^{-\frac{1}{2}} .$$

According to the model of Ingersoll and Pollard, the ratio $|2\Omega(\frac{1}{M}\frac{dM}{dr})|$: β is about three, so matching of interior structure to a barotropic surface layer with the same jet structure would require a baroclinic boundary layer in which the magnitude of $\bar{u}$ decreases by about a factor of three.

Because the Rossby number and the scale ratio L_j/a are small, the surface layer circulation can be described by quasi-geostrophic dynamics on the β-plane. The important dynamical quantity is the quasi-geostrophic potential vorticity q which can be separated into eddy and zonal mean components, q' and $\bar{q}$:

$$q' = \psi'_{xx} + \psi'_{yy} + \frac{f^2}{p} \frac{\partial}{\partial z} (\frac{p}{N^2} \frac{\partial \psi'}{\partial z}) , \qquad (5a)$$

$$\bar{q} = \int \{\beta - \bar{u}_{yy} - \frac{f^2}{p} \frac{\partial}{\partial z} (\frac{p}{N^2} \frac{\partial \bar{u}}{\partial z})\} \, dy . \qquad (5b)$$

The vertical coordinate is the log-pressure coordinate,

$$z = - H\ell n(p/p_s)$$

where p is pressure and p_s is a constant; ψ' is the geostrophic stream-function for the eddy component of the flow and f is the Coriolis parameter. The conservation of potential vorticity equation governs q',

$$(\frac{\partial}{\partial t} + \bar{u} \frac{\partial}{\partial x}) q' + v' \bar{q}_y = G' - J(\psi', q') , \qquad (6)$$

where G' represents generation of q' by convective eddies at the scale L_R. Multiplication of q' and zonal averaging yields the equation for eddy enstrophy, $1/2 \overline{q'^2}$:

$$\frac{\partial}{\partial t} 1/2\overline{q'^2} + \overline{v'q'} \, \bar{q}_y = \overline{q'G'} - \overline{q'J(\psi', q')} . \qquad (7)$$

Changes in the zonal flow are described approximately by

$$\frac{\partial \bar{u}}{\partial t} - f\bar{v}_* = \overline{v'q'} \tag{8}$$

where $\bar{v}_*$ is the residual mean meridional velocity. The residual mean circulation satisfies the continuity equation

$$\frac{\partial \bar{v}_*}{\partial y} + p^{-1} \frac{\partial}{\partial z} (p\bar{w}_*) = 0 \tag{9}$$

where the vertical residual mean velocity $\bar{w}_*$ is closely related to the zonal mean radiative heating rate $\bar{Q}$,

$$\bar{w}_* \simeq g\bar{Q}/ (c_p T_s N^2) \tag{10}$$

where g, c_p, and T_s are gravitational acceleration, constant pressure specific heat, and a mean reference temperature. The heating rate can be approximated by the radiative damping representation,

$$(\bar{Q}/c_p T_s) = - \alpha_r T_s^{-1} (\bar{T} - \bar{T}_e) \tag{11}$$

where $\bar{T}$ is the latitude dependent zonal mean temperature, $\bar{T}_e$ is the corresponding radiative equilibrium temperature, and $\alpha_r(z)$ is the radiative damping rate. The zonally averaged wind and temperature fields are in geostrophic balance:

$$\bar{u}_z = - (g/fT_s)\bar{T}_y . \tag{12}$$

Neglecting meridional variations of $\bar{T}_e$, equations (10)-(12) yield

$$\bar{w}_{*y} = \frac{f\alpha_r}{N^2} \bar{u}_z . \tag{13}$$

If the zonal wind shear distribution diminishes the amplitude of both easterly and westerly jets, equation (13) indicates that subsidence occurs in cyclonic shear zones and ascent occurs in anticyclonic shear zones (Fig. 2).

Using (9), (13), and the steady state versions of (7), and (8), integrating over a layer of finite thickness Δz gives

$$\Delta(\frac{\alpha_r p}{N^2} \bar{u}_z) = \Delta(p \bar{w}_{*y}) = - \int_{\Delta z} p \bar{v}_{*yy} dz = \int_{\Delta z} p \overline{(v'q')}_{yy} dz . \tag{14}$$

The behavior of the factor $\alpha_r p/N^2$ is sketched in Fig. 3. Above the cloud tops N^2 increases upward, and $\alpha_r p$ decreases upward, so $\alpha_r p/N^2$ decreases upward.

Figure 2. Possible dynamical relationships in a capping layer.

Figure 3. Schematic representation of $\alpha_r p/N^2$ as a function of height. Wind shear differences are taken across a layer such as (z_a, z_b) connecting levels where this factor has the same values.

Below the cloud tops $\alpha_r p$ decreases very rapidly downward, probably more rapidly than N^2, at least at intermediate depths. Under these conditions the layer can be taken to span the maximum of $\alpha_r p/N^2$ as indicated with end points at levels with equal values of $\alpha_r p/N^2$ in Fig. 3. Between these points the jump in wind shear is proportional to the pressure weighted integral of $\overline{v'q'}$,

$$\Delta \bar{u}_z \sim \left(\frac{N^2}{\alpha_r p}\right)_{za,zb} \frac{\partial^2}{\partial y^2} \int_{\Delta z} p \ \overline{v'q'} \ dz \ . \tag{15}$$

If the shear is relatively small at the base of the layer, and if the jet structure and associated eddy potential vorticity flux is oscillatory in y, the wind shear at the top of the layer is opposite in sign to $\int p \, \overline{v'q'} \, dz$. This is illustrated in Fig. 2.

According to (7), $\overline{v'q'}$ is closely related to potential enstrophy generation, either through stirring by upwelling turbulence (the term $\overline{G'q'}$), or through non-linearity (the term $\overline{-q'J(\phi',q')}$). The latter term is important where $\overline{q}_y$ vanishes on the shoulders of Jupiter's westward jets. It may also be important near the cores of the westward jets since the quasi-geostrophic instability condition, $\overline{q}_y < 0$, is likely to be satisfied there as a result of vertical as well as horizontal curvature of $\overline{u}$. In general

$$\overline{v'q'} \; \overline{q}_y \approx \overline{G'q'} - \overline{q'J(\phi',q')} \; , \tag{16}$$

and the right side will be positive where there is eddy stirring or baroclinic instability in westward jet cores, so that the sign of $\overline{v'q'}$ is the same as that of $\overline{q}_y$ in these regions. If eddy forcing occurs nearly everywhere, $\overline{v'q'} > 0$ in westerly jets, and $\overline{v'q'} < 0$ in easterly jets. Under these circumstances, according to (15) $\Delta \overline{u}_z > 0$ in easterly jets and $\Delta \overline{u}_z < 0$ in westerly jets. Thus, eddy forcing by upwelling convective eddies would generate shears in the capping layer as a result of the induced meridional circulation and associated Coriolis torques. These shears would reduce the magnitude of the internal jets through the cloud top region (Fig. 2).

This model is consistent with two observations: (a) If the flow is quasi-barotropic at the level of the observed cloud level winds,

$$\frac{\partial}{\partial y} (\overline{u'v'}) \simeq - \overline{v'q'} \tag{17}$$

there. The eddy momentum flux divergence would be negative in eastward jets and positive in westward jets. That is, it would act to intensify the jets. This relationship has been observed in some analyses of Voyager wind measurements, but this result is still somewhat controversial. (b) Zonal mean temperature at the cloud top level would be relatively low in anticyclonic shear zones and relatively high in cyclonic shear zones. This pattern is consistent with IRIS observations.

Clearly many details of this "capping layer" model have yet to be worked out, including the roles of thermal energy sources due to spatially varying solar and thermal radiation in the surface layer.

THE ROLE OF BREAKING WAVES

McIntyre and Palmer (1984) have recently argued that breaking planetary waves may play a very important role in the meridional transport of potential vorticity and passive tracers. Breaking occurs when initially adjacent fluid

184

parcels rapidly separate and lose all correlation of their positions and velocities. For waves such as Rossby waves superimposed on a background zonal flow, an approximate criterion for breaking is $|u'| > |\overline{u}-c|$ where u' is the eddy zonal velocity and c is wave phase speed. An effect of wave breaking is to produce a region in which tracers are well mixed (the region of breaking waves or "surf zone", to use the evocative terminology of McIntyre and Palmer), adjacent to relatively narrow regions of strong tracer gradient. Figure 4 illustrates this structure for the tracer ozone in Earth's stratosphere. Note that a spiraling band of strong ozone gradient coincides with a spiraling wind maximum. The wind maximum is a manifestation of a maximum in the potential vorticity gradient in the same band. The band bounds an apparent region of planetary wave breaking.
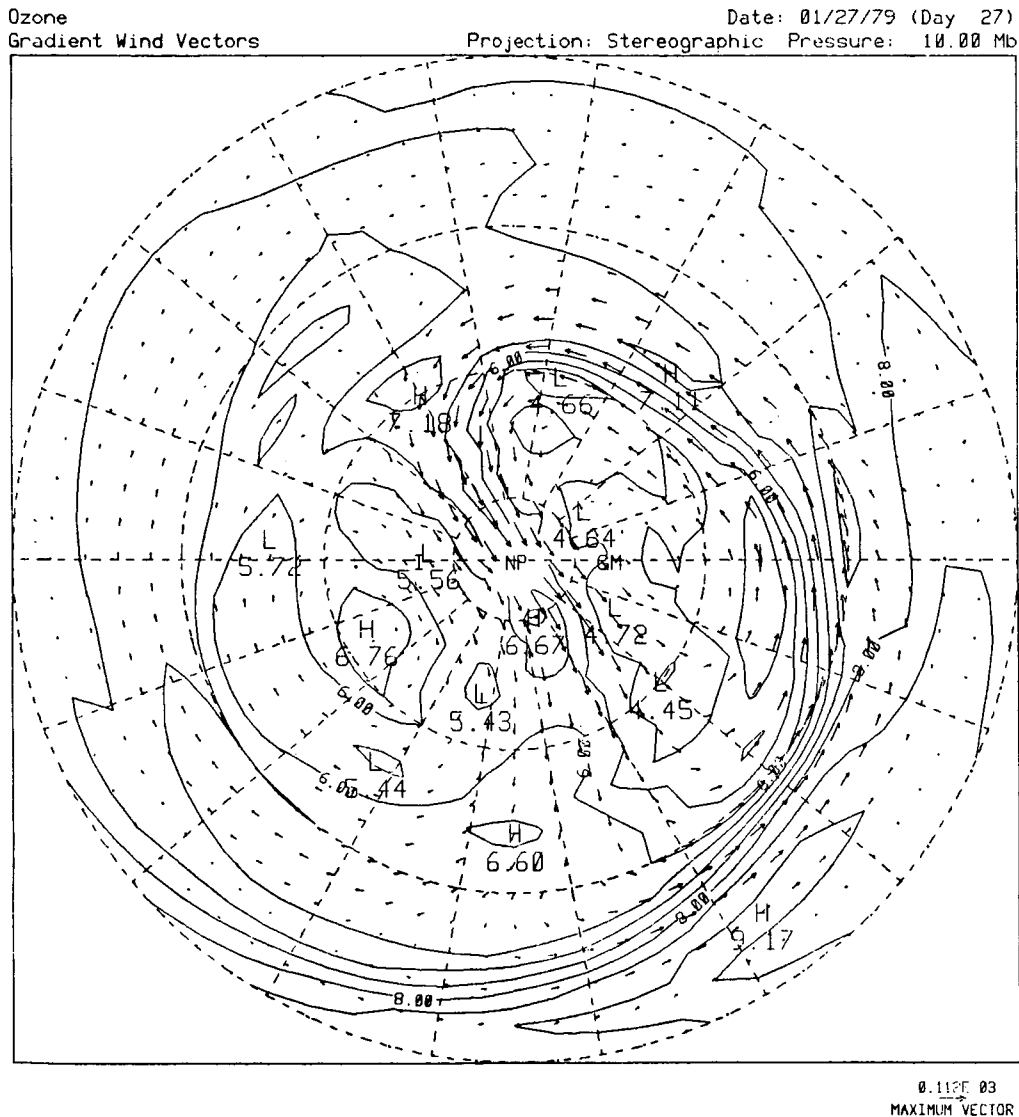
Figure 4. The "surf zone" structure at the 10mb level in the Earth's atmosphere. Ozone isopleths (ppmv) and gradient wind vectors (maximum speed 112 ms^{-1}). Note the correlation between ozone gradient and wind speed.

The cloud top region of Jupiter's atmosphere shares some characteristics with Earth's stratosphere. Potential vorticity is the important quasi-conservative dynamical variable, and there are observable "passive tracers", colored clouds in the case of Jupiter. Are there any features in the Jovian atmosphere which correspond to the wave-breaking/"surf zone" structure?

In the Cathedral of St. John the Divine nearby, several of us saw a stained glass window showing the planets, dating, I am told, from 1934. In rendering Jupiter, the artist has depicted the well-known zonally aligned belt and zone structure, and has chosen to show, in addition, a band stretching diagonally around the planet connecting two belts. A similar feature can be seen on Jupiter itself. Figure 5 shows a diagonal band extending from the equatorward edge of the GRS south westward to the polar edge. The region in which the band originates just west of the GRS is a region of particularly intense wave activity. It seems likely that this band is a manifestation of wave breaking on Jupiter analogous to the stratospheric structure shown in Fig. 4. What one sees in the Jupiter image is a sharp gradient of passive tracer, a cloud edge, with a spiral structure. Its tentative identification as the edge of a wave breaking zone would be confirmed if it was also found to be the locus of strong potential vorticity gradient, i.e., a wind maximum.

Breaking internal gravity waves are also important in Earth's atmosphere in that they exchange momentum between the surface and troposphere and the region above about 1 mb where these waves break. At the breaking level, they are very effective in shifting the zonal flow speed toward the wave phase speed. This is probably the reason zonal winds in the upper mesosphere are weak. Gravity wave breaking tends to reduce the flow speed to the phase speed of the waves, and for waves originating near the ground this phase speed is usually centered around zero. The same phenomenon must occur on Jupiter, so that zonal wind speeds in Jupiter's stratosphere, above about 1-0.01 mb, might reflect zonal wind speeds near the level of origin of the upward propagating waves, perhaps near the base of the stable layer where convection from the deep interior can generate gravity waves.

Figure 5. Possible evidence for spiral structure due to a "surf zone" in Jupiter's atmosphere in a cylindrical projection Voyager image showing about 220 deg of Jovian longitude.

There is an important exception to this tendency for upper-stratospheric zonal winds to resemble those at much lower levels. In the deep tropics, within 5-7 degrees of the equator, Kelvin waves would be generated, and these eastward propagating waves would be transmitted upward in preference to westward propagating Rossby-gravity waves that have short vertical wavelengths. Thus, Kelvin waves could produce systematic eastward acceleration in the equatorial stratosphere.

MIXING AND THE ORTHO-PARA H_2 DISTRIBUTION

It may be possible to understand the distribution of the ortho-para ratio given by Conrath and Gierasch (1984) in terms of a simple model of meridional mixing recently proposed by Holton (1986). At ~ 250 mb in Jupiter's atmosphere the time scale for ortho-para conversion is ~ 10^9 seconds. This is much longer than the radiative time scale at the same level. Consequently, the relatively steeply sloping isopleths of ortho-para ratio in the meridional plane closely approximate fluid parcel trajectories, while the relatively flat isentropes do not. The slope of the ortho-para ratio isopleths is determined by a balance between the tendency for the thermally driven residual mean circulation to tilt them and the tendency for meridional mixing to flatten them. Thus, the isopleth slope, $(dy/dz)_i$ is approximately

$$(\frac{dy}{dz})_i \sim \frac{\overline{v'^2}}{w_* a \tau_e}$$

where $\overline{v'^2}$ is eddy meridional velocity variance and τ_e is characteristic eddy time scale. Thus, correlations between this isopleth slope and the belt-zone structure would occur only to the extent that $\overline{v'^2}/\tau_e$ correlates with the belt-zone structure.

REFERENCES

Conrath, B. J., and P. J. Gierasch (1984). Global variations of the para-Hydrogen fraction in Jupiter's atmosphere and implications for the dynamics on the outer planets. *Icarus* 57, 184-204.

Holton, J. R. (1986). On the meridional distribution of stratospheric trace constituents. *J. Atmos. Sci.* 43 (in press).

Ingersoll, A. P., and D. Pollard (1982). Motions in the interiors and atmospheres of Jupiter and Saturn: scale analysis, anelastic equations, barotropic stability criterion. *Icarus* 52, 62-80.

McIntyre, M. P., and T. N. Palmer (1984). The 'surf zone' in the stratosphere. *J. Atmos. Terr. Phys.* 46, 825-850.

Williams, G. P. (1979). Planetary circulations: 2. The Jovian quasi-geostrophic regime. *J. Atmos. Sci.* 36, 932-968.

DR. BEEBE: Before I ask for questions I am going to excercise the chair's option and make some comments. With respect to your breaking waves--there are spiral patterns in both equatorial belts. As a matter of fact, the barges in the North Equatorial Belt are nested in spiral patterns. There are also spiral patterns in the North Temperate Belt, even when it is browner than it is in the Voyager data. On the front cover of the conference program notebook there is a feature which is schematically drawn along the south edge of the Equatorial Zone. This feature actually distorts the zonal wind flow and when it catches up and passes the Red Spot, it carries white cloud material from west of the Red Spot along with it. This forms a white cloud with a strong north-south wave pattern east of the Red Spot. The maxima of the wave translate at a constant velocity but the north-south extent of the pattern grows and becomes increasingly turbulent as it is sheared apart in the zonal flow. It is destroyed in about 40 hours. The location of the barges and the destruction of this wave pattern are located in the equatorial belts at latitudes where there is a bump in the latitudinal gradient of the zonal wind. Considering the fact that you have a discontinuity in the zonal wind shear where these phenomena occur, it may indicate that your surf zone is visible in the average zonal wind profile.

DR. LEOVY: Yes. Looking at the data from this point of view one may find a lot of things. It seems to me that there are two kinds of slanted patterns. One is that of a smaller scaled chevron which probably consists of individual systems and these have a relatively steep slope. On the other hand, the net effect of the mixing of potential vorticity or tracers produces, I suspect, a more gradual spiral.

DR. HUNTEN: Do you have a number for the angle specifying the slope of the stratospheric surface?

DR. LEOVY: That depends on the root-mean-square velocity and I haven't looked carefully at that. But the expected angle of such a spiral can be crudely estimated as follows. The rate of lateral spread of a breaking zone should be of order V/L, where V and L are characteristic eddy velocity and length scales. The zonal stretching rate should be of order $\overline{u}_y$. Hence, the angle of the spiral with respect to latitude circles is of order $V(L\overline{u}_y)^{-1}$. For the Jovian band, L appears to be comparable to the scale of zonal wind shear. Hence, the observed angle, $\sim 1/20$, might be attributable to eddies whose characteristic speed is $\sim 1/20$th of the scale for the zonal mean flow in the latitude belt.

DR. STONE: Conway, in your discussion of the shallow layer quasi-geostrophic dynamics you showed the definition of the potential vorticity gradient and related it to the stability criterion. You said that you thought that the vertical derivative term would really be negligible but you also estimated that the radius of deformation was 2000 km or less and the scale of the jets is the order of 20,000 km; so I would have thought that the opposite would be correct, that the vertical derivative term would be much more important than the horizontal derivative term.

DR. LEOVY: Well, I'm not sure. It's pretty hard to see how you can piece together a vertical and horizontal jet structure to make a stable

configuration. In other words you have to make a funny looking jet, one which looks like an antijet in the vertical in order to stabilize the system.

DR. STONE: Ah, I wasn't saying it would be stable if you could calculate the vertical term. I'm just suggesting that the zeros might be very differently located.

DR. LEOVY: They might be quite differently located, and that's one of the problems we have. We can't ignore that term. But the observed cloud drift winds may nevertheless be at a level at which horizontal shears dominate.

DR. ALLISON: Conway, your quasi-geostrophic representation of the thin layer dynamics, as I understand it, is of a class with the order one Burger number regime for which the Rossby radius is roughly the same, in order of magnitude, as the observed length scale. But some of us think it's possible that Jupiter might have a thin layer system with a very weak stratification and such a small Burger number that a different type of quasi-geostrophic dynamics prevails. Gierasch and I have studied a thin layer system with a very nearly adiabatic lapse rate, for which the horizontal variation of the geostrophic winds is the same at all altitudes. The vertically integrated vorticity equation for such a system, assuming appropriately small vertical velocities at the bottom of the layer, leads to a shear stability criterion which will admit a zonal flow curvature as large as 3β. But the instability constraint for this system applies to the westward jets, unlike Andy Ingersoll's new 3β instability constraint on eastward jets for deep cylindrical flow. It's possible that Reta Beebe can help us distinguish between these two very different systems by assessing the relative frequency of instability features at westward as compared with eastward jets.

DR. LEOVY: Yes. I would only claim that the picture of a forced zonal wind "capping" layer that I have described is only one of several possible pictures and you have to look at several kinds. The underlying assumption of this view is that the eddies that are important are those at the Rossby radius of deformation scale. The others are irrelevant in determining the modification of the jet structure in the stable layer. That may or may not be true. So far, I don't believe it is ruled out.

DR. READ: Just to comment along the same lines or the same sort of topic: You mentioned the possibility of the Rossby radius being the order of 2000 km and it being significantly smaller than the Red spot and white oval spots. In our experiments with laboratory systems we can actually produce a flow in which N^2 varies very strongly with height. The definition of the Rossby radius then becomes very much more complicated. In particular I would certainly like to argue for the possibility that things like the Red Spot and the white ovals could in fact reflect the true scale of the Rossby radius. It depends on where you put the top boundary. A second point, which is related, is connected with looking at the q_y shape and where it goes to zero. In the particular laboratory system that I spend part of my time looking at, it is possible to observe a configuration where q_y actually goes through zero both in the vertical and in the horizontal and yet which still maintains the presence of a stable wave train.

DR. LEOVY: How is that wave train generated?

DR. READ: Well, it's generated initially primarily by baroclinic instability. The point is that the profile would suggest that both baroclinic and barotropic instability processes can operate. I think the crucial thing to be borne in mind also is that these criteria are necessary conditions, they're not sufficient conditions.

DR. LEOVY: Yes, that's right, they're necessary but usually sufficient for some combination of baroclinic/barotropic instability. However, I'd like to comment on the idea that the Rossby radius is large. The 2000 km Rossby radius is based on the static stability near the tropopause, not low down. Since static stability decreases downward I don't see how you could get an effective Rossby radius which is very much larger than that.

DR. READ: The crucial thing is what you take for H. It's been customary to just plug in the pressure scale height but I don't think there's any fundamental reason why that should be.

DR. LEOVY: It's customary to plug in the pressure scale height and the effective vertical scale may be smaller than that, but it can't be larger. In a compressible atmosphere, the largest vertical scale for an unforced disturbance is the scale height.

DR. FELS: Am I correct in understanding that you were saying that selected vertical propagation of Kelvin waves in the tropics may account for the eastward acceleration of the equatorial stratosphere?

DR. LEOVY: I think one could draw that implication from what I said, but that's really not what I think is the mechanism for the equatorial superrotation in the Jovian case.

DR. FELS: Why couldn't one equally well have the mixed gravity-Rossby waves propagating?

DR. LEOVY: Well I think you could but as you know it's going to have a generally smaller vertical scale and it's not going to be able to penetrate as deeply and for that reason the Kelvin wave tends to be more effective. The reason I think Kelvin waves are nevertheless unimportant for what we see in the Jovian clouds is because these clouds occur at relatively high densities. If we saw an equatorial acceleration up around 0.1 mb or so, then I'd be more inclined to attribute that to Kelvin waves.

DR. EMANUEL: In one sense it seems to me that this discussion of scales relative to the deformation radius is irrelevant in assessing the stability and I suppose I can explain it this way. The Ertel potential vorticity is conserved regardless of scale; it's a three dimensional vorticity. In fact the Charney-Stern theorem can be generalized to say that you essentially have to have a local extremum of that quantity on an isentropic surface. In a sense you could ask the question, in view of the fact that it's a conserved variable, how are you ever going to produce that situation? Of course on the

Earth that constraint is not generally satisfied and the reason baroclinic instability exists is because of the effect of the rigid lower boundary. Again an internal maximum of potential vorticity in a fluid seems to be problematic regardless of scale.

DR. LEOVY: We do have, I think, an example in the Earth's atmosphere where one does get an internal instability and that's in the easterly jets of the stratosphere. Aside from that I think you're right. The Rossby radius is probably only relevant, if at all, in a consideration of the relative importance of the vertical derivative term as compared with the horizontal term in the potential vorticity, as Peter Stone pointed out.

DR. EMANUEL: I really don't see what that has to do with practicality and necessity.

DR. ORTON: Would you comment briefly on relevance to putative anticorrelative meridional temperature structures between tropospheres and stratospheres?

DR. LEOVY: If I understand your question, the reason that I emphasize the gravity waves is that we have good reason to believe that gravity waves in the Earth's atmosphere drive the winds in the mesosphere where the waves break, reducing the wind speed to that region where the waves are formed. That's how the mesosphere knows that it should have a zero wind velocity at some level. So what one has to ask for on Jupiter is: how do the winds at an upper level know that they ought to have some velocity and what velocity should that be? They might want to have the velocity associated with the zonal flow speed at the level where the waves are generated.

DR. BEEBE: Thank you. Before we leave I would like to call your attention to the fact that there are poster papers associated with this session. Please consider the first one. I would really like input from you. This poster deals with IAU standards for atmospheric nomenclature and I think this is probably the biggest group of users that we would get together for this sort of situation, so the input you would have would be quite significant.

192

MESOCALE WAVES AS A PROBE OF JUPITER'S DEEP ATMOSPHERE

F. M. Flaser
NASA/Goddard Space Flight Center

P. J. Gierasch
Cornell University

The presentation by Flasar and Gierasch is largely contained in a paper submitted to *The Journal of the Atmospheric Sciences*. The abstract of their presentation for the conference is reproduced here:

Images from the Voyager north/south mapping sequences have been searched for waves. A remarkable class of mesoscale waves has been identified, with the following features: 1) The wavetrains are usually aligned zonally, i.e., wavecrests are north-south. 2) The average wavelength is 300 km with a standard deviation of only 20%. 3) The wavetrains are long, ~20 crests. 4) The waves occur within 25 degrees of the equator, the bulk being at the equator itself. 5) The waves are centered at the extrema (in latitude) of the zonal flow. 6) The meridional extent of the waves is typically 1 degree of latitude.

We interpret these observations as evidence of gravity waves propagating vertically within a leaky duct. We assume a three-level model composed of a stable duct which extends up to the base of the NH_3 cloud deck near 600 mb. Above this is a thin wave-trapping region characterized by a Richardson number Ri <1/4 and containing a critical level, where the local value of the zonal flow velocity equals the phase speed of the wave. This in turn is overlain by a stable region, representing the tropopause region and stratosphere. We search for the "almost free" modes of the model. The critical level ensures that the upward propagating waves are totally or over-reflected back into the duct and naturally explains (3) above. The requirement that only one "almost free" mode be observable ((2) above) constrains the Richardson number of the duct itself. We conclude that just below the NH_3 cloud deck, Ri≈1. The requirement that the frequencies of vertically propagating inertial-gravity waves exceed the Coriolis frequency explains the tropical confinement of the waves (4), and implies wave frequencies, relative to the mean flow, ~10^{-4} s^{-1}. A meridional waveguide which results from the north-south shear in the background flow effects the meridional trapping ((5) and (6)) and zonal alignment (1) of the waves. The contribution to trapping from the variation of the Coriolis frequency with latitude is secondary.

DR. READ: Have you looked at the momentum fluxes in terms of the super-rotation problem?

DR. FLASAR: Actually, the only thing I really looked at before was the $\overline{w'\phi'}$, which is the vertical energy flux, and that turns out to be about 1000-fold below the σT^4 flux, the internal flux of the planet. Energywise, it seems to be small potatoes. I probably should look at $\overline{u'w'}$ a little more closely.

DR. LEOVY: Just to comment on that again, the waves you're looking at are trapped waves, so they'll have relatively little momentum flux. On the other hand, one expects that the trapped waves are the signatures of wave forcing, so you very likely, in those regions and times, have an ample amount of propagating waves, whose signature is just harder to see.

DR. INGERSOLL: With a Richardson's number of one in the ammonia cloud, I'm wondering what happens when you plug in some numbers? Let's say the shear of the zonal wind is given by the difference between its measured value and zero over two scale heights. Let's say the static stability is what you might get from the latent heat associated with evaporating ammonia. What do you get?

DR. FLASAR: The easy thing to do is to use the static stability values given by the ortho-para mixing theory that Barney and Peter did. That gave a Brunt frequency of 2×10^{-3} s^{-1}. This is a working number. That corresponds to $\partial u / \partial z$ of about 2 m s^{-1} km^{-1}, which I think is 40 m s^{-1} per scale height. And they scale linearly with each other.

DR. INGERSOLL: You're in the right ballpark. Big shear?

DR. FLASAR: They could be small shears, but then the Brunt frequency would have to go down to keep track of it. There's a lower limit on the Brunt frequency given by the fact that it has to exceed the Coriolis frequency of about 10^{-4} s^{-1}, so you have constraints there, although I don't think you can distinguish between big or small $\partial u / \partial z$ yet.

DR. STONE: Mike, I wasn't too clear about your middle region there. What you had to assume; you said it wasn't too sensitive to conditions there, but you did assume it was a small Richardson number...

DR. FLASAR: I need a Richardson number less than 1/4 to trap the waves. I need a quantum mechanical tunneling problem basically...

DR. STONE: Yeah, but won't that give you lots of instability there?

DR. FLASAR: I assume that region is maintained below a Richardson number of 1/4 by all kinds of convective instabilities and that this won't be affected by the waves. In other words, the waves aren't going to drive the Richardson number up or anything like that.

DR. STONE: The waves, you are saying, will survive any small scale instabilities too?

DR. FLASAR: Well, I still think that they'll be reflected back down if the conditions are right. But you're correct. I'm not treating in detail the interaction between the gravity waves and the convective instabilities. I'm treating the middle, wave-trapping region as a homogeneous medium with a small index of refraction.

THE SATURNIAN RIBBON FEATURE--A BAROCLINICALLY UNSTABLE MODEL

D. Godfrey
Imperial College, London

The presentation by Godfrey is largely contained in a paper submitted to *Icarus*. The abstract of his conference presentation is reproduced below.

We examine in detail, using measurements made by the Voyager spacecraft, an oscillatory feature in the northern midlatitudes of Saturn. Measurements made by the imaging and infrared instruments are used to estimate its horizontal wavelength and vertical extent. Some of these characteristics suggest that the feature could be due to baroclinic instability. We will describe a numerical model of such an instability with parameters based upon the Voyager observations, and using the lower boundary condition developed by Gierasch et al. (1979, Icarus 40, 205) for the Jovian planets.

DR. STONE: What about the propagation characteristics?

DR. GODFREY: I did calculate the phase velocity, but the feature exists in a very rapid jet, in a bland region of the planet, where the local material velocity cannot be accurately determined. Since the calculated phase velocity of 10 m s^{-1} was less than the errors in the velocity profile it was of little use for constraining the model.

QUASI-GEOSTROPHIC 'FREE MODE' MODELS OF LONG-LIVED JOVIAN EDDIES: FORCING MECHANISMS AND CRUCIAL OBSERVATIONAL TESTS

P. L. Read

Meteorological Office, U. K.

The presentation by Read is largely contained in a paper which appears in the special issue of *Icarus* (1986; 65, 304-334). The abstract of his conference presentation is reproduced here.

Recent modelling studies concerning the nature and generation of the longest-lived eddies in the atmospheres of Jupiter and Saturn (including Jupiter's Great Red Spot and White Ovals) are reviewed and shown to reduce to the derivation of steady, shape-preserving solutions to an appropriate homogeneous potential vorticity equation in a zonal shear flow as their (zeroth order) starting point. Crucial differences between the models arise from the ways in which the solutions maintain themselves against the inevitable effects of weak dissipation. Ingersoll and Cuong (1981, J. Atmos. Sci. 38, 2067-2076), for example, invoke small-scale transient eddy-forcing to maintain a time-averaged large-scale eddy, while the laboratory analogue of Read and Hide (1983, Nature 302, 126-129; 1984, Nature 308, 45-49) is shown to correspond to the diabatic forcing of a quasi-steady eddy. From a consideration of the potential vorticity budget for closed-streamline quasi-geostrophic flows, and of the nature of small-scale transient eddies as either a 'dissipation' or 'forcing,' the crucial difference between diabatically- and transient eddy-forced recirculating flows is shown to lie in the resultant direction of the cross-streamline flux (in the time average) of potential vorticity. By Ertel's theorem, the direction of the transport of other passive, quasi-conserved tracers can also be inferred, hence suggesting a potentially conclusive observational test of these models, provided adequate maps of suitable passive chemical tracers can be obtained. Some suggestions for the use of Galileo observations will be made, with particular reference to the use of the Near Infrared Mapping Spectrometer (see also the paper by Lewis et al. in this proceedings).

DR. WEST: I suggest perhaps stratospheric aerosols as a possible tracer which has interesting vertical and latitudinal concentrations towards the pole.

DR. INGERSOLL: I'm also concerned about how you can test things. You see things entering and leaving what is, on a time average, a closed eddy. You do see that all the time because things like the Red Spot are gulping smaller spots and the smaller spots are identifiable and the gulping is always incomplete. Maybe you've got it right in the movie.

DR. READ: Maybe I have, but has anyone actually looked at such a system using time-average statistics? Just because the Red Spot gulps in spots sometimes and expels them at other times, what you actually want to determine is what

the final...what net exchange of material takes place between the long-lived eddy and the smaller spots outside. That's what I'm asking.

DR. BEEBE: When we see a small spot enter the Red Spot or White Oval they go in and they leave a trail, and simply spiral and get stretched out to the point that they become translucent. You can see structures underneath them, through the trails as they wind in.

DR. READ: OK, but is it just between individual spots of either sense of circulation?

DR. BEEBE: We see the anticyclonic ones.

DR. READ: So what does coalescence amount to in these interactions in the presence of strong shear?

DR. BEEBE: I don't think I've ever seen anything come out of the spot. You almost get the impression that any of the subsiding regions are covered by an overlying cloud layer that masks the activity.

DR. READ: I think we ought to be rather careful to make sure we're actually looking at something that's a conserved tracer as well.

DR. BEEBE: That's right.

DR. READ: In interactions between spots, material (and potential vorticity) may be exchanged. If the interactions involve changes in the vertical motion field, however, the cloud structures may be affected on a similar timescale to that of the interaction itself. This is why we must look at [the budgets of long-lived] chemical tracers, as well as tracking cloud systems, because it's the motion of the individual fluid parcels that you want to infer. Not necessarily the products of upward and downward motion.

DR. BEEBE: You have to remember that almost all the observations we have of Jupiter have resolutions larger than the pressure scale height. We haven't seen any features with smaller dimensions.

DR. READ: What you're wondering is why I've listed all these chemical tracers is it, as a way of attributing direction rather than use the clouds themselves?

DR. LEOVY: One encouraging thing that I think there is in the cloud images is the correlation between the edges of the belts and zones, and the jets. One has the impression, and I don't know whether it's valid, but I think maybe look-ing at some of your images from this point of view that in some regions, such as as the latitudinal band of the GRS, the clouds are relatively long-lived. What someone would expect to see for a true long-lived tracer is a correlation between the edge of a tracer and velocity maxima. This is because long-lived tracers would correlate with potential vorticity, which is essentially vorticity itself at the jet level. Consequently, tracer cloud edges would correlate with velocity extrema over a range of scales. If one sees this behavior in areas other than the belt-zone edges, and on a somewhat finer scale, then one would be encouraged that in those regions you've got a long-lived tracer.

MOISTURE DRIVEN CONVECTION ON JUPITER: A MECHANISM TO PRODUCE THE EQUATORIAL PLUMES

C. Stoker
National Center for Atmospheric Research

The presentation by Stoker is largely contained in a paper to appear in *Icarus*. The abstract of her conference presentation is reproduced here.

Cloud condensation and moist convection processes on Jupiter are examined using an idealized model of a cumulus cloud. A cumulus cloud is represented as a spherical parcel of air which is warmed by latent heat release. Condensation is assumed to occur in the parcel and not in the surrounding environment. The entrainment rate, or the rate at which surrounding air mixes with the parcel, is a free parameter in the model. In the convective lower troposphere, rising air parcels can remain bouyant to high altitudes and reach high vertical velocities. Condensation occurring in deep cloud layers can lift air parcels far enough to produce lifting and condensation of higher cloud layers. The bouyant parcel model is used to demonstrate that moist convection can produce Jupiter's Equatorial Plumes and can account for the vertical distribution of aerosols associated with these features. The Plumes form when ammonia condenses in rising air parcels. The condensation of ammonia clouds does not provide enough bouyancy to produce the vigorous rising motion observed in the Plumes (1982, Hunt et al., Nature 295, 491-494). However, bouyant parcels originating at the water cloud level can lift air up to the ammonia cloud level and higher. The associated rapid transport of hydrogen from a high to low temperature region may be responsible for the observed disequilibrium of the ortho-to-para hydrogen ratio in Jupiter's Equatorial region.

DR. TRAFTON: If we're going to have upward moving elements, then we must have downward moving elements. It's not clear to me that you've accounted for these downward movements of air. Is the problem uncoupled, or how did you account for them?

DR. STOKER: Well, if you're referring to upward moving parcels entraining with downward moving parcels, or mixing with them, I haven't considered that at all. In fact this is a very preliminary model of convective processes and it doesn't get into a lot of the sophistication that's done in terrestrial cloud models.

DR. LUNINE: Am I correct in inferring from your model that if the water abundance determination of Bjoraker is right, then there is not enough water at 4 bars to initiate these moist convective effects?

DR. STOKER: If that model is correct, the moist convection will have no observable consequences on Jupiter. They just won't go.

DR. BJORAKER: They won't do that with ammonia? Suppose that you were to shift your cloud model higher up instead of being 2-4 bars, shift the action up around 500 mb, at the ammonia cloud level.

DR. STOKER: I showed a slide of basically that case. You could do it if you had a 10^{-3} mixing ratio of ammonia, but it's actually ten times smaller than that. It's actually the total energy available from latent heat release that drives moist convection. Unless you have a lot of that energy there you can't do it.

DR. ROSSOW: There's another process which can affect your bouyant parcel since you appear to have done your calculations under the assumption of adiabatic ascent. Of course, these parcels must also explosively produce precipitation which can fall out. I agree that at Mach point-something, vertical motions may well suspend a lot of precipitation, but you had to really assume that the environment was saturated in order to get anything sensible as far as the initial lift in order to get the beast going.

DR. STOKER: Right.

DR. ROSSOW: And that means the environment is probably sitting there and precipitating when you start, so you're not going to get nearly as much lift as you calculated from your adiabatic effect because most water is going to be stripped out by the precipitation. If you did an Earth cloud from that view-point, how close to the adiabatic amount would you actually get in an Earth cloud?

DR. STOKER: I haven't done that and I think that it's a good idea. In this model, cloud rises at the pseudo-adiabat which assumes that all condensate falls out immediately. It's an approximation. However, I haven't considered the production of downdrafts by drag of the aerosols that are falling out.

DR. ROSSOW: Let me just say two things about what you're saying. First, that pseudo-adiabat that you are referring to assumes that what falls out is precisely equal to the difference between well-mixed and vapor pressure equilibrium. The whole point of clouds on Earth is that you see two things in ascending cumulonimbus clouds. One is you never see the adiabatic density of cloud mass. You get within a factor of two or three, but you never get that dense. Second, the precipitation mechanism strips more moisture out of the ascent than what you calculate that way. It's not nearly as efficient a system as you're assuming. That doesn't neccessarily mean you get no plume, but you might get something less than Mach-whatever updraft velocities.

DR. STOKER: I agree that those vertical velocities are outlandishly high, but this is kind of a theoretical maximum. I have calculated the absolute maximum altitude that ascending parcels can reach assuming solar composition of water.

DR. BELTON: Do you have a reason why they're all so nicely spaced around the planet and why they're all at the same latitude and why they're all at the same state of development?

DR. STOKER: Well, no, but I think Mike Allison could answer that.[*] Clearly there has to be some kind of forcing that is triggering them in the first place. I'm not really worried about how they get triggered, I only worry about what happens once they do.

DR. BEEBE: There are some observational factors in the Voyager data. During the observational phase, you are taking a consistent movie. If you make strip charts out of an equatorial region, you will see that the translation of velocity in the individual plumes vary. It's not just a trapped wave. They seem to translate in local winds, which would imply that that large annular structure is rotating in the local wind. If it's rotating in the local wind, it's anti-cyclonic, so we expect it to be stable. The site of convection is west of the leading edge of the large plume structure. We also see interaction between convective structures, that are drifting equatorward in the North Equatorial belt, and the plumes. The convection associated with the plumes is not as simple as it looks when you first see it.

DR. WEST: To complicate it even further, one of the methane to continuum image ratios taken by the Voyager 1 camera shows that the northern part of at least one of these plume heads has enhanced methane absorption, which would imply that we're seeing deep down into it. The region immediately north of it is a 5 micron hotspot region which has not had so much enhanced methane, which implies that you're not seeing deep down into that region. How you try to pull all these facts together into a consistent model is... I don't know how to do it.

DR. STOKER: I'd like to respond to one thing that you just said. That is that these are cloud processes and you can't look at one feature and measure one thing on one feature and extrapolate this through all the clouds. The other point is that the Voyager resolution is not good enough to tell you if you have small scale cumulonimbus (that's small-scale compared to very large-scale Earth 1 km cumulonimbus) that is where actual rising motion is occurring. It's only when you get up into the negative shear zone that they form the anvil. In Voyager images, they could appear to be relatively clear and still have patchy clouds that are relatively small in the core region.

---

[*]Editor's note: Allison has performed a diagnostic assessment of Jovian equatorial cloud and temperature features in terms of linear wave theory. (cf. 1983, *Bull. Am. Astron. Soc.*, 15, 836.) This work suggests that the plume features might be planetary Rossby waves drifting westward at around 10 m s^{-1} with respect to the mean equatorial flow and latitudinally trapped by the beta effect. It is not clear, however, that he can answer all of Dr. Belton's questions or that the wave interpretation is correct. (See Dr. Beebe's comment following.)

TUESDAY POSTER PRESENTATIONS

ATMOSPHERIC DYNAMICS

A PROPOSAL FOR ADOPTING A STANDARD COORDINATE SYSTEM FOR DEFINING ATMOSPHERIC NOMENCLATURE FOR THE GIANT PLANETS

R. Beebe
New Mexico State University

Although the albedo of specific belts and zones varies as a function of time, there is evidence that wind maxima may be fixed in latitude. Before considering a standard notation for wind jets, it is necessary to establish a coordinate system within which the nomenclature would be defined. Traditionally, the BAA has used planetographic latitudes; however, this system is based not only on an accurate determination of the polar diameter but also on the assumption that the equipotential surfaces can be represented by biaxial ellipsoids.

The International Astronomical Union strives to adopt unambiguous nomenclature that will be universally acceptable. We propose that planetocentric coordinates be utilized and that a standardized value of the ratio of the polar diameter to the equatorial diameter be established for each planet to facilitate transformation into planetographic coordinates.

INVESTIGATION OF LONG-LIVED EDDIES ON JUPITER

S. R. Lewis, S. B. Calcutt and F. W. Taylor
Oxford University

P. L. Read
Meteorological Office, U. K.

Quasi-geostrophic, two layer models of the Jovian atmosphere are under development; these may be used to simulate eddy phemonena in the atmosphere and include tracer dynamics explicitly. The models permit the investigation of the dynamics of quasi-geostrophic eddies under more controlled conditions than are possible in the laboratory. (See the presentation by Read at this conference.) They can also be used to predict the distribution and behavior of tracer species, and hence to discriminate between different models of the mechanisms forcing the eddies, provided suitable observations can be obtained. At the same time, observational strategies are being developed for the Near Infrared Mapping Spectrometer on the Galileo Orbiter, with the objective of obtaining composition measurements for comparison with the models. Maps of features at thermal infrared wavelengths near 5 μm, and reflected sunlight maps as a function of wavelength and phase angle will be obtained. These should provide further useful information on the morphology, composition and microstructure of clouds within eddy features. Equilibrium chemistry models which incorporate advection may then be used to relate these results to the dynamical models and provide additional means of classifying different types of eddies.

The poster presentation summarizes recent and ongoing work on these problems with some preliminary results.

Compact, oval eddies, comparable in scale to the east-west bands of wind and cloud (belts and zones) are observed at various latitudes in the Jovian atmosphere, centered in shear zones between jets close to where the gradient of potential voticity with latitude is zero (e.g., Ingersoll et al. 1981), the most striking example being the Great Red Spot centered at 25 deg S of the equator. Other examples include the White Ovals, Brown Barges and White Spots. Most seem to be anticyclonic in circulation, with many similarities in shape, morphology of flow and thermal fields, cloud texture, etc. Some cyclonic examples exist (e.g., Barges) with opposite characteristics. All have long lifetimes compared with a typical advection timescale (L/U). Remote sensing instruments on the Galileo Orbiter will produce a wealth of new information about the planet's atmosphere. The complexity of the dynamics and radiative transfer within the atmosphere makes direct interpretation of much of this data difficult. The aim of the work described here is to produce physical models of processes within the Jovian atmosphere and to use these models to predict the values of observables and to test dynamical theories in an efficient way.

Hide (1980, 1981) has suggested that the long-lived eddies observed on Jupiter may be dynamically similar to the steady, regular baroclinic eddies produced in laboratory experiments on thermal convection in an internally heated rotating fluid. Read and Hide (1983) show a streak photograph of an anticyclonic eddy in a rotating annulus which appears to have many of the features of the Great Red Spot on Jupiter including a stagnant, relatively warm core, a peripheral jet stream, and a descending collar.

Baroclinic eddies have several aspects in common with other, recently suggested, models of Jovian eddies, especially "modon" solutions (Ingersoll 1973, Ingersoll and Cuong 1981) since both are characterized by a potential vorticity equation where the Jacobian of stream function and potential vorticity vanishes to first order in a frame moving with the zonal velocity of the shape-preserving solution. The essential difference is that weak, steady effects (in particular diabatic heating) are invoked to balance dissipation in the case of baroclinic eddies whereas Ingersoll and Cuong (1981) invoke transient effects to balance friction.

A quasi-geostrophic, two-level model is currently under development to investigate such eddy solutions. The flow is decomposed spectrally into zonal mean and wave components, which allows calculation of the non-linear interactions between modes represented to be exact. Currently a zonal mean mode is forced which corresponds to internal diabatic heating, but other means of forcing may be incorporated. Dissipation is achieved via various viscous terms.

The model may be used to study the stability of long-lived features in a background flow of suitable configuration, the role of interaction of transients with an eddy and internal forcing processes in the maintenance of the flow against dissipation, and may be used to simulate the transport of quasi-conserved passive Lagrangian tracers given suitable source and sink functions. The vertical motion field may also indicate the cloud morphology expected in the region of an eddy, especially once the resolution of the model is extended.

Advantages of such a model over laboratory experiments such as those performed by Read and Hide (1983) are that the types of forcing and dissipation in use may be specified explicitly, the 'beta effect' (variation in Coriolis parameter with latitude due to the curvature of the planet) may be included, and flow configurations unattainable in the laboratory may be investigated.

Observations of minor chemical species made by instruments on the Galileo Orbiter, e.g., the Near Infrared Mapping Spectrometer, are potentially extremely valuable in helping to discriminate between dynamical models of eddy features. Provided that the mixing and advection timescales are of the right order (see e.g. Read 1985) such species may be used as quasi-conserved passive Lagrangian tracers. For example, McIntyre and Palmer (1983) use satellite observations of ozone in the Earth's atmosphere to derive maps of Ertel potential vorticity on isentropic surfaces.

The NIMS instrument will produce maps of the planet at 408 wavelengths between 0.7 and 5.2 μm with a spatial resolution of better than 400 km at closest approach. (The Great Red Spot has a diameter of around 26,000 km.) This spectral range may provide measurements of the abundances of the minor

constituents PH_3, H_2O, NH_3, GeH_4 and CH_3D for example (Taylor and Calcutt 1984). At the shorter wavelength end of the spectrum ($\lesssim 3\mu m$) scattered sunlight becomes more important than emitted radiation and should provide more information on the morphology and microstructure of clouds within and around eddy features. This may provide further means of classifying different types of eddies.

REFERENCES

Hide, R. (1980). Jupiter and Saturn: giant, magnetic rotating fluid planets. *Observatory* 100, 182-193.

Hide, R. (1981). High vorticity regions in rotating thermally-driven flows. *Met. Mag.* 110, 335-344.

Ingersoll, A. P. (1973). Jupiter's Great Red Spot: a free atmospheric vortex? *Science* 182, 1346-1348.

Ingersoll, A. P. and P. G. Cuong (1981). Numerical model of long lived Jovian vortices. *J. Atmos. Sci.* 38, 2067-2076.

Ingersoll, A. P., R. F. Beebe, J. L. Mitchell, G. W. Garneau, G. M. Yagi, and J. P. Muller (1981). Interaction of eddies and mean zonal flow on Jupiter as inferred from Voyager 1 and 2 images. *J. Geophys. Res.* 86, 8733-8743.

McIntyre, M. and T. N. Palmer (1983). Breaking planetary waves in the stratosphere. *Nature* 305, 593-600.

Read, P. L. and R. Hide (1983). Long-lived eddies in the laboratory and in the atmospheres of Jupiter and Saturn. *Nature* 302, 126-129.

Read, P. L. (1985). Stable, baroclinic eddies on Jupiter and Saturn: a laboratory analogue and some observational tests. *Icarus* 65, 304-334.

Taylor, F. W. and S. B. Calcutt (1984). Near infrared spectroscopy of the atmosphere of Jupiter. *J. Quant. Spectrosc. Radiat. Transfer* 31, 463-477.

CHAOTIC MOTION IN THE JOVIAN ATMOSPHERE

Joseph Pirraglia
NASA/Goddard Space Flight Center

Strong nonlinear interactions among unstable waves and the mean flow occur in a simplified quasigeostrophic spectral model of the upper troposphere of Jupiter. The upper boundary of the layer inhibits vertical motion while at the lower boundary perturbations of the potential temperature are not permitted. On an infinite beta plane the forced flow of alternating zones of prograde and retrograde zonal winds, decreasing with height, are linearly unstable, and it is shown that the nonlinear terms stabilize the flow by bounding the growth of the eddies. Explicit viscosity terms are not needed. This does not imply that energy would not cascade to the small scale flow but suggests that the nature of the large scale flow is independent of the viscosity at small scales. Numerical time integration shows the flow to be chaotic but, in some cases, with transient propagating features and meandering zonal flow.

A spectral potential vorticity model of the upper troposphere of Jupiter has been constructed to study the nonlinear behavior of baroclinic flow on an infinite beta plane. The model imposes a basic zonal flow of alternating jets (longitudinal wavenumber 0 and latitudinal wavenumber 1) which decreases in amplitude with height. The vertical velocity is set equal to zero at the upper boundary of the flow layer (the tropopause) and potential temperature perturbations are required to vanish at the lower boundary. The imposed static stability for two different experiments corresponds to Burger number settings of $S = 0.5$ and 1.0. A schematic depiction of the basic state flow is shown in Figure 1.
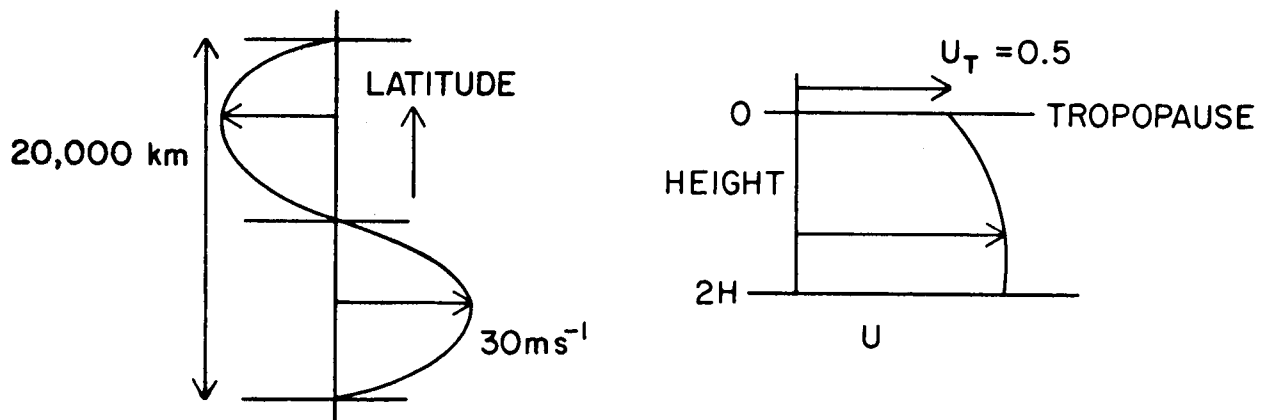
Figure 1. Basic state velocity profile.

The basic state flow is unstable to small perturbations which then grow and interact with the nonlinear terms of the model equations. Figure 2 displays contour plots of the evolving stream functions for the case of S = 1.0 at two different times separated by approximately 6 days. Figure 3 displays stream functions for the case of S = 0.5 at two different times again separated by 6 days.

40,000 KM

LONGITUDE
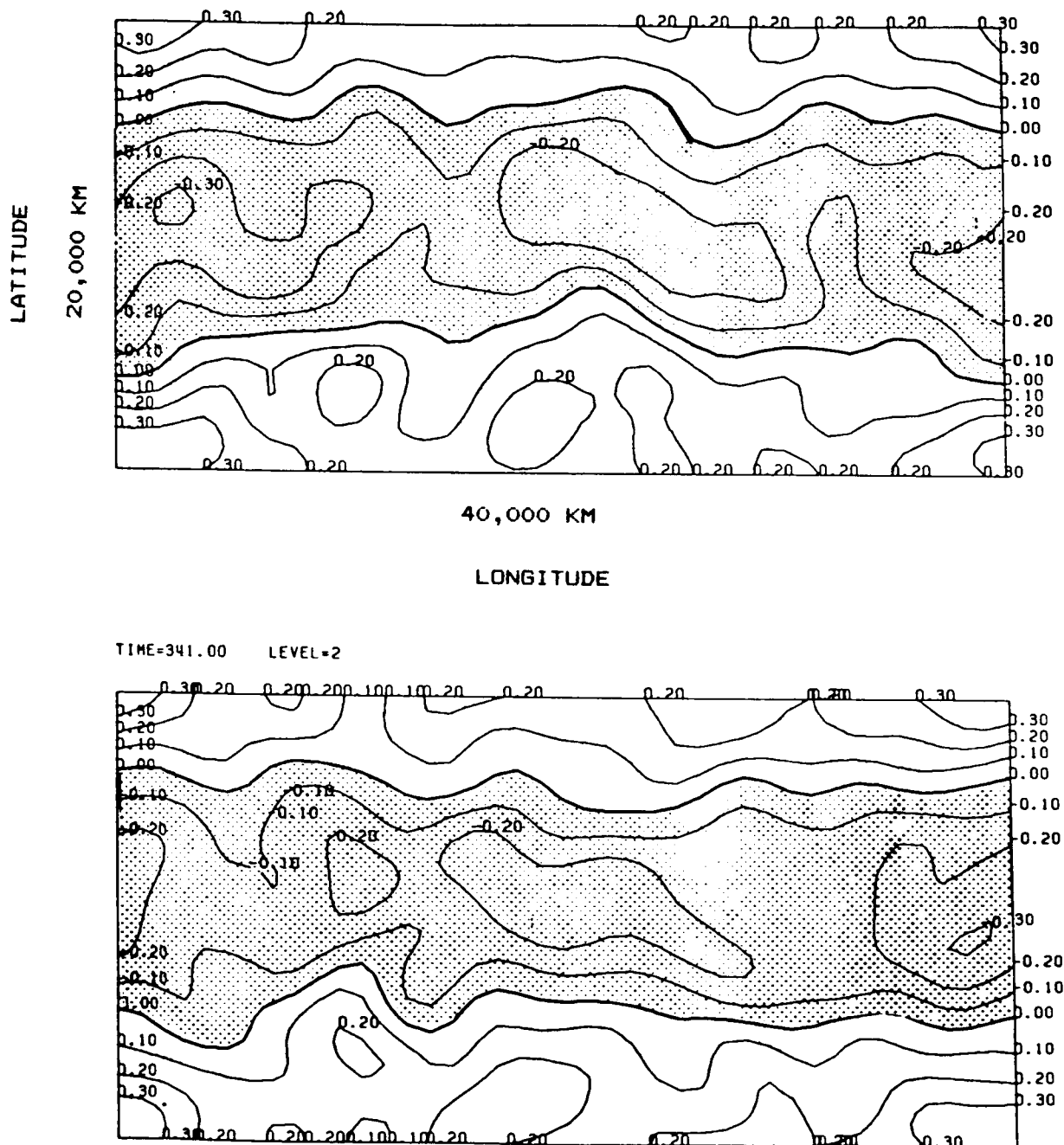
Figure 2. Stream functions for the case of S = 1.0
after "day" 1017 (top) and 1023 (bottom).

208
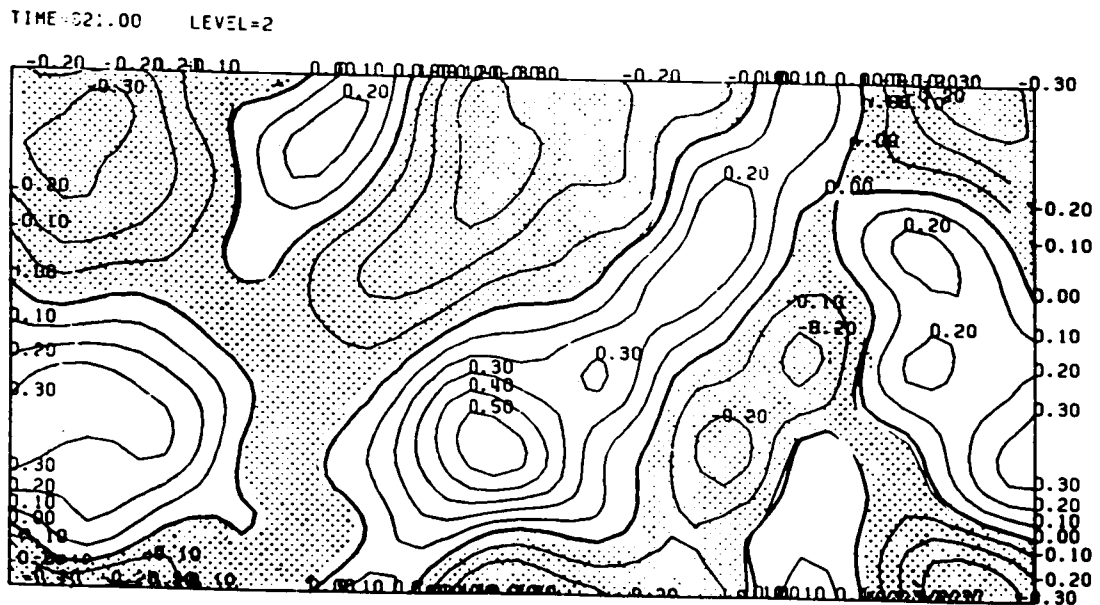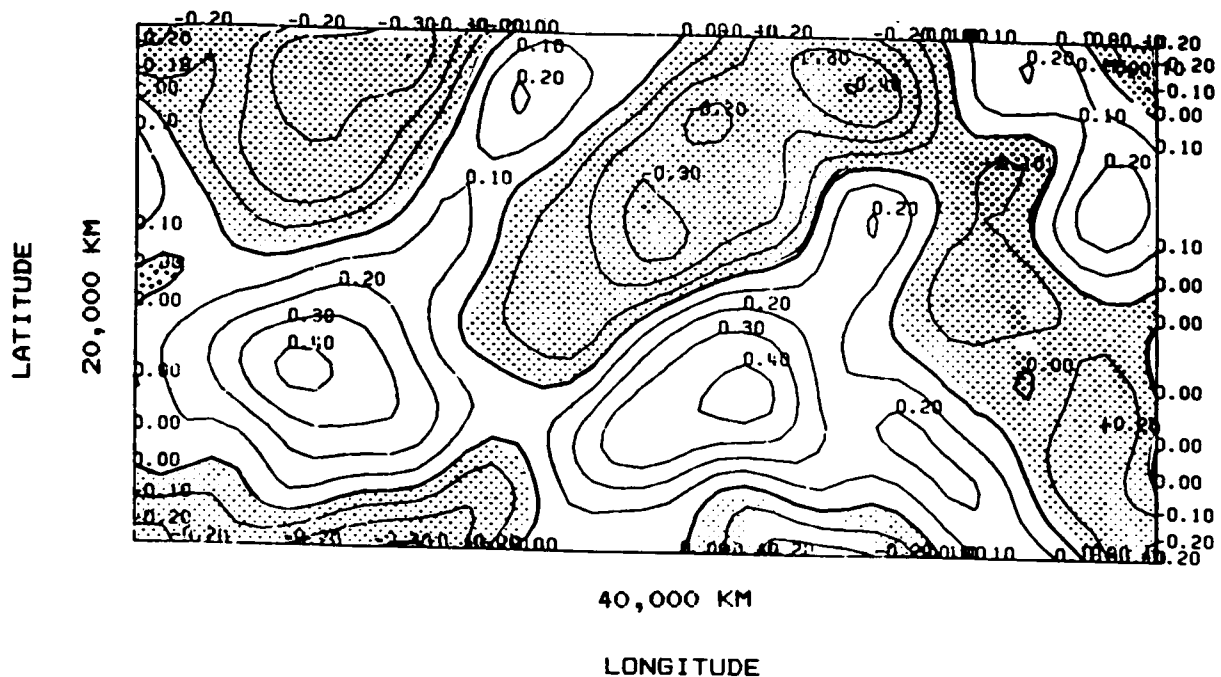
Figure 3. Stream functions for the case of S = 0.5
after "day" 957 (top) and 963 (bottom).

The results of the model experiments show that although the instabilities have exponential growth the nonlinear terms alone bound the solutions. (No explicit damping is required.) There is no equilibrium solution. The evolving zonal flow fluctuates and meanders by an amount dependent upon the parameter settings. The experiments also suggest that specific features propagate in the retrograde sense with respect to the mean flow.

209

TRANSPORT OF ABSOLUTE ANGULAR MOMENTUM IN QUASI-AXISYMMETRIC EQUATORIAL JET STREAMS

P. L. Read

Meteorological Office, U. K.

It is well known that prograde equatorial jet streams cannot occur in an axisymmetric inviscid fluid, owing to the constraints of local angular momentum conservation ("Hide's theorem"). For a viscous fluid, the constraints of mass conservation prevent the formation of any local maximum of absolute angular momentum m without a means of transferring m against its gradient ∇m in the meridional plane (e.g., Held and Hou, 1980, J. Atmos. Sci. $\underline{37}$, 515-533.) The circumstances under which m can be diffused up-gradient by normal molecular viscosity are derived, and illustrated with reference to numerical simulations of axisymmetric flows in a cylindrical annulus. Viscosity is shown to act so as to tend to expel m from the interior outwards from the rotation axis. Such an effect can produce local super-rotation $(m > \Omega R^2)$ even in a mechanically-isolated fluid (e.g. contained by rigid stress-free boundaries), and is illustrated in a further numerical experiment. The tendency of viscosity to result in the expulsion of m is shown to be analogous in certain respects to a "vorticity-mixing" hypothesis for the effects of non-axisymmetric eddies on the zonally-averaged flow. We show how the advective and 'diffusive' transport of m by non-axisymmetric eddies can be represented by the Transformed Eulerian Mean meridional circulation and the "Eliassen-Palm" (EP) flux of Andrews & McIntyre (1976, J. Atmos. Sci. $\underline{27}$, 15-30) respectively, in the zonal mean. Constraints on the form and direction of the EP flux in an advective/"diffusive" flow for such eddies are derived, by analogy with similar constraints on the diffusive flux of m due to viscosity. From a consideration of these constraints on $\underset{\sim}{E}$, $\nabla \cdot \underset{\sim}{E}$, and $\underset{\sim}{v}*$, and the properties of the super-rotating numerical simulations discussed above, we suggest ways of using observations of the zonal mean flows on Jupiter and Saturn to infer the sources and sinks of m required to maintain the observed flow. The associated form of $\underset{\sim}{E}$ can also be used to infer some of the properties of the non-axisymmetric eddies responsible for the transport of m within Jupiter's equatorial jet.

It is well known from cloud-tracked wind data, obtained from ground-based observations and the Voyager spacecraft that both Jupiter and Saturn exhibit strong westerly (prograde) jet streams near their equators. When measured with respect to the "interior" rotation rate (defined by their radio rotation frequencies), these equatorial jet streams are found to be extremely intense ($u>100$ m s^{-1} on Jupiter and $u\sim 500$ m s^{-1} on Saturn), and are remarkably persistent features in the large-scale circulations of the major planets. Some recently measured velocity profiles are shown schematically in Fig. 1.
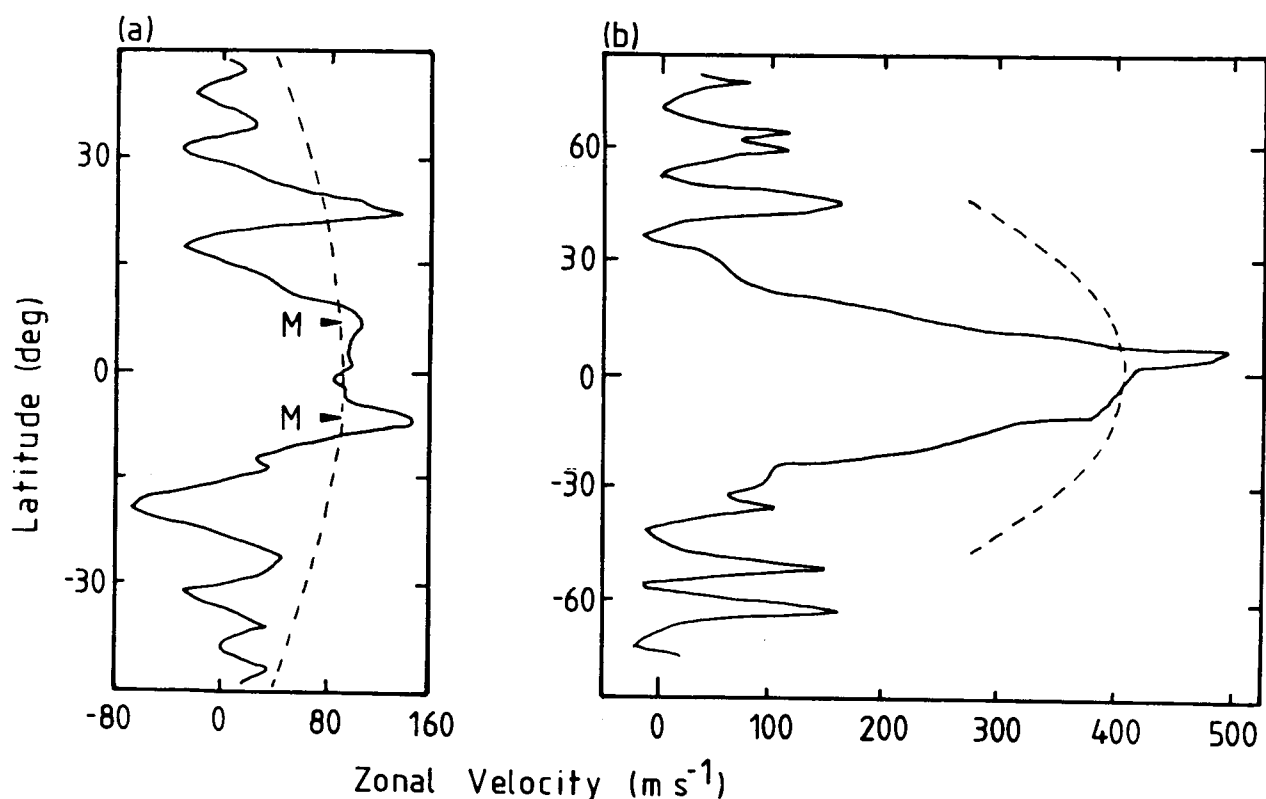
Figure 1. Latitudinal profile of mean zonal velocity (with respect to the measured radio rotation rate) at the cloud tops of (a) Jupiter (adapted from the data of Ingersoll et al., 1981) and (b) Saturn (adapted from the data of Smith et al., 1982). Also shown (dashed) are velocity profiles corresponding to a uniform angular velocity with latitude, equivalent to the approximate rotation period measured at the equator on each planet. The latitudes of the maximum observed angular velocity in Jupiter's equatorial jet are indicated in (a) by M.

The existence of these apparently steady equatorial jet streams poses some intriguing dynamical questions, especially regarding the origin of their angular momentum and the nature of the processes which maintain them. If we consider the simplest possible configuration, in which only axisymmetric motions (e.g., driven by a latitudinal distribution of diabatic heat sources and sinks) are permitted (i.e., we exclude non-axisymmetric pressure gradients, hydromagnetic effects etc.), prograde equatorial jets cannot occur without rather special initial conditions. This is because, in inviscid axisymmetric flow, the angular momentum per unit mass

$$m = (\Omega R \cos \lambda + u) R \cos \lambda \qquad (1)$$

(where Ω is the planetary rotation rate, R the planetocentric radius and λ is latitude) is conserved following the motion in the meridional plane, i.e.,

$$Dm/Dt = 0 \quad (\text{where } D/Dt = \partial/\partial t + \underset{\sim}{v} \cdot \nabla) \qquad (2)$$

Since $u>0$ at the equator requires that $m>\Omega R^2_{max}$, (2) requires the initial flow also to contain fluid elements with $m>\Omega R^2_{max}$, i.e., with more m than any fluid element initially at rest in the rotating frame (This is sometimes referred to as "Hide's theorem"--see Hide 1969). The volume-integrated angular momentum is similarly constrained to a constant value at all times.

EFFECTS OF INTERNAL VISCOSITY

Since an inviscid, axisymmetric system (initially at rest) cannot produce an equatorial jet, it is natural to consider the effects of Newtonian (molecular) viscosity, while still preserving an axisymmetric flow. Viscosity removes the formal conservation of m but, for a steady flow, some constraints on the flow can still be obtained (using arguments similar to Schneider 1977; Held and Hou 1980) as follows. With viscosity, Eq. (1) becomes

$$Dm/Dt = -\nabla \cdot \underset{\sim}{F} \qquad (3)$$

where $\underset{\sim}{F}$ is the diffusive flux of m due to viscosity which, for an isotropic fluid, is given by

$$\underset{\sim}{F} = -\nu R^2 (\cos^2 \lambda) \nabla \gamma \qquad (4)$$

where ν is the kinematic viscosity and

$$\gamma = u/(R \cos \lambda) \qquad (5)$$

the local relative angular velocity.

If we consider any local maximum in m (necessarily, though not exclusively, associated with an equatorial jet), $m = m_0$ (say), we may draw a closed m contour in the meridional plane at $m_0 - \varepsilon$ (where ε may be arbitrarily small; see Fig. 2). Integrating the steady form of (3) over the toroidal volume enclosed by the $m - \varepsilon$ contour, we get

$$\iiint \nabla \cdot (v m) \, d\tau = (m_0 - \varepsilon) \oint v \cdot n \, ds$$

$$= 0 \text{ (by mass conservation)}$$

$$= - \oint F \cdot n \, ds \tag{6}$$

Thus, either $F \cdot n = 0$ everywhere, or else F must possess both inward and outward components in different regions of the m contour (i.e., F must act up-gradient with respect to ∇m somewhere in the flow). Since F is (anti-) parallel to $\Delta \gamma$, and not to ∇m (see (4) and (5) above), a necessary condition for the existence of a steady viscous jet is for $\nabla \gamma \cdot \nabla m$ to take either sign in different parts of the flow. It is not necessary to invoke "negative viscosity" phenomena, which are fundamentally associated with non-axisymmetric effects.
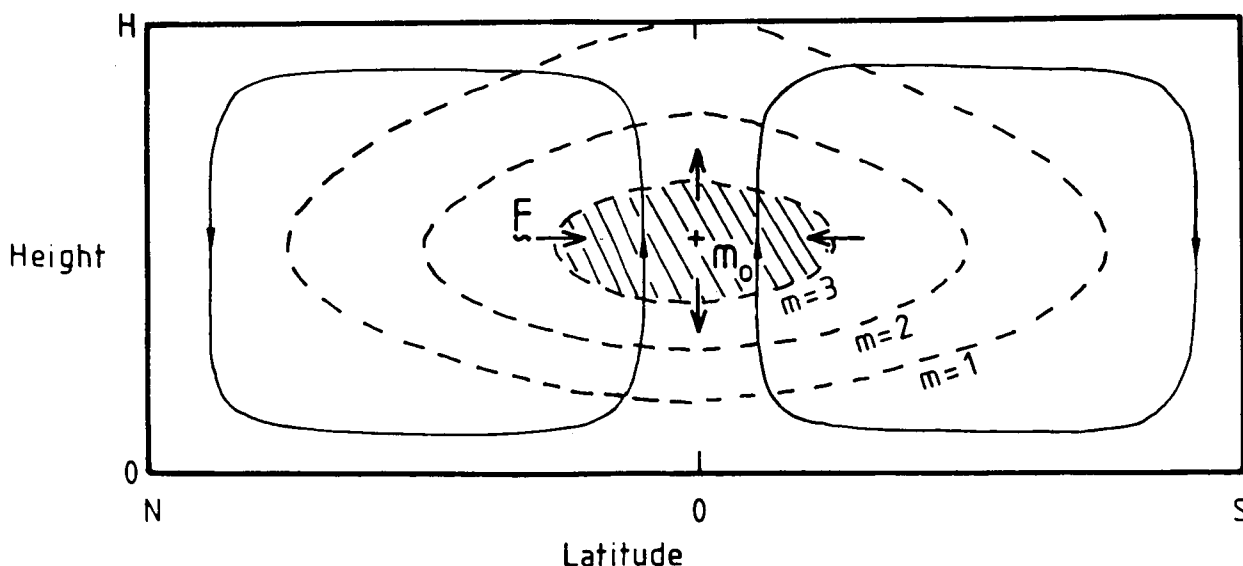
Figure 2. Map of m in a hypothetical flow on a sphere, with a local maximum in m near the equator. Constraints derived for such a flow, associated with a balance between advection (in a meridional circulation, shown by continuous lines) and diffusion, result in a need for F to act inwards in some places and outwards in others for a closed m contour region (shaded), with $\oint F \cdot n \, ds = 0$.

(a) TEMPERATURE (b) ANGULAR VELOCITY (c) ANGULAR MOMENTUM DIFFUSIVE AM FLUX VECTORS

(d) STREAM FUNCTION (e) VISCOUS TORQUE
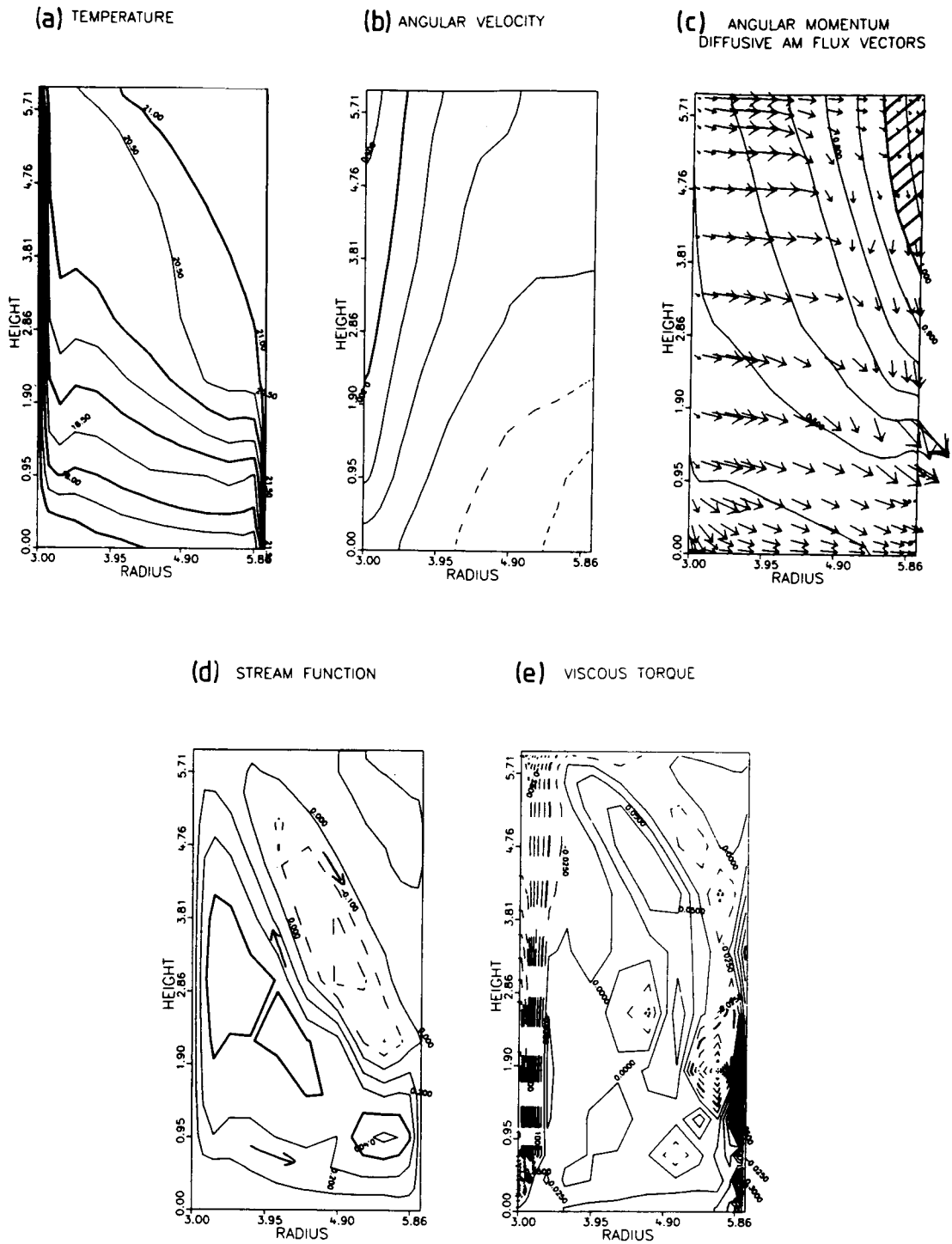
Figure 3. Steady state fields shown in the (r,z) plane for thermally-driven flow (by differential heating at the sidewalls) in a system with stress-free boundaries. (a) Temperature T. (Contour interval [CI] 0.5 deg C); (b) Angular velocity $\gamma = u/r$ (CI = 0.1 rad s^{-1}); (c) m and vectors of F (CI = 0.1 m/Ωb^2); (d) Meridional stream function χ_*. (CI = 0.1 cm^2 s^{-1}); (e) Local viscous torque ($-\nabla \cdot F$). (CI = 0.025 cm^2 s^{-2}).

214

AN EXAMPLE IN THE CYLINDRICAL ANNULUS

We illustrate the application of these ideas in a numerical simulation of axi-symmetric flow in a rotating cylindrical fluid annulus. The fluid is incompressible and Boussinesq (for simplicity), and contained between two coaxial cylindrical surfaces (at r=a,b) and horizontal boundaries at z = 0,H. Motion is driven by maintaining the two sidewall boundaries at different (constant) temperatures (T_a and T_b), and in the present example, all boundaries are rigid and stress-free (so that $\nabla\gamma\cdot\underset{\sim}{n}=\underset{\sim}{F}\cdot\underset{\sim}{n} = 0$, and the fluid cannot exchange m with its environment). The model used is a grid-point finite-difference formulation of conventional design, with a stretched mesh to resolve boundary layers, and a realistic representation of molecular viscosity and thermal conductivity (being the only sub-gridscale processes, see Hignett *et al.*, 1985 and Read 1986a for further details).

Figure 3 shows a selection of steady state fields in the (r,z) plane. With $T_a = T_b$, a meridional overturning circulation is driven between the two side-walls which is predominantly thermally-direct (cf. Figs. 3(a) and (d)), though some smaller, indirect cells also occur owing to the effects of a diffusive instability for Prandtl number $\sigma \gg 1$. During the "spin-up" of the flow, m is redistributed by the main meridional circulation (though because of the boundary conditions, the total amount must remain constant). It accumulates near the top of the inner cylinder (top left in Fig. 3), generating a local maximum in γ (see Fig. 3(b)). Since F is related to $\nabla\gamma$ (see Eq. (6)), viscous diffusion transfers m outwards from the γ maximum, tending to transfer m horizontally against its local gradient ∇m. In the steady state, this outward transfer of m exactly balances advection by the meridional circulation, and the resultant distribution of $\underset{\sim}{F}$ and $\underset{\sim}{m}$ is shown in Fig. 3(c). Note that fluid elements near r=b, z=H have now acquired $m > \Omega_b^2$ in a wedge-shaped region of the flow (shaded in Fig. 3(c)), even though the total angular momentum is unchanged from the initial rest state. Thus, viscosity has acted as a mechanism for __angular momentum expulsion__ towards the outer cylinder.

Since Eq. (6) is satisfied not only for a region bounded by contours of m, but also by impermeable boundaries, it applies to Fig. 3. This can be seen in Fig. 3(c), with $\underset{\sim}{F}$ being largely up-gradient (with respect to ∇m) in the horizontal, and down-gradient in the vertical. The corresponding local torque on the fluid ($-\nabla\cdot\underset{\sim}{F}$) is shown in Fig. 3(e), and consists of a complicated array of sources and sinks which, when integrated over the volume of the fluid, have a resultant of zero.

APPLICATION TO REAL EQUATORIAL JETS

The configuration considered in Fig. 3 is analogous in some respects to an equatorial jet in a thermally-driven flow on an entirely fluid spherical planet (i.e., without a solid underlying surface), if we regard the (r,z) plane as equivalent to the latitude, height) plane and r=b as representing the equator. The resulting advective/diffusive flow is similar in some respects to some simple models of the Jovian atmosphere (e.g. Williams and Robinson 1973; Mayr and Harris 1983), although such models have tended to require a stress-bearing lower boundary to generate a prograde equatorial jet. The experiment in Fig. 3

uses a stress-free lower boundary, yet still supports a local maximum in $m > \Omega_b{}^2$ in the steady state. The main criterion is that $\nabla\gamma\cdot\nabla m < 0$ somewhere in the flow, implying that maxima in γ cannot coincide with maxima in m.

Some evidence for this is apparent in Jupiter's equatorial jet (Fig. 1(a)), which clearly shows a local minimum in u (and $\bar{\gamma}$) at the equator itself, and maxima in u (and $\bar{\gamma}$) at the poleward extremes of the jet. Transfers of m by molecular viscosity are unlikely to be significant for Jupiter and Saturn's jets, however, and are probably dominated by eddy mixing (which is fundamentally non-axisymmetric). Since $\underset{\sim}{F}$ is related to the gradient of (relative or absolute) vorticity $\bar{\zeta}$, however, viscosity is seen to act in some respects like a vorticity-mixing process (tending to even out gradients in $\bar{\zeta}$), such as has been suggested for a variety of eddy phenomena in fluid mechanics and geophysics (e.g., Taylor, 1915; Rossby, 1947; Green, 1970; Read, 1986b). The experiment in Fig. 3 can be regarded, therefore, as indicating in a general way how an equatorial super-rotation can be driven and maintained by a thermally-driven meridional circulation interacting with eddies which act to mix vorticity.

Are there any useful constraints on non-axisymmetric flows? We present an eddy transfer theorem for closed m contours. If we form the equation for the conservation of zonally-averaged angular momentum m, using the residual Eulerian mean circulation of Andrews & McIntyre (1976), we get (e.g., in spherical geometry using pressure coordinates in the vertical)

$$\partial\bar{m}/\partial t + \underset{\sim}{v}_*\cdot\nabla\bar{m} = -\nabla\cdot\underset{\sim}{E} \;(-\nabla\cdot\underset{\sim}{F}) \tag{7}$$

where

$$\underset{\sim}{v}_* = [\,\bar{\underset{\sim}{v}} - (\,\overline{v'\theta'}/\theta_p)_p, \;\bar{\omega} + (\,\overline{v'\theta'}\cos\lambda/\bar{\theta}_p)_\lambda/(R\cos\lambda]\tag{8}$$

and represents the (quasi-Langrangian) mean meridional circulation associated with diabatic heating, eddy dissipation and transience. $\underset{\sim}{E}$ is related to the so-called Eliassen-Palm flux, and given by

$$\underset{\sim}{E} = R\cos\lambda[\overline{u'v'} - \bar{u}_p\overline{v'\theta'}/\bar{\theta}_p \;,$$

$$\omega'u' + \{(\bar{u}\cos\lambda)_\lambda/(R\cos\lambda) - 2\Omega\sin\lambda\}\,\overline{v'\theta'}/\bar{\theta}_p]\tag{9}$$

216

(cf. Andrews & McIntyre 1978). Since $\underset{\sim}{v}_*$ obeys a similar continuity equation to $\underset{\sim}{v}$, $\underset{\sim}{E}$ must obey a constraint similar to Eq. (6) for closed, steady m contours, provided we may ignore molecular viscosity. Thus,

$$\oint \underset{\sim}{E} \cdot \underset{\sim}{n} \, ds = 0 \qquad\qquad (10)$$

around any closed m contour.

Further aspects of the ideas presented in Sections 1-4 above are discussed in greater detail by Read (1986a,b).

DIAGNOSTICS FOR JUPITER'S EQUATORIAL JET?

Given the framework of constraints on equatorial jets associated with a balance between advection of m and its transfer by non-axisymmetric eddies, it may be possible to use observations of Jupiter's equatorial jet to obtain information concerning the processes by which the jet is maintained. We suggest below some strategies for possible diagnostic studies of Jupiter's atmosphere which may bear on this important problem:

a) From detailed observations of the zonal mean flow on Jupiter, we may investigate the properties of candidate eddy processes and their associated sources and sinks of m. The equatorially-localized structure of the jets might suggest the relevance of equatorially-trapped Kelvin and Mixed Rossby-Gravity (MRG) modes, for example, as studied in a simple model of Jupiter's equatorial jet by Maxworthy (1975). Given the thermal and velocity structure of the mean zonal flow, it is possible (subject to certain assumptions) to calculate the properties of steady modes which are compatible with that (steady) mean flow. An example of such a procedure was given by Plumb and Bell (1982), who undertook a similar study in connection with the quasi-biennial oscillation in the terrestrial stratosphere. Given the form of $u(y,z)$ and N^2, the mode structure can be obtained, together with quantities analogous to $\underset{\sim}{E}$ and $\nabla \cdot \underset{\sim}{E}$ for the main Kelvin and MRG modes. The latter could then be tested against the constraints of Eq. (10) for consistency with the distribution of m and a suitable meridional circulation.

b) Since the meridional circulation compatible with the constraints on $\underset{\sim}{E}$ and $\nabla \cdot \underset{\sim}{E}$ is quasi-Lagrangian, it primarily reflects the distribution of diabatic heat sources and sinks in the Jovian atmosphere. This can also be compared, therefore, with the known sources and sinks, e.g., due to radiative forcing obtained from radiation budget studies, to check for consistency of the solution, and to provide further requirements which the eddy processes need to satisfy.

The feasibility of such strategies have yet to be demonstrated for Jupiter, although some progress on a similar scheme for the analysis of data for Venus (from Pioneer Venus project) has been made by Hou (1984), Hou and Goody (1985) and Valdes (1984 and private communication).

REFERENCES

Andrews D. G. and M. McIntyre (1976). Planetary waves in horizontal and vertical shear: The generalized Eliassen-Palm relation and the mean zonal acceleration. *J. Atmos. Sci.*, 33, 2031-2048.

Andrews D. G. and M McIntyre (1978). Generalized Eliassen-Palm and Charney-Drazin theorems for waves on axisymmetric mean flows in compressible atmospheres. *J. Atmos. Sci.*, 35, 175-185.

Green J. S. A. (1970). Transfer properties of the large-scale eddies and the general circulation of the atmosphere. *Quart. J. R. Met. Soc.*, 96, 157-185.

Held, I. M. and A. Y. Hou (1980). Nonlinear axially symmetric circulation in a nearly inviscid atmosphere. *J. Atmos. Sci.* 37, 515-533.

Hide, R. (1969). Dynamics of the atmospheres of the major planets with an appendix on the viscous boundary layer at the rigid bounding surface of an electrically-conducting fluid in the presence of a magnetic field. *J. Atmos. Sci.* 26, 841-853.

Hignett, P., A. A. White, R. D. Carter, W. D. N. Jackson, and R. M. Small (1985). A comparison of laboratory measurements and numerical simulations of baroclinic wave flows in a rotating cylindrical annulus. *Quart. J. R. Met. Soc.*, 111, 131-154.

Hou, A. Y. (1984). Axisymmetric circulations forced by heat and momentum sources: A simple model applicable to the Venus atmosphere. *J. Atmos. Sci.* 41, 3437-3455.

Hou, A. Y. and R. Goody (1985). Diagnostic requirements for the super-rotation of Venus. *J. Atmos. Sci.*, 42, 413-432.

Ingersoll, A. P., R. F. Beebe, J. L. Mitchell, G. W. Garneau, G. M. Yagi and J.-P. Muller. *J. Geophys. Res.*, 86, 8733-8743 (1981).

Maxworthy, T. (1975). A wave-driven model of the Jovian equatorial jet. *Planet. Space Sci.* 23, 1223-1233.

Mayr H. G. and I. Harris (1983). Quasi-axisymmetric circulation and superrotation in planetary atmospheres. *Astron. Astrophys.* 121, 124-136.

Plumb, R. A. and R. C. Bell (1982). Equatorial waves in steady zonal shear flow. *Quart. J. R. Met. Soc.*, 108, 313-344.

Read, P. L. (1986a, b). Super-rotation and diffusion of angular momentum. *Quart. J. R. Met. Soc.* 112, 231-272.

Rossby, C.-G. (1947). On the distribution of angular velocity in gaseous envelopes under the influence of large-scale horizontal mixing processes. *Bull. Amer. Met. Soc.*, 28, 53-68.

218

Schneider, E. K. (1977). Axially symmetric steady state models of the basic state for instability and climate studies. Part II. Non-linear calculations. *J. Atmos. Sci.*, 34, 280-296.

Smith, B. A., L. Soderblom, R. Batson, P. Bridges, J. Inge, H. Masursky, E. M. Shoemaker, R. F. Beebe, J. Boyce, G. Briggs, A. Bunker, S. A. Collins, C. J. Hansen, T. V. Johnson, J. L. Mitchell, R. J. Terrile, A. F. Cook, J. Cuzzi, J. B. Pollack, G. E. Danielson, A. P. Ingersoll, M. E. Davies, G. E. Hunt, D. Morrison, T. Owen, C. Sagan, J. Veverka, R. Strom, and V. E. Suomi (1982). A new look at the Saturn system: The Voyager 2 images. *Science,* 215, 504-537.

Taylor, G. I. (1915). Eddy motion in the atmosphere. *Phil. Trans. R. Soc. Lond.,* A215, 1-26.

Valdes, P. J. (1984). *D. Phil. Thesis.* University of Oxford.

Williams, G. P. and J. B. Robinson (1973). Dynamics of a convectively unstable atmosphere: Jupiter? *J. Atmos. Sci.* 30, 684-717.

WEDNESDAY MORNING

FUTURE SPACEFLIGHT OPPORTUNITIES

CHAIR: WILLIAM B. ROSSOW

OPENING REMARKS

Henry C. Brinton
Solar System Exploration Division, NASA Headquarters

I want to commend GISS and the conference organizers for staging this meeting.
I think everyone here feels that it has been a very valuable and interesting
get-together. We encourage such topical conferences as this. As Jim Hansen
said the other day, I hope it's not another ten years before this group gets
back together.

Geoff Briggs is sorry that he couldn't be here. He was scheduled to speak
this morning. His father has been ill and in the hospital in England, and
Geoff is on his way to visit his father now. But I did bring his greetings, I
talked to him about the meeting before I came up here, and I want to convey
his optimism about the planetary program.

The recommended core program for future planetary exploration was put together
by the Solar System Exploration Committee some years back. We are on track
with implementing this program. The first two missions, Venus Radar Mapper,
and what is now called Mars Observer, are both approved and are being funded
for development. The Comet Rendezvous Asteroid Flyby or CRAF mission is the
first of the Mariner Mark II series.

The Titan Probe Mission and the Saturn Orbiter are now combined in what's
called Cassini. Some of you are, I know, heavily involved with the study of
the Cassini Mission and I think that Toby Owen is going to talk about this
later. It is our expectation that Cassini will be the second of the Mariner
Mark II's. This is going to be a joint NASA/ESA mission with a Saturn Orbiter
and Titan probe. The joint assessment study of this mission is underway now.
Geoff Briggs is confident that in November of this year both ESA and the U.S.
will approve an official Phase A study of this mission. That would lead to
the issuance of an instrument AO in January of 1988. The fiscal year 1990
would be the new start with a launch in 1994 and arrival at Saturn in 2002.
The SSEC program calls for a Mariner Mark II new start every three years.

So CRAF and Cassini are the first two missions in the Mariner Mark II series
we are working toward at Headquarters. This is going to be tough. I think
most of you know what the competition is. If CRAF slips beyond '87, a number
of things happen. One is that this could force a delay in the start of
Cassini. It also means that a different target comet would have to be selec-
ted. I think that it also means that the nature of the Earth-Comet trajectory
changes. I think we have to go into a delta-VEGA (Earth gravity assist) mode
of trajectory in order to reach the comet if we don't get the new start in
'87. Beyond Cassini, the choice of the next Mariner Mark II mission hasn't
yet been made. But I think we have a lot to look forward to in planetary ex-
ploration, and in particular, in planetary atmospheres research.

PRECEDING PAGE BLANK NOT FILMED

AN UPDATED HYDROCARBON PHOTOCHEMICAL MODEL FOR THE JOVIAN ATMOSPHERE FROM THE TROPOSPHERE THROUGH THE HOMOPAUSE: A PRELUDE TO GALILEO

M. Allen
Jet Propulsion Laboratory, California Institute of Technology

G. R. Gladstone and Y. L. Yung
California Institute of Technology

A photochemical model for the atmosphere of Jupiter, including 1-D vertical eddy diffusive transport, has been developed. It extends from the upper troposphere (pressure <5 bar) through the homopause. The hydrocarbon chemistry involves species containing up to four carbon atoms (and polyynes through C_8H_2). The calculations show that a large fraction of photochemical carbon may be contained in molecules with more than two carbon atoms. At the tropopause ($\approx$ 164 mb), C_2H_6 is the major photochemical species and C_2H_2, C_3H_8, and C_4H_{10} are of comparable abundance and down from C_2H_6 by a factor of ten. These species may be detectable with the mass spectrometer of the Galileo Probe. The vertical distributions of the photochemical species are sensitive to the magnitude of eddy diffusive mixing in the troposphere and stratosphere and the details of the interface region.

I presume that our paper was placed in this session on future spaceflight opportunities because of the last four words of our title. It is not necessarily inappropriate because I wish at the end to throw out a challenge to the Galileo Probe to detect something predicted by our models to exist but which has not yet been detected. You may have noticed that in his review Darrell Strobel did not emphasize the hydrocarbon chemistry modeling, essentially because nothing much has occurred in the past few years. Most of the action has been centered on phosphorus. There has been a fair amount of new observational information coming from Voyager, and with an eye towards Galileo we've decided to reopen the analysis of hydrocarbon modeling of Jupiter. Some of you may have heard me talk about some of the results from our work at the DPS Meeting in Hawaii. I'd like to talk about other new results this morning.

As for the basic details of the model, we now run the model from the 5 bar level in the troposphere up through the homopause. The Voyager data are used to define the temperature-pressure profile. We have expanded the model to include more complex hydrocarbon species than you find in other published hydrocarbon models for Jupiter. Much of this is a result of our work for Titan where, because of the complex molecules that were seen, it was necessary for us to make a major effort to expand the reaction set. Now we are going back to see if the same basic reactions will help us understand Jupiter. One hopes that the chemistry is the same, independent of where you are in the solar system.

Since this is still a classic one-dimensional model, the transport is vertical mixing through eddy diffusion. We employ a stratospheric profile for the eddy diffusivity that Randy Gladstone used in his thesis; it is similar to what other people have used in the past. Then there is the question of how fast is the mixing in the troposphere? Darrell Strobel mentioned values of the eddy diffusivity for the upper troposphere on the order of 10^4 cm^2s^{-1} based on work with Marty Tomasko, but dynamical arguments suggest that at some level in the troposphere the mixing may imply a coefficient as large as 10^8 cm^2s^{-1}. The modeling that I will describe assumes a constant value of 10^4 cm^2s^{-1} throughout the troposphere, but I'll surmise about what would be the effects if you had more rapid mixing. So the basic eddy diffusion profile we use has fast mixing (10^7 cm^2s^{-1}) up high as inferred by the Voyager UVS observations, decreases to a more stagnant layer ($<10^3$ cm^2s^{-1}) in the stratosphere, and then jumps up to faster mixing in the troposphere. This kind of profile is similar to what is used in Earth modeling, with a sharp discontinuity occurring at the tropopause.

We use diurnally averaged radiation field calculations, which should be valid for most species on Jupiter given their lifetimes. In addition to the basic reactions involving C_1 and C_2, we have a reaction set for a host of C_3 and C_4 compounds. Rather than describe the many pathways, I want to emphasize the fact that you get these more complex species through 3-body recombination between C_1 and C_2 radicals. So combination of C_2H_3 and C_2H_5 produces C_4H_8, and the C_4H_{10} comes from C_2H_5. With recombination between C_1 and C_2H_2, one gets allene and methyl-acetylene. There are tentative detections reported for some of these species, but many are undetected. I should note that our reaction set at the C_4 level is not thoroughly complete, so that the results we obtain for butane may be an upper limit. Another point that I should make is that some of these reactions were previously discussed by Jack McConnell at a DPS meeting some years ago.

Among the basic results of our model is the fact that we have allene, methyl-acetylene, and ethene, which are species that have been reportedly detected very recently. However, I particularly want to point out that in the lower stratosphere, we find abundances of propane and butane that are almost equal to the abundance of acetylene.

In fact, when you count up the number of carbon atoms, you find that there may be as much "photochemical" carbon contained in these species as is contained in acetylene. It is very interesting that none of these species have been reported so far. I would like to suggest a reason for that and relate it to the question of potential Galileo measurements.

The molecules with multiple bonds such as acetylene, methyl-acetylene, and ethene have spectroscopic characteristics that are significantly different from molecules that are fully saturated and hence have no multiple bonds (e.g., ethane, propane, and butane). The saturated molecules tend to have very smooth absorption that cuts off very sharply between 1600 and 1700 Å, whereas those with multiple bonds have a tendency to absorb at much longer wavelengths. This situation leads to problems in trying to detect the more saturated species because of the rapid decrease in solar illumination at shorter wavelengths in the ultraviolet. It makes things very difficult for

the IUE. The lack of structure also makes the identification of the signature for a particular species problematic. At the same time, the molecules with multiple bonds have fairly intense bands in the infrared, while those of the saturated molecules are relatively weak (down by a factor of 10 to 100). In fact, the only reason that one might see ethane is that it is so abundant relative to acetylene. When you start looking for saturated species which have abundances on the order of that for acetylene, then you will have trouble because you are fighting the spectroscopy.

Now I would like to pose the challenge for the mass spectrometer on the Galileo Probe, namely, the detection of one or more of these trace species. Because of the predicted decrease in mixing ratio towards the troposphere, a crucial issue in addition to its sensitivity will be the altitude at which the mass spectrometer begins to obtain data. It is my understanding that the mass spectrometer turns on at the 100 mb level and has a sensitivity of one part in 10^9. Because we have added a rapidly mixed troposphere instead of cutting off our model at the tropopause as most previously published models, the vertical mixing propagates up into the stratosphere. Even though the species in the lower stratosphere tend to be long-lived, there is sort of a "vacuum cleaner" effect on the troposphere, leading to a decrease in the mixing ratio profile starting somewhat above the tropopause and extending down into the troposphere. This is in contrast to the kinds of modeling that are done for remote sensing analyses in which constant vertical mixing ratios are assumed throughout the stratosphere. If the mass spectrometer has sufficient sensitivity starting at 100 mb, one might even see the decrease in the profile above the tropopause predicted by our more realistic modeling of the transport in the one-dimensional limit. If you increase the mixing in the troposphere by taking an eddy diffusivity of 10^8 cm^2s^{-1} instead of 10^4 cm^2s^{-1}, then the tropospheric profiles will drop even further, and there will be even sharper cut-offs in the stratosphere. In that case, we may miss completely any potential window for detection of the trace species by the mass spectrometer. Whether or not we see these trace species may therefore give us some information about the transport in the atmosphere.

DR. LUNINE: Mark, a lot of the photochemistry that you've talked about is also applicable to the other outer planets and also to Titan. There are some uncertainties I know, that have plagued these models for a while. Which of these uncertainties will be at least constrained, or possibly eliminated by the ability to measure vertical profiles through one of these atmospheres? Or will all the uncertainties remain buried in vertical transport?

DR. ALLEN: I think that, given our ability to do remote sensing, and the observations that are just coming out now based on some Voyager and IUE data, there is a possibility that we can attempt to confirm our reaction sequence to some extent in the upper stratosphere from remote sensing. Then hopefully, if we gain more confidence from looking at species in the stratosphere, tying that in with our understanding of Titan and the visibility of propane on Titan, maybe in the end we can have some hope of then saying that the ability to detect species depends on the sensitivity threshold. So you see, the mass spectrometer may actually succeed and we can then back out some statement about transport and mixing on Jupiter.

226

DR. NIEMANN: I suppose you would like to know what the probe mass spectrometer can do to verify your predictions. This is quite a challenge to the mass spectrometer. The present mission design does not cover the altitude or pressure range where you predict the relatively high and measurable hydrocarbon concentrations. However, we have a chemical enrichment cell in the instrument, and our laboratory tests have shown that we may get a factor of 200 or more enrichment depending on the species. This will be one sample averaged over an altitude of several kilometers. Mass spectrometers have a problem, particularly when they are operated in hydrogen, of generating their own hydrocarbons up to the C_3 level, which effectively lowers the detection threshold for these species. So in the direct measurement mode, without the enrichment cells, we will be below the detection threshold of the instrument, but with the enrichment cells we have a chance to see some of the species. However, we will not have any altitude resolution.

DR. ORTON: The Stony Brook group and I are reporting a detection of propane over the infrared bright region in the northern hemisphere in the Voyager IRIS data.

DR. ALLEN: I was in fact talking with Ken and Richard Wagener about those results and interestingly enough, the fact that you see these species in the North Polar region may not be a function of unique chemistry there, but may be an observability factor. When you are looking from Ken's point of view, the contribution level of the atmosphere that you're seeing near the pole is much higher than it is when you're looking towards the equatorial regions. If you remember, our profiles show a maximum in the stratosphere rather than a constant mixing ratio. That means that if you're looking up at <10 mb, you have sensitivity for these various species that I'm talking about. When you're looking more at the 20 mb level corresponding to observations at lower latitudes, you have less sensitivity. So it may turn out that in fact there is nothing funny in the chemistry at the poles that makes propane more abundant; it may be which level in the atmosphere you're observing.

NON-SOLAR NOBLE GAS ABUNDANCES IN THE ATMOSPHERE OF JUPITER

Jonathan I. Lunine
University of Arizona

David J. Stevenson
California Institute of Technology

The presentation by Lunine and Stevenson is largely contained in a paper appearing in the *Astrophysical Journal Supplement* (1985; 58, 493-531). The abstract of the conference presentation along with the discussion following that presentation is reproduced here.

We assess the possibility that the ratios of noble gases in the atmosphere of Jupiter, which will be measured by the Galileo Probe, could test the hypothesis of massive early bombardment of the planet by outer solar system planetesimals. It has been suggested (Stevenson, 1982, Lunar Planet. Sci. Conf. Abstract XIII, p. 770) that the two-fold enhancement of carbon relative to solar in the atmosphere of Jupiter (Gautier et al., 1982, Astrophys. J. 257, 901-912) might be due to the accretion of several Earth masses of cometary material on the planet. This material could contain carbon as CH_4 or CO ices or as these gases enclathrated in water ice. Temperatures and pressures in the environment of the accreting Jupiter (Lewis, 1974, Science 186, 440-443) were probably not conducive to the formation of methane clathrate or solid methane; hence the initial supply of methane in the Jovian envelope would have been gaseous and presumably solar in abundance. Doubling the gaseous methane abundance implies dredging >2 Earth masses of CH_4 from the core, an unreasonable quantity if the core material did not originally contain CO or CH_4 clathrate. Alternatively, if the enhanced carbon were derived from clathrate-bearing planetesimal debris, the noble gas signatures would be distinctive, with the ratios of xenon/argon and krypton/argon enhanced, and neon/argon depleted, relative to solar values. Moreover, with the possible exception of Ne/Ar, these ratios will not be altered by chemical partitioning at high pressures in the planet (Stevenson, 1985, Lunar Planet. Sci. Conf. Abstract XVI). The noble gas abundance ratios as a function of total carbon enhancement in the Jovian atmosphere are presented based on the above model. Application is also made to the other giant planets which may have incorporated clathrate in their cores. Challenges to the model, such as the recently determined depletion of water in the atmosphere of Jupiter (Bjoraker, 1985, this conference), are also discussed. Measurements of noble gas abundance by the Galileo Probe may provide a test of this hypothesis against others which do not involve clathrate as the source of carbon.

DR. LANE: I had a question, Jon. Do you have some feeling for the altitude distribution in the half bar to three-or-four bar region for this enhancement?

DR. LUNINE: Well, as long as one is looking at the convective region, which is the region that you are talking about, one would expect the noble gases to be well-mixed, as would all gases that are not going to be condensed. In fact, noble gases should be uniformly distributed through the deep interior of Jupiter with the possible exception of neon. Some work done recently by Stevenson suggests that in fact neon may precipitate out in the deep interior. As far as these other gases go, the mixing ratios are sufficiently small that they are carried along in the well-mixed convective zone, so the mixing ratio should be uniform.

DR. POLLACK: I'd like to take issue with you, Jonathan. One of the basic points you made was that in the place where Jupiter formed, one would not expect carbon present in the condensed phase except as a clathrate. This is fine up until a certain point, but we know that there are meteorites which are very rich in carbon, and there is a strong suspicion that many of the asteroids in the outer asteroid belt are very rich in carbon. There is some evidence that the irregular satellites of Jupiter, which presumably were captured in its early history, are also very rich in carbon. All those things would raise some questions about the assumption you made.

DR. LUNINE: I agree that carbon may be present in a meteoritic component that could be incorporated in the core of Jupiter. However, the enhancement of carbon that one sees in the atmosphere, if it extends throughout the interior, is quite substantial and is in fact 10 percent or more of the total mass of the core. One would therefore have to contemplate dredging up, or introducing in some way into the atmosphere, an amount of carbon that is essentially equal to, or perhaps a fifth of the abundance of the rock. That's a lot of carbon, even for meteorites. But I agree in principle that that is one possible source.

DR. POLLACK: Two points are relevant. One, carbonaceous chondrites have carbon abundances that go anywhere from 1 to 20 percent, so in that sense you're not in an implausible range. Secondly, and perhaps more importantly, if you think in terms of plausible models of how the outer planets formed, namely, the core forms first and then captures the gas, core material comes in as a gas envelope builds up. It's hard to imagine an immaculate process which is going to produce a core first in its entirety, and then suddenly obtain all its gas.

DR. LUNINE: I agree that it won't be immaculate. Noble gases may be enhanced in that case as well. The other thing to think about is whether one gets a very strong D to H enhancement coming in as well in this regards.

DR. ROSSOW: We have time for two more questions.

DR. PODOLAK: I just want to add one more point to what Jim Pollack said. That is that experiments have been done by Bar-Nun in which he has deposited water ice at low temperatures and then allowed methane or CO or N_2 or any

other kind of gas you like to flow around it. He has also deposited them simultaneously. The results are that as long as the water ice is deposited at temperatures below 100 K, you can get large abundances of CO, N_2 or anything you like. It's not a clathrate.

DR. LUNINE: Right, it's adsorbed.

DR. PODOLAK: It's not adsorbed...well, there are several things that go on. If you deposit it at 15 K or 30 K and let it heat up slowly, you'll find that at 30 K you get a big burst of N_2 coming off. That's the adsorbed stuff. When you go to 140 K you get another burst, and that seems to be because the water is going from amorphous to crystalline and releasing some of the stuff that's occluded. Then when you let the water get to about 160 K, it starts sublimating and you then get another release. So there is a substantial amount of volatile gas that could be kept in the water, and you can put it in even at 100 K. So it could be that when you're building up stuff from material in Jupiter's zone—certainly in Saturn's zone, you can have a lot of volatile gases there.

DR. LUNINE: Yes, you also have to remember though that the ratio of carbon to the bulk species has to be on the order of 10-20 percent, otherwise you have to put an amount of water and rock in that is a ridiculously large mass.

DR. PODOLAK: That's no problem.

DR. LUNINE: That's satisfied for clathrate. It may be satisfied as well for certain adsorption processes which have a large adsorbing surface area. It's also satisfied for carbonaceous chondrites, as Jim Pollack correctly pointed out. But it does have to be a fairly large abundance of carbon. They have to be, in some sense dominated by carbon.

DR. PODOLAK: It is. It varies with conditions, but it can be much more than you get for clathrates, so that's not a problem at all. You can get 20 percent easily.

DR. HUBBARD: The other possible test of this model would be to compare the abundance of methane in the atmospheres of Jupiter and Saturn. The Jupiter hydrogen envelope is about 4 or 5 times as massive as the hydrogen envelope of Saturn. If one could predict the flux rate of these carbon-bearing planetesimals into both bodies, one could then compute the dilution factor. It seems to me that that's something that could be modeled and maybe should be checked.

DR. LUNINE: Well, the other thing is that when one gets out to Saturn and actually more so for Uranus, the core size is more comparable to the envelope size, and dredging may therefore be a more important process. Also, one may get clathrate formation in the ice out at that distance. So the carbon could be very much enriched in the core, and then whether it actually comes out or not depends on how efficient one regards the dredging process to be.

THE CASSINI MISSION

Tobias Owen
State University of New York at Stony Brook

This is an interim report on an assessment study of a Saturn-Orbiter plus Titan-probe mission. The study was jointly undertaken by the European Space Agency (ESA) and NASA in response to recommendations from a committee established by the European Science Foundation and the U. S. Space Science Board. This committee relied in part on earlier work by European and U.S. scientists.

The NASA Solar System Exploration Committee (SSEC) had recommended two separate missions to the Saturn system, in keeping with its charter to design low-cost, dedicated planetary missions. These were a Titan probe, to be carried by a small spacecraft that would include some type of radar mapping device, and a Saturn Orbiter that would be a more sophisticated spacecraft, to be launched separately. This proposal became part of the SSEC Core Program of missions planned to occur before the year 2000. A competitive plan, to fly a duplicate of the Galileo spacecraft (including a Saturn probe) to Saturn had floundered because of budgetary considerations. At about this time (fall of 1983), a group of European scientists led by D. Gautier and W.-H. Ip had proposed to ESA to combine a Saturn orbiter and a Titan probe in a single mission that would be carried out in collaboration with NASA. Each agency would assume responsibility for one of the major components. It is this proposal, called the Cassini Project, which was approved by NASA and ESA in January 1984 for an assessment study to be carried out over the next year and a half.

Obviously, to do better than Voyager did at Saturn, we must either get more specialized or more sophisticated, or both at once if we can possibly do it. Having recovered from the extreme conservatism that dominated mission planning in the early stages of the SSEC work, the Cassini Science Study Team perhaps went overboard in assembling a strawman payload. That meant adding instruments that Voyager didn't have, and taking instruments that Voyager did have and making them better, or more suited to the Saturn-Titan system. We certainly wanted to fly a radar in order to study the surface of Titan through the satellite's ubiquitous aerosol cover, and to do much better studies of the rings. We can get closer to the various components of the system by using an orbiter, and we can do so several times. Of course the probe of Titan's atmosphere is an enormous step forward. We can spend up to four years in a series of orbits around Saturn, exploring much more of the magnetosphere than Voyager could. This would include measurements from orbits at high inclination angles. Yet we must keep expenses down. This requires collaboration between at least two partners to divide up the cost of the mission.

The Cassini Project is easy to divide. NASA is taking on the commitment to build the orbiter, which will be one of the new Mariner Mark II spacecraft the agency is planning. The Europeans are building a new lightweight probe, especially configured for the atmosphere of Titan. Europeans and Americans

will share in the experiments to be included in both the probe and the orbiter in various ways that have not yet been formally defined.

At the present time, the launch date is set for 1994, with a Delta-Vega trajectory that leads to arrival at Saturn in the year 2002. This puts a strain on most people's calendars, but that's the best we can do if everything goes exactly as planned at present. (Since this preview was presented in May 1985, the Assessment Study was completed on schedule in June. Copies may be obtained by writing to Mr. John Beckman at JPL. The formal evaluation of this study by the ESA review panels occurred in January 1986. The panel recommended initiation of a Phase A study in January of 1987.)

A list of the people involved in the Study is given in Table 1. In addition to these individuals, we have invited a number of other scientists to attend our meetings in Europe and in the U. S. The spacecraft configuration is still being changed in response to science and engineering requirements. A major driver for the orbiter is to achieve overall compatibility with other Mariner Mark II missions. The June 1985 version of the spacecraft is shown in Fig. 1.

Table 1

Participants in Cassini Assessment Study

ESA	NASA
G. Haskell	W. Piotrowski
D. Gautier	T. Owen
W.-H. Ip	M. Allison
S. Bauer	J. Cuzzi
M. Fulchigoni	D. Hunten
	T. Johnson
	H. Masursky
	R. Samuelson
	E. Sittler
	F. Scarf

Unlike the Jupiter system that Galileo is visiting, Saturn has only one large satellite, so the spacecraft repeatedly encounters Titan to "power" the orbital tours. We get over 20 encounters with Titan at about 1000 km, so we can actually use the orbiter as an upper atmosphere probe. Therefore, the aeronomy instruments will be on the orbiter rather than on the probe. We'll also get two close encounters with Iapetus and frequent close visits to the interesting inner satellites. Radar mapping of Titan is one of the key experiments being proposed for the orbiter. The level of sophistication of this device is still being studied. The magnetospheric scientists would like the orbiter to move up to a high inclination orbit toward the end of the nominal four-year mission.
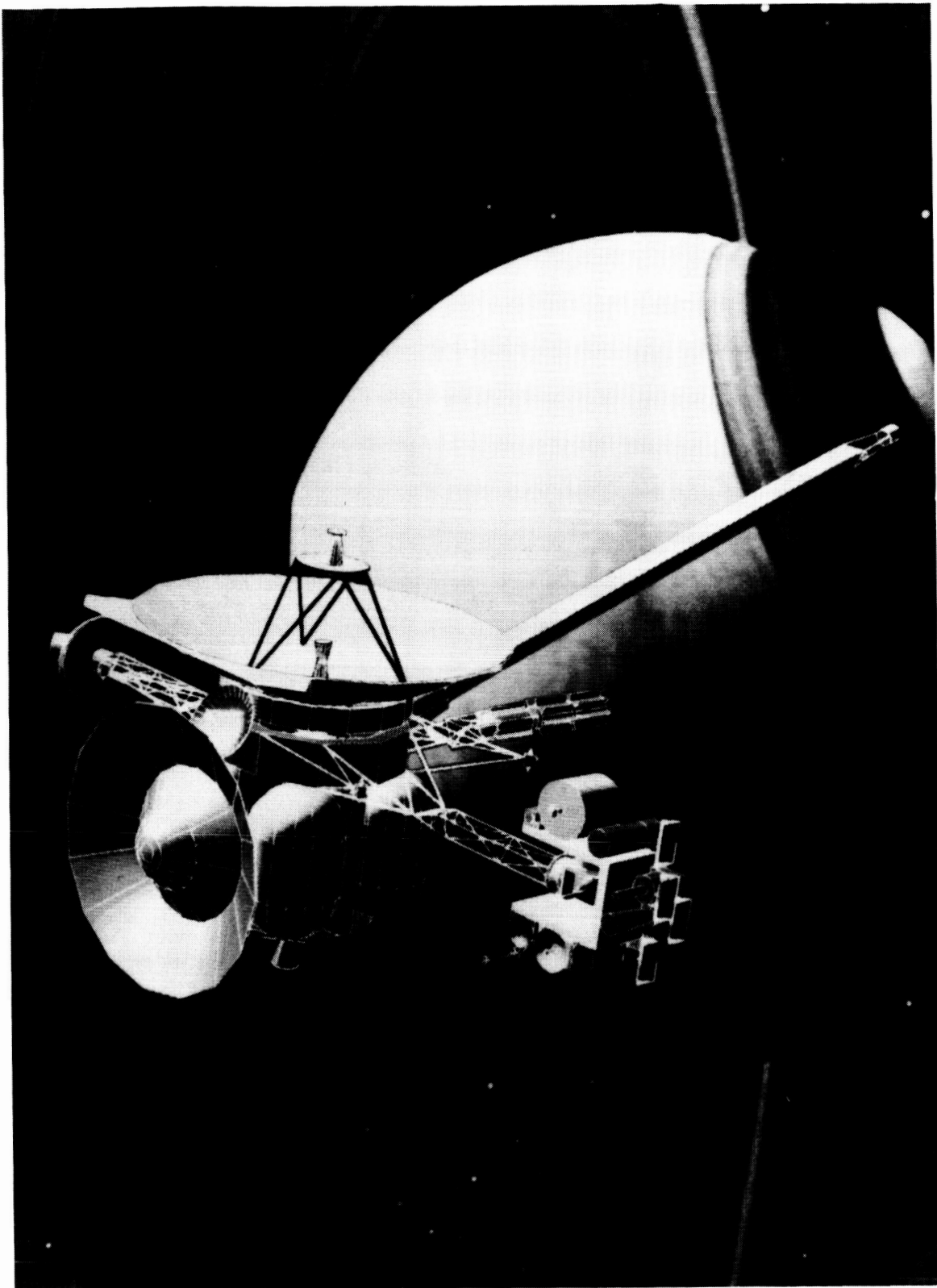
Figure 1.   The configuration of the Cassini spacecraft as of December 1985.

DR. HUNTEN: I think planetary people would like a high inclination too.

DR. ALLISON: But not in the magnetotail.

DR. OWEN: The consensus of the group is remarkable as you can see. The Titan probe entry and descent is very different from the Galileo entry probe profile. We have nearly four hours of descent time through Titan's atmosphere, which means that one can capture samples and analyze them almost at leisure. There are proposals for imaging in the near infrared, and possibly with radar as well. The probe will land or splash-down at relatively low velocities, 3 to 4 meters per second. Byron Swenson, who has worked this out, says the impact is similar to a drop from a height of 18 inches on Earth. So if you can jump 18 inches, you'll find out what the impact on Titan will be like.

DR. HAPKE: Can the probe float?

DR. OWEN: The probe can indeed float. A quick study of the splash-down indicates that the probe would be completely submerged on impact, but would then bob up to the surface. However, immersion in this 94 K ocean poses a tough thermal problem, and no effort is being made to solve it. The guidelines we're working with are that surface science must not drive the mission, but if the probe can carry out some useful measurements after the landing with no extra effort, it will certainly do so.

Figure 2 provides an idea as to what the satellite encounters are like. It is based on a presentation by Walter Flury of ESOC for one of the orbital tours that has been studied. Voyager 1 and Voyager 2 miss distances are compared with Cassini. It is apparent that except in the case of the Voyager 1 encounter with Titan, we get much better satellite encounters than Voyager was able to achieve. And we get more of them. In place of Voyager's single, intensely interesting Titan encounter, Cassini will provide over 30 such visits.

Highlights of the proposed orbiter payload include the fact that we are insisting on both a long-focus and a short-focus camera in order to provide adequate resolution at various distances. The radar is very much under discussion, and there is a battery of infrared instruments which is also not yet well-defined. More detailed definition of these instruments will be a prime early task for the Phase A studies. What are the trade-offs between using a microwave radiometer to study Titan's surface, and using the radar instrument? What combination of infrared instruments gives the greatest amount of information about the atmospheres of Titan and Saturn? And so on.

Most of the instruments on the probe have been flown before. There is a proposal to try to combine a gas chromatograph and a mass spectrometer, but this requires careful evaluation. An aerosol collector should be included as one of the inlet systems for this instrument if its efficacy can be demonstrated. Imaging on the way down, perhaps combined with some new infrared capability is also under review. Just to give a feeling for what kind of "free" surface science can be done, note that a GCMS on a probe that lands in an ocean can do some pretty nice experiments just by having a suitably designed, heated inlet.

234
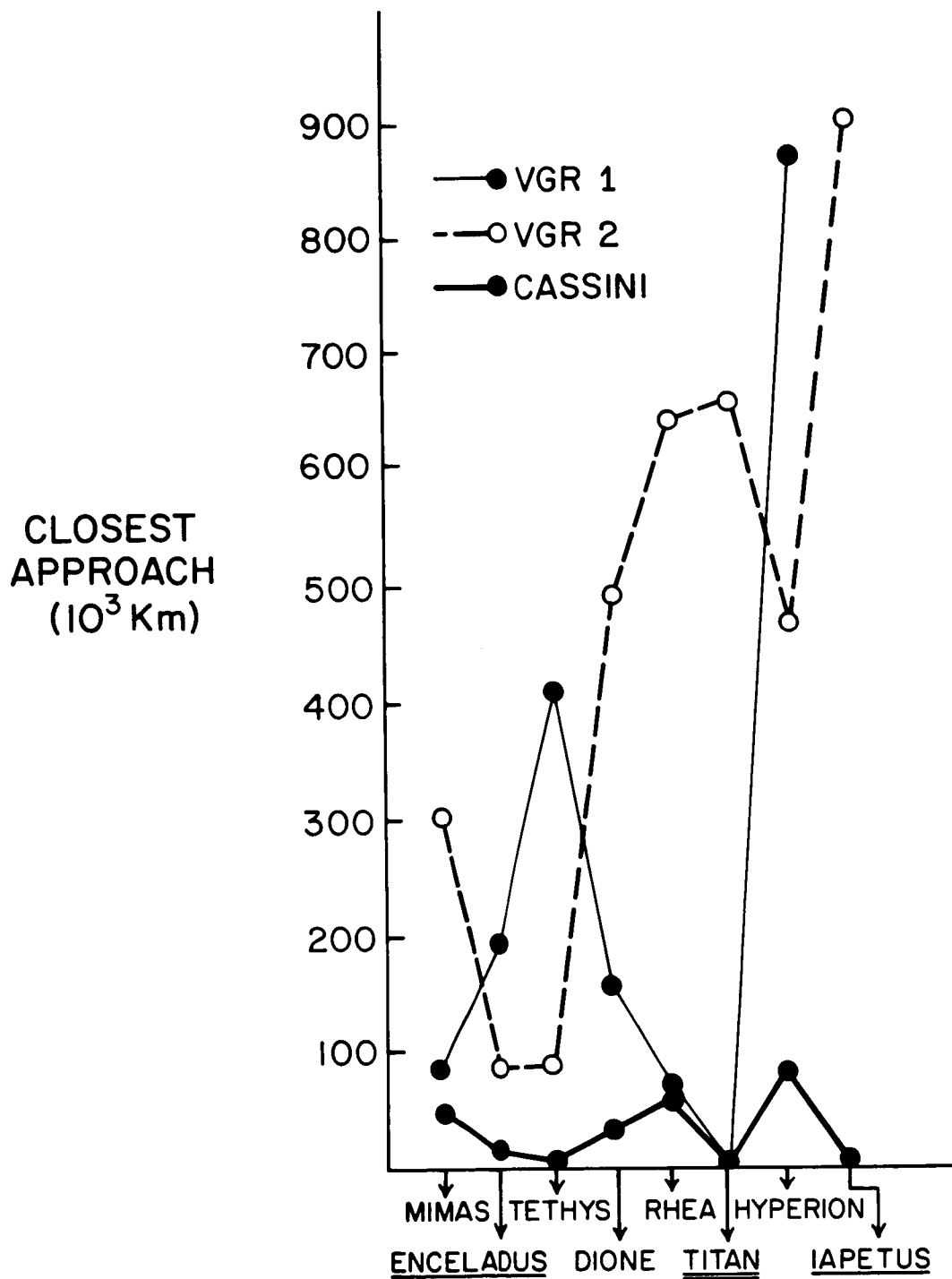
Figure 2. A comparison of flyby distances in the Saturn system for
Voyagers 1 and 2 and the Cassini Orbiter.

The four-year lifetime of the orbiter mission means that there will be an opportunity to do quite a lot of surveying on various aspects of this system. We expect many new phenomena to be discovered, since the Voyager encounters were very brief. The details of the tour have not been worked out, but we are very, very early in the design of the mission and orbital tours are one of many aspects that will receive lots of additional study in the years ahead. I am sure that many readers of this short report will become participants in the future studies and in the mission itself, if it is approved. All suggestions for improving the science return from this exciting enterprise will be very welcome.

DR. ROSSOW: We have time for a few comments.

DR. HUNTEN: Let me make one comment about the prospects. A couple of weeks ago the meeting of the Space Science Board was attended by ESA top management—namely the Director General and the Scientific Director. They seemed to be taking it for granted that the Cassini study is going to go into Phase A. They don't even regard it as an issue.

DR. POLLACK: I'd like to make a couple of quick comments on something that's germane to Cassini as well as some other missions, and has to do with the possibility of gaining very significant meteorological information by measuring horizontal winds by Doppler tracking of the probes. Some of you may know that I've been working very hard in terms of examining the feasibility of this for the Galileo probe. The good news is that if we can do it for Jupiter, and I am optimistic that we can, then it's much easier to do so for the other planets including Saturn, Uranus and Neptune as well as for Titan. I just want to quickly give people a feeling for what the status of that is. First, why is measuring the horizontal winds as a function of altitude by Doppler tracking of the probe important? The point is that depending upon whether the winds are driven by deep convection as Andrew Ingersoll indicated, or driven by water condensation or solar energy deposition, you have distinctly different altitude profiles for the resulting zonal winds. Consequently, there is a significant amount of useful information to be gained for any outer planet or any satellite that has an appreciable atmosphere by Doppler tracking a probe. In the case of Galileo, the reason that this is such a tremendous challenge is that unless you know quite accurately what the longitude of the probe is (and 1 degree is really not good enough because of the large rotation), you may potentially have a serious problem in determining the wind profile. In the case of Saturn and even more so for Titan, it would be a somewhat easier situation. Even in the case of Galileo going into Jupiter, we are optimistic that we really can recover wind information. Work that I've done with David Atkinson at Ames indicates that given significant probe uncertainties in longitude for even a relatively difficult test case profile, we would in fact have been able to obtain a very good recovery on wind profile and the longitude of entry with a linear least squares technique. The bottom line is that we think Doppler tracking of probes has something very relevant to offer in terms of putting good constraints upon dynamical theories of Jupiter, Titan, Saturn and the rest of the outer planets.

236

DR. BELTON: I was very glad to see that you have two cameras, i.e., complimentary optical systems on Cassini. I hope that you will pursue this, and maintain this right through the whole exercise.

DR. OWEN: That was the voice of Galileo imaging, which was unfortunately denied the possibility of two cameras through budgetary constraints. It is certainly our intent to maintain this dual camera capability, if at all possible.

THE VOYAGER ENCOUNTER WITH URANUS AND NEPTUNE

Ellis D. Miner
Jet Propulsion Laboratory, California Institute of Technology

Most of you have seen, I believe, the previews of coming attractions that were developed during the Saturn encounter to show the Uranus and Neptune encounter geometries. I would like to show the film clip again just to remind you of those geometries before I start discussions of what it is that we plan to do during the Uranus and Neptune encounters. Let's run the movie.

You notice that Voyager 2 approaches Uranus at a relatively low phase angle and high southerly latitude. Only when the spacecraft is very close to Uranus does the geometry change appreciably. Most of the important observations occur within six hours of closest approach. Voyager flies through an earth and solar occultation zone and leaves Uranus at a relatively high phase angle of about 145 degrees. We don't have much opportunity to look at the equatorial region of the planet.

At Neptune, on the other hand, the approach is more nearly equatorial (about 35 deg S lat). Voyager 2 will come much closer to Neptune than to any of the other gas giants as it skims within about 2000 km of Neptune's cloudtops. It will pass through earth and solar occultation zones at both Neptune and its satellite, Triton. Again, Voyager 2 will leave Neptune at about 35 deg S latitude. That completes the film clip.

The operational instrument complement aboard Voyager 2 has not changed since launch (see Table 1). However, there is one change in personnel. Robbie Vogt has found his duties as Provost of Caltech to be such that he cannot continue as Principal Investigator, so Ed Stone has been officially named the Cosmic Ray Principal Investigator for the Uranus and Neptune encounters. He'll carry a dual role as both Principal Investigator and Project Scientist.

DR. POLLACK: Does he argue with himself?

DR. MINER: He argues with himself on occasion. Actually, we've had notably little argument with the Cosmic Ray experiment, because it has almost no interaction with any of the other experiments. Ed's dual role works out pretty well.

Let me briefly recount the past and future Voyager encounters illustrated in Fig. 1. Voyager 1 completed its planetary mission with the Saturn encounter in November of 1980. It is leaving the solar system at an angle of about 35 degrees above the ecliptic plane. It will not come close to any of the other planets, but it is headed in approximately the direction of the incoming interstellar wind. Voyager 2, on the other hand, encounters Uranus on January 24, 1986, and will continue on to an August 1989 encounter with Neptune. The timing of the Neptune encounter has been changed slightly from our earlier plans. Voyager 2 will now arrive on August 25th at 0400 UT. Of course, it will be August 24 in the United States.
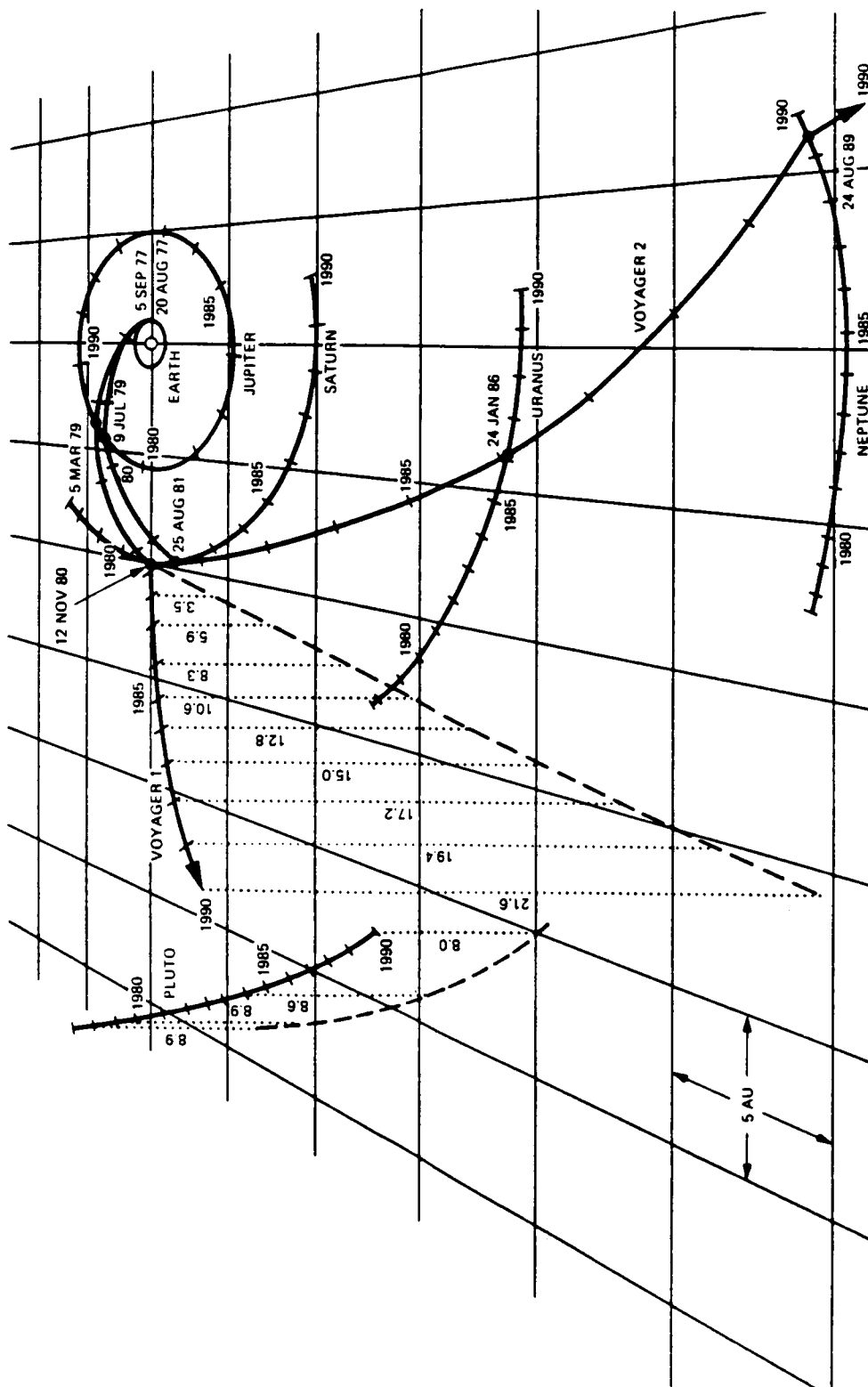
Figure 1. Interplanetary trajectories and planetary encounters
of Voyagers 1 and 2

Table 1

Voyager Science Investigations

Investigation	Principal Investigator/Organization
Imaging Science	B. Smith, University of Arizona (Team Leader)
Infrared Spectroscopy and Radiometry	R. Hanel, Goddard Space Flight Center
Photopolarimetry	A. Lane, Jet Propulsion Laboratory
Ultraviolet Spectroscopy	L. Broadfoot, University of Arizona
Radio Science	L. Tyler, Stanford University (Team Leader)
Magnetic Fields	N. Ness, Goddard Space Flight Center
Plasma	H. Bridge, Massachusetts Institute of Technology
Plasma Wave	F. Scarf, TRW
Planetary Radio Astronomy	J. Warwick, Radiophysics, Inc.
Low-Energy Charged Particles	S. Krimigis, Johns Hopkins University
Cosmic Ray	E. Stone, California Institute of Technology

Small adjustments have been made to the trajectory of Voyager 2 at Uranus. The spacecraft is now following a path that will bring it within 29,000 km of Miranda. The best imaging will be done at a range of about 30,000 km. I will not say more about the satellite science planned for this encounter; nor will I talk about the ring science. I intend to spend the remainder of my time talking about those observations that have to do with the planet itself: either the atmospheric observations or those observations that provide information about the interior.

Voyager 2 will pass through an occultation zone that includes both Earth and Sun occultations. Within a couple of hours after Uranus closest approach, the spacecraft will enter the occultation zone at a rather oblique angle, resulting in a substantial difference in range between entrance and exit occultation measurements.

As the movie illustrated, the subspacecraft latitudes are near 70 deg S (IAU convention) during Voyager 2 approach. At 24 hours before closest approach the latitude is 69 deg S; 12 hours before closest approach the spacecraft is still 64 degrees south of the equator. By closest approach, Voyager 2 is 23 degrees north of the equator on the dark side. At +12 hours, we again see a very similar bulls-eye view, but this time of the dark side of the planet.

The trajectory at Neptune is still undergoing some discussion. Final decisions have not been made. The trajectory correction which adjusts the timing of the Neptune encounter occurs in mid-February of 1986, during the latter portions of the Uranus encounter. One remaining concern is that Voyager 2 will cross the equatorial plane inbound at approximately three Neptune radii. Of course, some of the recent measurements indicate that a

ring (or arc) might be located at that distance from Neptune. We will be interested in receiving information on any ring parameters deduced from telescopic observations. It is possible that the trajectory will have to be revised to avoid potential damage to spacecraft instrumentation.

Voyager scientists have been planning for a 10,000 km miss at Triton. If we revert to the 40,000 km originally planned, Voyager 2 will cross Neptune's equator well outside the possible danger zone at three Neptune radii. If we don't have any problems with a ring at that distance, we can target for the 10,000 km miss distance at Triton that we hoped for.

DR. TAYLOR: What will be the criteria for trajectory selection? Can the decision be delayed?

DR. MINER: I think that much will depend on our estimates of the potential dangers at ring-plane crossing. The Triton encounter is of significant enough scientific importance that we do not want to chance damaging the spacecraft before we get to Triton.

The Neptune views from Voyager 2 are equatorial during approach. Because of the very close approach to Neptune the perspective doesn't change much until the spacecraft is very near the planet. Voyager 2 then flies over the north pole of Neptune. Incidentally, this will be the first time for any of the major planets that a spacecraft will fly over an auroral zone (if Neptune has an auroral zone). The fields and particles experiments are looking forward to that particular encounter with great enthusiasm. As the spacecraft recedes from the planet the illuminated south polar region will again be viewable; near-equatorial dark-side observations will also be possible.

As Voyager 2 approaches Uranus and Neptune we plan to do atmospheric dynamics observations, with narrow-angle imaging starting about 2,000 hours before closest approach and continuing until about 50 hours before closest approach. For Uranus, the cameras will see a planet rotating in the field of view with very little change in the latitude/longitude coverage. Voyager 2 will execute a series of time-lapse movies taken at intervals that correspond to improvements of a factor of 1.4 in resolution. Each of the movies is 36 hours in length, providing imaging coverage over two complete rotations of Uranus. These movies should enable imaging scientists to study atmospheric dynamics at a variety of scales. For Neptune, we revert to the class of atmospheric imaging that was done at Jupiter and Saturn; the spacecraft will obtain five-color imagery every 72 degrees of longitude, so that we can create zoom movies for Neptune similar to those created from Jupiter and Saturn imagery.

Near 10 days before and after closest approach to each planet the IRIS field of view is filled by the planet. Infrared observations of the planets at those times will provide two important pieces of information. Firstly, the IRIS data will determine the precise, disk-integrated temperature of both the illuminated and the unilluminated hemispheres. Secondly, the IRIS radiometer will measure the bolometric reflectivity of each planet on the illuminated side. Because of the unusual orientation of its rotation axis, Uranus can be expected to have a heat balance quite different from the other giant planets.

For Jupiter, Saturn and Neptune most of the incoming solar energy is absorbed at near-equatorial latitudes. At Uranus, most of the solar input is presently near the pole. Since the amount of energy is probably relatively constant with latitude for each of the gas giants, a different sort of energy transport is occurring at Uranus than was seen at Jupiter and Saturn, and than we expect to see at Neptune. The ratio of the total emitted energy to the absorbed energy from the Sun has been measured by Voyager at both Jupiter and Saturn, and both planets appear to have substantial internal heat sources. Uranus appears to have little or no internal heat source. One of the purposes of doing the infrared measurements discussed above is to measure (or set upper limits on) the internal heat from Uranus. The internal heat source within Neptune is probably even larger relative to solar input than it is at Saturn and Jupiter.

Some concern has been expressed about the low sensitivity of IRIS at Uranus and Neptune, whether it is capable of making the measurements that need to be made. In the thermal infrared there is really no difficulty; even with a single spectrum, obtained in 48 seconds, IRIS sensitivity is more than adequate. At longer wavenumbers, where the energy is from reflected solar radiation, there is a problem, and IRIS will probably need relatively long integrations in order to be able to determine the chemical composition of the atmosphere.

Accurate heat balance calculations require measurements of atmospheric bright-ness at different phase angles to determine the atmospheric phase functions for Uranus and Neptune. Figure 2 depicts the phase angle coverage planned for the Uranus encounter. The Photopolarimeter and the Wide-Angle Imaging Camera participate in each of these observations, which cover six different phase-angle ranges as indicated by the rectangles. The two curves in the figure represent phase angles at the center of the planet (lower line) and at the illuminated limb (upper line) as a function of encounter-relative time in hours.

The chemical composition of each of these atmospheres is of interest, partic-ularly the abundances of He, C, N, and O relative to H. Table 2 summarizes the current knowledge. Measurements have been made for both Jupiter and Saturn, although the oxygen content in Saturn's atmosphere is still relatively unknown. For Uranus, there have been various estimates of the relative carbon abundance. We think nitrogen is somewhat underabundant, but we really know very little about either helium or oxygen abundances. Neptune's atmospheric composition is thought to be very similar to that of Uranus. Voyager 2 should provide relative abundances of H, He, C, and N. Oxygen will be more difficult to determine because of the low temperatures and the extreme depth of water ice clouds.

The IRIS, UVS, and Radio Science experiments will provide information on atmospheric temperatures from the microbar region down to 2 or 3 bars as illustrated by Fig. 3. At Uranus and Neptune, IRIS covers intermediate pressure levels, the Ultraviolet experiment overlaps IRIS somewhere in the upper portions of the Uranus and Neptune atmospheres, and the Radio Science experiment should extend the pressure-temperature profile down to several bars. At both planets there may be some opacity caused by methane clouds.
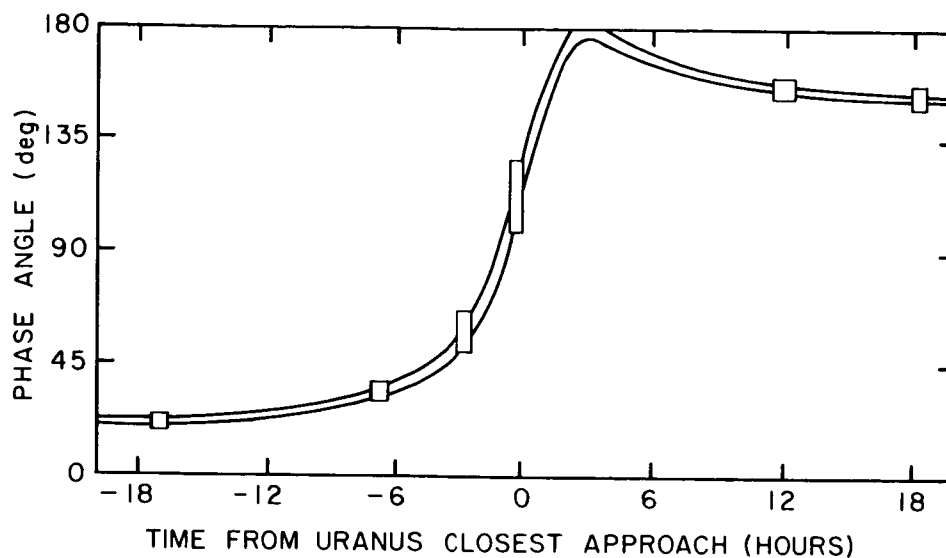
Figure 2. Phase angle coverage of Photopolarimeter and Wide-Angle Imaging Camera observations planned for the Uranus encounter. The six scheduled observation periods denoted by rectangles are shown along with the variation of phase angle of disk center (lower curve) and the illuminated limb (upper curve).
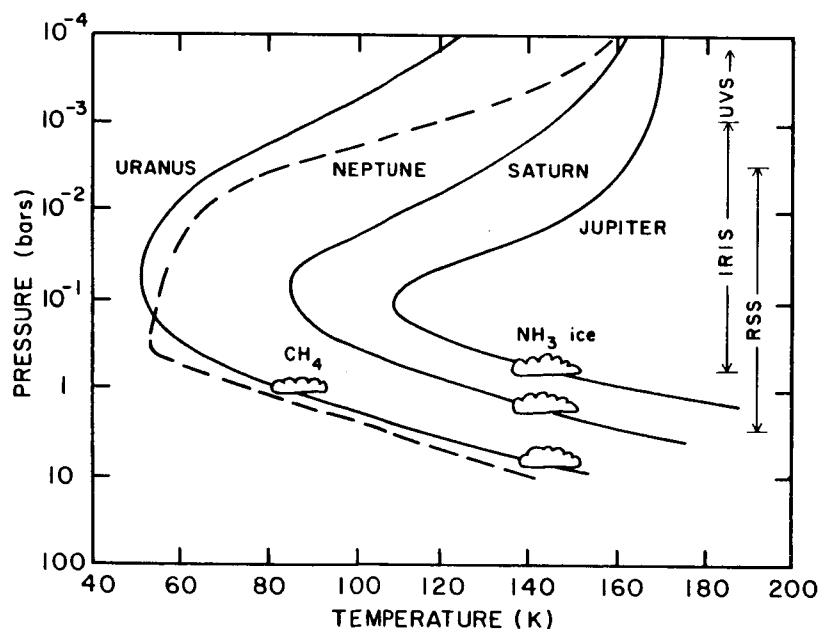
Figure 3. Vertical temperature profiles for the four giant planets and the respective range of vertical coverage by the IRIS, UVS and Radio Science experiments.

243

Table 2

Elemental Abundances for the Atmospheres of the Major Planets

Abundance Relative to Solar

Planet	He	C	N	O
Jupiter	0.87 ±0.18	2.32 ±0.18	1.0 ±0.5	≈0.03
Saturn	0.61 ±0.29	2.1 +1.6/−0.5	≈2.4	?
Uranus	?	1.3−4	<1	?
Neptune	?	0.3−16	<1	?

Radio Science experiments will include earth-based monitoring of the occultation of Voyager 2 by the planet between 2.5 and 4 hours after closest approach. Occultations of the spacecraft by the rings will also be monitored on both ingress and egress sides. We had hoped to be able to do an ultraviolet solar occultation experiment at both ingress and egress of the sun. Unfortunately, at solar egress the spacecraft is still being maneuvered to track the planetary limb for the Radio Science experiment. So we're limited to only an ingress measurement of solar occultation by the UV experiment. There are also two stellar occultations which will be observed using the Ultraviolet experiment; these provide data on the structure of the atmosphere near the polar regions. (The Radio Science and UVS Solar occultation observations are limited to equatorial measurements.) The UVS observes gamma Pegasi, both at ingress and egress, to get the south polar and north polar measurements. It will also observe a grazing occultation by nu Geminorum that will provide better altitude-resolution data for near-equatorial regions of the upper atmosphere.

The spacecraft trajectory for Neptune encounter results in an occultation of the spacecraft by the planet from about 10 minutes after closest approach until about 50 minutes after closest approach. Ingress is near the north pole; egress is slightly south of the equator. If there exists a ring (or arc) near three Neptune radii and it has particles that are centimeter size or larger, then we may observe their effect on the spacecraft radio signals near the time of closest approach to Neptune and again 1.5 hours later.

The internal composition of the planets is also of interest. Inferential information on the internal structure is provided in part by carefully tracking the spacecraft as it flies by the planets in order to determine the detailed characteristics of the planetary gravitational field. The relative mass distribution in the interior of the planet affects both the oblateness and the gravitational harmonic coefficients, so different models of the interior correspond to different allowed relations between oblateness and J_2. Thus, by comparing measurements of the optical oblateness obtained with the Imaging System to the J_2 gravitation harmonic term determined from Radio Science analysis, the range of acceptable interior models can be restricted.

Since the relationship between oblateness and J_2 depends on planetary rotation rate, an improved determination of the rotation period coupled with an accurate estimate of the oblateness and/or J_2 will be particularly useful for inferring internal structure.

Elliot and his co-workers have been able to determine J_2 for Uranus from ring measurements. Their estimated uncertainty of 5×10^{-6} is about six times better than the expected Voyager precision. However, Voyager Imaging and Radio Astronomy experiments should provide a direct determination of the rotation period to a precision far better than any of the present estimates.

For Neptune, the contribution by Voyager will be even stronger. Voyager measurements can improve by a factor of four the precision of J_2 compared to the current estimates. Again, the Imaging and Planetary Radio Astronomy experiments should tie down the Neptune body rotation period fairly well. The rotation period of Neptune has been estimated using ground-based photometry, but photometry is not always reliable. Data from 1980 indicate a reasonably well-defined period on the order of 18 hours, but observations just a year later reveal no clear periodicity.

DR. INGERSOLL: That may not be the observer's fault. It may be that the photometry is simply reflecting changes in the cloud features.

DR. MINER: That's very true. I wasn't implying that the observers didn't use proper techniques. For Neptune sequence development, we are planning to use a period of 17.8 hours, which is consistent with the recent photometry and CCD imaging estimates. However, note that present determinations of J_2 and optical oblateness imply a period of 13.7 hours. It is possible that the recent CCD and photometric measurements are overly influenced by rapid cloud motions and may not measure the true body rotation rate.

Also of interest for internal composition of the planets are the magnetic field measurements. The current estimate of the Uranus magnetic field is based on the Lyman alpha flux. IUE observations show an excess of about a kilorayleigh of Lyman alpha radiation coming from Uranus. IUE observers interpreted this Lyman alpha emission as auroral activity, which implied that Uranus possesses a magnetic field. The estimated intensity of Lyman alpha radiation from Uranus corresponds to 0.5 to 3×10^{12} W of power in such an auroral emission. Only an upper limit exists for possible auroral emissions from Neptune. Based on thse estimates, Voyager scientists predict that if the planet possesses an iron core, Voyager 2 should encounter the magnetopause between 9 and 19 Uranus radii. For Neptune, the number would be in the range of 10-22 Neptune radii. If an ice layer is the source of the magnetic field, then the numbers would be somewhat larger. So, for example, we would expect Voyager 2 to encounter the Uranian magnetopause somewhere around 20 hours before closest approach; the outbound magnetopause probably would occur several days after closest approach.

Voyager 2's closest penetration into the magnetic field at Uranus occurs fairly near the time of closest approach of the planet. Voyager 2 will penetrate the field down to an L-shell of just under 4.5. Miranda's orbit is at an L-shell of 5.1; Voyager would cross that L-shell about an hour before

closest approach and again near the moment of closest approach. The known rings are well inside the spacecraft trajectory. At Neptune the spacecraft goes very near the pole of magnetic field space (assuming the magnetic field is aligned with the rotation axis). Field penetration is down to a minimum L-shell of 2.45 Neptune radii inbound; outbound it will be a little further out. That summarizes the Voyager atmospheric investigations of Uranus and Neptune.

DR. BELTON: I was just wondering, does this ring around Neptune really exist? I haven't seen anything. What's the story?

DR. HUBBARD: Yes, the ring really does exist, except that it's not a complete ring. The information suggests that 90 percent of the time we're in no danger of getting an occultation from the ring; so 90 percent of the time it isn't there. Whether it's intermittent in time or space, we don't know at the moment. We had a very clean detection last year.

DR. ALLISON: Ever since Monday afternoon I've been wanting to make a remark which I'm finally going to offer now, because I think it's relevant to this session. We've all been impressed by the work of Gordon Bjoraker on the five micron data and its implication of low water abundance at the IR sounding level on Jupiter. I think it's important to remember (and Bill Rossow could say this better than I can) that if Jupiter has a strongly water-enriched atmosphere, then condensation will occur at deeper levels than predicted by the canonical models. One can imagine dynamical and microphysical processes which would deplete the saturation vapor curve above the cloud condensation level where we have infrared data. And yet there could still be a massive water cloud at deeper levels in Jupiter's atmosphere. Since this is a session on future space flight opportunities, I just want to say that I hope Hasso Niemann will still do everything possible to calibrate the Galileo Probe neutral mass spectrometer for water. It's been said that the purpose of the Galileo mission is to measure the water abundance on Jupiter. Although that's probably an exaggeration, I think that it is an extremely important measurement for us to keep in mind.

WEDNESDAY AFTERNOON

URANUS AND NEPTUNE

CHAIR: GLENN S. ORTON

THE ORTHO-PARA H_2 DISTRIBUTION ON URANUS: CONSTRAINTS FROM THE COLLISION-INDUCED 3-0 DIPOLE BAND AND 4-0 S(0) AND S(1) QUADRUPOLE LINE PROFILES

K. H. Baines and J. T. Bergstralh

Jet Propulsion Laboratory, California Institute of Technology

The presentation by Baines and Bergstralh is largely contained in a paper which appears in the special issue of *Icarus* (1986; 65, 406-441). The abstract of the conference presentation is reproduced here.

S(0) and S(1) absorptions by H_2 are prominent in Uranus' spectrum, both as broad ($\approx$60 Å) collision-induced dipole features and narrow ($\simeq$0.08 Å) quadrupole lines. The 3-0 and 4-0 bands near 6400 and 8200 Å are useful for deriving atmospheric properties since they are much stronger than higher overtones and occur in regions of relatively weak CH_4 absorptions. Three features seem to be particularly free of CH_4 extinction effects: the 3-0 S(1) collision-induced feature at 8260 Å, and the profiles of the 4-0 S(0) and S(1) quadrupole lines at 6435 and 6369 Å. Current analysis suggests that the distribution of ortho-para H_2 departs significantly from equilibrium on a global scale, with perhaps as much as 60% of the gas being distributed "normally." The interpretation of these data, however, depends strongly on three controversial issues: the line strengths and time constants for the 4-0 quadrupole and 3-0 dipole features, the dependence of the background methane absorption on temperature, and the nature of the aerosol distribution in the Uranian atmosphere. The latter two issues are discussed in particular, drawing upon our experience in modeling other portions of the existing Uranian spectral data set. Our current analysis indicates that an ortho/para distribution wherein approximately 75% of the gas is in the equilibrium state is most consistent with theoretical 4-0 quadrupole line strengths.

DR. BELTON: Could you just go over that hand-drawn representation of the methane band data?

DR. BAINES: Perhaps Bill Smith should describe it. It's his data. My main point was to emphasize the change in character of the 6190 Å band as a function of temperature.

DR. W. H. SMITH: We recently obtained data on the absorption in the region of the 6190 Å methane band using the photoacoustic technique. At present this is all raw data, and it has not been normalized. So there is a baseline slope which is dependent on the detailed conditions of the measurement. At room temperature you get a nice symmetric band shape for the 6190 Å feature after you remove the baseline slope. But when you make the measurement at

cold temperatures, the band changes shape. There are apparently two bands in this region. At the cold temperatures, you lose a lot of absorption on the blue side of the feature, whereas on the red side, it doesn't change very much.

DR. LUTZ: What was the resolution for the spectrum you showed of Uranus?

DR. BAINES: It was 10 Å resolution.

DR. LUTZ: I tried to get a feeling for scale and ask you about this before. The laboratory spectrum is one angstrom resolution. Even at 10 Å, I'm surprised that in the Uranus spectrum you don't see the shoulder evident in the low-temperature lab spectrum.

DR. BAINES: We may be...

DR. LUTZ: Well, the spectrum you showed didn't show it...

DR. BAINES: Well, it's a very steep curve on the spectrum and it's very hard to see...

DR. LUTZ: But Uranus is a low-temperature "laboratory," isn't it?

DR. BAINES: Yes.

DR. LUTZ: So it should have had a low-temperature shape, shouldn't it have?

DR. BAINES: It may be in there, I don't know.

DR. CONRATH: At which levels are your observations most sensitive?

DR. BAINES: Basically what happens is that we are sampling different levels depending on what part of the line profile you look at. A point near the peak corresponds to about 100-200 millibars, whereas out in the wing it is more like two bars. The average line formation is one bar, but it depends on how you want to analyze this. Basically, it's a lot like the infrared where you sample different places in the atmosphere depending on where on the shoulder of a line you are. If you had really high resolution data, it could be used in that way to probe a number of levels in the atmosphere.

DR. MCKINNON: Why did you emphasize the theoretical line profile estimate of $S(1)/S(0)$, as opposed to existing measurements?

DR. BAINES: Well, theoretical line profiles agree pretty well with the other quadrupole lines, 2-0, 3-0, 1-0. Most of the time they tend to agree. It's only in 4-0 that it seems like the few laboratory measurements have been in disagreement with the theoretical. Those laboratory measurements have been all over the place. The latest ones, at least for $S(1)$, have been in agreement with theoretical. The controversy there is the $S(0)$ measurement, and that's why the ratio, $S(1)/S(0)$ is so different. It's the $S(0)$ line, and there has only been one of those measurements made, by Sue Bragg. There's some speculation that it may be a little off. There's only this one real laboratory measurement of $S(0)$.

250

DR. PODOLAK: Could you just say something about where the aerosols fit in the model.

DR. BAINES: That's constrained by the other parts of the broadband spectrum. Basically, it's wavelength dependent. In this case, the optical depth can go from zero to about 0.75 or so to limits...

DR. PODOLAK: Optical depth? What kind of depth do you have here?

DR. BAINES: Depending on the models you use, basically starting around 700 mb and going anywhere up to--it could be as high as 200 mb, but normal models stop around 400 mb.

C -4

RADIATIVE-CONVECTIVE EQUILIBRIUM MODELS OF URANUS AND NEPTUNE

J. F. Appleby
Jet Propulsion Laboratory, California Institute of Technology

The presentation by Appleby is largely contained in a paper appearing in the special issue of *Icarus* (1986; 65, 383-405). The abstract of that paper is reproduced here.

A study of radiative-convective equilibrium models for Uranus and Neptune is presented, with particular emphasis on the stratospheric energy balance, including the influence of aerosol heating and convective penetration. A straightforward numerical method is employed (Appleby and Hogan, 1984, Icarus 59, 336-366) along with standard opacity formulations and the assumption of local thermodynamic equilibrium. A range of models was considered for Uranus, reflecting uncertainties in observational constraints on the middle stratospheric temperatures. The results indicate that a "continuum absorber" could be significant in the stratosphere, despite Uranus' great distance from the Sun. Also, test runs are presented to illustrate the influence of uncertainties in the gas composition and changes in the effective mean insolation. A longstanding theoretical problem for Neptune has been to explain the unexpectedly high stratospheric temperatures without invoking supersaturation of CH_4. The results show that a "continuum absorber" could contribute significantly to the energy balance within a localized stratospheric region; however, it probably cannot provide enough power to explain the observed infrared spectrum, regardless of its vertical distribution. One alternative is "convective penetration" which could arise if, for example, vertical mixing is so rapid that CH_4 condensation cannot occur before the gas is swept upward, above the condensation region. In the example considered here, the CH_4 mixing ratio in the middle and upper stratosphere is equal to that below the condensation region in the troposphere. The infrared emission from this model was found to be in generally good agreement with the observations. Such a model could also apply to Uranus, in lieu of aerosol or other "additional" heating mechanisms, to an extent that is commensurate with weaker convective uplifting.

DR. ORTON: Could you explain why two of your models seem to be able to fit some of these points, but the third seems not to fit the 150-200 micron region?

DR. APPLEBY: Well there are slight differences in the effective temperatures of these models. Since effective temperatures for Uranus and Neptune carry relatively large error bars (±2 K roughly), I don't constrain the models to produce effective temperature to within tenths of degrees in contrast to what I do for Jupiter. That just means that the flux of the one model is probably

a little bit too high, and it could be brought down a bit by changing boundary conditions.

DR. HUNTEN: You seemed very concerned about those four points at 28-30 microns, which is rather a small spread of wavelengths. They must have error bars comparable to the other point which you plotted there. I don't think you can even say that they are defining a flat curve in any sense whatsoever. If you have four points that close together with typical error bars, the slope is almost unconstrained. You are not required to fit the points. You are required to draw a line through the error bars. That's all I'm saying; it doesn't necessarily define a slope.

DR. APPLEBY: That's certainly true to some extent, but variation of two or three degrees seems to be ruled out.

DR. BELTON: Why don't Orton's points have vertical error bars?

DR. ORTON: The error bars are smaller than the squares representing the observations.

DR. BELTON: Then why couldn't you know what wavelength you were looking at?

DR. ORTON: I think that it's fair to say that those aren't really error bars; they are discrete filters that wide.

DR. LUTZ: You showed the JPL version of the Uranus albedo, but our group at Lowell Observatory published a similar albedo, and showed that the geometric albedo does change significantly with time. What does that do to your matching data from various sources, and to your model?

DR. APPLEBY: I believe you are referring to measurements that indicate a brightening of ≈14 percent in the integrated geometric albedo spectrum, comparing data from 1981 versus 1961-1963 (Lockwood *et al.*, 1983, *Astrophys. J.* 266, 402). The uncertainties discussed here, associated with locating the haze-free continuum in the recent data of Neff *et al.* (1984) correspond to differences (haze-free versus 'observed' continuum) that are two to three times greater than this 20-year secular change.

A MODEL OF THE SPATIAL AND TEMPORAL VARIATION OF THE URANUS THERMAL STRUCTURE

B. Bezard and D. Gautier
Observatoire de Meudon

Seasonal variability of the temperature structure of Uranus is modeled for all latitudes in the 10^{-4} to 2 bar pressure range in anticipation of the Voyager encounter in January 1986. Atmospheric heating in the model results on the one hand from an internal heat source and, on the other hand, from absorption of solar energy by methane and by non-conservative aerosols located between the 0.5 and 2 bar levels. Various cases for the behavior of the internal heat flux are investigated, such as constant with latitude or constrained to yield a time-averaged thermal emission independent of latitude. Meridional transport of heat in the stably stratified atmosphere is not taken into account. The results indicate that at the Voyager encounter time, very small north-south temperature asymmetry should be expected. Moreover, the northern hemisphere, although not illuminated, should emit as much energy (within one percent) as the southern hemisphere at this date. At a given latitude, extreme temperatures are reached at the equinoxes. At the poles, seasonal amplitudes of about 10 K in the upper stratosphere and 6 K at the 0.6 bar level are predicted, and the variation with time of the emission to space is found to be at most 20 percent. The atmosphere of Uranus appears to be characterized by very long radiative response times (mainly due to its cold temperature) which inhibit the large seasonal variations that one could otherwise expect in view of the high obliquity of the planet and its long orbital period.

We have developed a seasonal radiative model for the atmosphere of Uranus. It is in fact an adaptation of previous modeling for Saturn's stratosphere (Bezard and Gautier, 1985). In such a seasonal model, temperature for a given pressure level p and at a given time t is derived from the simple equation:

$$\frac{dT(p,t)}{dt} = \frac{mg}{C_p} \frac{dF(p,t)}{dp} ,$$

(1)

where m is the mean molecular weight, g is the gravitational acceleration, C_p is the specific heat, and F is the net upward flux.

Temporal variation of temperature is then directly related to the variation of the total flux with pressure. The flux consists of two parts: the thermal flux essentially in the far-infrared ($\lambda > 7\mu m$), and the solar flux which is predominantly absorbed in the visible and near-infrared.

To compute the solar heating, we first consider absorption by methane bands (0.45-1.5, 1.7, 2.3 and 3.3 μm groups). Methane is constrained to follow the saturation law in the troposphere above the condensation level, and a constant mixing ratio is assumed above the temperature minimum. We also include deposition of solar flux by non-conservative aerosols located below the 0.5 bar level following the model of Bergstralh and Baines (1984).

The second part of the flux, the part concerned with thermal emission, is calculated through a multilayer monochromatic radiative transfer treatment for wavelengths longer than 7 μm. Calculations incorporate opacity due to CH_4, H_2-H_2 and H_2-He for a H_2 mole fraction of 0.90. This approach is quite different from that adopted by Wallace (1983) to model the seasonal variation of the thermal emission over Uranus' disk. Wallace's model is essentially a grey atmosphere model. Moreover, the use of the Rosseland mean opacity τ_R restricts its validity to deep atmospheric levels where $\tau_R \gg 1$, which corresponds to pressure higher than 1-2 bar.

When the calculated temperature profile is found to be unstable, the tempera-ture lapse rate is set to the adiabatic value, and this criterion then defines the location of the convective zone. On the other hand, the internal heat flux behaves as a lower boundary condition in the calculation of the layer-by-layer transfer of energy. Three different assumptions have been investigated in this work. In the first case (1), the thermal structure in convective layers is not allowed to vary with time or latitude. Some meridional heat transfer thus takes place through the convective zone. In the second case (2), the heat flux is taken to be independent of latitude, and we adopted a value of 70 erg $s^{-1}cm^{-2}$ consistent with ground-based measurements. Such a model does not incorporate any kind of pole-to-equator transport of heat and will yield a thermal emission-to-space which is dependent on latitude. Finally, a third case (3) has been investigated in which a latitude-dependent heat flux is set at the base of the model so that the annual average of the emission-to-space does not vary over the disk. Meridional heat transfer thus occurs in the deep interior. Note that in any case horizontal advection of heat in the *radiatively-controlled* region is not taken into account. The model is also constrained to match some observational constraints: the Bond albedo A_b = 0.35±0.05, the effective temperature as measured from the Earth in 1977-1982 T_e = 58.5±2 K, and a methane abundance CH_4/H_2 $\approx$ 0.03 with large uncertainties.

The solid line in Fig. 1 indicates the synthetic temperature profile corres-ponding to an average over the southern hemisphere—the one which is presently sunlit—and was as well for year 1982.[*] That year, Moseley et al. (1985) made far-infrared measurements of Uranus, and the temperature profile they retrieved is displayed here as a dashed line. It is about 3 K warmer than the theoretical profile in the vicinity of the tropopause. This discrepancy may reveal the need for additional atmospheric heating at these levels, possibly by absorption of

---

[*]This is consistent with the conventional definition which identifies the pole corresponding to the direction of the positive angular momentum vector of rotation for Uranus as the South Pole because that vector direction is less than 90 degrees from the South Ecliptic Pole.

solar flux by dust particles as discussed by John Appleby in the preceding
paper. The model exhibits a temperature minimum located around the 50 mb level
with a very shallow lapse rate in the vicinity (10-100 mb). The temperature
lapse rate reaches the adiabatic value near the 0.45 bar level, but it is
noteworthy that it becomes subadiabatic again at the deepest layers of the
model below the 1.5 bar level. In fact this special feature occurs because at
these levels the solar flux no longer penetrates efficiently so that solar
heating is negligible, and on the other hand the internal heat flux is too weak
to maintain alone an adiabatic lapse rate. However, at even deeper layers
corresponding to high far infrared optical depths, the lapse rate is likely to
be adiabatic again for a non-zero internal heat flux.
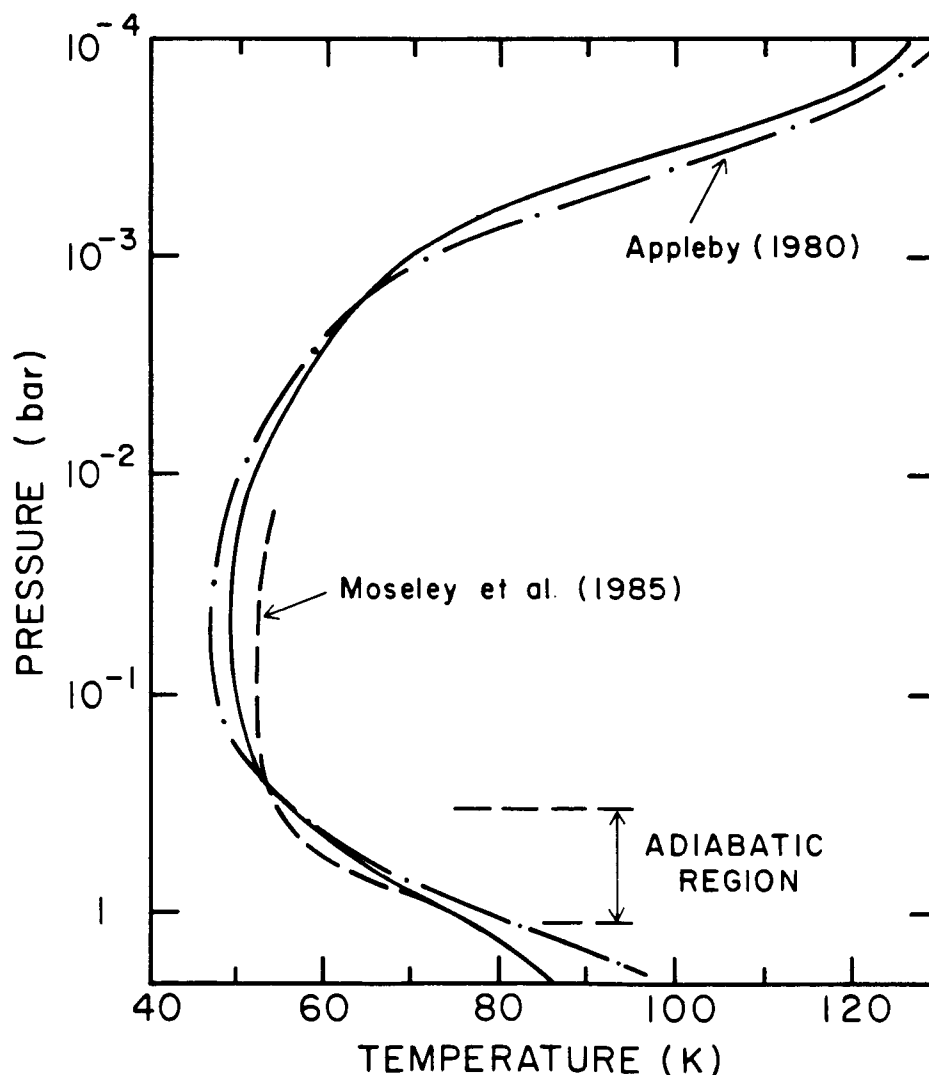
Figure 1. Synthetic temperature profile (solid line)
corresponding to an average over the southern hemi-
sphere compared to the result obtained by Appleby (1980)
and the retrieved profile by Moseley et al. (1985).

When you perform ground-based spectrophotometry of Uranus to determine its effective temperature, a potential error might be introduced in that you measure the thermal emission of the sunlit hemisphere, which may differ from the global planetary emission. We have therefore compared, in the framework of this seasonal model, the actual planetary effective temperature to that measured from the Earth as a function of time. In Fig. 2 the curves labelled 1, 2 and 3 correspond to the above mentioned cases concerning the behavior of the internal heat source. The corresponding dashed lines indicate the expected seasonal variation of observations from Earth as estimated by our model. One can see that, at most, the discrepancy between the "true" and the "apparent" effective temperature is less than 2 K and thus lies within the typical uncertainties associated with ground-based measurements. The maximum discrepancy corresponds to no more than a 10 percent variation in the emitted flux; it is reached at the equinoxes, and in case 1 or 2 at the solstices to a lesser extent. We can then conclude that fortunately the inference of Uranus' effective temperature from ground-based studies is not too strongly biased despite the nature of the planetary seasonal cycle.
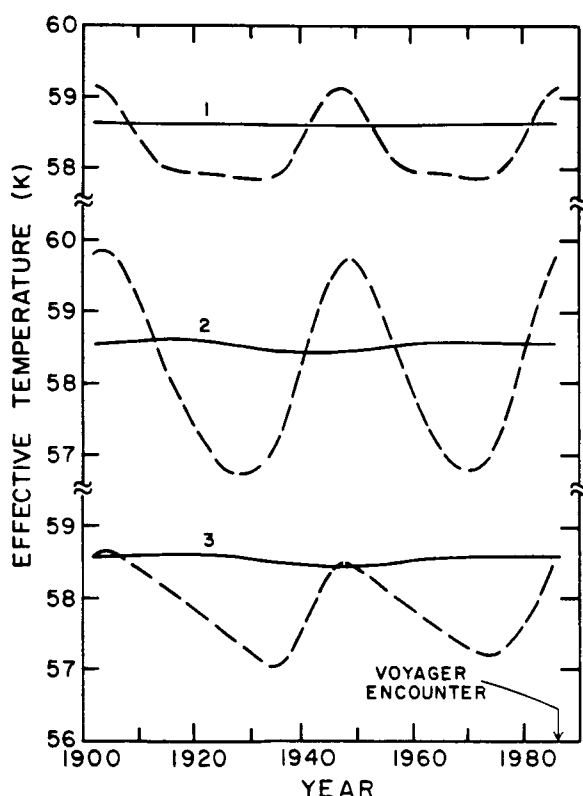
Figure 2. Seasonally dependent effective temperature for cases 1-3. The solid line curve indicates the actual planetary effective temperature, and the dashed line shows that predicted to be measured from Earth.

Figure 3 shows the predicted seasonal cycles of polar and equatorial temperatures for the 0.35 bar level for cases 1 and 2. This level is close to the emission-to-space level. Maximum seasonal variations occur at the poles with amplitudes at 0.35 bar in the range 1-3.5 K depending on the assumed redistribution of heat at deeper levels. Larger seasonal changes, typically 5-10 K, are predicted in the high stratosphere. The variation with time of the emission-to-space is at most 25 percent. At the equator, the 0.35 bar temperature does not vary by more than 0.1 K, and seasonal changes do not exceed 1 K at any atmospheric level. Two important characteristics should be noted. First, the seasonal cycle of the atmosphere is lagging behind the solar heating by approximately one-quarter of the orbital period, so maximum north to south asymmetry occurs at the equinoxes and minimum at the solstices. Secondly, the temporal variations of temperature are indeed very weak in view of the high obliquity of Uranus, its small internal heat source if any, and its long orbital period (84 years). These characteristics result from the very long radiative response time of the Uranian atmosphere mainly due to its cold temperature.

The Voyager 2 spacecraft encounters Uranus in January 1986, only four months after the summer solstice for the southern hemisphere. Because of the phase lag between the insolation cycle and the response of the atmosphere, very small north-south asymmetry should be expected. Within the atmospheric range which will be sounded by the infrared spectrometer IRIS (approximately 0.1-0.6 bar), the difference is expected to be less than 2 K at any level.
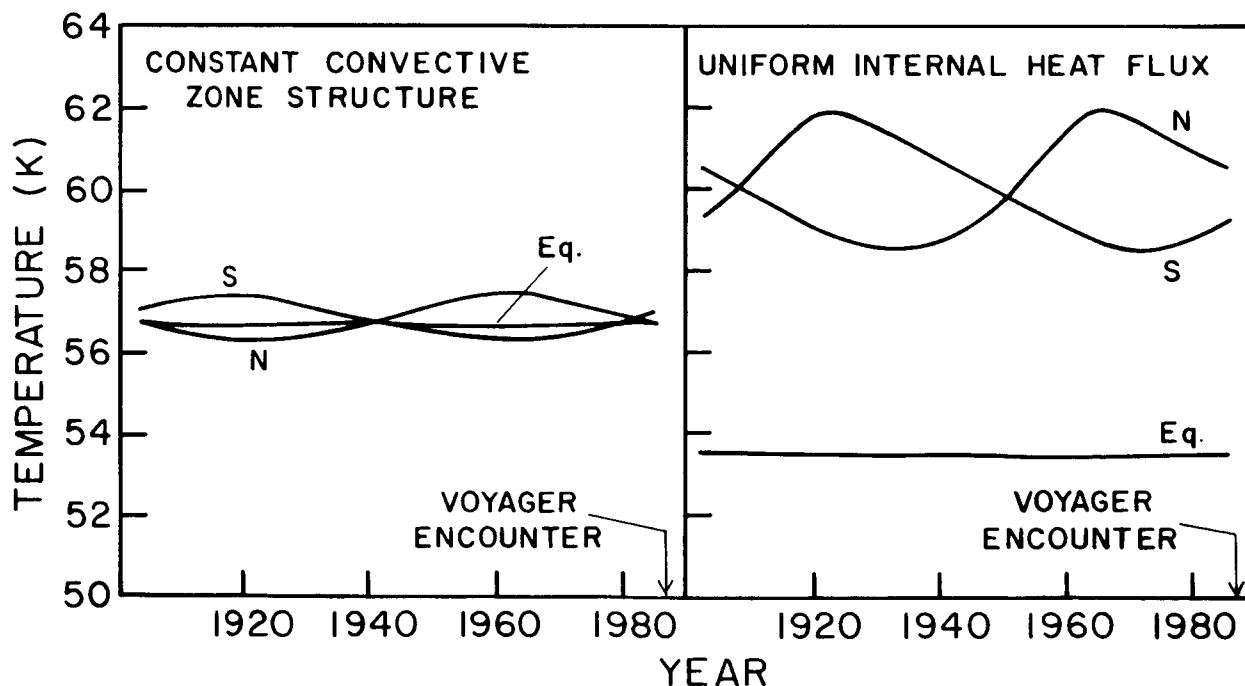
Figure 3. Predicted seasonal cycles of polar and equatorial
temperatures for the 0.35 bar level for cases 1 and 2.

The lack of north-south asymmetry is also illustrated in Fig. 4 where the cal-
culated local effective temperature is plotted as a function of latitude for
the time of Voyager encounter. For any redistribution of heat at deep levels
(case 1, 2 or 3), the two hemispheres are predicted to emit the same amount of
energy within one percent. However, a pole-to-equator gradient as high as 6 K
would result if no redistribution of heat takes place to compensate for the
minimum insolation at low latitudes (case 2). This difference is less than 0.5
K if some transfer of energy takes place in the upper convective layers (case
1) or through the deep interior (case 3). Now, it only remains to be seen
whether seasonal radiative models give a realistic representation of the actual
thermal structure of Uranus. Undoubtedly, the forthcoming Voyager encounter
will give important clues towards the answer to that question.
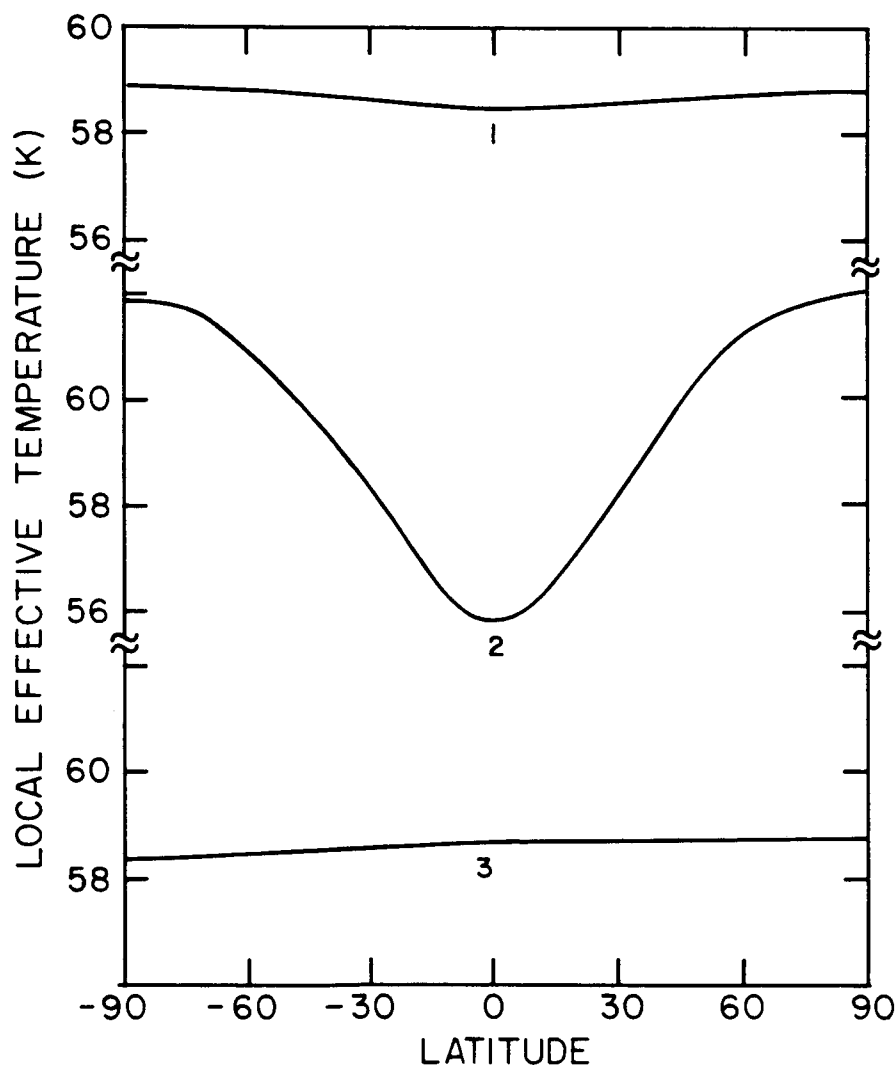
Figure 4. Local effective temperature for the three
model cases as a function of latitude for the time of
Voyager encounter.

REFERENCES

Bergstralh, J. T., and K. H. Baines (1984). Properties of the upper tropo-
    spheres of Uranus and Neptune derived from observations at visible to
    near-infrared wavelengths. In *Uranus and Neptune* (Ed. J. T. Bergstralh),
    pp. 179-212. NASA CP 2330.

Bezard, B., and D. Gautier (1985). A seasonal climate model of the atmospheres
    of the giant planets at the Voyager encounter time: I. Saturn's strato-
    sphere. *Icarus* 61, 296-310.

Moseley, H., B. Conrath, and R. F. Silverberg (1985). Atmospheric temperature
    profiles of Uranus and Neptune. *Astrophys. J.* 292, L83-L86.

Wallace, L. (1983). The seasonal variation of the thermal structure of the
    atmosphere of Uranus. *Icarus* 54, 110-132.

DR. STOKER: Isn't the radiative time constant, even at the levels you are
looking at, longer than the seasonal time scale? How can you get seasonal
variations, or how can you account for that by your models?

DR. BEZARD: Yes, in fact that was the problem. The radiative time constants
are very long at any level. That is why you see only weak variations of
temperature along the Uranian year. We still have some variation because
there is a very long day and a very long night, and also a negligible internal
heat flux.

DR. INGERSOLL: I think you are saying that the big variation in the middle
curve (Fig. 4) is not a seasonal variation at all. It's just the Sun coming
onto the equator and then the pole.

DR. BEZARD: Yes. There is no north to south asymmetry predicted for Voyager
encounter.

VERTICAL STRUCTURE OF AEROSOLS AND CLOUDS IN THE ATMOSPHERES OF URANUS AND NEPTUNE: IMPLICATIONS FOR THEIR HEAT BUDGETS

James B. Pollack and Kathy Rages[*]
NASA/Ames Research Center

Jay Bergstralh, Kevin Baines, and Daniel Wenkert
Jet Propulsion Laboratory

G. Edward Danielson
California Institute of Technology

The presentation by Pollack *et al.* is largely contained in a paper appearing in the special issue of *Icarus* (1986; 65, 442-466). The abstract of that paper is reproduced here.

We have attempted to bound the wavelength averaged phase integrals and bolometric albedos of Uranus and Neptune by fitting a wide range of aerosol model atmospheres to their observed geometric albedo spectra. These models are characterized by an upper haze layer of finite optical depth and a lower cloud layer of infinite optical depth at discrete altitudes. Alternative models differ in the assumed value of the particles' single scattering phase function and the wavelength dependence of the haze optical depth. Phase functions ranging from isotropic to those characteristic of particles in the atmospheres of Titan, Jupiter, and Saturn are considered. We have partially tested the models of Uranus by comparing the dependence of their disk integrated brightness on phase angle with that derived from a combination of ground-based and Voyager 1 data that span phase angles from 0° to 85° and by comparing the predicted shapes of several H_2 quadrupole lines with observed shapes. Predictions of the Neptune models were compared with determinations of the planet's disk integrated brightness from 0° to 48° phase angle.

The derived model parameters lie within useful bounds. In the case of Uranus, the cloud pressure for all 7 models considered falls between 2.2 and 2.5 bars, implying methane mixing ratios in the deeper portion of the atmosphere that are at least 30 times higher than expected from solar elemental abundances if the cloud is interpreted as being a methane condensation cloud. The range of haze pressure (< 0.5 bars) and optical depths (0.06 to 0.6 at a wavelength of 0.6435 µm) imply that haze aerosols are a significant absorber of sunlight and hence constitute a significant heating source in Uranus' upper troposphere and stratosphere. The haze aerosols absorb strongly at both short and long visible wavelengths, unlike the aerosols in Titan's atmosphere.

---

[*]Also at Mycol Inc., Sunnyvale, CA.

Qualitatively similar conclusions apply to our model atmosphere of
Neptune, with the cloud pressure being somewhat higher than for Uranus
(2.7-3.2 bars) and the methane abundance being at least 60 times
higher than expected from solar elemental abundances.

At the current epoch, the wavelength averaged phase integrals of
Uranus and Neptune equal 1.26 ± 0.11 and 1.25 ± 0.1, respectively. The
corresponding bolometric albedos are 0.343 ± 0.055 and 0.282 ± 0.044
respectively. When averaged over an orbital period, these albedos
may be 7 percent lower for Uranus and little altered for Neptune,
based on measurements of their secular brightness variability.
Comparison of these results with thermal observations implies that the
internal heat source for Uranus is less than 0.27 times the solar input
(specific luminosity $< 1.6 \times 10^{-7}$ erg $s^{-1}g^{-1}$), while this value for
Neptune is (1.85 ± 0.56) times its solar input (specific luminosity =
3.4 ± 1.1) $\times 10^{-7}$ erg $s^{-1}g^{-1}$). These results imply that the meteoro-
logical regimes in the observable atmospheres of Uranus and Neptune
may be very different, with internal heat flux playing a much more
important role for Neptune than for Uranus.

DR. APPLEBY: I don't understand how you can come up with tight constraints on
the phase integral for the following reason. Marty Tomasko did some test cal-
culations to help me with the aerosol heating problem, and everything he did
indicated that uncertainties in the phase function of the cloud material in
the troposphere, not to mention variations in the phase function of the haze
particles higher up in the atmosphere, influence the phase integral by as much
as 25 percent at 7000-8000 angstroms. What constrains the phase integral to
the much smaller range indicated in your figure?

DR. POLLACK: Our basic strategy here was to pick a wide range of feasible
single scattering phase functions to range all the way from isotropic to high-
ly anisotropic ones that are typical for Titan, Saturn, and Jupiter. Surpris-
ingly, we did indeed find out that the phase integral has turned out to be
reasonably constrained. I think there are several reasons for that. Number
one, there is a very large contribution from molecular Rayleigh scattering,
and that tends to make the overall effect more isotropic in character than you
would tend to think. Secondly, the differences between the different single
scattering phase functions actually become important only at the largest and
smallest phase angles. So what that means is that when you're computing the
phase integral, much of the contribution comes from the range of phase angles
where you would expect it to be relatively insensitive. For the whole range
of models calculated, our differences were approximately ± 10 percent.

DR. LUTZ: I just want to emphasize something you said to make sure that peo-
ple remember it. When you bootstrap your way with the absorption coefficients
using liquid methane in the centers (and that's what we've got to do), it's
really a little risky; so it's important to remember that we've got to do the
absorption coefficients right at low temperatures. I think that Bill Smith's
cell data shows us interestingly enough that the band centers could shift and
everything. If we don't do it right in the lab, we may be in bad shape.

DR. POLLACK: First of all, I couldn't agree with you more. I really think that the sort of measurements that Bill has been doing is tremendously important, and I must say that I'm very dismayed to hear that he may have a problem in continuing to do this work in the future because of questions about support. I think it's very vital that such work get done. To explain some of the logic behind our approach, let me point out that Larry Giver was kind enough to make some comparisons between his room temperature gas measurements and liquid methane absorption coefficients. It is really incredible, but for almost every band that one makes a comparison, the absorption coefficients are very similar in the band center. So our philosophy was to avoid the wings of bands where you do in fact expect the temperature effects to be the largest and to focus on the band centers where you expect them to be small.

DR. MCKINNON: I take it that the internal heat flux limit you gave of 0.27 times solar does not include the phenomena that the previous speaker, Dr. Bezard, mentioned, where the long-term average and what one measures could be different by several degrees.

DR. POLLACK: Yes, in fact I think that is really one level of sophistication that is going to be needed. Once one has the Voyager data, I think one wants to think very hard about some seasonal effects in terms of the secular variations of brightness to really pin things down. I think Voyager will be very helpful in the sense that it will be the first time that we are able to observe both bright and dark sides.

DR. ORTON: I find it personally very interesting that both you and Kevin Baines independently came up with a methane mixing ratio that evolved into these calculations. To some extent they are independent results. I might ask one question as sort of a follow-up to the results which you described. Is there any constraint given by the level of sophistication of the models that displaces current Voyager observations of Uranus?

DR. POLLACK: I'd like to say two things. First, because I had a limited time, I didn't adequately acknowledge the very important contributions that Kevin has made in this area. Many of the qualitative conclusions we came to in terms of cloud pressure bounds and in terms of absorption in the near infrared, were really first made by Kevin's modeling, and we should acknowledge him for that. In terms of bounds by Voyager at present, our original thought was that now that we have some phase angle data, we can really start eliminating some of the models. In fact, when you're at intermediate phase angles, that's the time when you have the least discriminability among models. So in retrospect, it would have been nice if Voyager data had covered more diagnostic phase angle ranges. That's water under the bridge, and I think the good point is that the encounter will really give us phase angles in the ranges where we do have discriminability.

ON THE OBLATENESS AND ROTATION RATE OF NEPTUNE'S ATMOSPHERE

W. B. Hubbard
Lunar and Planetary Laboratory, University of Arizona

Recent observations of a stellar occultation by Neptune (Hubbard et al., 1985, Astron. J. 90, 655-667) give an oblateness of 0.022 ± 0.004 for Neptune's atmosphere at the 1-microbar pressure level. This result is consistent with hydrostatic equilibrium at a uniform atmospheric rotation period of 15 hours, although the error bars on quantities used in the calculation are such that an 18-hour period is not excluded. The oblateness of a planetary atmosphere is determined from stellar occultations by measuring the times at which a specified point on immersion or emersion occultation profiles is reached. We critically evaluate whether this standard procedure for deriving the shape of the atmosphere is consistent with what we know about vertical and horizontal temperature gradients in Neptune's atmosphere. We then consider the nature of the constraint placed on the interior mass distribution by an oblateness determined in this manner, considering the effects of possible differential rotation. A 15-hour Neptune internal mass distribution is approximately homologous to Uranus', but an 18-hour period is not. We discuss the remarkable implications for Neptune's interior structure if its body rotation period is actually 18 hours.

This morning, you heard Ellis Miner talking about two different values for the rotation period of Neptune. Some questions came up about which one was correct. The purpose of this talk is to try to elucidate that matter and to attempt to convince you that there is some possibility that maybe both are correct.

The first point I want to make is the reason that I, at least, would like to know the rotation period of Neptune is because of what it tells us about the interior. If we expand the external gravity potential V_e of the planet in the usual form where θ is the colatitude and J_2 is the second-degree zonal harmonic:

$$V_e = (GM/r) \ [1 - J_2 \ (a/r)^2 \ P_2(\cos \ \theta)] \qquad , \qquad (1)$$

where a is the equatorial radius; then for a rotating body in hydrostatic equilibrium, J_2 is going to be proportional to a small parameter given by

$$q = \omega^2 a^3/GM \qquad , \qquad (2)$$

where ω is the angular rotation rate, G is the gravitational constant, and M is the mass. We express the proportionality in the form

$$J_2 = \Lambda_2 \, q \quad , \tag{3}$$

to lowest order in q. Λ_2 is the response coefficient. For the Jovian planets, we can look at these values which are known for Jupiter and Saturn, compare them with the homogeneous case, and we see that these planets are centrally condensed. The more centrally condensed they are, the smaller Λ_2. For a sixteen-hour period of Uranus, which is sort of becoming a consensus value (although there may still be some holdouts), we obtain for Uranus, $\Lambda_2 = 0.09$.

Now the 18-hour period for Neptune, which was discussed this morning, and which comes from looking at cloud features going around on Neptune, gives us $\Lambda_2 = 0.20$, derived from the fact that the J_2 of Neptune is 4×10^{-3}. Now $\Lambda_2 = 0.20$ means that Neptune is less centrally condensed than any of the Jovian planets, and that leads to very weird interior models. For example, one may have to consider models that are composed entirely of water. Morris Podolak recently completed a study with Ray Reynolds and Rich Young, and he might want to say a word or two about this.

There is another way to measure the rotation period, and this is where the atmosphere comes in. One can look at the shape of the planet's surface, and the way one does this is to assume that the atmosphere defines an equipotential surface. Then we calculate the potential at the pole of the planet where b is the polar radius, and we equate that to the full corotating potential at the equator, where we add the centrifugal potential to expression (1). We then equate these potentials, use that to calculate the relative difference in the equatorial and polar radius, and that then can be expressed in terms of J_2 and this rotation parameter q, which can also be expressed in terms of these other variables as previously described:

$$e = (a-b)/a = (3/2)J_2 + (1/2)q$$

$$= q(3\Lambda_2 + 1)/2$$

$$= J_2(3 + \Lambda_2^{-1})/2 \quad . \tag{4}$$

In 1983, we had a very good stellar occultation by Neptune, which was observed by our group, and we obtained data from eight stations over a rather large baseline (Hubbard et al., 1985). We were able to observe from extremely southern locations as well as extremely northern locations. The timings were used to define the equipotential surface. There was a very measurable difference between a spherical and oblate object. Thus, we were able to deduce the oblateness. One of the difficulties that comes in when one is trying to measure oblateness is that the planets with atmospheres have fuzzy edges.

We get a lot of scattering of light due to refractive focusing and defocusing. It's difficult to say where a particular pressure level occurs, but there is a standard procedure for doing this; namely, we look for the half intensity point as obtained by fitting an isothermal light curve (i.e., a theoretical light curve computed for a strictly isothermal atmosphere) to the observed data. That seems to work reasonably well, although I should point out that you see variations from one station to another which don't reproduce. So, in detail, the planet is not globally layered, at least beyond some limit. The immersion and emersion profiles are grossly similar: we have non-correlation in detail although the overall structure is similar.

If we considerably idealize the atmosphere, in terms of a perfectly isothermal quiet atmosphere, then the rays of light coming from the star to the observer will fall in a pattern such that the angle through which Neptune bends each ray will increase exponentially with depth of penetration of the ray into Neptune's atmosphere. At the ideal half intensity point, the linear deflection of the ray at the Earth is precisely equal to the scale height H, which in the case of Neptune is about 50 km. Now the argument in trying to say how accurately we can define the edge of the planet, goes as follows: We have density fluctuations (with respect to the ideal isothermal atmosphere) which are perturbing the rays so that they actually don't fall in the idealized path, but they, in fact, sometimes converge, producing a spike. At other times they may diverge by an extra amount. But the argument is that any extra bending that they will suffer due to imperfections in the isothermal atmosphere will be small compared with the value of the overall bending angle. The reason for that is that we assume that the density fluctuations are small compared to the background density, which is certainly quite reasonable. If that argument is true, then any residuals that we get in our fit to the overall profile of the atmosphere should be considerably less than the scale height. That is the type of accuracy for which we aimed in fitting the solution. With suitable discarding of anomalous data points, we succeeded.

Some of the data were affected by known systematic problems, and indeed it was those stations that turned out to have the largest residuals. On the ingress side, we got residuals less than a kilometer at our Taiwan station, and at our Hobart station it was again less than a kilometer (a very nice fit to the best fit solution). A portable station gave a 37 km residual and was thrown out in the final solution, though I could mention that we did include it in one solution, which gave a slightly shorter rotation period. On the emersion side, there was a measurable separation between the spherical profile and the oblate profile. The residual was −1 km at Chung Li, Taiwan. The Guam station was thrown out. The overall fit had all retained stations with residuals of substantially less than 50 km. The results of this solution I'll give to you in a moment. Let me also mention that as a by-product of this analysis, we obtained the temperature at the occultation level, which was computed by fitting an isothermal light curve to the data, and obtaining the scale height. The scale height was then corrected for the variable gravity, due to the oblateness of the planet. Finally, the temperature at the one microbar level was deduced as a function of the latitude. What we find is in general not really any indication of a large temperature gradient as a function of latitude. In fact, at this level in the atmosphere it looks like the temperature is reasonably constant, both with latitude and with time. The average value turns out to be

about 155 K. So if that is the case, then that is further support for the model that we are assuming, that we are dealing with a surface that is at a constant potential and a constant density.

We had to fit not only to the oblateness of course, but also solve simultaneously for the equatorial radius as well as the center of figure. Though we have a very nicely defined minimum in the rms residuals, because of the large number of the parameters that we had to vary, the probability that the solution actually lay within a narrow interval in the oblateness e is still rather small. But the deduced value is e = 0.022 ± 0.004, which is an improved result over the one that I reported at the Uranus/Neptune meeting (which led to a 13.6 hour period, which was mentioned by Ellis Miner this morning). What we did in this analysis was to use Harris' (1984) improved pole position for Neptune. That leads to a reasonable value for Λ_2: 0.12, and a period P = 15^h ($+3^h$, -2^h). However, notice that because of the large error bars we still can't rule out an 18-hour period. Nevertheless, as I mentioned earlier, I don't like the 18-hour period.

Here is the model for the atmospheric dynamicist to figure out. Suppose that we had differential rotation on cylinders, and suppose that the bulk of the planet is actually rotating with a period consistent with the models and the J_2 value (say, P = 15^h). Suppose that we have an equatorial zone which is in differential rotation, but unlike Jupiter and Saturn, it's going backwards. In other words, it's rotating at a slower rate of, say, 18 hours. We have spots on it, so that's what we see going around. We want the q of the planet as a whole to be 0.033, of course, the value corresponding to a 15-hour rotation period. The oblateness is now going to be given by this formula:

$$e = (3/2)J_2 + (1/2)q_0 + (1/2)\;\Delta q \quad , \qquad (5)$$

where $q_0 = q(15^h)$ is the q corresponding to the deep interior (about 0.033), and Δq is a correction due to the differentially rotating outer layer. But we want this oblateness to remain almost the same as the one we just got [eq. (4)]. Thus we want Δq to be much smaller than q_0. It turns out that if you do the calculation, assuming the planet is rotating on cylinders so that you can derive the centrifugal force from a potential, then the correction $\Delta q/q_0$ is just given by the formula:

$$\Delta q/q_0 = -0.31 \cos^2\theta_0 \quad , \qquad (6)$$

where θ_0 is the colatitude where the bounding cylinder pierces the surface, the bounding cylinder being the one which divides the inner region which rotates with a period of 15^h from the outer region which rotates with a period of 18^h. Thus, by adjusting the parameters an appropriate amount (for example, taking θ_0 to be 60 deg which gives you a big band in latitude of ± 30 deg to have spots in), you can make $\Delta q = -0.076\; q_0$, less than a tenth of q_0. Thus one can construct a model which would do the job, i.e., reconcile a 15^h deep-interior period with an 18^h equatorial-atmospheric period. But as to whether that seems plausible or not, I would have to refer you to a dynamicist.

REFERENCES

Harris, A. W. (1984). Physical properties of Neptune and Triton inferred from the orbit of Triton. In *Uranus and Neptune* (Ed. J. T. Bergstralh), pp. 357-373. NASA CP 2330.

Hubbard, W. B., H. P. Avey, B. Carter, J. Frecker, H. H. Fu, J.-A. Gehrels, T. Gehrels, D. M. Hunten, H. D. Kennedy, L. A. Lebofsky, K. Mottram, T. Murphy, A. Nielsen, A. A. Page, H. J. Reitsema, B. A. Smith, D. J. Tholen, B. Varnes, F. Vilas, M. D. Waterworth, H. H. Wu, B. Zellner (1985). Results from observations of the 15 June 1983 Occultation by the Neptune System. *Astron. J.* 90, 655-667.

DR. PODOLAK: I'd like to pick up on the speaker's first statements. In order to match models to Uranus with a 16-hour period you need very much different models from those required to match an 18-hour period for Neptune. The amount of ice necessary is not so unreasonable, but the distribution differences between Uranus and Neptune are great.

Briefly, there are three types of material you have to worry about: things that are always solid in the solar nebula (like things we call rock), things that are always gaseous like hydrogen and helium, things that could be solid or gaseous depending on the temperature that we call ice (it's just a generic name not meaning the stuff is solid and frozen) and that would be water, methane, ammonia or similar substances. Then if you try to construct models made up of those three materials that match Uranus with a 16-hour period and Neptune with an 18-hour period, what you find is that the amount of rock that you put in the core is similar for both planets. It's a little bit more for Neptune because Neptune has a slightly higher density. The amount of ice that you put in the planets is similar, and in fact the ice-to-rock ratio is about three, which is exactly what you'd expect for solar compositions. All that is very nice except that for Uranus, most of the ice sits in a shell around the core (it's very centrally condensed like Bill said). For Neptune, most of the ice has to spread out throughout the envelope because it's rotating so much more slowly that you still want to have a high moment of inertia. The problem is, why do these things have such different structure? Just to give you a feeling for how strange this is, if you were to say "O.K., suppose the stuff on Uranus just fell down and the stuff on Neptune is going to fall down in another couple of years." It turns out that the amount of gravitational energy you release is so large that even with an effective temperature of about 100 K, it would still take two billion years to radiate away. You're talking about a really substantial amount of energy and a really big difference in structure. It is hard to see how that came about. That is the reason that I would like a 15-hour period for Neptune too.

DR. ORTON: Does anyone else want to reconstruct the solar system?

DR. ALLISON: Bill, do you think that there is a realistic prospect of eventually refining these occulatation measurements to the point where they could be used as a discriminant between models of rotation on cylinders versus thin-layer models?

DR. HUBBARD: I think that it could be done if we can find a way to pin down the location of the center of Neptune accurately. In the case of Uranus, we have the advantage of the rings. They don't have atmospheres, so you can determine excatly where they are. Now if we can get enough observations of a Neptunian ring, or portions of a Neptunian ring to do the same, then yes, in the long run it should be possible to do the same thing. In that case, I believe that enough precision would be possible to check this point out.

WEDNESDAY POSTER PRESENTATIONS

OUTER PLANETS

ARE THE AEROSOLS ON URANUS AND NEPTUNE COMPOSED OF METHANE PHOTOPOLYMERS?

M. Podolak[*], L. Giver, and D. Goorvitch
NASA/Ames Research Center

*We have used the measured optical properties of photochemically pro-
duced aerosols in an adding-doubling radiative transfer code to match
various points in the spectra of Uranus and Neptune. We show how well
these points are fit by different assumptions regarding the size and
distribution of these aerosols in the Uranus and Neptune atmospheres.
The consistency of these derived distributions with those expected
from computations of the sedimentation rate of such aerosols is
discussed.*

---

[*]Permanent address: Dept. of Geophysics and Planetary Sciences, Tel Aviv
University, Ramat Aviv, Israel

THE HD/H$_2$ RATIO IN THE ATMOSPHERE OF URANUS

J. T. Trauger
Jet Propulsion Laboratory

High resolution spectra of HD and H$_2$ have been brought together to derive the D/H ratio for Uranus. The deuterium concentration in the dominant molecular hydrogen phase is least susceptible to the effects of isotope fractionation in the planetary atmosphere, and the determination of relative abundances of HD and H$_2$ is unambiguous due to nearness (at 6000 and 6300 Å, respectively) and relative weakness of the chosen spectral lines. The HD 5-0 R(0) and R(1) dipole lines and the H$_2$ 4-0 S(0), S(1), and S(2) quadrupole lines were obtained with a PEPSIOS instrument at the Palomar 5-meter telescope. The H$_2$ spectra, which resolve the asymmetric line profiles resulting from pressure shifts in the deep stratified Uranus atmosphere, unambiguously define the line-of-sight hydrogen abundance for comparison with the HD spectra. The 5-0 band of HD was chosen to minimize interference from blended CH$_4$ lines. However, weak interfering lines have been found in the 5-0 bands from Uranus as well, and some uncertainties remain regarding the intrinsic line strengths in molecular hydrogen, complicating the analysis of the HD/H$_2$ data. Nevertheless, it is established that the D/H ratio in the atmosphere of Uranus is smaller than the Jovian value, and is significantly smaller than recent theoretical predictions for Uranus based on estimates of isotope fractionation in the pre-planetary solar nebula.

CLOSING SESSION

CONFERENCE REVIEW

ANDREW P. INGERSOLL

CONFERENCE REVIEW

Andrew P. Ingersoll
California Institute of Technology

Obviously, I can't review everything that was said here. Besides, you've heard it before. Why do you want to hear it again? On the other hand, I would like to tell you what are the really exciting questions, as I see them. I would define an exciting, thrilling question as one where what we think we know disagrees with what we think we know by another means. So, there will be many occasions where I will say, "Well here's the model but...," and then there will be the observation. I think some of the best questions in planetary science can be framed or phrased in terms of this violation of our intuition leading to a deeper understanding of something. What can we expect to learn during the rest of this century? There are a few remarks I have to make on that. I'm going to try not to mention your names, because I might leave someone out.

First, let's start out with the chemical models that are all getting pecked full of holes. The solar composition model comes first. Jupiter and Saturn are made out of solar material, right? But of course Saturn and possibly Jupiter have less helium. I'll get back to what might be causing that, but this was the original model, right? Now, they have more carbon, catastrophically less oxygen perhaps, deuterium varies all over from giant planet to giant planet, and no one has seen sulfur yet. Well, there are some modifications to this model. You didn't just take a chunk of solar material and put it together to make a giant planet. You brought things in later, and perhaps all the atmsopheres of the solar system are due to comets and big meteorites. Well, O.K., if they are enriched in nitrogen and carbon, maybe that's consistent with some type of later enrichment by volatile-rich bodies, but where's the oxygen to go with this? So we have this discrepancy here between what we thought we knew, and what we think we know by another means. Now we have the chemical equilibrium model. You look at the atmosphere, and everything is supposed to be in chemical equilibrium in accordance with that naive model. We recognize that it's naive, and of course we part with things that aren't right. The ortho-para H_2 for Jupiter is not in thermal equilibrium. It has a hot signature, as if it came from someplace deeper down, or some other place. Maybe even though it appears to have a hot signature, maybe it's a forgery. Maybe it has nothing to do with temperature. We have a currently popular model to explain the depletion of helium in Saturn's atmosphere, namely, the idea that Saturn has cooled to the point where helium has started to precipitate in the metallic core, or metallic region of Saturn. However, it's quite obvious that if you start taking helium out of the atmosphere and the outer envelope covering one-half the radius of Saturn, you're going to decrease the moment of inertia. Yet we have estimates of the moment of inertia which are somewhat higher than if the whole outside envelope were simply hydrogen. So if you take out helium, then you have to add something back in to this outer one-half of the radius.

277

Is Uranus a wet adiabatic planet? This is a separate issue that I thought of this morning because I remembered some discussions that we had in COMPLEX. We were discussing a proposed requirement that any Uranus probe (this was for the year 2020, of course) should measure the base of the water clouds. Someone pointed out that the base might be the center of the planet! So we scrubbed that one. Well, you can surely see my prejudices; I like this disagreement between models and observations. This is a plea; let's get some models so that Galileo can shoot them down, and so we can stand up at press conferences when Galileo gets there and say, "...and look, here was this model and now we've proved that it was wrong." The press will love it. Is any element uniformly mixed? Let me rephrase that. What I really mean is, can we find any element that can deal with limits in the atmosphere? Nothing seems to be sacred--noble gases were wrong, nearly everything has misbehaved. But that's the way it is, and that's the way it should be if we're going to have an exciting program.

Now, turning to clouds, we find similar kinds of questions. Chemistry is certainly involved there. Remember the chemical equilibrium model that everything was just the kind of precipitate that you'd get if you raised the solar composition parcel up adiabatically and let things precipitate out and stay there. Of course, when that model was published, immediately the modelers recognized that you would have a bunch of white cloud layers and no colors. Nor do you have holes in the clouds to see through. So we still have the big question of what we are seeing when we look at the beautiful color on the giant planet. Sulfur has the right color, but no one's really seen sulfur. That's the way it should be also--we've got mysteries.

I may show my ignorance on some of these issues. I'm searching for the controversies. Perhaps I'm searching a little too hard, and looking in the wrong place, but it appears to me that the different photochemical models imply inconsistencies. According to this particular photochemical model, the eddy mixing coefficient is too high for Jupiter, higher for Jupiter by a factor of 100 than for Saturn. Then according to another photochemical model, which admittedly refers to a different altitude, the eddy mixing coefficient is the other way; Saturn is more vigorous than Jupiter. Someone's got to put all that together and reconcile the inconsistencies if it's not just my misunderstanding.

I sort of like aurora and lightning. They are oddball things. They don't fit into anything, but we're beginning to get a data base about lightning and auroras in the solar system. Lightning is particularly fascinating, especially because it exists in such different atmospheres. As for aurora, of course it's there on Jupiter, because you're getting zapped all the time by particles.

We have this old model, rising motions in the zones so the clouds are high, sinking in the belts, and the clouds are depressed or thinned out or something. But yet, the more we observe it and try to say how high the clouds are in the zones or the belts, the more things disagree. I was afraid for a time yesterday, that there was going to turn out to be no difference at all between the belts and the zones; they would disappear. I'm not sure what photochemical haze is. I'm not sure what the surprises there are. I don't yet know whether they contribute to the color. I'm not sure what the experts say.

Let's go on to temperatures. I'll try to point out the questions which seem exciting and fight with intuition. The kind of thing which often defies your intuition, or mine is that in meteorology, one often finds that things seem to spontaneously act as refrigerators, rather than heat engines. In other words, things seem to be defying the Second Law of Thermodynamics, even though they of course never do. That's always interesting. But we're not basic physicists; we're trying to show the basic physicists how complex the real world is when you apply their simple laws.

We are narrowing our error bars on the internal energy fluxes from all these giant planets. Do we understand why the different planets have the fluxes they do? Why does Uranus have none, while Neptune does? I don't know the answer. It certainly looks sort of odd. A fundamental quantity, the equator-to pole temperature gradient or difference in an atmosphere is obviously related to how much of a difference there is in sunlight absorption, how much difference in internal energy coming up there is and how much the atmosphere is transporting energy. It galls me that we have never measured the atmospheric energy transport for Jupiter or Saturn or any planet except the Earth--how embarrassing! It is a very important and fundamental quantity, and I'm sure that there will be some surprises if we are ever able to get a good measurement. It's even harder to measure what the internal energy flux is doing. Is it constant with latitude or is it variable? Is there some feedback whereby it tries to compensate for the solar flux?

We've got at least six examples of planets with very different kinds of seasonal forcing. Not much has been said at this meeting about Triton's seasons, but they are odd, perhaps the oddest of all. I haven't even talked about the old idea of rising and sinking zones and belts. The observations seem to disagree even on something that simple. Is there any way we can measure and confirm that the interior is adiabatic, and if so, to what level of approximation? Can we say that the interior is uniformly rotating by any observational means? I don't know.

Let me consider some dynamical questions and then I'll turn to the issue of future data sets. Getting back to the theme of observations defying your intuition, perhaps we should start with the Earth's atmosphere, where the only long-lived atmospheric features are attached to continents. We have no continents on the Jovian planets. So your intuition says that atmospheric features there shouldn't be very long-lived. But yet we have zonal jets and oval spots, all very stable. If anything, Voyager increased the discrepancy between our intuition and these long-lived things because one of the big surprises (I can personally attest as a dynamicist) when Voyager got there was to see how energetic the eddies were, how short-lived they were, and that they were infinitely capable of destroying all this structure and yet they didn't. So our intuition was further strained by the Voyager observations. All of this kind of thing involves questions that are very interesting to dynamicists, not just meteorologists, not just fluid dynamicists, but dynamicists in general interested in systems with many degrees of freedom. In funny ways, in some situations, these systems can somehow maintain large-scale order in spite of small-scale payouts. We may have some of the best examples in nature to look at. So we have a responsibility.

I have several more interesting things on my list. We keep learning things about convection. Often from theoretical studies, and also lab studies, but studies that are motivated at least by giant planets. We didn't hear much about a discrepancy that seems to exist according to Voyager. The Jovian atmosphere rotates faster, except for one or two very minor latitudes, than the interior. For Saturn, the whole atmosphere, not just the equator, but the whole atmosphere is going faster than the magnetic field. Is there any way that the magnetic field could be lying to us? I don't know. Again, controversy is healthy. Deep versus shallow pictures of the atmospheric circulation is just what we want. The Galileo probe probes to 20 bars. Can we do seismology and probe deeper? In other words, by observing waves and eddies in the atmosphere, will we find that they are somehow telling us about deeper levels analogous to how people use seismology or Earth-free oscillation to study the interior of the Earth.

Now I'm going to change gears. Let's talk about data sets. I am going to emphasize planetary observations, but there are other important data sets such as spectroscopic and chemical data, and theoretical data sets. With modern computers you can get a big program, just put it on the computer, let it run and treat it as an experimental system (turning the knobs to see how it varies), and those are theoretical data sets. I'm really talking primarily about data sets of observations of the planets. Let's first talk about all the data already returned from Pioneer and Voyager. How much more should we be doing with this data? I don't know. But my feeling is that with all of the images it's worth doing just about everything you've heard about today at least once again. I also feel that the movies show that there is an infinitely more complicated way that fluid structures behave. We almost have to go back to just inventing nomenclature and cataloging just what's going on on this planet. I'd like to see the cloud experts put together one model starting from the physical properties of the cloud particles that explains all the observations at once. I personally don't know whether the IR data from Voyager, for instance, has been milked dry.

With respect to ground-based observations, high resolution spectroscopy keeps on discovering things in a prolific way. Also, there are dynamical things that you should do from the ground simply because of the long time base line, and the fact that there are some myths that we keep repeating such as the jets never change. Well, some things change. If we are to find out what changes with them, and what stays constant, we've got to keep that long base-line data set going.

What will Space Telescope do? It has a ten year lifetime. It has resolution comparable to sort of an intermediate useful Voyager resolution. It has much better wavelength coverage, if you look in methane bands for example. An ideal thing to use Space Telescope for would be to get at least two rotations of the planet (20 hours) so you could see motion, and then come back every three months. While you're doing that, you could measure just about everything else in the Jupiter system: the magnetosphere, the aurora, the volcanoes, and the key word—coordinated observations—to see these things all happening at once. This should be done certainly not only for Jupiter, although I would say that Jupiter and Saturn, in my opinion, deserve more attention than Uranus and Neptune from Space Telescope.

280

DR. POLLACK: Viewing the development of a global dust storm on Mars with the Space Telescope could be very exciting.

DR. INGERSOLL: I'm not talking about Mars. This is the Jovian planets, right?

Let's talk about future Voyager data sets. You've heard about that today. Well, we're going to learn the temperature profiles, pole-to-pole and equator-to-pole temperature gradients, and if there are any winds to be seen we'll see them. If there are bands or spots, we'll see them. Probably we will get the carbon to hydrogen ratio. Triton is just full of surprises. It is probably the best place to go if you're a planetary scientist, because you can more than double your knowledge about this object. I have still that kind of emotion in me; I like to double my knowledge no matter how small it is.

As for Galileo, I am familiar with some of the aspects, and it's not all good news. The plus side is that you have broad wavelength coverage: UV, visible out to one micron, including methane bands, photometry. You have near-infrared out to five microns, and far-infrared out from 15 microns—not really a spectrometer like IRIS, but well-chosen bands. Here is the bad news. Apojove is on the dark side, so you spend most of your time working with a thin crescent. There is no wide-angle camera, so when you go zooming by at perijove, you are so close that most of your fields-of-view are "postage stamps" a little more than a tenth of a radius of the planet. There is a period of a few days when the planet is at half-phase (90° phase angle), and that's where we get the global views. It's going to be quite a different mission from Voyager. I'm hoping that the following things will be learned, however. I think that there will be a very good measurement of cloud particles because there is all this wavelength coverage. You can really see things on the limb. You get vertical structure. I also think there will be some dynamical information at smaller scales by a good factor of 10 better than on Voyager. So we'll get samples, but not everywhere on the planet by any means. Getting down to small scales is very important. I want to try very hard to get a heat transport at least one place around one feature. In other words, we need a correlation between a wind and a temperature over some field of eddies. But it won't be another Voyager movie. It will be small scales and vertical structure.

The Galileo probe of course goes down to 20 bars. At least at that one place near the equator, you get a very good temperature profile, cloud profile, velocity profile, compositional profile, isotope, lightning and heating profiles. But let's not feel guilty if we don't answer all the questions. When I was younger, I used to feel very guilty when a layperson would say to me, "You guys come up with more questions than you do answers." Now I say, "Damn right!"

DR. HUNTEN: I'd like to make a comment. Galileo does not die after 20 months, at least it may not die. If it lasts less time than either Voyager or Pioneer Venus then the apojove will be right smack over the sub-solar point. I think we should all keep that in mind because this isn't too early to start thinking about it and working on it.

DR. LEOVY: Might there not be an opportunity to get distributions of lightning and higher resolution data even on the day side?

DR. INGERSOLL: I should of course mention that by using Space Telescope and Galileo together, we can put the high resolution information that we get from Galileo in the global context.

DR. TAYLOR: Would you answer my question from yesterday now like you said you would?

DR. INGERSOLL: Well, his question from yesterday was "What would I like to do not with Galileo, but just in general if I had my druthers?"

DR. TAYLOR: No. You showed us your model with all the cylinders going through Jupiter and resonances going through the planet and all that sort of stuff, but I asked you specifically what would you measure to put that model to the test.

DR. INGERSOLL: I assume you mean with realistic measurements. I didn't realize that was the question. That's a harder question. I don't have great optimism of settling these arguments by observation unless we actually get into the atmosphere. Remote sensing observations are going to have trouble. On the other hand, my greatest hope for optimism is the one I alluded to here. Somehow, from looking at the time-dependent, two-dimensional behavior of all the structures, waves, spots and eddies that we see (which is a lot of bits of information and a very powerful constraint when coupled with Newton's laws, which we also know are a constraint), I hope we can back out what is going on much deeper down just from that kind of information.

DR. TAYLOR: Can't you use your model to tell us what sort of observations to strive for?

DR. INGERSOLL: If the model were complete now—yes. I gave you some examples such as the shear and the zonal velocity profile, but I think the big thing that we really want more of and don't have right now from a dynamics point of view is "imaging" of temperatures. The temperature instruments just typically have too poor a resolution to resolve eddies. It's not their fault, but it's a fact.

DR. SROMOVSKY: In the case of Saturn, is this worth it? Saturn's whole atmosphere is rotating, perhaps to great depths. It seems like that should be verifiable from gravity data with the right type of orbiting object.

DR. INGERSOLL: You're right. If you know the equation of state reasonably well, then from the gravity harmonics, you can solve for the other unknown, the rotation of the interior, and in fact get that as a function of the altitude in the interior.

DR. SROMOVSKY: What would it take to solve that problem unambiguously?

DR. INGERSOLL: You probably know the answer to this. You have to get close in, so you need a polar orbiter perhaps, or any kind of orbiter at close range.

DR. HUBBARD: Actually, I think that the best hope for this is to use the rings, because my understanding is that an analysis is going on right now of the motions of an eccentric ringlet in the Saturn system. That serves as your probe. It's fairly clear that's the best method.

DR. ORTON: I want to put in a plug if I may for continued observations of the stratosphere whether it's us doing it, or the IRTF operation doing it with any newly-developed technology with two-dimensional ten or seven micron cameras. I wouldn't have believed it if someone had told me that there is a structure there that was going to be completely changed compared to 1983. It's changed even over one year. I don't know why...

DR. INGERSOLL: The stratosphere of Jupiter?

DR. ORTON: Jovian stratospheric temperature structure has been observed to change substantially on the order of months or days, and I just don't know why. Is it a tracer of tropospheric motion? I don't really know; but it's a pretty big question.

DR. MCKINNON: One more question on differential rotation; would you care to comment on Bill Hubbard's suggestion of global retrograde rotation for Neptune and whether you think that it is possible?

DR. INGERSOLL: I learned long ago that meteorological dynamics is not a deductive science. More often than not, you rationalize observations. Still, on the other hand, there are good theories and there are bad theories. The answer is...anything, sure. I'd believe anything. Wait—there is a difference between good and bad theory. A good theory is one that has enough steel in it to convince its author that his or her initial intuition was wrong. A bad theory is one that is so yielding that the author can manipulate it to whatever result is desired. For that particular question, I have no answers.

DR. MCKINNON: O.K., but we have some evidence that there is differential prograde rotation, and is that easier to explain?

DR. INGERSOLL: No, as someone in this room said yesterday. For instance, the Earth's atmosphere has no equatorial maximum of angular momentum. That's somewhat easier to explain than a planet which has this band sitting up in the atmosphere that's going faster, faster than anything else on the planet. This requires some sort of counter gradient transfer of momentum into it, to keep it going.

Mike! Mike Allison wherever you are. Thanks again.

DR. ALLISON: Thank you.
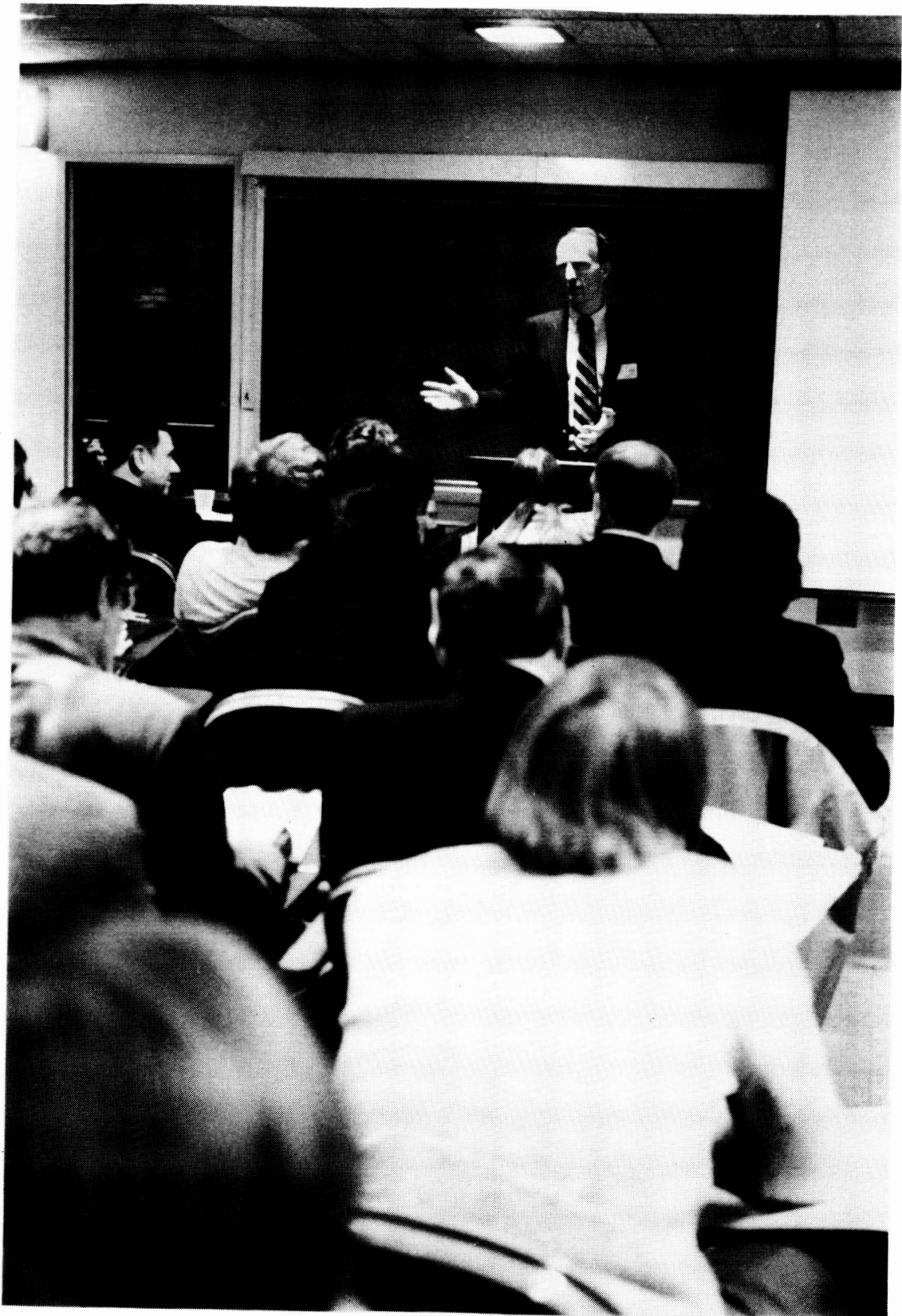
LIST OF PARTICIPANTS

Mark Allen
Jet Propulsion Laboratory
MS 183-601
4800 Oak Grove Drive
Pasadena, CA 91125

Michael Allison
NASA/GISS
2880 Broadway
New York, NY 10025

Venkata Anne
Sigma Data Services
Institute for Space Studies
2880 Broadway
New York, NY 10025

John Appleby
Jet Propulsion Laboratory
MS 183-301
4800 Oak Grove Dr.
Pasadena, CA 91109

Paul Ashcraft
Dept. of Atmospheric Science
SUNY/Albany
Albany, NY

Sushil K. Atreya
Atmospheric and Oceanic Science
Space Research Building
University of Michigan
Ann Arbor, MI 48109

Kevin H. Baines
Jet Propulsion Laboratory
MS 183-301
4800 Oak Grove Drive
Pasadena, CA 91109

Alessandro Battaglia
Institute for Space Studies
2880 Broadway
New York, NY 10025

J. Kelly Beatty
Sky and Telescope Magazine
49 Bay Street Rd.
Cambridge, MA 02238

Reta Beebe
Department of Astronomy
New Mexico State University
Box 4500
Los Cruces, NM 88003

James W. Beletic
Center for Earth and Planetary Physics
Harvard University
29 Oxford St.
Cambridge, MA 02138

Michael J.S. Belton
National Optical Astronomy Observatories
950 N. Cherry Ave.
Tucson, AZ 85726

Christian Bezanger
Laboratoire d'Astronomie Infrarouge
Pl J. Janssen.
92195 Meudon
France

B. Bezard
Laboratoire d'Astronomie Infrarouge
Observatoire de Meudon
92195 Meudon Principal Cedex
France

Gordon Bjoraker
Goddard Space Flight Center
Code 693.2
Greenbelt, MD 20771

Lee Branscome
University of Miami
4600 Rickenbacker Causeway
Miami, FL 33149

Henry C. Brinton
Code EL
NASA Headquarters
Washington, DC 20546

Harold Brooks
308 N. Orchard, Apt. 2
Urbana, IL 61801

William Cabot
Sigma Data Services
Institute for Space Studies
2880 Broadway
New York, NY 10025

Simon Calcutt
Department of Atmospheric Physics
Clarendon Laboratory
Oxford OX1 3PU
England

Vittorio Canuto
NASA/GISS
2880 Broadway
New York, NY 10025

Barbara Carlson
NASA/GISS
2880 Broadway
New York, NY 10025

Barney J. Conrath
NASA/Goddard Space Flight Center
Code 693.2
Greenbelt, MD 20771

Cindy C. Cunningham
Department of Planetary Sciences
University of Arizona, LPL
Tucson, AZ 85721

Catherine de Bergh
Observatoire de Meudon
92195 - Meudon
France

Imke de Pater
Astronomy Department
Campbell Hall
University of California
Berkeley, CA 97720

Anthony D. DelGenio
NASA/GISS
2880 Broadway
New York, NY 10025

Pierre Drossart
Observatoire de Paris-Meudon
92190 - Meudon Principal Cedex
France

Kerry A. Emanuel
Rm 54-1622
Massachusetts Institute of Technology
Cambridge, MA 02139

Larry W. Esposito
Lab for Astrophysics and Space Research
Campus Box 392
University of Colorado
Boulder, CO 80309

Steven Fels
Geophysical Fluid Dynamics Laboratory
P.O. Box 308
Princeton University
Princeton, NJ 08540

Joseph Ferrier
Sigma Data Services
Institute for Space Studies
2880 Broadway
New York, NY 10025

F. Michael Flasar
NASA/Goddard Space Flight Center
Code 693.2
Greenbelt, MD 20771

Ernest Fontheim
Code EL
NASA Headquarters
Washington, DC 20546

James Friedson
Geological and Planetary Science
Caltech 170-25
Pasadena, CA 91125

David Godfrey
Blackett Laboratory
Prince Consort Road
London SW7 2BZ
United Kingdom

Rangasayi Halthore
Earth and Space Sciences
SUNY/Stony Brook
Stony Brook, NY 11794

James E. Hansen
NASA/GISS
2880 Broadway
New York, NY 10025

Bruce Hapke
321 Old Engineering Hall
University of Pittsburgh
Pittsburgh, PA 15260

Greg Hartke
Sigma Data Services
Institute for Space Studies
2880 Broadway
New York, NY 10025

David H. Hathaway
Mail Code ES52
NASA/Marshall Space Flight Center
Huntsville, AL 35812

William B. Hubbard
Lunar and Planetary Laboratory
University of Arizona
Tucson, AZ 85721

Olenka Hubickyj
Sigma Data Services
Institute for Space Studies
2880 Broadway
New York, NY 10025

Donald M. Hunten
Department of Planetary Science
University of Arizona
Space Science Building
Tucson, AZ 85721

Andrew P. Ingersoll
Geological and Planetary Sciences
Caltech 170-25
Pasadena, CA 91125

Fred Jaquin
Department of Astronomy
Cornell University
Ithaca, NY 14850

Gordon Johnston
MS 156-246
Jet Propulsion Laboratory
4800 Oak Grove Drive
Pasadena, CA 91103

Ralph Kahn
Earth and Planetary Science
Campus Box 1169
Washington University
St. Louis, MO 63130

Rosemary Killen
Space Physics and Astronomy
Rice University
Houston, TX 77251

Sang J. Kim
GSFC/NSSDC
Code 633
Greenbelt, MD 20771

The Rev. Jonathan King
Cathedral of St. John the Divine
Amsterdam Ave. and 112th St.
New York, NY 10025

Edward Kinsella
Sigma Data Services
Institute for Space Studies
2880 Broadway
New York, NY 10025

Arvydas Kliore
Jet Propulsion Laboratory
MS 161-228
4800 Oak Grove Drive
Pasadena, CA 91109

Roger Knacke
Earth and Space Sciences
SUNY
Stony Brook, NY 11794

Andrew Lacis
NASA/GISS
2880 Broadway
New York, NY 10025

W. Alexander Lane
University of Illinois
Urbana, Illinois 61801

Arthur L. Lane
Jet Propulsion Laboratory
MS 264-626
4800 Oak Grove Drive
Pasadena, CA 91109

Sergej Lebedeff
Sigma Data Services
Institute for Space Studies
2880 Broadway
New York, NY 10025

Conway Leovy
Dept. of Atmospheric Sci., AK-40
University of Washington
Seattle, Washington 98195

Stephen Lewis
Department of Atmospheric Physics
Clarendon Laboratory
Oxford OX1 3PU
England

Sanjay S. Limaye
Space Sciences and Engineering Center
University of Wisconsin-Madison
1225 W. Dayton St.
Madison, WI 53706

Jonathan Lunine
Lunar and Planetary Laboratory
University of Arizona
Tucson, AZ 85721

Dr. Barry L. Lutz
Lowell Observatory
P.O. Box 1269
Flagstaff, AZ 86002

Julio Magalhaes
Department of Astronomy
Cornell University
Ithaca, NY 14853

Terry Z. Martin
Jet Propulsion Laboratory
MS 183-301
4800 Oak Grove Drive
Pasadena, CA 91109

William B. McKinnon
Earth and Planetary Sciences
Washington University
St. Louis, MO 63130

Marie Christine Migozzi
Park de LaVillete
National Museum of Science
211 Ave. Jean Jaures
75019 Paris; France

Ellis D. Miner
Jet Propulsion Laboratory
MS 264-331
4800 Oak Grove Drive
Pasadena, CA 91109

Hasso B. Niemann
NASA/Goddard Space Flight Center
Code 615
Greenbelt, MD 20771

Keith S. Noll
Earth and Space Sciences
SUNY/Stony Brook
Stony Brook, NY 11794

Roger Opstbaum
46-20 193 St.
Flushing, NY 11358

Glenn S. Orton
Jet Propulsion Laboratory
MS 183-301
4800 Oak Grove Drive
Pasadena, CA 91109

Tobias C. Owen
Earth and Space Sciences
SUNY/Stony Brook
Stony Brook, NY 11794

Carl Pilcher
Institute for Astronomy
2680 Woodlawn Drive
Honolulu, HI 96822

Joseph A. Pirraglia
NASA/Goddard Space Flight Center
Code 693.2
Greenbelt, MD 20771

Morris Podolok
NASA/Ames Research Center
MS 245-3
Moffett Field, CA 94053

James B. Pollack
NASA/Ames Research Center
MS 245-3
Moffett Field, CA 94035

Michael Prather
NASA/GISS
2880 Broadway
New York, NY 10025

Boris Ragent
NASA/Ames Research Center
MS 245-1 Space Science Division
Moffet Field, CA 94035

Michael Rampino
Institute for Space Studies
2880 Broadway
New York, NY 10025

Peter L. Read
Geophysical Fluid Dynamics Lab.
Meteorological Office (Met021)
Bracknell, Berkshire RG12 2SZ
England, U.K.

William B. Rossow
NASA/GISS
2880 Broadway
New York, NY 10025

Makiko Sato
Sigma Data Services
Institute for Space Studies
2880 Broadway
New York, NY 10025

Makoto Sato
Sigma Data Services
Institute for Space Studies
2880 Broadway
New York, NY 10025

Thomas Scattergood
NASA/Ames Research Center
MS 239-12
Moffett Field, CA 94035

Alvin Seiff
NASA/Ames Research Center
MS 245-1
Moffett Field, CA 94035

William A. Shaffer
NRC Resident Research Associate
NASA/GSFC Code 693.2
Greenbelt, MD 20771

Peter H. Smith
Lunar and Planetary Laboratory
University of Arizona
Tucson, AZ 85721

288

William Hayden Smith
Earth and Planetary Science
Washington University
St. Louis, MO 63130

William Smythe
Jet Propulsion Laboratory
MS 183-301
4800 Oak Grove Drive
Pasadena, CA 91109

Ralph Snyder
Earth and Space Sciences
SUNY/Stony Brook
Stony Brook, NY 11794

Larry Sromovsky
Space Sciences and Engineering Center
Univ. of Wisconsin-Madison
Madison, WI 53706

Paul G. Steffes
School of Electrical Engineering
Georgia Institute of Technology
Atlanta, GA 30332

Louis J. Stief
Code 691
Goddard Space Flight Center
Greenbelt, MD 20771

Carol Stoker
NASA/Ames Research Center
MS 245
Moffett Field, CA 94035

Peter H. Stone
Massachusetts Institute of Technology
Rm 54-1420
4 Trowbridge Pl.
Cambridge, MA 02139

Richard Stothers
NASA/GISS
2880 Broadway
New York, NY 10025

Darrell F. Strobel
Earth and Planetary Sciences
Johns Hopkins University
Baltimore, MD 21218

Jean-Louis Tassoul
Department of Physics
University of Montreal
P.O. Box 6128, Station A
Montreal, P.Q. H3C 3J7; Canada

Monique Tassoul
Department of Physics
University of Montreal
P. O. Box 6128, Station A
Montreal, P.Q. H3C 3J7; Canada

Fred W. Taylor
Department of Atmospheric Physics
Clarendon Laboratory
Oxford OX1 3PU
England

W. Reid Thompson
Department of Astronomy
Cornell University
Ithaca, NY 14853

Martin Tomosko
Lunar and Planetary Laboratory
University of Arizona
Tucson, AZ 85721

Larry Trafton
Department of Astronomy
University of Texas at Austin
Austin, TX 78712

John T. Trauger
Geological and Planetary Sciences
Caltech MS 170-25
Pasadena, CA 91125

Larry D. Travis
NASA/GISS
2880 Broadway
New York, NY 10025

Richard Wagener
Earth and Space Sciences
SUNY/Stony Brook
Stony Brook, NY 11794-2100

Andrew Weir
Department of Astronomy
Cornell University
Ithaca, NY 14853

Paul Weissman
Jet Propulsion Laboratory
MS 183-301
4800 Oak Grove Drive
Pasadena, CA 91109

Robert A. West
Jet Propulsion Laboratory
MS 183-301
4800 Oak Grove Drive
Pasadena, CA 91109

R. John Wilson
Geophysical Fluid Dynamics Laboratory
Princeton University
P. O. Box 308
Princeton, NJ 08540

John Yatteau
Pierce Hall, 29 Oxford Street
Harvard University
Cambridge, MA 02138

ASTRONOMICAL, PHYSICAL, AND METEOROLOGICAL PARAMETERS

FOR PLANETARY ATMOSPHERES

ASTRONOMICAL, PHYSICAL, AND METEOROLOGICAL PARAMETERS
FOR PLANETARY ATMOSPHERES

Michael Allison and Larry D. Travis
NASA/Goddard Institute for Space Studies

A newly compiled table of astronomical, physical, and meteorological parameters for planetary atmospheres is presented together with formulae and explanatory notes for their application and a complete listing of sources.

Although the reconnaissance of the Solar System by spacecraft in the past fifteen years has virtually recalibrated the measure of planetary parameters, there is an evident lag in the comprehensive digestion of the new data into a form that can serve as a ready reference for comparative planetology. Certainly there is not yet available anything like a Solar System analogue to Allen's *Astrophysical Quantities* (1973) for the everyday use of the practicing space scientist. The tabular appendix to *The New Solar System*, "Planetary and Satellite Characteristics" (Beatty, O'Leary, and Chaiken, 1982) is a useful reference for orbital and physical parameters, though already partly out of date. Hubbard's (1984a) *Planetary Interiors* textbook contains a number of excellent tables for the comparison of internal structure, heat flow, and magnetic field characteristics of the planets and satellites. What is still lacking, however, is a succinct tabulation of specifically atmospheric and meteorological parameters, updated with the most recent Voyager measurements of the Jovian planets, together with the relevant astronomical and physical structure data.

The purpose of this appendix is to offer a partial remedy in the form of a single table designed specifically to provide a listing of the most important parameters for the comparative study of planetary atmospheres. It represents a compilation not only of such fundamental and well-measured quantities as the planetary rotation period and emission temperature but also provides estimates for such equally important but more elusive parameters as the static stability and vertical mixing coefficient.

Although the table is designed for nominal comprehension without external reference, this appendix also provides explanatory notes for the tabulations, including a brief summary of formulae for their simple application, and a complete reference listing of published data sources. Although the estimation of error bounds is an essential part of the observational assessment of planetary parameters, they have been omitted from the table not only for economy of space but also to avoid their misrepresentation out of context of the real uncertainties (e.g., in many cases where systematic errors associated with model dependent assumptions may exceed estimates of the formal statistical error). Some assessment of the precision of individual tabulations is

given in the explanatory notes. In general numbers have usually been rounded so that the claimed uncertainties affect at most the last decimal place reported. For critical applications, however, users are urged to consult the references to obtain a further account of assumptions and limitations as well as to confirm accurate citation!

ORBITAL PARAMETERS

The mean solar distance R (or semi-major axis) and the orbital eccentricity are specified as the (rounded) values for the osculating elements on 1987 January 5 as tabulated in *The Astronomical Almanac* (1986). (These describe the unperturbed two-body orbit that the planets would follow if the perturbations imposed by their neighbors were to cease instantaneously.) Distances are given in Astronomical Units (with 1 A.U. = 1.49598×10^8 km). For Venus, Earth, Mars, and Jupiter these parameters are nearly invariable to within the given precision over decadal time scales within the current epoch, although they change by much larger amounts over several centuries (cf. Ward, 1974). For Saturn (and Titan), Uranus, and Neptune the osculating mean distances change by as much as a few tenths of a percent. Their eccentricities mostly change by no more than ten percent of their tabulated values with the notable exception of Neptune, whose osculating eccentricity has varied in recent years between 0.004 and 0.009. The numbers in the table have been rounded so that secular variation affects at most only the last decimal place reported.

The orbital periods τ_{orb} (in days = 86,400 s and tropical years = 365.24 days), measured with respect to the fixed stars and rounded to five significant figures, are from Allen's *Astrophysical Quantities* (1973). For the outer planets, these are slightly shorter than their two-body Kepler period about the Sun, owing to the perturbing influence of their neighbors in inferior orbits.

The perihelion and Southern Summer Solstice dates (the first for each planet since 1985 May) and the L_S angle at perihelion are compiled or extrapolated from data in Allen (1973) and *The Astronomical Almanac*. (L_S is the planeto-centric longitude of the sun measured eastward in the plane of the orbit from the ascending node on its equatorial plane, so that the Vernal Equinox corresponds to L_S = 0 deg.) The Southern Summer Solstice corresponds to the time for which L_S = 270 deg and was chosen for reference here because of its apparent relevance to the Martian global dust storms, the Voyager approach to Uranus encounter, and coincidentally, with possible arrival times planned for Galileo at Jupiter and Cassini at Saturn. (Projected calendar dates for perihelion and Solstice for the Jovian planets are reported here in tenths of years but may be in error by as much as 1% of their orbital periods.) L_S values at perihelion are given to facilitate the estimate of calendar dates for any L_S but may be in error by as much as a degree for the Jovian planets.

The obliquity is the inclination of a planet's equator to its orbital plane. The tabulated values are from *The Astronomical Almanac* (1986) and refer to the current epoch.

294

PLANETARY ROTATION AND PHYSICAL STRUCTURE PARAMETERS

The <u>sidereal</u> <u>rotation</u> <u>period</u> τ_{rot} is measured with respect to the fixed stars. The value for the Earth is from the *Astronomical Almanac* (1986). The rotation period for Mars has been derived from telescopic observations of the transit of surface features (cf. Ashbrook, 1953). The sidereal rotation of Venus has been determined from radar measurements of its surface (Shapiro et al., 1979). Jupiter's rotation is determined from measurements of its decametric radio emission (cf. Duncan, 1971). Titan's is taken to be the same as its orbital period about Saturn (as reported by Davies et al., 1980), assuming that its rotation is tidally locked to the planet. The rotation periods for Saturn (Desch and Kaiser, 1981) and Uranus (Warwick et al., 1986) are based on measurements of their periodic radio emissions by the Voyager Planetary Radio Astronomy investigation. The rotation period for Neptune can at present be only crudely estimated from determinations of its oblateness and gravitational moment according to principles briefly summarized below or from photometric observations of atmospheric periodicities (cf. Hubbard, 1986 and Belton et al., 1981). The periods for Venus and Uranus are given with negative signs to indicate that they rotate in a retrograde sense with respect to the pole that lies to the north of the invariable plane of the Solar System.

The <u>equatorial</u> <u>radius</u> values for Earth, Mars, Venus and Titan are referred to their solid surfaces and rounded to four significant figures. The value for the Earth is taken from *The Astronomical Almanac* (1986). The value for Mars is derived from a study by Christensen (1975) employing occultation, radar, spectral, and optical measurements. The Venus radius has been determined by Pettengill et al. (1980) using Pioneer Venus radar altimetry. The appended altitude for the haze level is derived from Pioneer Venus cloud photopolarimeter limb scan measurements by Lane and Opstbaum (1983). Titan's radius has been derived from Voyager radio occultation measurements, assuming that the satellite is spherical (Lindal et al., 1983). The indicated altitude of the main haze level on Titan corresponds to the elevation of its optical limb as measured by Voyager imaging (Smith et al., 1981). Tabulated values for the equatorial radius of the Jovian planets (again rounded to four significant figures) refer to the 1-bar pressure level of their atmospheres. Values for Jupiter and Saturn have been derived by Lindal et al. (1981, 1985) from a calculated geodetic fit to Voyager radio occultation measurements at different latitudes. The 1 bar equatorial radius value for Uranus has been derived by Hubbard (1984b) from stellar occultation observations of the planet by Elliot et al. (1981). The result agrees with Voyager imaging measurements (25,600 to 25,700 km, as reported by Smith et al., 1986) for the visible cloud deck which, according to Voyager radio science, is expected to reside at about 1.3 bar (Tyler, et al., 1986). The 1 bar radius for Neptune has been derived from stellar occultation data by Hubbard et al. (1985).

The <u>oblateness</u> $\varepsilon = (a_e - a_p)/a_e$ is a measure of the fractional difference between a planet's equatorial and polar radii. The tabulated value for Earth is from *The Astronomical Almanac* (1986), rounded to five significant figures. The Mars (optical) oblateness is from the study by Christensen (1975). Measurements of Venus altimetry by Pettengill et al. (1980) suggest that its oblateness is less

than about 10^{-5}. The Titan oblateness is presently unknown. The geometrical oblateness of the fluid envelopes of the Jovian planets serves as an important measure of their rotational and gravitational structure. (Table sources are cited below together with a brief discussion of the inferred relationships to other parameters. Question marks follow the tabulated values for Saturn and Uranus as an indication of slight discrepancies between optical measurements and dynamical inferrence. The oblateness, once determined, provides a simple relationship between the planetocentric latitude coordinate ϕ_c, measured along the oblate surface with respect to the center of the planet, and the planetographic coordinate ϕ_g, measured with respect to the local normal to the same surface:

$$\tan \phi_g = (1-\epsilon)^{-2} \tan \phi_c \quad . \tag{1}$$

The differences between the two coordinates at midlatitudes on the Jovian planets are sufficiently great to warrant careful discrimination in reference to published results of atmospheric observations.

The gravitational parameter $\underline{GM}$ is the product of the gravitational constant and planetary mass (in $km^3 s^{-2}$). (Although $G \cong 6.673 \times 10^{-3}$ is known to less than four-place precision, the product for most of the planets is now known to much greater accuracy.) Tabulated values for Earth, Mars, and Venus are taken from *The Astronomical Almanac* (1986). The value for Titan is from the tracking of Voyager radio science data reported by Tyler et al. (1981). Values for Jupiter (Null, 1976) and Saturn (Null et al., 1981) have been derived from the analysis of radio tracking data from the Pioneer spacecraft which, because of its close-encounter geometry with the two planets, provides the best available determination. The GM value for Uranus is a new result of the Voyager encounter (Tyler et al., 1986). The value for Neptune is that reported by Gill and Gault (1968) based on an analysis of the motion of Triton.

J_2 and J_4 are the two lowest order coefficients in the multipole expansion expression for (an axially symmetric) planetary gravitational potential. Including the centrifugal potential associated with planetary rotation this expression may be written as

$$V(r,\phi) = -\frac{GM}{r} \left\{ 1 - \left[\sum_{i=1}^{\infty} J_{2i}(a/r)^{2i} P_{2i}(\mu) \right] + (q/3)(r/a)^3 [1 - P_2(\mu)] \right\} \tag{2}$$

where (r,ϕ) denote radial and (planetocentric) latitudinal coordinates, $\underline{a}$ is the normalizing radius for the expansion, $\mu = \sin \phi$, $q = \Omega^2 a^3/GM$ ($\Omega = 2\pi/\tau_{rot}$ is the planetary rotation frequency), and $P_{2i}(\mu)$ denotes the $(2i)$th Legendre polynomial with $P_2(\mu) = 1/2(3\mu^2 - 1)$, $P_4(\mu) = (35/8)\mu^4 - (30/8)\mu^2 + 3/8$, etc. Then to second order in the expansion:

$$V(r,\phi) = -\frac{GM}{r} \left\{ 1 - J_2(a_e/r)^2 [(3/2)\sin^2\phi - 1/2] \right.$$

$$- J_4(a_e/r)^4[(3/8)\sin^4\phi - (30/8)\sin^2\phi + 3/8]$$

$$\left. + (q/2)(r/a_e)^3 \cos^2\phi \right\} \tag{3}$$

296

where the equatorial value a_e has been taken as the normalizing radius. Evaluating the potential at the equator (a_e, 0°) and the pole (a_p, 90°) and then equating the two results to solve for the relationship between a_e and a_p on an equipotential surface yields (for $\varepsilon \ll 1$)

$$\varepsilon \cong (3J_2/2 + q/2)(1 + 3J_2/2 - q/2) + 5J_4/8 \qquad (4a)$$

or (to order J_2):

$$\varepsilon \cong 3J_2/2 + q/2 . \qquad (4b)$$

Alternatively, the relationship for the rotation period in terms of ε, J_2, and J_4 may be written as

$$\tau_{rot} = 2\pi \left[\frac{a_e^3(1-\varepsilon)(1+3J_2/2)}{2GM(\varepsilon - 3J_2/2 - 9J_2^2/4 - 5J_4/8)} \right]^{1/2} \qquad (5a)$$

or (to lowest order in J_2 and ε):

$$\tau_{rot} = 2\pi[a_e^3/2GM(\varepsilon-3J_2/2)]^{1/2} \qquad (5b)$$

Clearly the nondimensional specification of the J_2 and J_4 coefficients as employed in Eq. (2) requires the adoption of a particular value for the normalizing radius $\underline{a}$ which, for various historical reasons, is often slightly different from atmospheric reference values for the equatorial radius. It has been traditional, for example, to employ a normalizing radius of 60,000 km for referencing the gravity moments of Saturn. For the purpose of specifying J_2 and J_4 for the Jovian planets in the present table, the published values have been renormalized to a reference radius equal to the tabulated 1 bar equatorial value. Gravitational studies of terrestrial planets often employ coefficient expansions with different normalizations, often including "off-diagonal" tesseral harmonics in addition to the zonal harmonics. Consequently, great care must be taken in comparing these for different planets (or different representations of a single planet.)

Tabulated J_2 and J_4 values for the Earth are from *The Astronomical Almanac*. J_2 for Mars is taken from the analysis of combined tracking data for the Viking and Mariner 9 spacecraft by Gapcynski et al. (1977). (The Mars J_4 value is omitted since it appears to be smaller than one of the second order tesseral harmonic coefficients.) J_2 for Venus is taken from the analysis of tracking data for the Pioneer Venus orbiter by Ananda et al. (1980). J_2 and J_4 for Jupiter (Null, 1976) and Saturn (Null et al., 1981) are from the gravity analysis of the Pioneer 10 and 11 tracking data. The J_2 and J_4 values for Uranus have been derived by Elliot et al. (1981) from stellar occultation determinations of the precession of the planet's rings. J_2 and J_4 as determined in this way are inferred in proportion to the square root of GM. The table values reflect a renormalization of the results of Elliot et al. in terms of both the tabulated radius a_e and the Voyager determination of GM. The J_2 value for Neptune is the (radius-renormalized) value derived by Harris (1984) from considerations of its spin-orbit coupling with Triton.

Accurate determinations of GM, J_2, and J_4 permit the dynamical inference of oblateness as indicated, for example, by Eq. (4). This relation assumes deformable fluid envelopes in hydrostatic balance. Solid planets may have non-equipotential surfaces with geometrical flattening different from the dynamical value inferred from Eq. (4), although in the case of the Earth these differences are small. For the Jovian planets, optical measurements of the geometrical oblateness provide an important check on the dynamical calculation. In the case of Jupiter the agreement is quite good. The tabulated number is the (rounded) value from a calculation by Lindal et al. (1981, 1985) which fits Voyager radio occultation data at various latitudes to the dynamical flattening of equipotential surfaces including the effects of the differential winds observed at cloud level. The same number also agrees with a stellar occultation measurement of Jupiter's oblateness by Hubbard (1977) and with the dynamical value inferred from Eq. (4), to within reported error limits. Determinations of Saturn's oblateness are more problematic. Equation (4), together with the tabulated values for GM, J_2, and J_4 yields $\varepsilon = 0.0963$. An optical measurement from Pioneer 11 imaging photopolarimeter data yields the value 0.088 ± 0.006 (Gehrels et al., 1980). Analysis of the geodetic fit to several radio occultation measurements by Lindal et al. (1985) yields 0.09796 ± 0.00018 and implies that the centrifugal potential associated with Saturn's equatorial jet produces a 100 km bulge above the reference geoid. The number for the present table is taken as their value, rounded to four places. The tabulated value for Uranus is from a geometric determination with stratoscope II photographs by Franklin et al. (1980) and agrees within error bounds with stellar occultation measurements by Elliot et al. (1981), although both are larger by slightly more than the reported errors from the dynamical oblateness of Eq. (4) using the new Voyager rotation period. The tabulated oblateness for Neptune is taken from the stellar occultation measurements reported by Hubbard (1985, 1986) and is as yet uncontested by any independent measure of planetary spin rate and dynamical flattening.

Measured values of GM and J_2 as applied to the multipole expansion of Eqs. (2) and (3) are also useful for the calculation of the gravitational accelera-tion g on an oblate equipotential surface of a rotating planet. This is given by the magnitude of the gradient of the total gravitational plus centrifugal potential normal to the surface, i.e.

$$g = [(\partial v/\partial r)^2 + (r^{-1} \partial v/\partial \phi)^2]^{1/2} \tag{6}$$

evaluated for the radial distance between the planetary center and its elliptical figure. For small values of the oblateness ε the ellipse equation gives

$$r = a_e(1 - \varepsilon \sin^2\phi) \ . \tag{7}$$

Neglect of the J_4 term, substitution of equation (3) into (6), and evaluation for the radial distance given by (7) yields, to first order in the small parameters ε, J_2, and q:

$$g = GM/a_e^2 \ [1 + 3J_2/2 - q + (2\varepsilon - 9J_2/2 + q) \sin^2\phi] \tag{8}$$

298

Evaluation at the equator and the pole gives

$$g_E = GM/a_e^2 (1 + 3J_2/2) - \Omega^2 a_e \tag{9}$$

and

$$g_p = GM/a_e^2 (1 + 2\epsilon - 3J_2) \tag{10}$$

It is then convenient to rewrite Eq. (8) in terms of these last results as

$$g = g_E + (g_p - g_E) \sin^2\phi \tag{11}$$

An estimate of the global area-weighted mean value for the gravitational acceleration may be obtained by the integration of the product of this last expression for g with the cosine of the latitude with the result

$$\langle g \rangle = g_E + (g_p - g_E)/3 \quad . \tag{12}$$

As already mentioned, planets with solid surfaces may exhibit small departures from equipotential geoids. Nevertheless, Eqs. (9) to (12) are good first-order approximations for the estimation of rotation and oblateness corrections to their surface gravities and have been employed in the determination of the tabulated values for the area-weighted mean $\langle g \rangle$. The difference between the polar and equatorial values δg_E^p is also given and may be used together with Eqs. (11) and (12) to estimate the gravitational acceleration at any latitude. In the case of Jupiter and Saturn, the most elaborate geodetic study published incorporating the Voyager radio occultation soundings is that of Lindal et al. (1985) and for these two planets the tabulated mean value has been derived by application of Eq. (12) to their results for the equatorial and polar gravities. All tabulated values for the gravitational acceleration have been rounded to three significant figures. Applications requiring the accurate determination of g on the Jovian planets should consider the appendix to Lindal et al. (1985) outlining the iterative computation of higher order corrections than are contained in the simple formulae provided here.

PLANETARY HEAT FLOW PARAMETERS

Tabulated values of the internal heating, albedo, and effective emission temperature provide important characterizations of the radiative-convective state of planetary atmospheres. These quantities are related by the heat balance relation:

$$E = I + L \tag{13a}$$

where

$$E = 4\pi a_e^2 \sigma T_e^4 \text{ , the power } \underline{\text{emission,}} \tag{13b}$$

$$I = \pi a_e^2 F_\odot (R/R_E)^{-2} (1-A) \text{ , the power } \underline{\text{insolation,}} \tag{13c}$$

$$L = 4\pi a_e^2 F \text{, the planet's internal } \underline{\text{luminosity,}} \tag{13d}$$

299

with $\sigma = 5.67 \times 10^{-5}$ mW m^{-2}K^{-4} designating the Stephen-Boltzmann constant, T_e the effective blackbody emission temperature, $F_\odot = 1.37 \times 10^6$ mW m^{-2} the solar flux constant at 1 A.U. (Willson et al., 1980), (R/R_E) the (heliocentric) planetary distance in A.U., $\underline{A}$ the Bond albedo, and F the planet's internal heat flux (as power per unit area). These relations (13a-d) neglect oblateness effects and complications related to the optical obscuration of planetary rings which are important for Saturn (cf. Hanel et al., 1983). For the case of a planet with an internal source, knowledge of both T_e and $\underline{A}$ permits the inferrence of the planet's self-luminosity or internal heat flux

$$F = \sigma T_e^4 - F_\odot (R/R_E)^{-2}(1-A)/4 \qquad (14)$$

The internal heat is also usefully characterized in terms of the ratio of emitted to insolated (or absorbed) power as

$$E/I = 4\sigma T_e^4 (R/R_E)^2 / [F_\odot(1-A)] \qquad (15)$$

Some researchers refer to the internal heating in terms of the fraction of solar input, sometimes denoted as

$$Q = (E/I - 1) = L/I \qquad (16)$$

A convenient expression for the conversion of internal heating in these terms to the flux (as power per unit area) may be written as

$$F = (E/I)^{-1}(E/I - 1)\sigma T_e^4 \quad , \qquad (17)$$

For the case of a planet with negligible internal heat source (14) reduces to

$$T_e \cong (279K)[(1-A)(R/R_E)^{-2}]^{1/4} \qquad (18)$$

so that knowledge of either one of T_e and $\underline{A}$ together with (R/R_E) permits the inference of the other.

The tabulated value for the very small but still measureable internal heat flux F for the Earth is from Zharkov and Trubitsyn (1978). Mars, Venus, and Titan may also have very small internal heating but it cannot be measured remotely from spacecraft. The internal heating values for Jupiter (Hanel et al., 1981) and Saturn (Hanel et al., 1983) are from the analysis of Voyager IRIS measurements. The internal heat flux values for Uranus and Neptune have been estimated by Pollack et al. (1986) from a combination of ground based and Voyager data. The values for F in the present table have been obtained from their values of $Q = (E/I-1)$ by application of equation (17). Tabulated values for E/I are from the same sources.

The Bond albedo $\underline{A}$ for the Earth is from a time and space mean analysis of observations from the Nimbus 7 spacecraft by Jacobowitz et al. (1984). The

300

Bond albedo for Mars is from an analysis of Mariner 9 infrared radiometric measurements by Kieffer et al. (1973) and confirms earlier ground-based photometric measurements by Irvine et al. (1968). The albedo value for Venus is from Pioneer Venus infrared radiometric measurements by Schofield and Taylor (1982). The value for Titan is derived from the effective temperature estimate of Lindal et al. (1983) by application of equation (18). Bond albedos for Jupiter and Saturn are from the Voyager IRIS analysis of Hanel et al. (1981, 1983). New estimates for Uranus and Neptune are from the work of Pollack et al. (1986).

The tabulated <u>effective</u> <u>temperature</u> values T_e are derived from the same sources as the Bond albedos, either by application of Eq. (18) (for Earth and Mars) or by reference to the separate specification of these by the authors of the papers cited for Titan, Jupiter, and Saturn. The tabulated value for the effective temperature of Neptune is taken as the upper limit estimated by Hanel et al. (1986) from Voyager IRIS measurements (rounded down to the nearest K) but is also within the error bounds on the number specified by Pollack et al. (1986).

It is also useful to evaluate the <u>emission</u> <u>pressure</u> <u>level</u> p_e corresponding to the emission temperature (sometimes called the "emission to space level") by reference to remotely retrieved or directly measured vertical structure profiles. The value for Earth is from the *U.S. Standard Atmosphere* (1976). The emission level for Mars is estimated in reference to an adopted model profile discussed below in the context of the surface temperature and pressure. The Venus emission level is determined by reference to *in situ* measurements of the pressure-temperature profile from Pioneer Venus probes by Seiff et al. (1980). The emission levels for Titan, Jupiter, Saturn, and Uranus are given by the same sources as referenced above for their measured albedo or effective temperature. The Neptune emission level is estimated from the radiative-convective model profile of Appleby (1986).

METEOROLOGICAL PARAMETERS

The <u>1-bar</u> <u>temperature</u> T_{1b} is tabulated as a useful reference level for the vertical structure profile of the atmosphere. (For the Jovian planets this is nearly the deepest level which can be reliably retrieved from Voyager radio occultation or IRIS data and is therefore a useful benchmark for adiabatic extrapolation to lower levels.) For the Earth T_{1b} nearly coincides with its surface temperature (cf. *U.S. Standard Atmosphere*, 1976). (Of course the Martian atmosphere has no such level.) The 1-bar level for Venus is estimated from the <u>in situ</u> measurements by Seiff et al. (1980). The 1-bar retrievals for Titan (Lindal et al. 1983) and for Jupiter and Saturn (Lindal et al., 1981, 1985) are from Voyager radio occultation measurements. The 1-bar temperature for Uranus is from Voyager IRIS retrievals by Hanel et al., 1986. The Neptune value is estimated from radiative-convective models by Appleby (1986).

The <u>surface</u> <u>temperature</u> and <u>pressure</u> (T_s and p_s) correspond to measurements of conditions at the solid surfaces of Earth, Mars, Venus, and Titan. The Earth values (from *U.S. Standard Atmosphere*) correspond to a time and space mean.

Determination of the time and space mean surface temperature for Mars is problematic. Diurnal, seasonal, as well as latitudinal variations are extreme, with temperatures ranging between 140 and 290 K. Kahn (1983) has assembled a cross section of diurnally averaged 20-μm brightness temperatures over latitude and L_S using Viking IRTM measurements from Martin et al. (1979) together with otherwise unpublished data supplied by private communication. The area-weighted, time averaged temperature for this cross section is about 207 K. Although the 20-μm channel is thought to provide a good measure of surface temperatures, this average may represent a slight underestimate of the actual mean surface value owing to the effect of measurements taken at non-zero emission angles. Although no Martian standard atmosphere is available, in a theoretical study of diurnal tides on Mars, Zurek (1976) offers a simple empirical model for the basic state temperature in the form

$$T_m(p) = 145K + (T_s - 145K) \exp[-\gamma ln(p_s/p)] \qquad (19)$$

where T_m is the mean (altitude-dependent) temperature, T_s and p_s are the surface temperature and pressure, and γ is a parameter related to the lapse rate. The high-altitude limit for this model gives a good fit to Viking lander descent data (cf. Seiff and Kirk, 1977). Zurek uses T_s = 220 K (as do many authors) and suggests that γ = 0.64 gives a good match to atmospheric lapse rates inferred from Mariner 9 IRIS measurements (Hanel et al., 1972). If, for average clear-air conditions, the Martian surface temperature is raised by a very weak greenhouse associated with the CO_2 absorption of its thin atmosphere, then the application of the Eddington approximation would indicate that

$$T_s = T_e (1 + 3\tau/4)^{1/4} \qquad (20)$$

where T_e is the effective emission temperature and τ the optical depth. τ = 0.1 may be taken as a lower limit value for the surface under clear conditions (according to Leovy, 1979). Then, with T_e = 210K as derived from the radiometric albedo measurement, Eq. (20) yields T_s = 214 K and coincidentally agrees with the average of the "canonical" value of 220 K and the IRTM result of 207K. On this (admittedly somewhat ad hoc) basis, the value of T_s ~ 214 is adopted for tabulation, although it is probably uncertain by as much as 8K from the actual time and space mean. (It is possible that on an average basis the radiative screening of the surface by residual air-borne dust largely compensates for the very weak greenhouse warming and produces a shallow inversion layer). Mars surface pressures also vary substantially with the seasons (because of the sublimation and evaporation of the South polar cap) and with the topographic elevation. A mean surface pressure value of p_s= 0.007 is estimated from Viking lander data (Ryan et al., 1978), adjusted for elevation with respect to the Mars geoid (cf. Seiff and Kirk, 1977). With these choices for the surface temperature and pressure, Zurek's (1976) model for the Martian pressure-temperature profile is modified to read

$$T_{Mars} (p) = 145K + (214-145)K (p/0.007bar)^{0.64} \qquad (21)$$

and has been used to derive the tabulated emission pressure corresponding to T_e.

The surface temperature and pressure for Venus are estimated from the Pioneer Venus probe measurements of Seiff et al. (1980).

The Jovian planets have no solid surfaces (except for relatively small rocky cores). For these the T_s and p_s are given instead as the estimated condensation level for water which, as a result of the associated latent heating and differentiation of mean molecular weight might act as a kind of (permeable) surface of strong buoyancy contrasts. Condensation levels are estimated by simple application of the integrated Clausius-Clapeyron equation which specifies that the saturation vapor pressure e_s changes with temperature according to

$$e_s = e_o \exp\left[(L_c m_v/R^*T_o)(1 - T_o/T)\right] \qquad (22)$$

where $e_o = 0.00611$ bar is the saturation vapor pressure of water at the triple-state temperature $T_o = 273$ K, L_c is the latent heat of condensation, m_v the molecular weight of vapor and $R^* = N_o k_B$ is the universal gas constant. (For water the factor $L_c m_v/R^*T_o \cong 20$.) The saturation vapor pressure can be expressed in terms of the molar mixing ratio of water f_{H_2O} using the partial pressure relation

$$e_s = (p - e_s)f_{H_2O} \cong p\, f_{H_2O} \qquad (23)$$

Neglecting the effects of latent heat and differentiated molecular weight on the adiabat, the temperature is assumed to increase with depth as

$$T = T_{1b}(p/1bar)^{R/c_p} \qquad (24)$$

where R is the gas constant for dry atmoshpere and c_p the specific heat at constant pressure. (Both quantities are discussed below.) Then using (23) and (24) to eliminate e_s and T in (22) gives

$$f_{H_2O} = (0.00611bar/p)\exp\left\{20[1 - (273K/T_{1b})(1bar/p)^{R/c_p}]\right\} \qquad (25)$$

for the variation of the saturated mixing ratio of water with depth. Above the lower base of the cloud condensation level, the water mixing ratio will be depleted with altitude as indicated by this last result and possibly more by the action of dynamics and microphysical processes (cf. Rossow, 1978). At sufficiently deep levels below the condensation level the molar ratio of the vapor is expected to be well mixed and approximately constant with increasing depth. The condensation level itself is expected to occur where the saturated mixing ratio as a function of the local temperature and pressure equals the value for the deep atmosphere. Unfortunately, the H_2O abundance for the deep atmospheres of the Jovian planets is unknown. The analysis of Voyager IRIS and ground based data by Bjoraker et al. (1986) suggests that at the 5 bar level it is a factor of 100 below the solar composition value. Levels below 7 bars are inaccessible to remote observation, however, so that condensation of larger molar fractions at deeper levels cannot be ruled out. Table values for T_s and p_s on the Jovian planets correspond to the solution of Eq. (25) for a molar ratio equal to three times the solar abundance value (cf. Cameron, 1982) so that $f_{H_2O} \cong 3.7 \times 10^{-3}$. This represents a solar enrichment factor comparable to that observed for CH_4 on Jupiter and Saturn. (cf. Gautier and Owen,

1983; Buriez and de Bergh, 1981.) It must be emphasized, however, that this is intended only as an illustrative example of the condensation parameters in the absence of any direct knowledge of the deep atmosphere.

The three most abundant <u>major gases</u> measured (or inferred) for each planetary atmosphere are listed along with their molar fractions. The measured ratios for the Earth's atmosphere are taken from Allen (1973). The major gas fractions for Mars are from an analysis of Viking lander data by Owen et al. (1977). The Venus gas fractions are those recommended by von Zahn et al. (1983) from a consideration of both Pioneer Venus and Venera spacecraft data. The approximate gas ratios for Titan have been inferred from a combination of Voyager IRIS and radio science data. The tabulated values are those suggested by Samuelson et al. (1981). The molar fractions for Jupiter are those derived from Voyager IRIS measurements by Conrath et al. (1984) as a revision of an earlier study by Gautier et al. (1981), also using the inferred CH_4/H_2 ratio of Gautier and Owen (1983). The molar fractions for Saturn are also taken from Conrath et al., 1984, together with the CH_4/H_2 ratio of Buriez and de Bergh (1981). The tabulated hydrogen and helium mole fractions for Uranus are the approximate results of a preliminary analysis of Voyager IRIS data by Hanel et al. (1986). The hydrogen-helium mole fractions of the Neptune atmosphere await precise measurement but are assumed to be roughly the same as the solar mixture (cf. Gautier and Owen, 1983).

The complex radiative, chemical, morphological, and microphysical properties of <u>clouds</u> in planetary atmosperes are still largely unknown. The present tabulation merely specifies the leading chemical constituents for the (upper level) clouds of each atmosphere. The probable three-component nature of Martian clouds and condensates is discussed by Pollack et al. (1977). The Venus clouds were identified as a highly concentrated solution of H_2SO_4 by Sill (1972) and Young and Young (1973). The haze and clouds of Titan are thought to be a complex mixture of hydrocarbons (cf. Kunde et al., 1981). The Jovian planets are thought to have both NH_3 and H_2O clouds, but the observations are still incomplete. (The current status of the relevant studies is reviewed by West, Strobel, and Tomasko, 1986.) Various metallic compounds such as MgH and SiH_4 may condense as clouds at pressure levels greater than 5000 bar (cf. Gierasch and Conrath, 1985) but are completely inaccessible to observation. It is likely that temperatures on Uranus and Neptune are cold enough to also effect the condensation of methane (cf. Atreya and Romani, 1985).

The <u>gas constant</u> R is given as the ratio of (the universal gas constant) $R^* = N_0 k_B = 8.314 \times 10^7$ g $cm^2 s^{-2} mol^{-1}$ (where N_0 is Avagadro's number and k_B is the Boltzmann constant) to the mean molecular weight per mole of the atmospheric gas mixture. The mean molecular weights and resulting value for R have been computed from a molar-weighted average as indicated by the inventory of major gas constituents specified by the references cited above.

c_p/R is the ratio of the molar specific heat at constant pressure to the gas constant. This is computed as

$$c_p/R = m\sum_i (f_i/m_i)(c_p/R)_i \qquad (26)$$

where f_i and m_i are respectively the molar fraction and molecular weight of the ith component and $m=R^*/R$ is the mean molecular weight of the total mixture. (The expression is derived from the assumption of an ideal gas mixture with a total specific heat equal to the molar weighted average of the specific heats of each of the components.) In the classical (high temperature) limit $(c_p/R)_i$ = $(2+n)/2$ where n is the total number of (translational, rotational, and vibrational) degrees of freedom of the molecules. Thus the ratio $(c_p/R)_i$ = 5/2, 7/2, or 9/2 in the classical limit for the case of a monatomic, diatomic, or triatomic gas respectively and is in good agreement with actual observations of the relevant gases at room temperature. (For pure methane, the ratio is taken to be 4.23 according to data in the 1980 CRC Handbook of Chemistry and Physics.) For the cold upper tropospheres of the Jovian planets, where $T \lesssim 300$ K, the molecular partition of internal energy and therefore the specific heat is significantly temperature dependent. The statistical ortho-para alignment of the hydrogenic protons also varies with temperature and adjusts to local equilibrium within a lag time that can be either as long as 10^9 s or much shorter, depending upon the presence of various catalyzing agents in the aerosols. Conrath and Gierasch (1984) have made a careful assessment of these effects in the context of the observations for Jupiter and Saturn. The size of the temperature-dependent effects on (c_p/R) for hydrogen is displayed in their Figure 9. (A similar plot for a Jovian hydrogen-helium mix is given by Conrath, 1986.) In view of the apparent variations, c_p/R = 3.3 is tabulated for Jupiter as a compromise between the minimum value for equilibrium hydrogen which would prevail for temperatures near the one bar level and the larger value in the high-temperature limit obtained near the 7 bar level below. For Saturn, Uranus, and Neptune, equilibrium hydrogen at the colder temperatures of their tropopause levels will have a higher c_p/R ratio than the high tempreature limit and an intermediate value of 3.6 is therefore adopted for tabulation.

The dry adiabatic lapse rate is computed as $\Gamma = g/c_p$ from the tabulated values for the mean acceleration of gravity $\langle g \rangle$, the gas constant R, and the ratio c_p/R. The tabulated results are rounded to the nearest tenth of a Kelvin per kilometer. This will be a slight overestimate of the true dry adiabatic lapse rate in the deep atmospheres of Venus and Titan owing to non-ideal gas effects there (cf. Seiff et al., 1980 and Lindal et al., 1983). On the Jovian planets, strong variations of g with latitude as outlined above will result in corresponding changes in the adiabat. Furthermore, variations in the hydrogen ortho-para spin state as well as the variation of the specific heat of a given state with temperature, will result in substantial changes in the dry adiabatic lapse rate with altitude.

The static stability $S = \Gamma + \partial T/\partial z$ is a measure of the bouyant restoring force acting on a parcel of atmosphere undergoing vertical displacements. The corresponding frequency of stable vertical oscillations is given by

$$N = (gS/T)^{1/2} \qquad (27)$$

and is called the Brunt-Väisälä frequency. The static stability will in general vary with both latitude and elevation. Tabulated values refer to

estimated averages over selected altitudes. The tabulated value for the Earth is from a global annual mass-weighted mean between 200 and 1000 mb computed by Stone and Carlson (1979). The tabulated value for Mars is estimated as an average over two logarithmic pressure intervals (or scale heights) above the surface by application of the model atmosphere Eq. (23). The result is in good agreement with results obtained by Mariner 9 IRIS retrievals (Hanel et al., 1972), radio occultation measurements (Rasool and Stewart, 1971), and *in situ* Viking Lander descent data (Seiff and Kirk, 1977). (During dust storm conditions, the static stability may be reduced by around a factor of two.) The static stability for Venus is estimated for levels just below the cloud level (at around 45 km altitude) from the *in situ* probe measurements of Seiff et al. (1980). The value for Titan is estimated as the mean tropospheric stability indicated by the radio occultation measurements of Lindal et al. (1983). Tropospheric static stabilities for the Jovian atmospheres are exceedingly difficult to measure. Voyager radio occultation retrievals for Jupiter are nearly indistinguishable from the dry adiabat at levels below 1 bar. There is, however, an indirect inference of Jupiter's effective static stability based upon a mixing length theory for the transport of the planet's internal heat in the presence of ortho-para hydrogen conversion processes. Conrath and Gierasch (1984) have concluded that the Brunt frequency for vertical oscillations with frozen composition in an adiabatic equilibrium mean structure (expected to prevail below the 600 mb level) is constrained to approximately 2×10^{-3} s^{-1} at 1 bar. The application of Eq. (27) to this result, together with tabulated values for g and T_{1b} implies a static stability of 0.03 K km^{-1}. The mixing length model also implies a rapid reduction in the stability with increasing depth. The tabulated value may therefore be regarded as an upper limit for levels below 1 bar in the absence of other phase change processes. Radio occultation measurements of lapse rates on Saturn between the 0.7 and 1.3 bar level (Lindal et al., 1985) imply a static stability of approximately 0.05 K km^{-1} when compared with a dry adiabat for dry normal hydrogen with a 3:1 ortho-para ratio. Since an equilibrium mixture will have a higher specific heat and therefore a lower adiabatic lapse rate, this result may also be regarded as an upper limit to the actual stability at that level.

The <u>scale height</u> H = RT/g where R is the gas constant, T the local temperature, and g the local gravity corresponds to an e-folding pressure depth of atmosphere. Values are computed for all planets at both the emission level and the surface (or estimated water condensation level on the Jovian planets) using the respective entries in the table.

The <u>meridional thermal gradient</u> (in Kelvins per 1000 km) is a useful scaling parameter for the analysis of the zonal momentum balance associated with large scale flows. The tabulated value for the Earth is estimated from the equator-to-pole drop at 500 mb as depicted in the Northern Hemisphere Winter cross section of Lorenz (1967). The value for Mars is estimated for the 7.6 km altitude (where the pressure is half the surface value) from the thermal cross section of Mariner 9 IRIS retrievals presented by Pollack et al. (1981). The meridional thermal gradient for Venus is estimated for the level of the main cloud deck (near 100 mb or 65 km altitude) from Pioneer Venus radio occultation data presented by Newman et al. (1984). The meridional gradient for Titan is

estimated from the Voyager IRIS brightness temperature analysis of Flasar et al. (1981) and refers to the 100 mb level. Meridional thermal gradients for Jupiter and Saturn have not been directly observed except above the cloud levels where the thermal wind analysis of Pirraglia et al. (1981) suggest a reduction of flow speeds with altitude. Nevertheless, estimates based on their measurements are adopted for tabulation and refer to changes over the horizontal scale of the jets.

The <u>radiative time constant</u>

$$\tau_{Rad} = (c_p\rho T)/(\sigma T_e^4/H) = (pT)/\Gamma\sigma T_e^4 \tag{28}$$

is equivalent to the ratio of the thermal energy content of the atmosphere (per unit volume) to the radiative heating rate for one local scale height (per unit volume). Values are computed at both the p_e and p_s levels using the required information in the table.

The <u>vertical eddy mixing coefficient</u> κ (a.k.a. diffusion, viscosity, or exchange coefficient) is one of the most notorious parameters ever to be employed in the atmospheric sciences. It represents an attempt to parameterize the transport of conserved quantities by analogy to molecular dissipation and suffers from vexing uncertainties as to its size, spatial variation, and differences in application to heat, momentum, and trace constituents. Nevertheless, it finds essential application to such apparently different subjects as boundary layer theory and stratospheric chemistry. Fixing attention on purely vertical transport in the absence of any external forces, the idea is to represent the conservation of some quantity J as

$$\rho\partial J/\partial t = -\partial/\partial z[\rho(wJ - \kappa\partial J/\partial z)] \tag{29}$$

where ρ is the density, t and z are time and altitude coordinates, w is vertical velocity and the mixing coefficient

$$\kappa = \langle w'J'\rangle/(\partial\langle J\rangle/\partial z) \tag{30}$$

where w' and J' are the eddy fluctuations of vertical velocity and J. (The angle brackets denote a suitably defined average.) The scaling of these relations suggests that

$$\kappa \sim w'D \tag{31}$$

and
$$\tau_e \sim D^2/\kappa \tag{32}$$

where D is the characteristic vertical scale of the transport (often the scale height) and τ_e denotes the eddy "turn-over" time scale. One person's eddy mixing is another's up (and down) draft. While for most applications meteorologists attempt to minimize their reliance on κ by explicit account of w, aeronomers often seek to absorb all vertical transport into a single eddy diffusion coefficient which includes large-scale motions as well as small-scale turbulence. (An excellent review of this subject from the aeronomical viewpoint is given by Hunten, 1975.) Horizontal transports are also sometimes parameterized with horizontal exchange coefficients. These are often much

larger (for global scales) than the vertical coefficients but are even more problematic and will not be considered any further here. For specific applications it is important to distinguish between the diffusion of heat and momentum, since certain atmospheric eddy motions may transport one more efficiently than the other. This difference is sometimes expressed in terms of the Prandtl number P, defined as the ratio of the momentum diffusion coefficient to the heat diffusion coefficient. Several studies have shown, however, that for many atmospheric applications the Prandtl number is of order unity. For example, in the terrestrial boundary layer P=0.7, according to Sutton (1953). Assuming this is the case, the eddy mixing coefficient for planetary atmospheres may be estimated from a variety of recipes applicable to specific types of observations. A number of similarity relations are given by Priestley (1959). One especially important application for rapidly rotating planets with solid surfaces is the analysis of the Ekman wind spiral within the lower boundary layer (cf. Holton, 1979). This theory accounts for the observed turning of the wind vector with altitude by 45 deg between the surface and the geostrophic level aloft within a characteristic depth

$$D_E = \pi(2\kappa/f)^{1/2} \ . \tag{33}$$

(Here f is the Coriolis parameter and is defined below.) Inference of this characteristic Ekman depth therefore yields a value for the strength of the eddy mixing. For applications to the very different context of Jovian atmospheres, useful estimates of eddy mixing may be made by application of the mixing length theory for the transport of heat in stellar interiors (cf. Clayton, 1983). This specifies that the mixing required to support the internal heat flux F is given as

$$\kappa = H(FR^2T/c_pp)^{1/3} \tag{34}$$

where it has been assumed that the mixing length is given by the pressure scale height H. Equations (33) and (34) are only two different examples out of many other methods for determining the eddy mixing coefficient including the theory of tidal waves, the diagnostic analysis of heat and momentum balances for observed winds and temperatures, and solutions of diffusion models for the best match to observed chemical tracer abundances.

The tabulated vertical eddy mixing coefficient for the Earth is estimated from the application of Eq. (33) to observed Ekman layer depths at Jacksonville, Florida by Brown (1970). The result is one-half the value recommended by Hunten (1975) based on aeronomical considerations. Above the terrestrial tropopause Hunten suggests that the mixing coefficient drops rapidly to a minimum of 2500 cm^2s^{-1}, then increases gradually with height, and this number is also appended in the table for stratospheric applications. Leovy and Zurek (1979) have used the Ekman layer theory to fit diurnally averaged wind and pressure variations on Mars observed by Viking Lander 2 and infer an eddy viscosity of about 10^5 cm^2s^{-1}. French and Gierasch (1979) have applied a viscous boundary layer model to the Martian polar vortex and obtain a good match of calculated surface stress to observations of eolian wind streak features in the polar region with the choice of 10^6 cm^2s^{-1}. The tabulated

value of 5×10^5 for the Mars eddy mixing coefficient is taken as a compromise between these two results and is the same as the value adopted by Kahn (1983). An estimated upper limit for the eddy mixing coefficient in the Venus atmosphere is derived from the scaling analysis for a meridional circulation model for the equatorial super-rotation by Gierasch (1975). This value is in good agreement with the inferrence of $\kappa = 1.3 \times 10^5$ from measurements of the vertical haze distribution observed by Pioneer Venus photopolarimeter limb scans as derived by Lane and Opstbaum (1983). The upper limit on the eddy mixing in Titan's atmosphere is derived by Flasar et al. (1981) as a diagnostic analysis of meridional flow balances implied by Voyager IRIS observations. Eddy mixing coefficients for the Jovian tropospheres are derived from the application of the mixing length expression of Eq. (34) to tabulated values for T_s, p_s, and the internal heat flux. Moist convection (cf. Gierasch, 1976) and ortho-para conversion processes (cf. Conrath and Gierasch, 1984) may act to reduce the strength of these large mixing coefficients by several orders of magnitude on scales smaller than the horizontal eddies associated with the zonal flow. Lewis and Fegley (1984) have argued, however, that vertical motions associated with the zonal winds may themselves produce vertical transports corresponding to eddy coefficients of nearly the same size as predicted by Eq. (34). It is important to understand that in such a case the "weather" produces the mixing and not the reverse. As for the Earth, the statically stable stratosphere overlying the emission level on the Jovian planets will be associated with a region of greatly reduced mixing compared with that of the deep atmosphere. Conrath and Pirraglia (1983) have argued that the reduction of the cloud-top winds with altitude inferred from the thermal wind shear may be understood in terms of a forced mean merdional circulation with eddy friction and radiative damping. Flasar (1986) has pointed out that the implied vertical damping scale suggests that the time scales for both dissipative processes is of comparable magnitude. Eddy mixing coefficients for the lower stratospheres of Jupiter and Saturn are therefore estimated by application of Eq. (32) with $\tau_e = \tau_{rad}$ and D = H as evaluated at the emission level. The results are comparable to eddy diffusion coefficients employed by Strobel (1986) to describe the vertical distribution of photochemical constituents.

The <u>Coriolis parameter</u> <u>f</u> = $2\Omega\sin\phi$ (where $\Omega = 2\pi/\tau_{rot}$) is the component of planetary vorticity normal to the local level surface (for latitude ϕ in planetographic coordinates). Tabulated values are determined for 30 deg latitude.

The <u>beta parameter</u> $df/d(a\phi) = (2\Omega/a)\cos\phi$ is the local planetary vorticity gradient. Tabulated values are determined for the equator.

The <u>characteristic weather length</u> <u>L</u> is used here to denote an estimate of the horizontal wavelength of meteorological features (pressure, temperature, and wind variations) divided by 2π. This amounts to a measure of the reciprocal horizontal (dimensional) wavenumber and is useful for estimating the horizontal derivative of meteorological field variables in the scaling analysis of the equations of motion. For the Earth, the tabulated value for L=1000km is chosen as a characteristic measure of the scale of zonal midlatitude variations in temperature and pressure (high and low centers). It corresponds to a

midlatitude zonal wavenumber of 6 at the high altitude jet stream latitude
(around 30 deg) as evident in hemispheric isobaric and isothermal cross-
sections (e.g. Palmen and Newton, 1969). The same zonal wavenumber is
evidenced in the spacing of midlatitude cloud forms as apparent, for example,
in the southern hemisphere of the "blue marble" Apollo 8 photo of Earth from
space. Thus $L = a_e\cos(30°)/6 \approx 920$km. The length scale may also be estimated
as the peak-to-peak separation of the northern and southern hemispheric 500 mb
jet streams (both at around latitude 30 deg for solstice conditions, as
depicted by Mintz, 1954), again divided by 2π. By this meridional reckoning,
therfore, $L = 2(30°/180°)(a_e/2) = 1060$km, in agreement with the zonal value.
For Mars, L can be similarly estimated from the observed zonal wavenumber 4-6
associated with the passage of high and low pressure centers at the Viking
Lander 2 site (Ryan et al., 1978). Then for Mars $L = a_e\cos(48°)/4 \approx 600$km. A
meridional estimate of the length scale on Mars may be inferred from the
thermal wind field presented by Pollack et al. (1981). This shows a high-
altitude jet stream at latitude 50 deg so that by analogy to the estimate for
the Earth $L = 2(50°/180°)(a_e/2) = 940$km in fair agreement with the zonal
determination. The tabulated length scale for Venus, L = 6000km, is inferred
from the visually obvious zonal wavenumber 1 "Y-feature" in the clouds (Belton
et al., 1976). Thus, the length scale for Venus is the same as the planet's
radius. This is also consistent with the qualitative character of the zonal
wind profile with latitude: a single super-rotating jet from pole-to-pole,
symmetric about the equator. (Cloud tracked wind data presented by Rossow in
1985 also shows evidence for superimposed mid-latitude jets which may be
associated with a secondary smaller length scale.) Voyager IRIS measurements
of meridional thermal gradients on Titan are the only presently available
evidence for atmospheric motions there, and show no sign of longitudinal
variation. The analysis of these data by Flasar et al. (1981) suggest the
presence of a cyclostrophic flow regime similar to that observed on Venus.
This inferrence and the qualitatively monotonic equator-to-pole thermal
gradient tentatively suggests a characteristic length scale for Titan equal
to its radius, so that L is estimated to be ~3000 km but is sufficiently
uncertain to warrant a question mark. The length scale for Jupiter is
estimated as the width of a jet-stream pair (as measured, for example, by
Limaye, 1986) divided by 2π. The same estimation method is applied to Saturn,
with observations reported by Ingersoll et al. (1984). Smith et al. (1986)
have presented a latitudinal extrapolation of Voyager imaging measurements of
drift speeds on Uranus suggesting a single prograde jet between 20 deg
latitude and the pole. Taking this interval as a measure of one-half
wavelength implies a horizontal scale L = 10,000km for Uranus. Horizontal
scale measurents for Neptune must await the Voyager encounter in 1989.

The characteristic weather speed is given for both midlatitude and equatorial
locations. (A plus sign designates prograde flow with respect to the planet's
rotation, a minus sign retrograde flow.) Values for the Earth are estimated as
the mean of Northern Winter and Southern Summer measurements at the 500mb level
reported by Mintz (1954). The midlatitude Mars value is estimated from the
thermal wind cross section of Pollack et al. (1981) as the average of the jet
maxima at the 7.6 km (half pressure) altitude in the Northern and Southern
Hemispheres. No equatorial wind measurement is available for Mars. Venus wind
speeds are from cloud-tracked drift measurements reported by Rossow (1985).

310

These are independently confirmed by Doppler tracking measurements of the Pioneer Venus probes (Counselman et al., 1980) and the cyclostrophic wind analysis of radio occultation data by Newman et al. (1980). The Titan wind speed at 45 deg latitude and the 100mb (tropopause) level is taken from the thermal wind analysis of Flasar et al. (1981). Wind speeds for Jupiter (estimated from results by Limaye, 1986) and Saturn (from Ingersoll et al., 1984) are for the cloud-tracked wind level (probably no more than a scale height above the 1-bar level). The midlatitude wind speed for Uranus is taken as the maximum of the extrapolated fit to Voyager cloud tracked wind measurements given by Smith et al. (1986). No equatorial wind speeds for Uranus are available although the extrapolation of available data suggest retrograde velocities there. The tabulated wind speed for Neptune is from differential drift rates implied by atmospheric periodicities reported by Belton et al. (1981). This is assumed to apply to midlatitudes but is of uncertain interpretation.

REFERENCES

Allen, C. W. (1973). *Astrophysical Quantities (Third Edition)*. The Athlone Press, London.

Ananda, M. P., W. L. Sjogren, R. J. Phillips, R. N. Wimberly, and B. G. Bills (1980). A low-order global gravity field of Venus and dynamical implications. *J. Geophys. Res.* 85, 8303-8318.

Appelby, J. F. (1986). Radiative-convective equilibrium models of Uranus and Neptune. *Icarus* 65, 383-405.

Ashbrook, J. (1953). A new determination of the rotation period of the planet Mars. *Astron. J.* 58, 145-155.

The Astronomical Almanac. (1984-1986). U.S. Government Printing Office, Washington D.C.

Atreya, S. K. and P. N. Romani (1985). Photochemistry and clouds of Jupiter, Saturn and Uranus. In *Recent Advances in Planetary Meteorology* (G. E. Hunt, Ed.) pp. 17-68. Cambridge University Press, Cambridge.

Beatty, J. K., B. O'Leary, A. Chaiken (1982). *The New Solar System* (Second Edition). Sky Publishing Corporation, Cambridge.

Belton, M. J. S., G. R. Smith, D. A. Elliot, K. Klaasen, and G. E. Danielson (1976). Space-time relationships in the UV markings on Venus. *J. Atmos. Sci.* 33, 1383-1393.

Belton, M. J. S., L. Wallace, and S. Howard (1981). The periods of Neptune: evidence for atmospheric motions. *Icarus* 46, 263-274.

Bjoraker, G. L., H. P. Larson, and V. G. Kunde (1986). Water vapor in Jupiter's atmosphere. In *the Jovian Atmospheres* (this volume) pp. 48-52.

Brown, R. A. (1970). A secondary flow model for the planetary boundary layer. *J. Atmos. Sci.* <u>27</u>, 742–757.

Buriez, J. C. and C. de Bergh (1981). A study of the atmosphere of Saturn based on methane line profiles near 1.1 μm. *Astron. Astrophys.* <u>94</u>, 382–390.

Cameron, A. G. W. (1982). Elementary and nuclido abundances in the solar system. In *Essays in Nuclear Astrophysics* (C. A. Barnes, D. D. Clayton, and D. N. Schramm, Eds.) pp. 23–43. Cambridge University Press, Cambridge.

Christensen, E. J. (1975). Martian topography derived from occultation, radar, spectral, and optical measurements. *J. Geophys. Res.* <u>80</u>, 2909–2913.

Clayton, D. D. (1983). *Principles of Stellar Evolution and Nucleosynthesis*. The University of Chicago Press, Chicago.

Conrath, B. J. (1986). Parahydrogen equilibration in the atmospheres of the outer planets. In *The Jovian Atmospheres* (this volume) pp. 5–18.

Conrath, B. J. and P. J. Gierasch (1984). Global variation of the para hydrogen fraction in Jupiter's atmosphere and implications for dynamics on the outer planets. *Icarus* <u>57</u>, 184–204.

Conrath, B. J. and J. A. Pirraglia (1983). Thermal structure of Saturn from Voyager infrared measurements: implications for atmospheric dynamics. *Icarus* <u>53</u>, 286–292.

Conrath, B. J., D. Gautier, R. A. Hanel, and J. S. Hornstein (1984). The helium abundance of Saturn from Voyager measurements. *Astrophys. J.* <u>282</u>, 807–815.

Counselman III, C. C., S. A. Gourevitch, R. W. King, and G. B. Loriot (1980). Zonal and meridional circulation of the lower atmosphere of Venus determined by radio interferometry. *J. Geophys. Res.* <u>85</u>, 8026–8030.

CRC Handbook of Chemistry and Physics. 61st Edition. (1980). West, R. C. and M. J. Astle (Eds.) CRC Press, Inc., Boca Raton.

Davies, M. E., V. K. Abalakin, C. A. Cross, R. I. Duncombe, H. Masursky, B. Morando, T. C. Owen, P. K. Seidelmann, A. T. Sinclair, G. A. Wilkins, and Y. S. Tjuflin (1980). Report of the IAU working group on cartographic coordinates and rotational elements of the planets and satellites. *Celestial Mech.* <u>22</u>, 205–230.

Desch, M. D. and M. L. Kaiser (1981). Voyager measurements of the rotation period of Saturn's magnetic field. *Geophys. Res. Lett.* <u>8</u>, 253–256.

Duncan, R. A. (1971). Jupiter's rotation. *Planet. Space. Sci.* <u>19</u>, 391–398.

Elliot, J. L., R. G. French, J. A. Frogel, J. H. Elias, D. J. Mink, W. Liller (1981). Orbits of nine Uranian rings. *Astron. J.* <u>86</u>, 444–455.

Flasar, F.M. (1986). Global dynamics and thermal structure of Jupiter's atmosphere. In *The Jovian Atmospheres* (this volume), pp. 119–123.

312

Flasar, F. M., R. E. Samuelson, and B. J. Conrath. Titan's atmosphere: temperature and dynamics (1981). *Nature* 292, 693-698.

Franklin, F. A., C. C. Avis, G. Colombo, and I. I. Shapiro (1980). The geometric oblateness of Uranus. *Astrophys. J.* 236, 1031-1034.

French, R. G. and P. J. Gierasch (1979). The Martian polar vortex: theory of seasonal variation and observations of eolian features. *J. Geophys. Res.* 84, 4634-4642.

Gapcynski, J. P., R. H. Tolson, and W. H. Michael, Jr. (1977). Mars gravity field: combined Viking and Mariner 9 results. *J. Geophys. Res.* 82, 4325-4327.

Gautier, D., B. Conrath, F. M. Flasar, R. Hanel, Y. Kunde, A. Chedin, and N. Scott (1981). The helium abundance of Jupiter from Voyager. *J. Geophys. Res.* 86, 8713-8720.

Gautier, D. and T. Owen (1983). Cosmogonical implications of elemental and isotopic abundances in atmospheres of the giant planets. *Nature* 304, 691-694.

Gehrels, T., L. R. Baker, E. Beshore, C. Blenman, J. J. Burke, N. D. Castillo, B. Da Costa, J. Degewij, L. R. Doose, J. W. Fountain, J. Gotobed, C. E. KenKnight, R. Kingston, G. McLaughlin, R. McMillan, R. Murphy, P. H. Smith, C. P. Stoll, R. N. Strickland, M. G. Tomasko, M. P. Wijesinghe, D. L. Coffeen, L. Esposito. (1980). Imaging photopolarimeter on Pioneer Saturn. *Science* 207, 434-439.

Gierasch, P. J. (1975). Meridional circulation and the maintenance of the Venus atmospheric rotation. *J. Atmos. Sci.* 32, 1038-1044.

Gierasch, P. J. (1976). Jovian meteorology: Large-scale moist convection. *Icarus* 29, 445-454.

Gierasch, P. J. and B. J. Conrath (1985). Energy conversion processes in the outer planets. In *Recent Advances in Planetary Meteorology* (G. E. Hunt, Ed.) pp. 121-146.

Gill, J. R. and B. L. Gault (1968). A new determination of the orbit of Triton, pole of Neptune's equator, and mass of Neptune. *Astron. J.* 73, 595.

Hanel, R., B. Conrath, W. Hovis, V. Kunde, P. Lowman, W. Maguire, J. Pearl, J. Pirraglia, C. Prabhakara, B. Schlachman, G. Levin, P. Straat, and T. Burke (1972). Investigation of the Martian environment by infrared spectroscopy on Mariner 9. *Icarus* 17, 423-442.

Hanel, R. A., B. J. Conrath, L. Herath, V. G. Kunde, and J. A. Pirraglia (1981). Albedo, internal heat and energy balance of Jupiter: Preliminary results of the Voyager infrared investigation. *J. Geophys. Res.* 86, 8705-8712.

Hanel, R. A., B. J. Conrath, V. G. Kunde, J. C. Pearl, and J. A. Pirraglia (1983). Albedo, internal heat flux, and energy balance of Saturn. *Icarus* 53, 262-285.

Hanel, R. A., B. Conrath, F. M. Flasar, V. Kunde, W. Maguire, J. Pearl, J. Pirraglia, R. Samuelson, D. Cruikshank, D. Gautier, P. Gierasch, L. Horn, P. Schulte (1986). Infrared observations of the Uranian system. *Science* 233, 70-74.

Harris, A. W. (1984). Physical properties of Neptune and Triton inferred from the orbit of Triton. In *Uranus and Neptune* (J. Bergstralh, Ed.), pp. 357-373. NASA CP 2330.

Holton, J. R. (1979). *An Introduction to Dynamic Meteorology* (Second Edition). Academic Press, New York

Hubbard, W. B. (1977). de Sitter's theory flattens Jupiter. *Icarus* 30, 311-313.

Hubbard, W. B. (1984a). *Planetary Interiors*. Van Nostrand Reinhold Company, New York.

Hubbard, W. B. (1984b). Interior structure of Uranus. In *Uranus and Neptune* (J. Bergstralh, Ed.), pp. 291-325. NASA CP 2330.

Hubbard, W. B. (1986). On the oblateness and rotation rate of Neptune's atmosphere. In *the Jovian Atmospherers* (this volume) pp. 264-274.

Hubbard, W. B., H. P. Avey, B. Carter, J. Frecker, H. H. Fu, J.-A. Gehrels, T. Gehrels, D. M. Hunten, H. D. Kennedy, L. A. Lebofsky, K. Mottram, T. Murphy, A. Nielsen, A. A. Page, H. J. Reitsema, B. A. Smith, D. J. Tholen, B. Varnes, F. Vilas, M. D. Waterworth, H. H. Wu, B. Zellner (1985). Results from observations of the 15 June 1983 occultation by the Neptune system. *Astron. J.* 90, 655-667.

Hunten, D. M. (1975). Vertical transport in atmospheres. In *Atmospheres of Earth and the Planets*. (B. M. McCormac, Ed.) D. Riedel Publishing Company, Dordrecht-Holland.

Ingersoll, A. P., R. F. Beebe, B. J. Conrath, and G. E. Hunt (1984). Structure and dynamics of Saturn's Atmosphere. In *Saturn* (T. Gehrels and M. S. Matthews, Eds.), pp. 195-238. Univ. of Arizona Press, Tucson.

Irvine, W. M., T. Simon, D. H. Menzel, J. C. Piloos, and A. T. Young (1968). Multicolor photoelectric photometry of the brighter planets. III. Observations from Boyden Observatory. *Astron. J.* 73, 809-828.

Jacobowitz, H., R. J. Tighe, and the Nimbus 7 ERB Experiment Team (1984). The Earth radiation budget derived from the Nimbus 7 experiment. *J. Atmos. Sci.* 89, 4997-5010.

Kahn, R. (1983). Some observational constraints on the global-scale wind systems of Mars. *J. Geophys. Res.* 88, 10189-10209.

Kieffer, H. H., S. C. Chase, E. Miner, G. Munch, and G. Neugebauer (1973). Preliminary report on infrared radiometric measurements from the Mariner 9 spacecraft. *J. Geophys. Res.* 78, 4291-4312.

Kunde, V. G., A. C. Arkin, R. A. Hanel, D. E. Jennings, W. C. Maguire, and R. E. Samuelson. C_4H_2, HC_3N, and C_2N_2 in Titan's atmosphere. *Nature* 292, 686-688.

Lane, W. A. and R. Opstbaum (1983). High altitude Venus haze from Pioneer Venus limbscans. *Icarus* 54, 48-58.

Leovy, C. B. (1979). Martian meteorology. In *Ann. Rev. Astron. Astrophys.* 17, 387-413.

Leovy, C. B. and R. W. Zurek (1979). Thermal tides and Martian dust storms: direct evidence for coupling. *J. Geophys. Res.* 84, 2956-2698.

Lewis, J. S. and M. Bruce Fegley, Jr. (1984). Vertical distribution of disequilibrium species in Jupiter's atmosphere. *Space Sci. Rev.* 39, 163-192.

Limaye, S. S. (1986). Jupiter: new estimates of the mean zonal flow at the cloud level. *Icarus* 65, 335-352.

Lindal, G. F., G. E. Wood, G. S. Levy, J. D. Anderson, D. N. Sweetnam, H. B. Hotz, B. J. Buckles, D. P. Holmes, P. E. Dorns, V. R. Eshleman, G. L. Tyler, and T. A. Croft (1981). The atmsophere of Jupiter: an analysis of Voyager radio occultation measurements. *J. Geophys. Res.* 86, 8721-8727.

Lindal, G. F., G. E. Wood, H. B. Hotz, and D. N. Sweetnam (1983). The atmosphere of Titan: an analysis of the Voyager 1 radio occultation measurements. *Icarus* 53, 348-363.

Lindal, G. F., D. N. Sweetnam, and V. R. Eshleman (1985). The atmosphere of Saturn: an analysis of the Voyager radio occultation measurements. *Astron. J.* 90, 1136-1146.

Lorenz, E. N. (1967). *The Nature and Theory of the General Circulation of the Atmosphere.* Geneva, World Meteorological Organization.

Martin, T., A. Peterfreund, E. Miner, H. Kieffer, and G. Hunt (1979). Thermal infrared properties of the Martian atmosphere, 1 Global behavior at 7,9,11 and 20 m. *J. Geophys. Res.* 84, 2830-2842.

Mintz, Y. (1954). The observed zonal circulation of the atmosphere. *Bull. Am. Met. Soc.* 35, 208-214.

Newman, M., G. Schubert, A. J. Kliore, and I. R. Patel (1984). Zonal winds in the middle atmosphere of Venus from Pioneer Venus radio occultation data. *J. Atmos. Sci.* 41, 1901-1913.

Null, G. W. (1976). Gravity field of Jupiter and its satellites from Pioneer 10 and Pioneer 11 tracking data. *Astron. J.* 81, 1153-1161.

Null, G. W., E. L. Lau, E. D. Biller, and J. D. Anderson (1981). Saturn gravity results obtained from Pioneer 11 tracking data and Earth-based Saturn satellite data. *Astron. J.* 86, 456-468.

Owen, T., K. Biemann, D. R. Rushneck, J. E. Biller, D. W. Howarth, and A. L. Lafleur. The composition of the atmosphere at the surface of Mars. *J. Geophys. Res.* 82, 4635-4639.

Palmen, E. and C. W. Newton (1969). *Atmospheric Circulation Systems*. Academic Press, New York.

Pettengill, G. H., E. Eliason, P. G. Ford, G. B. Loriot, H. Masursky, and G. E. McGill (1980). Pioneer Venus radar results: altimetry and surface properties. *J. Geophys. Res.* 85, 8261-8270.

Pirraglia, J. A., B. J. Conrath, M. D. Allison, and P. J. Gierasch (1981). Thermal structure and dynamics of Saturn and Jupiter. *Nature* 292, 677-679.

Pollack, J. B., D. Colburn, R. Kahn, J. Hunter, W. Van Camp, C. E. Carlston, and M. R. Wolf (1977). Properties of aerosols in the Martian atmosphere, as inferred from Viking Lander imaging data. *J. Geophys. Res.* 82, 4479-4496.

Pollack, J. B., C. B. Leovy, P. W. Greiman, Y. Mintz (1981). A Martian general circulation experiment with large topography. *J. Atmos. Sci.* 38, 3-29.

Pollack, J. B., K. Rages, K. H. Baines, J. T. Bergstralh, D. Wenkert, and G. E. Danielson (1986). Estimates of the bolometric albedos and radiation balance of Uranus and Neptune. *Icarus* 65, 442-466.

Priestly, C. H. B. (1959). *Turbulent Transfer in the Lower Atmosphere*. The University of Chicago Press, Chicago.

Rasool, S. I. and R. W. Stewart (1971). Results and interpretation of the S-band occultation experiments on Mars and Venus. *J. Atmos. Sci.* 28, 869-878.

Rossow, W. B. (1978). Cloud microphysics: Analysis of the clouds of Earth, Venus, Mars, and Jupiter. *Icarus* 36, 1-50.

Rossow, W. B. (1985). Atmospheric circulation of Venus. *Adv. Geophys.* 28A, 347-379.

Ryan, J. A., R. M. Henry, S. L. Hess, B. B. Leovy, J. E. Tillman, and C. Walcek (1978). Mars meteorology: three seasons at the surface. *Geophys. Res. Lett.* <u>5</u>, 715-718.

Samuelson, R. E., R. A. Hanel, V. G. Kunde, and W. C. Maguire (1981). Mean molecular weight and hydrogen abundance of Titan's atmosphere. *Nature* <u>292</u>, 688-693.

Schofield, J. T. and F. W. Taylor (1982). Net global thermal emission from the Venusian atmosphere. *Icarus* <u>52</u>, 245-262.

Seiff, A. and D. B. Kirk (1977). Structure of the atmosphere of Mars in Summer at midlatitudes. *J. Geophys. Res.* <u>82</u>, 4364-4378.

Seiff, A., D. B. Kirk, R. E. Young, R. C. Blanchard, J. T. Findlay, G. M. Kelly, and S. C. Sommer (1980). Measurements of thermal structure and thermal contrasts in the atmosphere of Venus and related dynamical observations: results from the four Pioneer Venus probes. *J. Geophys. Res.* <u>85</u>, 7903-7933.

Shapiro, I. I., D. B. Campbell, and W. M. DeCampli (1979). Nonresonance rotation of Venus? *Ap. J. Lett.* <u>230</u>, L123-L126.

Sill, G. T. (1972). Sulfuric acid in the Venus clouds. *Comm. Lunar Planet. Lab.* <u>9</u>, 191-198.

Smith, B. A., L. Soderblom, R. Beebe, J. Boyce, G. Briggs, A. Bunker, S. A. Collins, C. J. Hansen, T. V. Johnson, J. L. Mitchell, R. J. Terrile, M. Carr, A. F. Cook II, J. Cuzzi, J. B. Pollack, G. E. Danielson, A. Ingersoll, M. E. Davies, G. E. Hunt, H. Masursky, E. Shoemaker, D. Morrison, T. Owen, C. Sagan, J. Veverka, R. Strom, V. E. Suomi (1981). Encounter with Saturn: Voyager 1 imaging science results. *Science* <u>212</u>, 163-191.

Smith, B. A., L. A. Soderblom, R. Beebe, D. Bliss, J. M. Boyce, A. Brahic, G. A. Briggs, R. H. Brown, S. A. Collins, A. F. Cook II, S. K. Croft, J. N. Cuzzi, G. E. Danielson, M. E. Davics, T. E. Dowling, D. Godfrey, C. J. Hansen, C. Harris, G. E. Hunt, A. P. Ingersoll, T. V. Johnson, R. J. Krauss, H. Masursky, D. Morrison, T. Owen, J. B. Plescia, J. B. Pollack, C. C. Porco, K. Rages, C. Sagan, E. M. Shoemaker, L. A. Sromovsky, C. Stoker, R. G. Strom, V. E. Suomi, S. P. Synnot, R. J. Terrile, P. Thomas, W. R. Thompson, J. Veverka (1986). Voyager 2 in the Uranian system: imaging science results. *Science* <u>233</u>, 43-64.

Stone, P. H. and J. H. Carlson (1979). Atmospheric lapse rate regimes and their parameterization. *J. Atmos. Sci.* <u>36</u>, 415-423.

Strobel, D. F. (1986). Photochemistry of the Jovian atmosphere. In *The Jovian Atmospheres* (this volume) pp. 45-47.

Sutton, O. G. (1953). *Micrometeorology: A Study of Physical Processes in the Lowest Layers of the Earth's Atmosphere*. McGraw-Hill Book Company, New York.

Tyler, G. L., V. R. Eshleman, J. D. Anderson, G. S. Levy, G. F. Lindal, G. E. Wood, T. A. Croft (1981). Radio science investigations of the Saturn system with Voyager 1: preliminary results. *Science* 212, 201-266.

Tyler, G. L., D. N. Sweetnam, J. D. Anderson, J. K. Campbell, V. R. Eshleman, D. P. Hinson, G. S. Levy, G. F. Lindal, E. A. Marouf, R. A. Simpson (1986). Voyager 2 radio science observations of the Uranian system: atmosphere, rings, and satellites. *Science* 233, 79-84.

U.S. Standard Atmosphere (1976). NOAA-5/T76-1562. U.S. Government Printing Office, Washington, D.C.

von Zahn, U., S. Kumar, H. Niemann, and R. Prinn (1983). Composition of the Venus atmosphere. In *Venus* (D. M. Hunten, L. Colin, T. M. Donahue, and V. I. Moroz, eds.) pp. 299-430. Univ. of Arizona Press, Tucson.

Ward, W. R. (1974). Climatic variations on Mars I. Astronomical theory of insolation. *J. Geophys. Res.* 79, 3375-3386.

Warwick, J. W., D. R. Evans, J. H. Romig, C. B. Sawyer, M. D. Desch, M. L. Kaiser, J. K. Alexander, T. D. Carr, D. H. Staelin, S. Gulkis, R. L. Poynter, M. Aubier, A. Boischot, Y. Leblanc, A. Lecacheux, B. M. Pedersen, P. Zarka (1986). Voyager 2 radio observations of Uranus. *Science* 233, 102-106.

West, R. A., D. F. Strobel, and M. G. Tomasko. Clouds, aerosols, and photochemistry in the Jovian atmosphere (1986). *Icarus* 65, 161-217.

Willson, R. C., C. H. Duncan, and J. Geist (1980). Direct measurement of solar luminosity variation. *Science* 207, 177-179.

Young, A. T. and Young, L. D. G. (1973). Comments on the composition of the Venus cloud tops in light of recent spectroscopic data. *Astrophys. J.* 179, 39-43.

Zharkov, V. N. and V. P. Trubitsyn (1978). *Physics of Planetary Interiors*. Pachart, Tucson.

Zurek, R. W. (1976). Diurnal tide in the Martian atmosphere. *J. Atmos. Sci.* 33, 321-337.

ASTRONOMICAL, PHYSICAL, AND METEOROLOGICAL PARAMETERS FOR PLANETARY ATMOSPHERES

	EARTH	MARS	VENUS	TITAN	JUPITER	SATURN	URANUS	NEPTUNE
Mean solar dist (AU)	1.0000	1.5237	0.7233	9.54	5.203	9.54	19.2	30.2
Orbital eccentricity	0.017	0.093	0.007		0.048	0.053	0.046	0.009
Orbital period τ_{orb}	365.26d 1.0000yr	686.98d 1.8809yr	224.70d 0.61521yr	*SATURN*	4332.6d 11.862yr	10759d 29.458yr	30685d 84.014yr	60189d 164.79yr
Perihelion Date L_S	1986Jan2 281	1986Sep25 251	1985Oct6 253	*SATELLITE*	1987.48 57	2003.5 278	2050.3 187	2042.0 357
So. Summer Solstice	1985Dec22	1986cOct25	1985cOct17	2002.6	1994.6	2002.6	1985.8	2001.8
Obliquity	23.45°	25.19°	177.3°	-	3.12°	26.73°	97.86°	29.56°
Rotation period τ_{rot}	$23^h56^m04^s$	$24^h37^m23^s$	-243.01^d	15.945^d	$9^h55^m30^s$	$10^h39^m24^s$	-17^h14^m	$\sim15\text{-}18^h$
Eqtr radius a_e (km)	6378	3397	6051[haze @+84]	2575[haze @+240]	71,490	60,270	25,660	24,820
Oblateness $\varepsilon=1-a_p/a_e$	0.00335	0.0059	≤0.00001	-	0.0649	0.0980?	0.022?	0.022
GM ($km^3 s^{-2}$)	3.986×10^5	4.283×10^4	3.249×10^5	8.976×10^3	1.267×10^8	3.794×10^7	5.794×10^6	6.88×10^6
$J_2\times10^6$} @ a_e $J_4\times10^6$	1082.6 -1.6	1956 -	6 -	- -	14694 -580	16330 -920	3490 -30	4400 -
Mean $<g>|\delta g_E^P$ (cm s^{-2})	980|5	371|3	887|0	135|0	2440|389	1000|318	875|51	1090|21
Internal heat flux F (erg $cm^{-2}s^{-1}$)	62	-	-	-	5400	2000	<150	~450
Emission/Insolation	1.0002	1.000	1.000	1.000	1.7	1.8	<1.3	~2.8
Bond albedo	0.306	0.25	0.76	0.22	0.34	0.34	0.34	~0.28
Effective emission temperature T_e (K) pressure p_e (bar)	255 0.5	210 0.006	229 0.02	85 1	124 0.4	95 0.3	59 0.4	59 0.5
1-bar temp (K)	288	-	346	86	165	134	78	75?
Surface [or Jovian H_2O cld if 3⊙mix] temperature T_S (K) pressure p_S (bar)	288 1.013	~214 0.007	731 92	94 1.5	[294] [7]	[313] [21]	[366] [260]	[360] [283]
Major gases [molar ratios]	N_2[0.781] O_2[0.209] Ar[0.009]	CO_2[0.953] N_2[0.027] Ar[0.016]	CO_2[0.965] N_2[0.035] Ar[70ppm]	N_2[0.822?] Ar[0.166?] CH_4[0.060?]	H_2[0.899] He[0.099] CH_4[0.002]	H_2[0.963] He[0.033] CH_4[0.004]	H_2[≈0.85] He[≈0.15]	H_2[~0.9?] He[~0.1?]
Clouds	H_2O	Dust,H_2O,CO_2	H_2SO_4	hydrocarbons	NH_3,H_2O?	NH_3,H_2O?	CH_4,NH_3,H_2O?	CH_4,NH_3,H_2O?
Gas const R($cm^2 s^{-2}K^{-1}$)	2.87×10^6	1.92×10^6	1.91×10^6	2.9×10^6	3.71×10^7	3.89×10^7	3.6×10^7	3.8×10^7
c_p/R	3.5	4.4	4.5	3.6	3.3	3.6	3.6	3.6
Dry adiabatic lapse rate $\Gamma=g/c_p$ (K km^{-1})	9.8	4.4	10.5	1.3	*varies with altitude and ortho-para H_2 ratio* 2.0	0.7	0.7	0.8
Static stability $S=\Gamma+\partial T/\partial z$ (K km^{-1})	4.6	? *var w dust*	3 *near clds*	0.7	<0.03 *below 1-bar level*	<0.05	?	?
Scale height H (km) @ emission level p_e @ surface[or H_2O] p_S	7.5 8.4	11 11	4.9 16	18 20	19 45	37 122	24 150	21 124
Meridional thermal gradient (K/10^3km)	-4	-8	-6	-1	<±2?	<±3?	?	?
Radiative time const (s) $\tau_{Rad}=pT/\Gamma\sigma T_e^4$ @ p_e @ p_S	5×10^6 1×10^7	3×10^5 3×10^5	3×10^5 4×10^9	2×10^9 3×10^9	2×10^8 8×10^9	9×10^8 2×10^{11}	5×10^9 2×10^{13}	5×10^9 2×10^{13}
Vertical eddy mixing coeff κ_v ($cm^2 s^{-1}$)	5×10^4 *trop* >2500 *aloft*	5×10^5	≤2×10^5	≤10^3	6×10^8 *deep trop* 2×10^4 *aloft*	8×10^8 *deep trop* 2×10^4 *aloft*	<2×10^8	2×10^8
Coriolis parameter $f(30°)=2\pi/\tau_{rot}$ (s^{-1})	7.292×10^{-5}	7.088×10^{-5}	-2.993×10^{-7}	4.561×10^{-6}	1.758×10^{-4}	1.638×10^{-4}	-1.012×10^{-4}	~1×10^{-4}?
Beta parameter $\beta_e=2f/a_e$ ($cm^{-1}s^{-1}$)	2.29×10^{-13}	4.17×10^{-13}	9.89×10^{-16}	3.54×10^{-14}	4.92×10^{-14}	5.43×10^{-14}	7.88×10^{-14}	~9×10^{-14}?
Characteristic weather length L (km) (wavelength/2π)	1000	600	6000	3000?	2000	3000	10,000	?
speed U @ mid-lat (m s^{-1}) @ eqtr	+15 -4	+30 -	+90 +100	+40 +?	±50 +100	+100 +500	+200 -?	100? -

NOTICE

BIBLIOGRAPHIC DATA SHEET

1. Report No. NASA CP-2441	2. Government Accession No.	3. Recipient's Catalog No.
4. Title and Subtitle The Jovian Atmospheres		5. Report Date October 1986
		6. Performing Organization Code 640
7. Author(s) Michael Allison and Larry D. Travis, Editors		8. Performing Organization Report No.
9. Performing Organization Name and Address NASA Goddard Institute for Space Studies 2880 Broadway New York, NY 10025		10. Work Unit No.
		11. Contract or Grant No.
12. Sponsoring Agency Name and Address National Aeronautics and Space Administration Washington, DC 20546		13. Type of Report and Period Covered Conference Publication
		14. Sponsoring Agency Code

15. Supplementary Notes

16. Abstract

This volume provides a printed record of the proceedings of the Conference on the Jovian Atmospheres which was convened at the Goddard Institute for Space Studies on May 6-8, 1985. It includes the abstracts for all conference presentations, the complete text of selected reviews and contributed papers, and a transcript of open discussion. Separate sections are specifically devoted to studies of the thermal and ortho-para hydrogen structure, clouds and chemistry, global dynamics, and synoptic features and processes in the atmospheres of Jupiter and Saturn. Additional sections are devoted to pre-Voyager studies of Uranus and Neptune and a discussion of future spaceflight opportunities. A review of the major problems and interpretive conflicts arising in the study of giant planet atmospheres is given by Andrew P. Ingersoll.

17. Key Words (Selected by Author(s)) Jupiter, Saturn, Uranus, Neptune, Planetary Atmospheres, Planetary Meteorology.	18. Distribution Statement Unclassified - Unlimited Subject Category 91		
19. Security Classif. (of this report) Unclassified	20. Security Classif. (of this page) Unclassified	21. No. of Pages 332	22. Price* A15

*For sale by the National Technical Information Service, Springfield, Virginia 22161